ASTRO
SCIENCES
CENTER

Report No. M-16

THE MULTIPLE OUTER PLANET MISSION (GRAND TOUR)

IITRI
IIT RESEARCH INSTITUTE
10 West 35 Street
Chicago, Illinois 60616

Report No. M-16

THE MULTIPLE OUTER PLANET MISSION (GRAND TOUR)

Compiled by

David L. Roberts

Astro Sciences Center
of
IIT Research Institute
Chicago, Illinois

Contributors

A. B. Binder
A. Friedlander
L. Golden
H. Goldman
M. Hopper
J. C. Jones
J. C. Niehoff
D. L. Roberts
K. Uherka

for

Lunar and Planetary Programs
Office of Space Science and Applications
NASA Headquarters
Washington, D. C.

Contract No. NASr-65(06)

APPROVED

C. A. Stone, Director
Physics Research Division

January 1969

THE MULTIPLE OUTER PLANET MISSION (GRAND TOUR)

SUMMARY

The Multiple Outer Planet Mission (Grand Tour) is possible in the late 1970's because of an unusual alignment of the outer planets. Such an alignment will not reoccur for some one hundred seventy-nine years. From its initial conception the mission appeared potentially rewarding, but many unknowns were associated with it and there were many questions which had not been answered. Accordingly, the Astro Sciences Center of IIT Research Institute undertook a study of the major problem areas associated with the Grand Tour mission in order to further verify the mission concept and to provide a background for later Phase A study.

The specific aims of the study were:

1. To determine the guidance requirements to perform the mission,
2. To identify the scientific commonality between the planets Jupiter, Saturn, Uranus, Neptune,
3. To define "minimum" and "representative" scientific payloads, and
4. To estimate the launch vehicle requirements to perform the mission.

Trajectory opportunities for the Grand Tour exist from 1976 through 1980. The 1976 opportunity requires a high risk penetration of the Jovian radiation belts, in order to achieve adequate gravitational deflection. Since later opportunities relax this constraint, the 1976 opportunity has not been considered in detail. The 1977 and 1978 opportunities are the most acceptable in terms of planet miss distances, characteristic velocity, and time of flight. These were examined in detail and the results used as inputs to the guidance and scientific experiment analyses. The 1979 and 1980 opportunities pass very far from Jupiter (greater than 30 radii) which reduces the significance of Jupiter in the mission concept. These opportunities also have relatively high launch energy requirements and were not considered in further detail.

The most critical planetary intercept profile is at Saturn, the miss distance being generally of the same order as the radius of its rings. A cursory study of the possible collision rates in the rings made it advisable not to permit direct penetration of the rings by the spacecraft. At each of the 1977 and 1978 opportunities, mission profiles that pass entirely outside the rings (exterior) and that pass between planet surface and the lower edge of the rings (interior) have been considered. These are designated the 1977 E, and 1977 I, 1978 E, and 1978 I missions. Once a

Saturn profile had been selected, the profiles at each of the other gravity assist planets were essentially fixed. The major trajectory parameters for the selected opportunities are shown in Table S-1.

Table S-1

TRAJECTORY PARAMETERS FOR GRAND TOUR

	1977 E	1977 I	1978 E	1978 E
Launch Date	Sept 1977	Sept 1977	Oct 1978	Oct 1978
Ideal Velocity ft/sec				
Center of Window	51,900	54,400	53,200	56,200
20 Day Launch Window	52,700	55,200	54,200	57,100
Time of Flight (yrs)				
Jupiter	1.87	1.40	1.60	1.28
Saturn	3.98	2.98	3.36	2.53
Uranus	8.40	6.37	7.53	5.71
Neptune	11.94	9.05	11.00	8.32

The guidance requirements were established for each of the selected trajectories. Guidance maneuvers were specified on both approach and departure at each swingby planet to correct for three major errors:

a. the ΔV execution error from the previous maneuver

b. orbit determination errors

c. planet ephemeris errors

Because each swingby effectively magnifies any error that exists on approach to a planet the guidance velocity requirements are sensitive to the size of the error and to the planet at which it occurs. The objectives of the guidance analysis were to determine realistic estimates of spacecraft propulsion ΔV requirements, the method and accuracy of orbit determination, and the trajectory selection. Two tracking modes were considered, one using an on-board planet tracker, as originally considered for the Mariner '69, and an alternative using earth based radar tracking as is current practice.

The guidance requirements for the Grand Tour mission are much more severe than for current missions although they are not beyond the current state of the art. The total velocity corrections are given in Table S-2 and it can be seen that interior ring passage missions are by far the more demanding.

Table S-2

TOTAL GUIDANCE VELOCITIES FOR GRAND TOUR

	1977 E	1977 I	1978 E	1977 I
On-Board Tracking (m/sec)	190	430	200	370
Earth Radar Tracking (m/sec)	450	1710	340	1010

The orbit determination process must extend well into the planetary approach phase at Uranus and Saturn. Thus some approach maneuvers must be made relatively close to the planet. However, from the standpoint of positional error, either tracking mode will provide accuracies within the tolerances of the scientific experiments at each target planet.

The largest ΔV contribution occurs at the Uranus encounter. The importance of this result is that if a problem of fuel depletion occurs, it would be significant only at Uranus and hence only the Neptune encounter need be sacrificed. In the interest of minimizing the guidance ΔV requirement a strong case is made for an on-board planet tracking capability.

The scientific objectives for the Grand Tour mission have been developed from the goal of understanding the outer planets of the solar system. A systematic and logical procedure was adopted to identify the parameters of interest (measurables) that should be measured at each planet, and their relative values. Potential experiments were identified for each of the measurables and the extent to which each experiment could fulfill the objectives, given the flyby profiles, was evaluated. By combining these two sets of results it was possible to identify the relative importance of a wide range of experiments to the goal and objectives of exploring the outer planets. A final rating for the experiments was expressed in terms of value per pound to aid the selection of typical payloads. The major results of this evaluation are presented graphically in Figure S-1. The order in which the experiments have been plotted was determined by their relative values.

The highest priority scientific objectives were related to the atmospheres of the outer planets, but the highest priority experiments were related to particles and fields. This resulted directly from the universality of these experiments throughout the mission and hence their high integrated total value. The value of the planetary experiments is approximately equal at each target for all weights. This results from the fact that all the flyby profiles are similar in terms of their viewing of the light and dark hemispheres of the planets. The major differences between the planetary profiles are in miss distance. Overall there is a clear scientific commonality between the targets. Furthermore, this commonality can be retained for both 1977 and 1978 opportunities and for the interior and exterior ring passages, although the detailed experiment design specifications will be different in each case.

Typical scientific payloads have been derived on the basis of the experiment value curves shown in Figure S-1 and are shown in Table S-3. The "minimum" payload for which the mission is considered worthwhile utilizes the first four

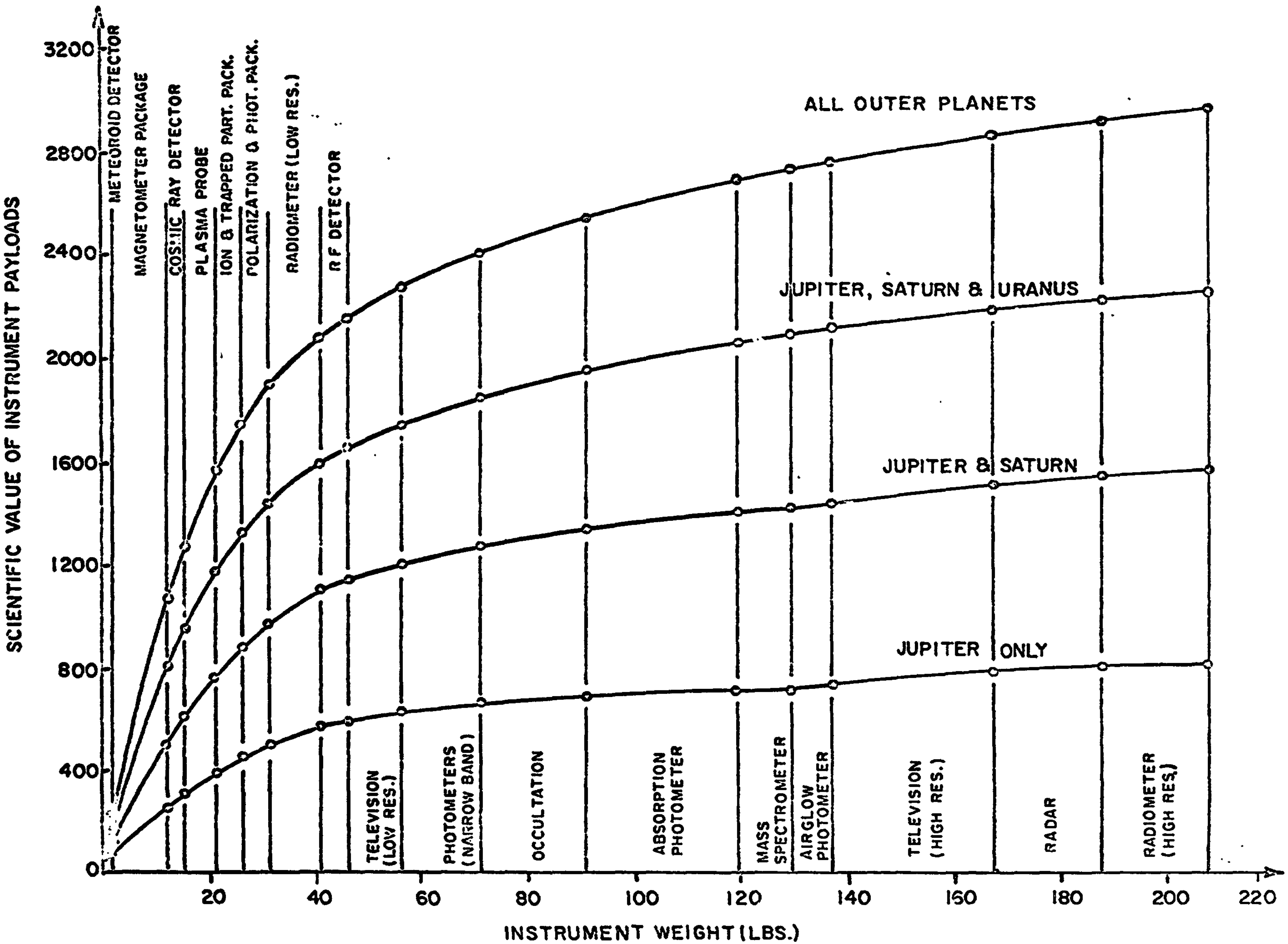

FIGURE S-1. VALUE OF INSTRUMENT PAYLOADS BASED ON "VALUE PER UNIT WEIGHT".

EXPERIMENT	WEIGHT LBS	VALUE/LB ARB. UNITS	DATA
MICROMETEOROID DETECTOR	2	124	NOMINAL
MAGNETOMETER PACKAGE	10	76	1 bps
COSMIC RAY DETECTOR	2.5	66	NOMINAL
PLASMA PROBE	6.5	48	3 bps
	21	314	$\simeq$ 5 bps
TRAPPED PARTICLE DETECTOR	5	41	10^4 bpp*
POLARIMETER - PHOTOMETER	5	41	10^5
IR, WAVE RADIOMETER	10	20	10^4
RF DETECTOR	5	14	10^4
	46	430	5 bps + 10^5bpp
LOW RES. TV	10	12	2 x 10^8 bpp
NARROW UV PHOTOMETERS	15	9	10^4
OCCULTATION (DUAL FREQU.)	20	6	10^4
ABSORPTION PHOTOMETERS	28	5	10^4
MASS SPECTROMETER	10	5	NOMINAL
AIRGLOW PHOTOMETERS	8	4	10^3
	137	471	5 bps + 2 x 10^8 bpp
HIGH RES. TV	30	3	2 x 10^8 bpp
RADAR (10 cm)	20	3	10^3
HIGH RES. IR RADIOMETER	20	1	10^6
	207	478	5 bps + 4 x 10^8 bpp

* bpp = bits per planet

TABLE S.3 SELECTED PAYLOADS FOR GRAND TOUR particles and fields experiments. This weighs approximately 20 pounds and will acquire some 5 bits per second of data. A "small" payload includes the first 8 experiments and is able to include 4 planetary experiments with a relatively low data requirement. The total weight is approximately 50 pounds. The "medium" payload includes television which adds some 2×10^8 bits to the data requirement. It was also possible to include the next five experiments without adding markedly to the power or data requirements. The payload weight is approximately 140 pounds. Finally a "large" payload includes all the experiments considered and weighs some 200 pounds. These selected payloads are used to define a typical range of total spacecraft weights and launch vehicle requirements.

In terms of the total spacecraft weight there are many Grand Tour mission options with different mission requirements. There are four selected trajectories, with their quite distinct midcourse correction requirements, depending on the tracking system used. There are four selected payloads each with its own weight, power, and data bulk. Rather than select a typical example, a matrix of spacecraft weights is presented in Table S-4 which bound the variables of the Grand Tour missions and launch vehicle capabilities. These weight totals are based on a brief analysis of the subsystem requirements for communications, power guidance, attitude control, sequencing and storage, thermal control, and structure.

		SPACECRAFT WEIGHT				LAUNCH VEHICLE CAPABILITY			
MISSION	TRACKING	MINIMUM	SMALL	MEDIUM	LARGE	SLV 3X -CENT-364	TIII D -CENT	TIII D -CENT-BII	TIII F -CENT
1977E	ON-BOARD	605	725	1180	1560	750	1900	2200	3300
	RADAR	760	930	1500	1950				
1977I	ON-BOARD	760	925	1480	1900	-	-	1450	2000
	RADAR	2270	2750	4060	4900				
1978E	ON-BOARD	620	730	1190	1510	-	1250	1700	2500
	RADAR	675	810	1330	1650				
1978I	ON-BOARD	720	850	1365	1710	-	-	1000	1200
	RADAR	1250	1300	2330	2850				

TABLE S.4 COMPARISON OF LAUNCH VEHICLE CAPABILITY WITH SPACECRAFT WEIGHT

From a total capability standpoint the exterior ring passages are strongly recommended, and an on-board tracker is the most effective tracking system. However for the exterior passages, the differences are such that radar tracking could be used as a back up, and only the Neptune intercept would be lost if the on-board system failed. If it is important that the same spacecraft design and launch vehicle be used at both opportunities, the minimum vehicle would be a Titan III-D-Centaur which has a capability for the exterior missions of 1900 lbs in 1977 and 1250 lbs in 1978. This will launch a "medium" payload with on-board tracking or a "small" payload with radar tracking.

The recommended missions would utilize the 1977 and 1978 opportunities, use an on-board planet tracker, have a payload in the 100 pound weight class, and require a total spacecraft weight of some 1200 pounds. In the light of the apparent tractability of all the subsystem requirements for the Grand Tour mission, it is strongly recommended that conceptual spacecraft designs be developed and that the complete feasibility of the mission be verified.

TABLE OF CONTENTS

TABLE OF CONTENTS (Continued)

LIST OF FIGURES

LIST OF FIGURES

LIST OF FIGURES

LIST OF FIGURES

LIST OF FIGURES

LIST OF FIGURES

LIST OF FIGURES

LIST OF TABLES

LIST OF TABLES

LIST OF TABLES FOR APPENDIX

SECTION 1

INTRODUCTION

THE MULTIPLE OUTER PLANET MISSION (GRAND TOUR)

1. INTRODUCTION

In the late 1970's a unique opportunity to conduct a grand tour of the outer planets will be possible utilizing gravity-assisted swingbys of Jupiter, Saturn and Uranus to achieve flyby missions of the planets and Neptune (Flandro 1966). A typical profile of this Grand Tour Mission is shown in Figure 1.1. In concept the Grand Tour offers a very significant exploration opportunity. For the investment of a single launch to Jupiter, scientific experiments are potentially possible at four outer planets. The most attractive opportunities occur in 1977 and 1978 with total mission times on the order of 9 to 12 years to Neptune. The opportunities offer a saving in trip time over direct outer planet missions but are rare in the sense that they will not reoccur until 2156 A.D.

In reality it is not obvious that the Grand Tour is practical. It is quite possible that the flyby profiles at each planet are so different as to demand different rather than common experimental payloads. One of the most critical aspects of executing the mission will be avoiding the rings of Saturn. Both interior and exterior ring flybys of Saturn have been considered (Silver 1967). It intuitively appears that a heavy guidance and control capability may be necessary to keep the spacecraft on course during the successive planet flybys.

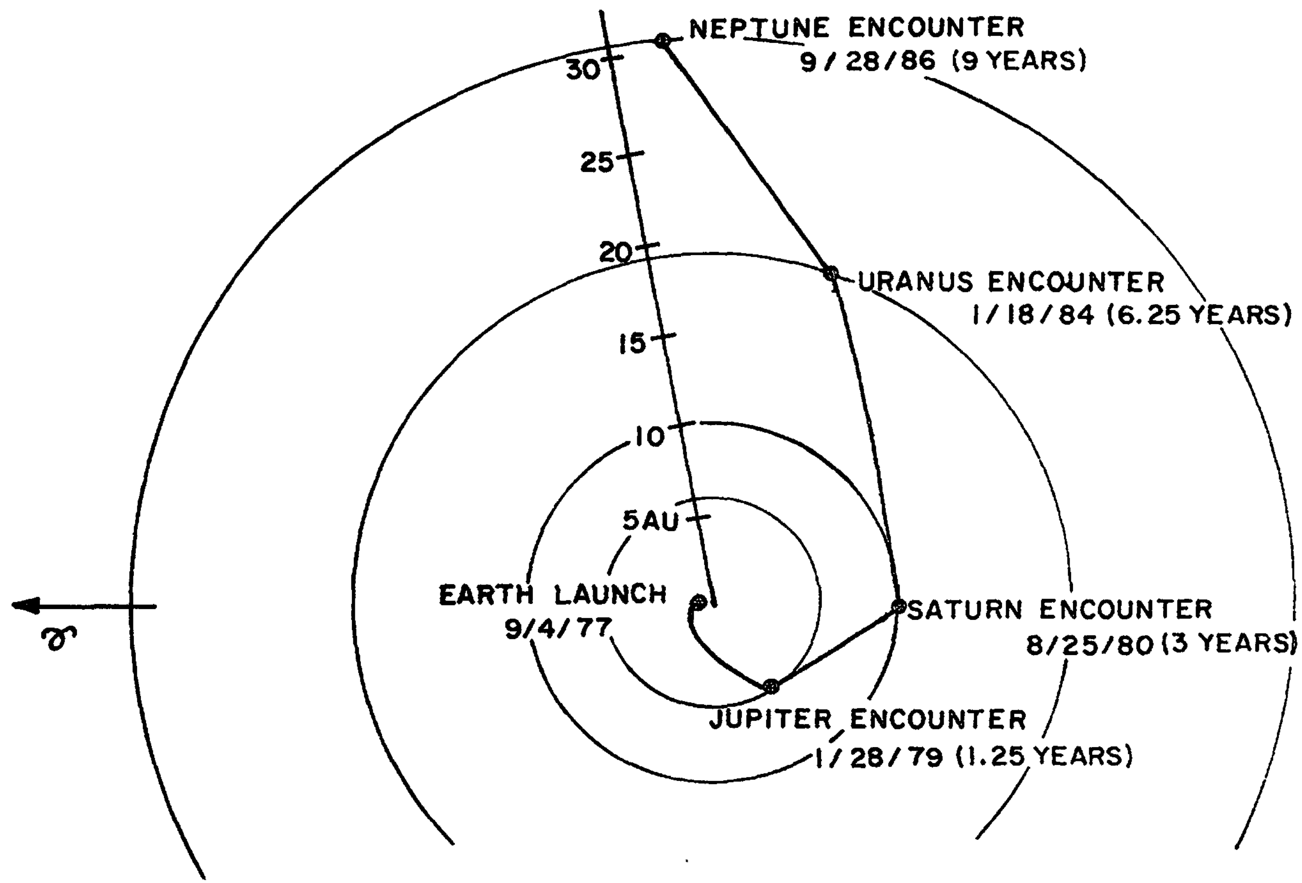

FIGURE 1.1. HELIOCENTRIC FLIGHT PATH, 1977-I GRAND TOUR.

It was in the context of this potentially rewarding mission concept, with many unknowns, that the Astro Sciences Center of IIT Research Institute performed the "Pre-Phase A" Study reported here. The specific aims of the study were:

1. To determine the guidance requirements to perform the mission.
2. To identify the scientific commonality between the planets (Jupiter, Saturn, Uranus, Neptune).
3. To define "minimum" and "representative" scientific payloads.
4. To estimate the launch vehicle requirements to perform the mission.

The flow chart for the study is shown in Figure 1.2. The trajectory selection exerts a strong influence on both the guidance and the science requirements in that it specifically defines each flyby profile. The sensitivity of the trajectory to guidance errors, and therefore the probability of completing all swingby maneuvers, is also dependent on the particular trajectory considered. Section II of this report presents four specific trajectories and the rationale for their selection. The four trajectories are designated exterior and interior Saturn Ring passages in 1977 and 1978 (1977 E, 1977 I, 1978 E, and 1978 I). By way of example Figure 1.3 shows the encounter profile at each of the planets for the 1977 E Grand Tour Mission.

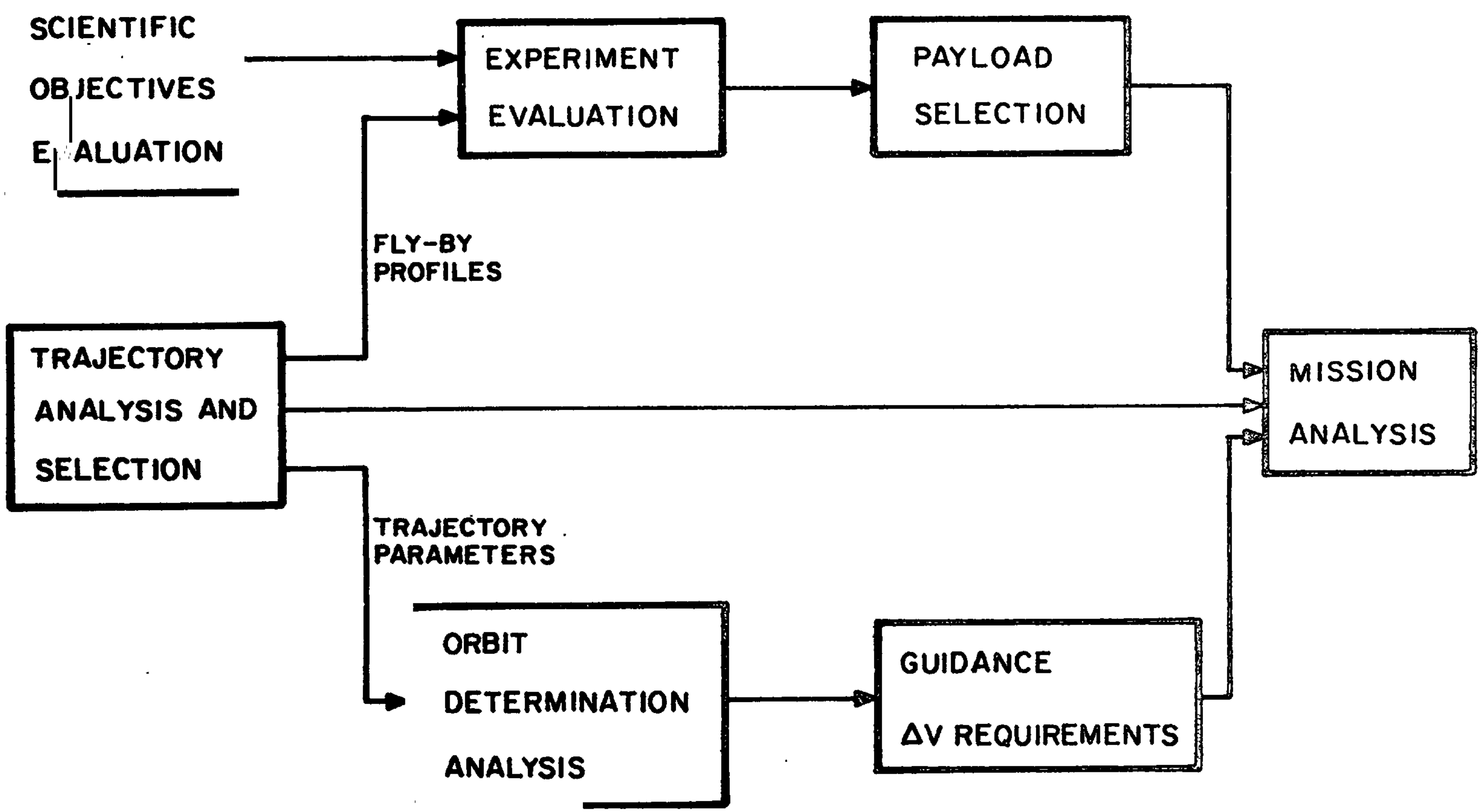

FIGURE 1.2. STUDY FLOW CHART — GRAND TOUR

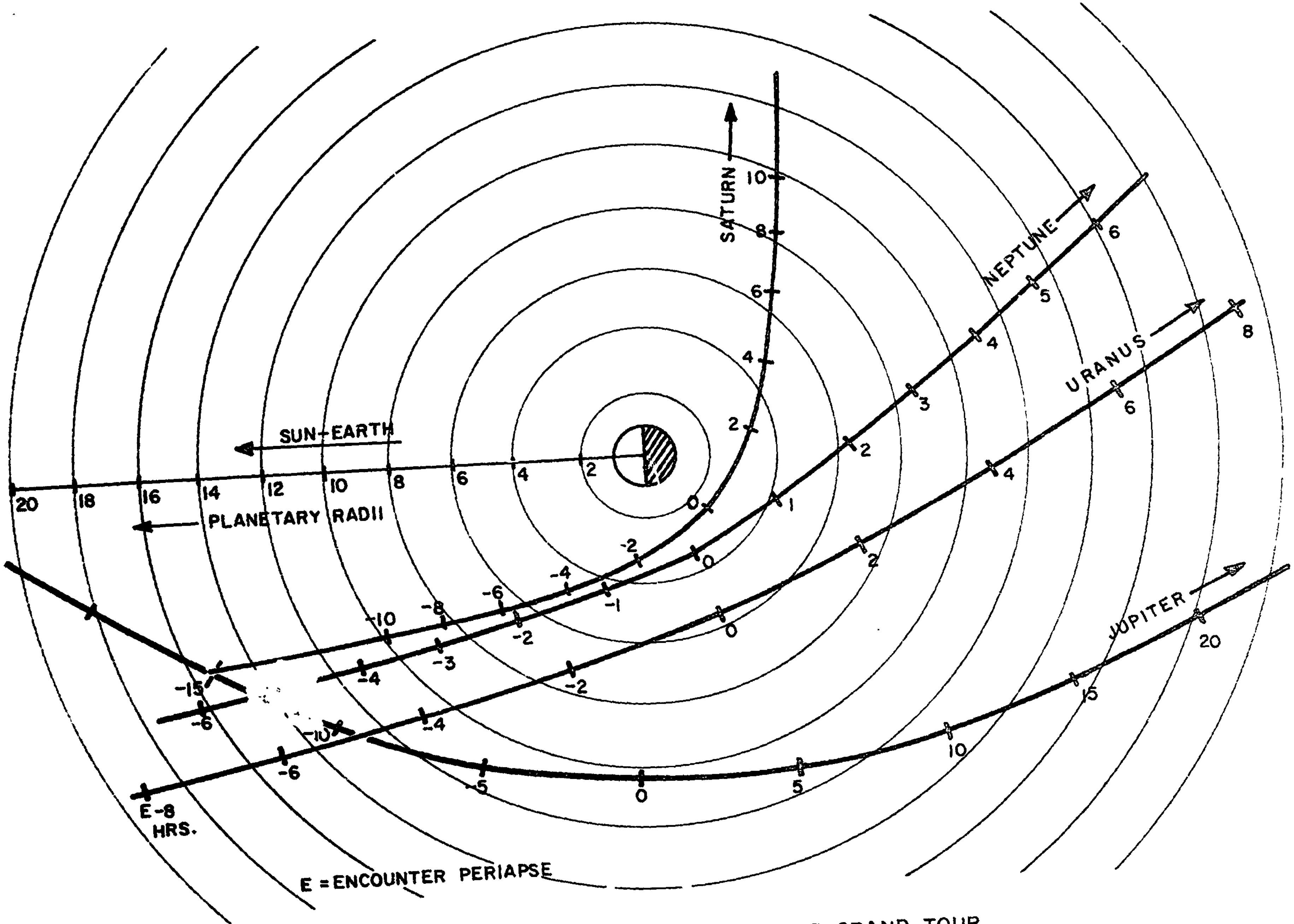

FIGURE 1.3. ENCOUNTER TRAJECTORY PROFILES, 1977-E GRAND TOUR

Section 3 describes the orbit determination analysis and the guidance requirements associated with each of the four selected trajectories. In defining the guidance velocity requirements both radar tracking from earth and on-board planet tracking (such as was proposed for Mariner '69) were evaluated.

Section 4 presents an evaluation of the scientific objectives for exploration of the outer planets. A method is presented which allows the relative priority of all the relevant scientific objectives to be assessed at each of the outer planets. These objectives are then considered in Section 5 together with the actual flyby profiles, and with available flyby measuring techniques, to select mission payloads. The results for each potential experiment are expressed in terms of value per pound at each target. A total of four representative payloads have been selected on the basis of this evaluation.

Section 6 discusses the major mission requirements which have resulted from the trajectory, guidance and payload analyses. Sample spacecraft weight breakdowns are presented as a guide to the identification of the launch vehicle requirements.

The study has provided a much better understanding of the mission requirements for the Grand Tour Mission. In particular guidance and experiment analyses had not been performed to this level prior to this study.

SECTION 2

TRAJECTORY ANALYSIS AND SELECTION

Compiled by

A. L. Friedlander

Contributors

A. L. Friedlander
M. Hopper
J. C. Niehoff

2. TRAJECTORY ANALYSIS AND SELECTION

The trajectory of an interplanetary spacecraft can be altered significantly if the spacecraft passes near a planetary body. This perturbation effect, due to the planet's gravitational field, is often referred to as a "gravity assist." When properly designed, a gravity assist can be used to modify the heliocentric trajectory in a desired manner. For example, the trajectory may be deflected to intercept another target planet at a later time. The technique of gravity-assisted or planetary-swingby trajectories has been studied extensively during the past several years (Minovitch 1963) and (Niehoff 1965). A number of studies have shown the advantage in reduced launch energy and trip time that accrues when this technique is employed for multiple-target missions in solar system exploration (Niehoff 1966) and Sturms 1967). This report is concerned with the "Grand Tour" mission, i.e., the successive swingbys of the Jovian or outer planets -- Jupiter, Saturn, and Uranus, with Neptune being the final target.

2.1 Principle of Planet Swingby

Viewed on a heliocentric scale, the result of a gravity assist is to change the spacecraft's velocity vector between the time that the spacecraft enters and leaves the planet's sphere of influence (see Table 2.1). Since this

Table 2.1 PLANET SPHERE OF INFLUENCE*

Planet	Radius	Sphere of Influence
EARTH	6,378 km	0.925×10^6 km
JUPITER	71,375	48.1×10^6
SATURN	60,500	54.6×10^6
URANUS	24,850	51.7×10^6
NEPTUNE	25,000	86.1×10^6

*Sphere of influence is defined as that distance from the planet where the perturbative forces due to the Sun and the planet are equal:

$$R_{sphere} = \left(\frac{\text{mass of planet}}{\text{mass of Sun}}\right)^{2/5} \times \left(\begin{array}{l}\text{mean distance of}\\ \text{planet from Sun}\end{array}\right)$$

time is relatively short compared to the interplanetary travel time, the planet's orbital velocity may be considered approximately constant. Furthermore, the spacecraft's motion with respect to the planet approximates a hyperbola. Figure 2.1 illustrates the geometry of the hyperbolic flyby.

The spacecraft approaches the planet initially along one asymptote of the hyperbola with velocity $\underline{V}_{h1}$. This asymptotic approach velocity is defined as the vector difference between the heliocentric velocity of the spacecraft and that of the planet,

$$\underline{V}_{h1} = \underline{V}_1 - \underline{V}_p \tag{2.1}$$

both of which are assumed determined at the nominal time of encounter. The gravitational attraction causes the planetocentric trajectory to bend through a rotation Ψ which is the turning angle between the approach and departure asymptotes. The asymptotic departure velocity, $\underline{V}_{h2}$, is equal in magnitude to $\underline{V}_{h1}$ but differs in direction. With reference to heliocentric coordinates, the changed velocity is now given by the vector addition.

$$\underline{V}_2 = \underline{V}_p + \underline{V}_{h2} \tag{2.2}$$

$\underline{V}_2$ differs from $\underline{V}_1$ in both magnitude and direction, the former reflecting a change in the energy of the heliocentric trajectory. In the case of successive swingbys of the outer planets, each swingby trajectory takes place along the trailing edge of the planet's motion, i.e., behind the planet as seen from the Sun.

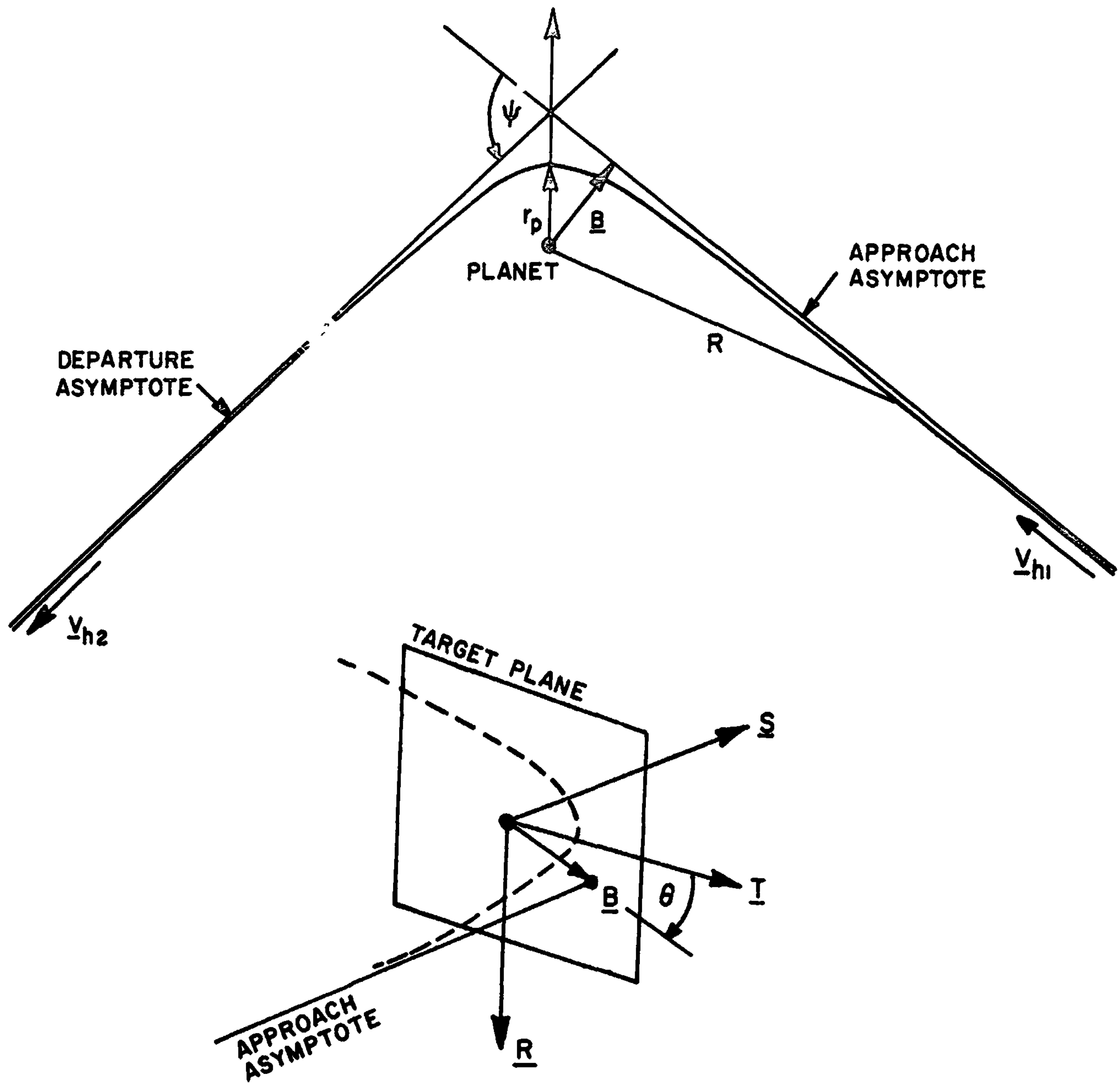

FIGURE 2.1 HYPERBOLIC FLYBY DIAGRAM

Hence, the heliocentric energy is increased by the gravity assist. Conservation of energy is preserved, of course, since the planet looses orbital energy in the gravitational exchange. However, this point is strictly academic inasmuch as the gravitational attraction of the massive planet by the spacecraft is negligible.

For a given gravity assist planet, the asymptotic departure velocity can be shown to depend on the approach velocity and the aim point parameters. The latter is expressed by the asymptotic miss vector $\underline{B}$ which is referred to the STR coordinate system of Figure 2.1. By definition, the target plane (T-R) passes through the planet's center and is perpendicular to the direction of the approach asymptote $\underline{S}$ (a unit vector).

$$\underline{S} = \frac{\underline{V}_{h1}}{|\underline{V}_{h1}|} \quad \underline{\text{ecliptic reference}} \tag{2.3}$$

$$\underline{T} = \frac{\underline{S} \times \underline{k}}{|\underline{S} \times \underline{k}|} \tag{2.4}$$

$$\underline{R} = \underline{S} \times \underline{T} \tag{2.5}$$

with $\underline{k}$ being a unit vector perpendicular to the ecliptic plane, $\underline{T}$ is defined as a unit vector perpendicular to $\underline{S}$, and also parallel to the ecliptic. The vector $\underline{B}$, from the planet center perpendicular to the approach asymptote, lies in the target plane with components

$$(\underline{B} \cdot \underline{T}) = b \cos \theta$$
$$(\underline{B} \cdot \underline{R}) = b \sin \theta \qquad (2.6)$$

where $b = |\underline{B}|$ is the miss distance (here, miss distance is a trajectory design parameter not to be confused with a guidance error Δb).

Several important conic formulas relating the swingby parameters are

Hyperbolic velocity: $V_h = |\underline{V}_{h1}| = |\underline{V}_{h2}|$ (2.7)

Periapse distance: $r_p^2 + \frac{2\mu}{V_h^2} r_p = b^2$ (2.8)

Turning (deflection) angle:

$$\cos \Psi = \frac{b^2 V_h^4 - \mu^2}{b^2 V_h^4 + \mu^2} \qquad (2.9)$$

Departure velocity vector:

$$\underline{V}_{h2} = \underline{V}_{h1} \cos \Psi - \left(\frac{\underline{V}_h \sin \Psi}{b}\right) \underline{B} \qquad (2.10)$$

where μ is the planet's gravitational constant $\left(\frac{km^3}{sec^2}\right)$ which is proportional to the planet's mass. Several comments can be made about the general effects of the above equations.

(1) The periapse (closest approach) distance is always less than or equal to the asymptotic miss-distance. The difference between these quantities will decrease as μ decreases or as V_h increases.

(2) The turning angle can vary between 0° and 180°. Turning angle will increase as μ increases, or as b decreases, or as V_h decreases.

2.2 Launch Opportunities

Practical launch opportunities for the Grand Tour mission are dictated by the relative orientation of the outer planets. The appropriate phase angle relationship reoccurs approximately once every 179 years. This long period is fixed largely by the synodic period of the two outermost planets considered in the combination. Uranus and Neptune have a synodic period of about 171.4 years. Once the proper phasing does occur, however, several consecutive launch years are available because of the slow motion of the outer planets. The next opportunity occurs during the period from 1976 to 1980. Launch windows in each of these years are approximately 13 months apart.

Previous trajectory analyses of the Grand Tour were helpful to the present study in that launch windows and velocity requirements were fairly well delineated (Flandro 1966) and (Silver 1967). These results allowed one to readily identify the best opportunities, and to minimize costly trajectory search computations.

The bar chart of Figure 2.2 shows the range of ideal launch velocities* and trip times to Neptune for five launch opportunities in the period 1976-1980. It is seen that ideal velocity generally increases with each successive launch year, whereas the trip time tends to decrease. In any given year, the faster trip times correspond to the higher launch velocities. Overall, the potential Grand Tour missions cover the range of velocities 51,400 to 60,700 ft/sec, and the range of trip times 8.1 to 12.8 years.

Another important parameter of the Grand Tour trajectories is the pericenter of closest approach distance at each planet. In the case of Jupiter, which moves faster than the other planets, the variation of pericenter distance with the launch year is quite large. A spacecraft launched in 1976 will pass very close to Jupiter (1.02 - 1.50 Jupiter

---

*Ideal velocity (in ft/sec) is that velocity required by a launch vehicle to achieve a given hyperbolic excess velocity (VHL) beyond Earth escape from a 100 n. mile parking orbit, assuming gravitational and frictional losses of 4000 ft/sec.

$$V_I = \left[(VHL)^2 + (36,178)^2 \right]^{1/2} + 4000 \text{ ft/sec}$$

$$= 3280.8 \left[C_3 + 121.5964 \right]^{1/2} + 4000 \text{ ft/sec}$$

where VHL is hyperbolic excess velocity in ft/sec

C_3 is injection energy in $\left(\frac{\text{km}}{\text{sec}}\right)^2$

IIT RESEARCH INSTITUTE

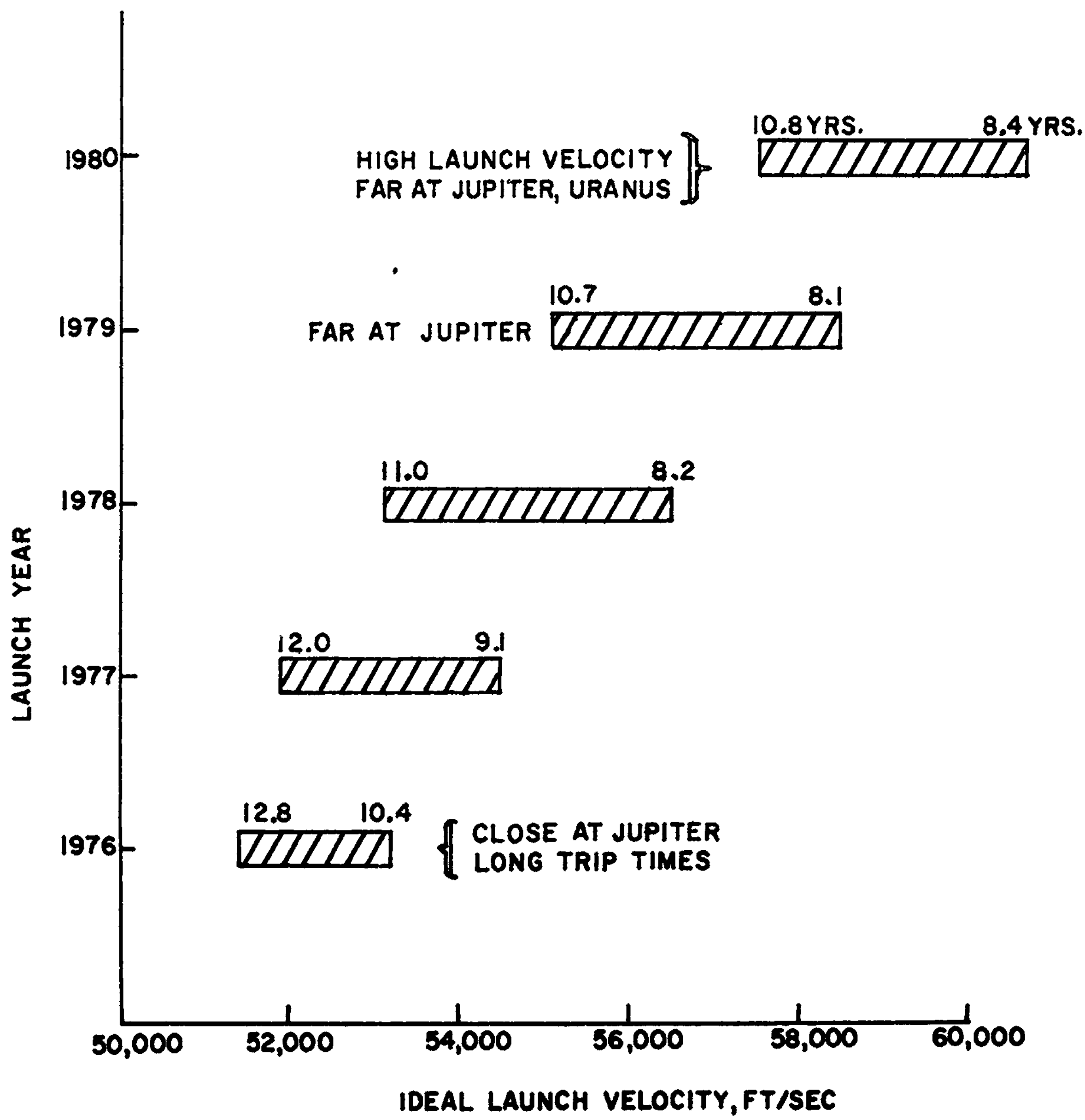

FIGURE 2.2 GRAND TOUR LAUNCH OPPORTUNITIES

radii). Later flights in 1979 and 1980 have very large pericenter distances (30-70 Jupiter radii). Although close flybys of Jupiter may be desirable from a science experiment standpoint, several disadvantages of the 1976 opportunity are worth noting. These are: (1) long trip times, (2) equipment shielding penalty due to Jupiter's radiation belts, (3) high guidance requirement, and (4) an earlier spacecraft development and flight program. The disadvantages of the later launch opportunities are clearly the high launch velocities required and the large passing distances at Jupiter.

On the basis of the above preliminary results and arguments, it was decided that the best launch opportunities for the Grand Tour mission occur in 1977 and 1978. Accordingly, this study was aimed at these two consecutive launch years.

2.3 Method of Trajectory Analysis

The various stages in the trajectory analysis are described by the block diagram shown in Figure 2.3. A computer program based on conic trajectory approximations was employed to generate the large amount of data representing potential Grand Tour trajectories throughout the launch opportunities. Trajectory selections were then made from the data map after imposing several conditions of constraint which define the regions of practical trajectories. The final stage in the analysis employs an N-BODY numerical integration

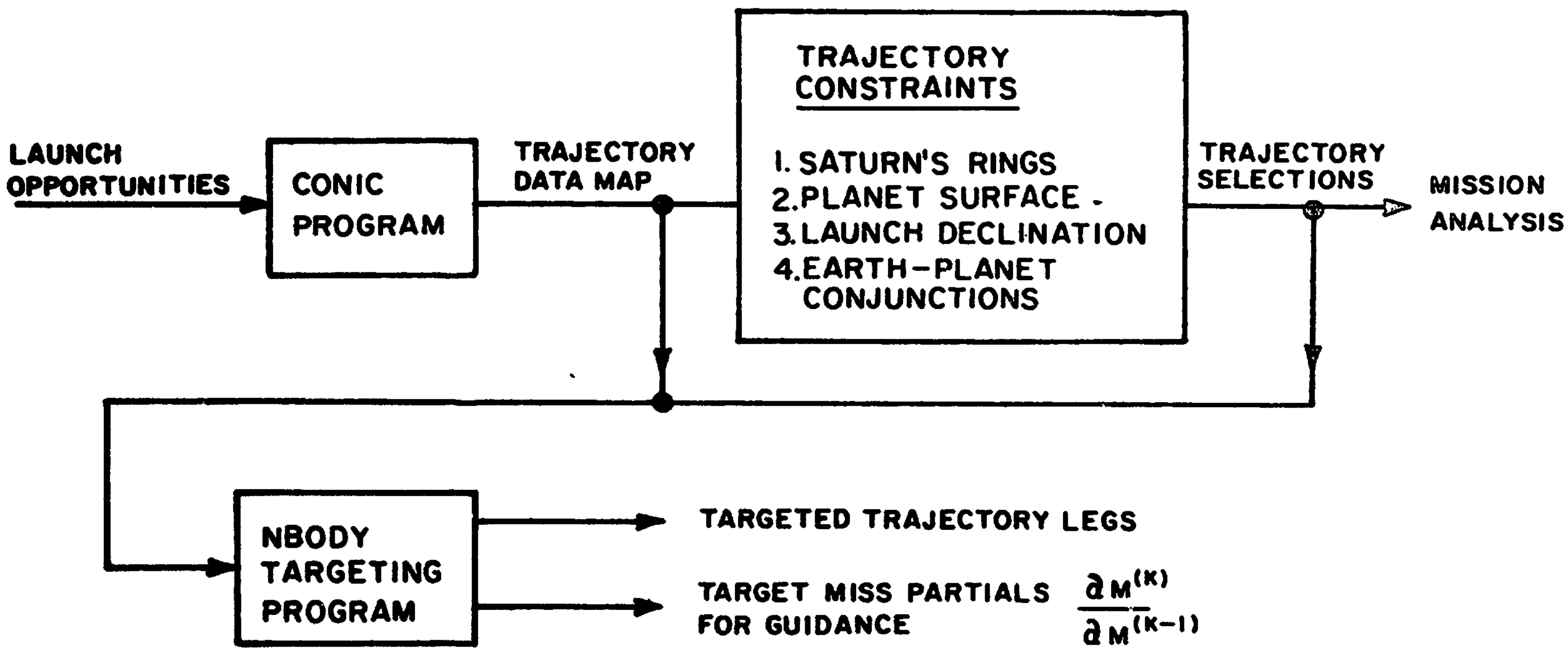

FIGURE 2.3 METHOD OF TRAJECTORY ANALYSIS

targeting program to check the validity of the conic results, and to generate the partial derivative (sensitivity) matrices needed for the guidance analysis.

2.3.1 Conic Analysis

Trajectory data was obtained from the Space Research Conic Program (SPARC) developed at JPL for investigations of multiple planet missions (Joseph 1966). The inputs to this program are specified values of the Earth-launch date and injection energy C_3. Using a matched conic approach between the successive heliocentric trajectory legs, a search is made to find the appropriate Earth-Jupiter transfer which results in subsequent planetary swingbys and finally Neptune encounter. The matching process insures equal magnitude of the approach and departure hyperbolic velocities at each swingby planet. All heliocentric trajectory legs were restricted to Type I, Class I transfers* in order to achieve the shortest possible flight times. Mean orbital elements of the planets were used to obtain the planetary positions and velocities at the encounter times.

*Type I trajectories have a heliocentric transfer angle less than 180°, whereas Type II trajectories traverse more than 180°. For either Type I or Type II, Class I trajectories have a smaller heliocentric transfer angle than Class II trajectories.

In operation, potential Grand Tour trajectories are obtained over a range of launch dates and injection energy (ideal velocity). For each trajectory, the computer program printout includes defining parameters of the geocentric and planetocentric hyperbolas, planet encounter dates, elements of the heliocentric transfer legs, and orientation angles of the Earth, Sun and Canopus as seen by the spacecraft at the encounter times. Trajectory data is obtained over a sufficiently fine grid of input variables to allow the use of cross-plotting techniques in the trajectory selection stage of the analysis.

2.3.2 NBODY Targeting Analysis

The NBODY Targeting Program indicated in Figure 2.3 was developed at IITRI as a modification of the Lewis Research Center NBODY code (Strack 1963). Because of the single precision arithmetic of this program and the high trajectory sensitivity of the Grand Tour, it was not possible to target a continuous trajectory from Earth to Neptune. In fact, attempts to target two legs at a time (e.g., Earth-Jupiter-Saturn) were not too satisfactory, although near convergence was obtained. The method adopted in this study was to target one leg at a time working backwards from the Uranus-Neptune leg and successively matching the arrival and departure target vector at each planet. This procedure is initialized with the conic trajectory parameters obtained from the SPARC program.

It should be made clear that the procedure of targeting each individual leg separately does not yield a continuous trajectory from Earth to Neptune. The discontinuity appears as a target plane velocity difference between the approach and departure trajectories. This is due to the fact that no attempt was made to converge on velocity but only on the miss vector $\underline{B}$ and the time of encounter. Generally, the conic and NBODY results are in excellent agreement for any one trajectory leg. On the basis of this result, it is expected that the conic trajectory data is sufficiently valid for preliminary mission analysis. Some results of the NBODY Targeting Program are described in the Appendix to this section of the report.

2.3.3 Conditions of Constraint

Four constraints are imposed on the trajectory selection process. Clearly, the "hard" constraint is that the point of closest approach at each swingby planet must be above the planet's surface. This applies initially to the nominal trajectory conditions, but the question of guidance accuracy must be factored in at a later stage in the analysis. Guidance accuracy is the dominant factor in selecting the nominal aim point at Neptune, which otherwise might be chosen arbitrarily since Neptune is the final target.

Another constraint is that the declination of the geocentric departure asymptote be limited to about 34°. Lower declinations provide launch azimuths within ETR range safety limits, thus avoiding costly dog-leg maneuvers during ascent to Earth orbit. Also, early orbit determination accuracy is enhanced if the declination is not too large.

To avoid a communications problem caused by solar activity interference, it is desirable that the planet not be behind the sun at the time of encounter. That is, the earth-Sun-planet angle at planet encounter should be somewhat removed from 180° (superior conjunction). A third constraint on the trajectory selection process, then, is a set of conjunction bands of ± 10 days (± 10°) for each planet encounter.

The fourth, and major, constraint is the apparent necessity of avoiding passing through the Ring of Saturn. Lying in Saturn's equatorial plane, the Rings extend from about 11,500 km to 76,500 km above Saturn's surface. The inclination of the spacecraft's swingby trajectory to the Ring plane is about 30° for the Grand Tour mission. The relative velocity between the spacecraft and Ring particles is about 12 km/sec as an average, and the component of the spacecraft's velocity normal to the Ring plane is also about 12 km/sec.

There is great uncertainity in the present knowledge of the Ring density and thickness. An estimate of the upper limit on density based on a gravitational stability analysis is 0.06 g/cm^3 (Cook 1965) but the actual density may be more than an order of magnitude lower. Earlier estimates of Ring thickness have an upper limit of about 10 km. However, a more recent analysis of observations fitted to a theoretical physical model indicates that the Rings may only be 10 cm thick (Franklin 1965).

A parametric analysis was performed assuming the average particle radius (r_p) to range from 0.01 cm to 100 cm, and the average particle density (ρ_p) to range from 1 g/cm^3 to 8 g/cm^3. It can be shown that the number of collisions (C) and the mass encountered (M) per unit spacecraft area are given by the following equations:

$$C = \left(\frac{V_R}{V_N}\right)\left(\frac{\tau}{\pi r_p^2}\right) \times 10^4 \quad \frac{\text{collisions}}{\text{m}^2} \qquad (2.11)$$

$$M = \left(\frac{V_R}{V_N}\right)\left(\frac{4}{3}\ \tau\ \rho_p\ r_p\right) \times 10^1 \quad \frac{\text{kg}}{\text{m}^2} \qquad (2.12)$$

where V_R is the relative velocity between the spacecraft and the Ring particles (~ 12 km/sec) and V_N is the spacecraft's velocity component normal to the Ring plane (~ 12 km/sec).

The normalized optical thickness of the Rings, τ, is assumed to be unity which is the maximum experimentally determined value. The following table lists several values of C and M.

r_p \ ρ_p	1 g/cm^3	8 g/cm^3
0.01 cm	$C = 3.2 \times 10^7 \frac{coll}{m^2}$ $M = 0.134 \frac{kg}{m^2}$	$C = 3.2 \times 10^7 \frac{coll}{m^2}$ $M = 1.07 \frac{kg}{m^2}$
100 cm	$C = 0.32 \frac{coll}{m^2}$ $M = 1340 \frac{kg}{m^2}$	$C = 0.32 \frac{coll}{m^2}$ $M = 10,700 \frac{kg}{m^2}$

Since the mass that would be encountered by a spacecraft is estimated to be in the range 0.1 kg/m^2 to 10,000 kg/m^2, it would appear that the Grand Tour trajectory should not pass through the Rings of Saturn.

2.4 Descriptive Trajectory Data

Launch opportunities for the Grand Tour in 1977 occur over a two to three week period in August-September of that year. A similar period 13 months later occurs during September-October in 1978. In this section of the report, certain characteristic trajectory parameters obtained from the SPARC computer runs are presented for these two launch years. Consideration of constraint conditions is deferred to the next section.

Figure 2.4 shows curves of ideal launch velocity in 1977 plotted on a grid of Jupiter arrival date (Julian Date) versus Earth launch date. Every point on the grid represents a potential Grand Tour trajectory to Neptune with swingbys at Jupiter, Saturn and Uranus. In selecting the range of design trajectories throughout a launch window, it is helpful to fix the Jupiter arrival date at some specified value. Therefore, the Jupiter arrival data is a convenient independent variable for representing other key trajectory parameters. The velocity curves are actually closed contours although this is not shown in the figure. In other words, for a given launch date and velocity, there are two possible Jupiter arrival dates. The later date corresponds to a Class II trajectory which has a significantly longer flight time. It is recalled that the Class II trajectories are not

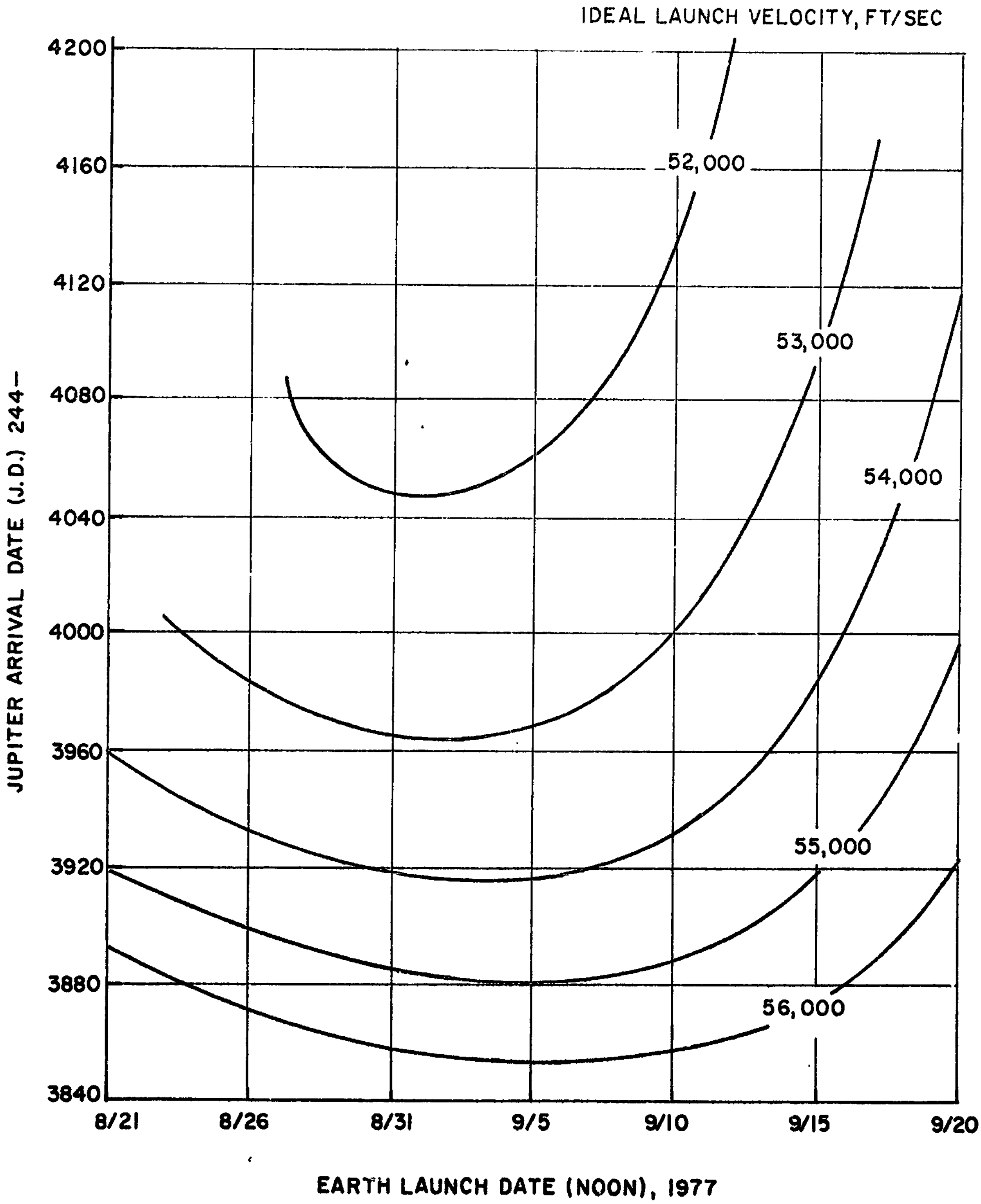

FIGURE 2.4 TRAJECTORY SELECTION GRAPH, 1977 GRAND TOUR

considered in the study. The minimum energy trajectory (Type I) has a launch date of Sept. 5 1977 and a Jupiter arrival date of Oct. 24 1979 (2444170). The corresponding minimum ideal launch velocity is 51,500 ft/sec.

Figure 2.5 shows the declination of the geocentric departure asymptote. This parameter is seen to be in the range 23° - 36° for the 1977 Grand Tour. The higher declinations are associated with lower values of launch velocity.

The minimum flight time to Jupiter is plotted as a function of launch velocity in Figure 2.6. This curve is obtained from the minimum points of the velocity contours of Figure 2.4. Flight time to Jupiter varies from 460 to 660 days as the ideal launch velocity decreases from 56,000 to 52,000 ft/sec.

Three additional descriptive parameters of the Grand Tour are the trip time, pericenter distance and hyperbolic approach velocity at each planet encounter. This data is plotted against the Jupiter arrival date in Figures 2.7 to 2.9. The curves shown are specifically for the optimum launch date, i.e., the minimum launch velocity for each value of Jupiter arrival date. Although there is a variation of the parameters with launch date, this variation is quite small for Grand Tour trajectories. Hence, when plotted against Jupiter arrival date, this form of data compression is quite representative of all trajectories throughout the launch windows.

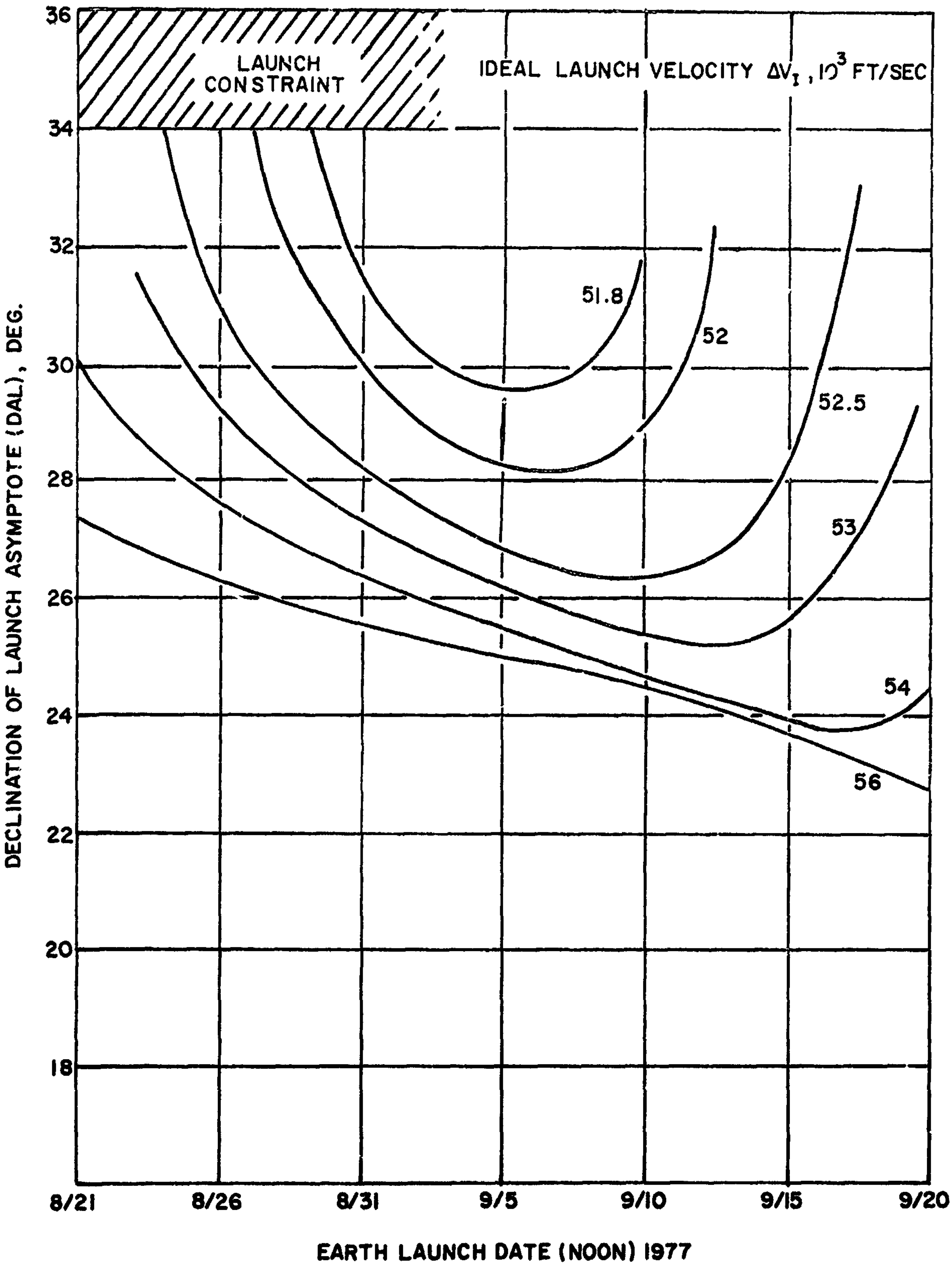

FIGURE 2.5. DECLINATION OF GEOCENTRIC DEPARTURE ASYMPTOTE, 1977 GRAND TOUR

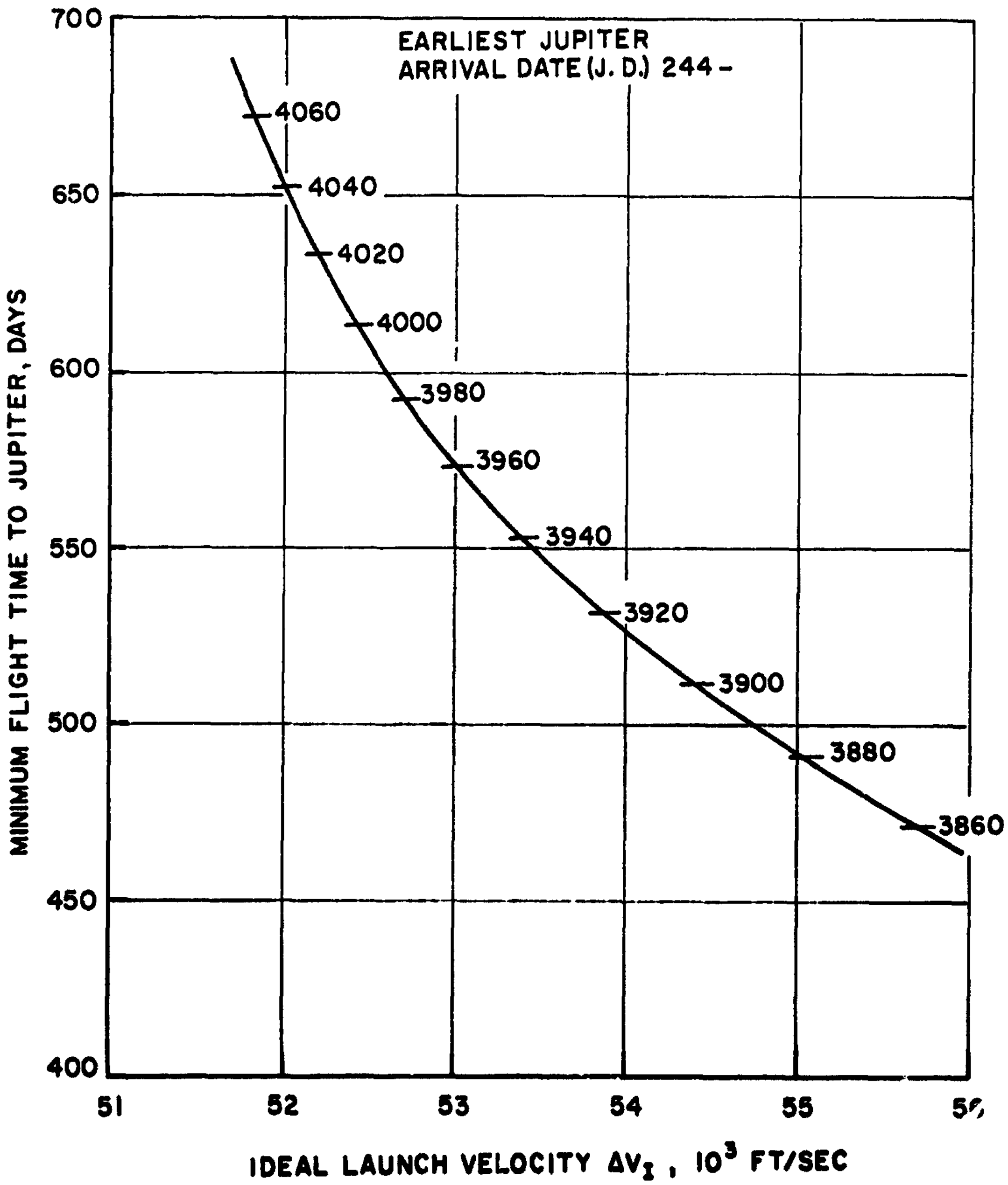

FIGURE 2.6 MINIMUM FLIGHT TIME TO JUPITER, 1977 GRAND TOUR

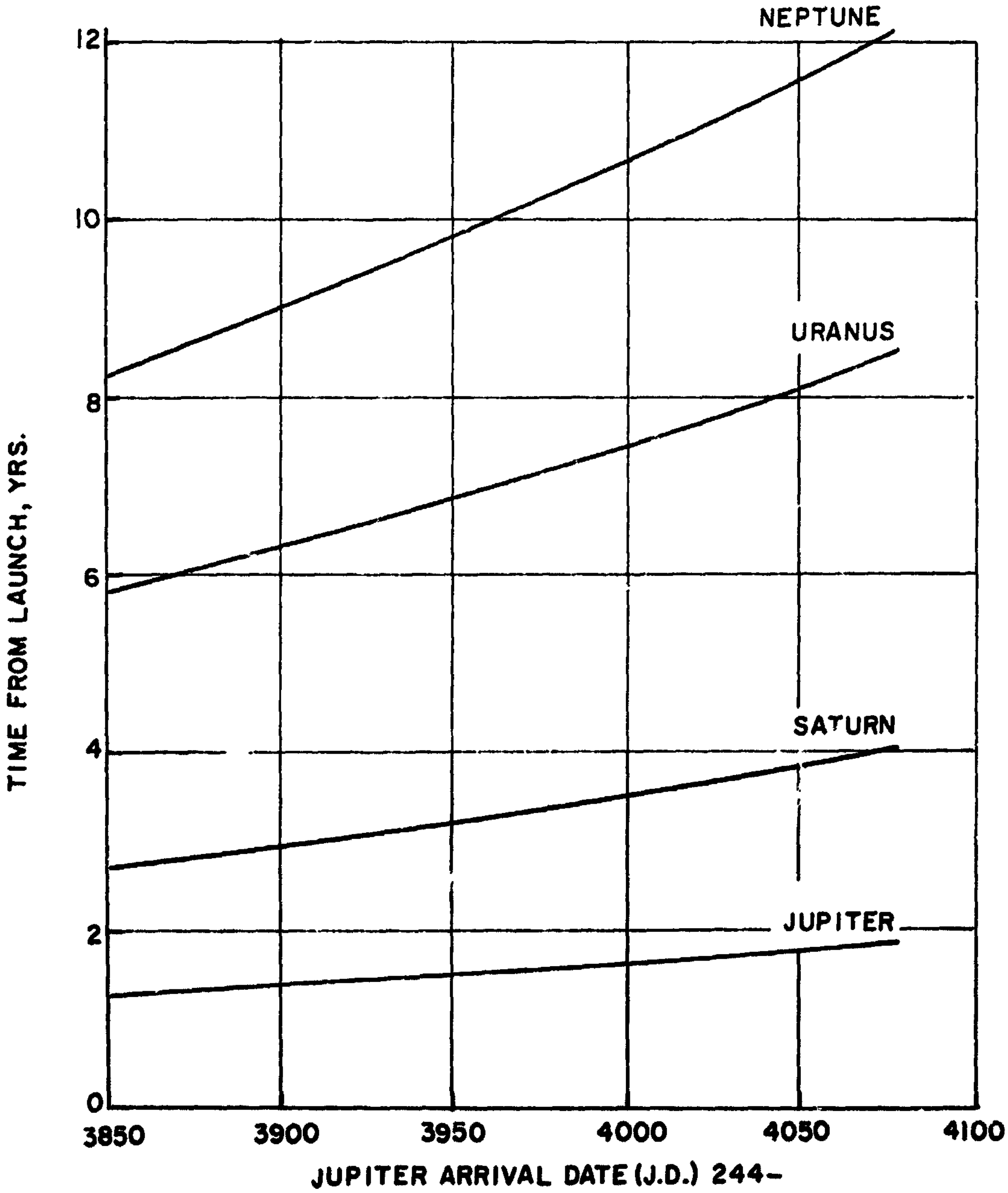

FIGURE 2.7 PLANET ARRIVAL TIMES, 1977 GRAND TOUR

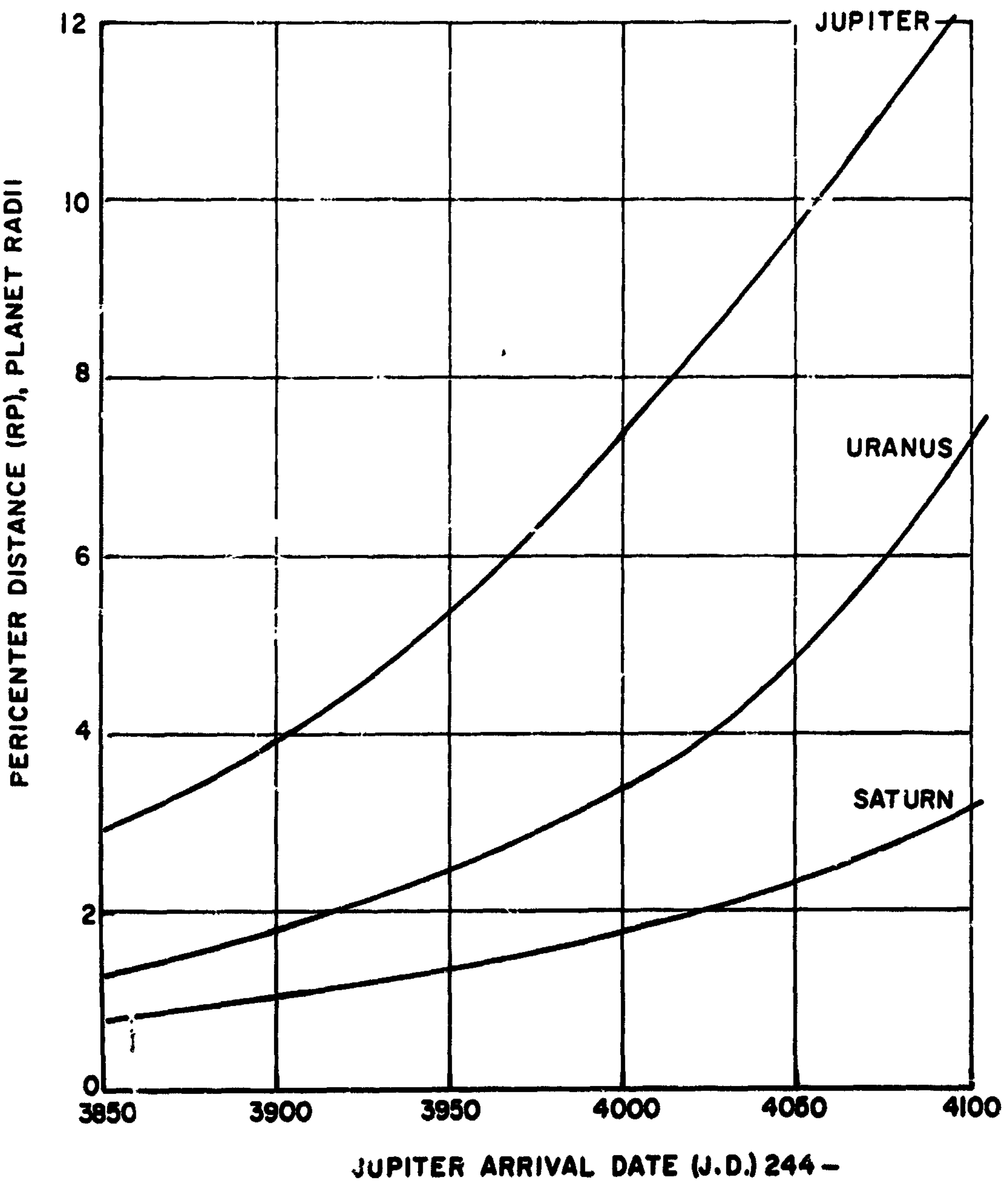

FIGURE 2.8 PLANET CLOSEST APPROACH DISTANCES, 1977 GRAND TOUR

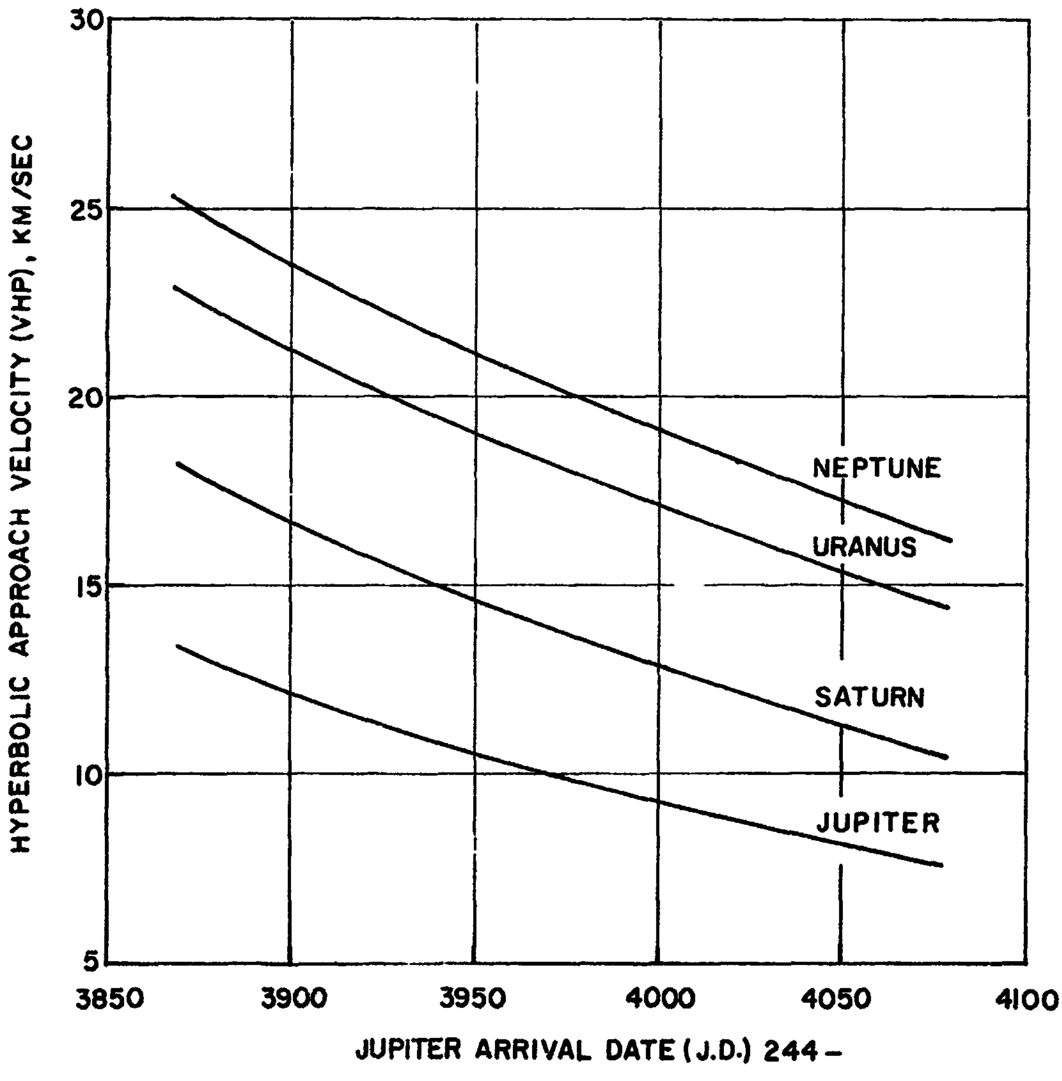

FIGURE 2.9 PLANET ARRIVAL VELOCITIES, 1977 GRAND TOUR

It is seen that the closest approach distance is largest at Jupiter and smallest at Saturn. Closest approach at Neptune is not shown since it is arbitrary and will be chosen by the selection process described later. Another important characteristic is that the closest approach at each swingby planet increases as the trip time increases (or, as the launch velocity decreases). The largest variation occurs for Jupiter (3-12 Jupiter radii), and the smallest variation for Saturn (1-2.7 Saturn radii).

Along a given trajectory, the approach velocity is found to increase at each successive planet encounter. Also, as the trip time increases, the approach velocity at each planet decreases. The velocity variation over the range of trajectories shown are 7.7-13.4 km/sec (Jupiter), 10.5-18.2 km/sec (Saturn), 14.5-22.8 km/sec (Uranus), and 16.3-25.3 km/sec (Neptune).

The above results have described the 1977 Grand Tour opportunity. Similar data is presented for the 1978 Grand Tour in Figure 2.10 to 2.14.

2.5 Trajectory Selections

The constraint conditions discussed previously are first applied to select trajectories for the 1977 launch opportunity. Figure 2.15 shows the constraint regions of the surface and Rings of Saturn projected onto the basic trajectory selection grid of Jupiter arrival date versus

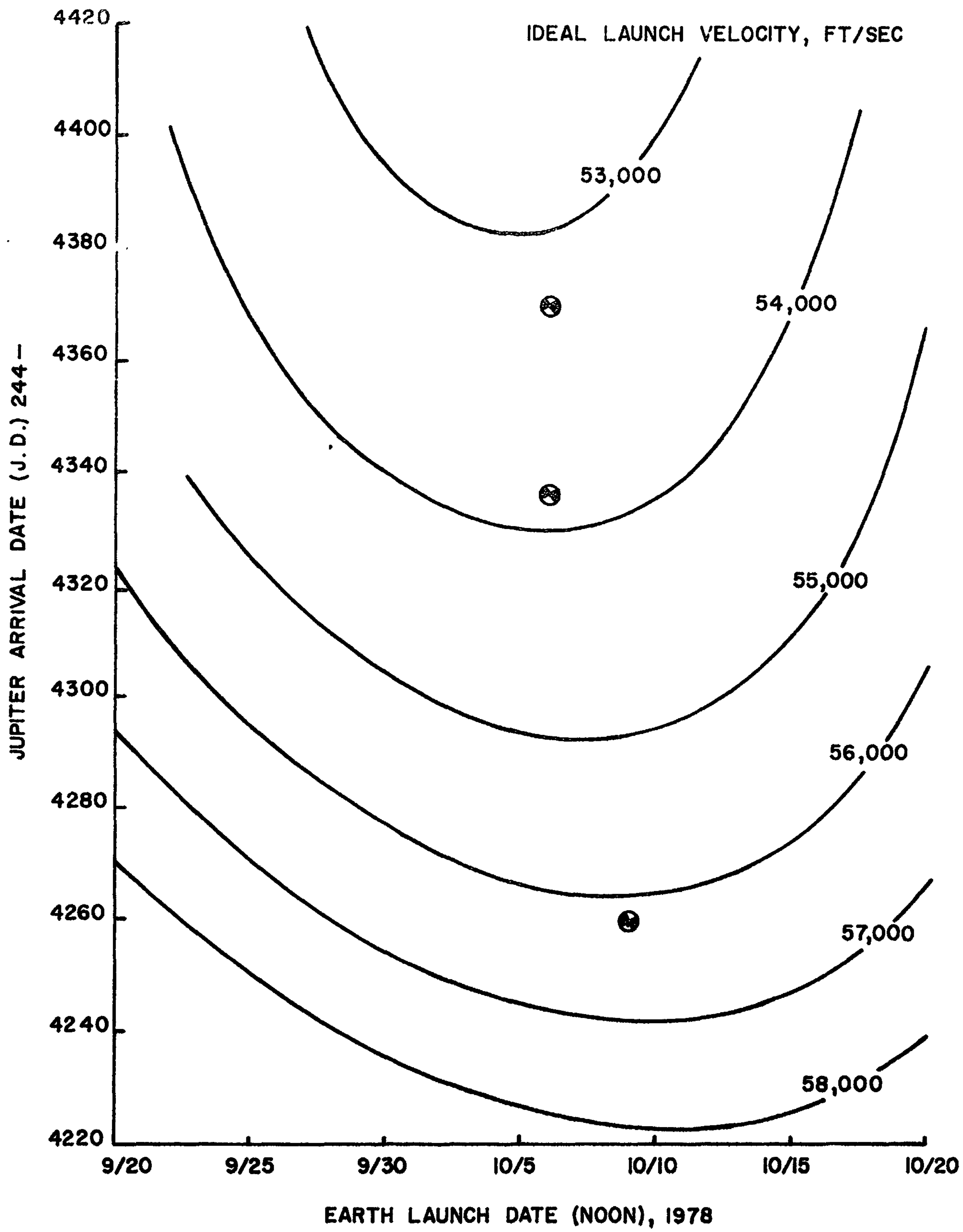

FIGURE 2.10 TRAJECTORY SELECTION GRAPH, 1978 GRAND TOUR

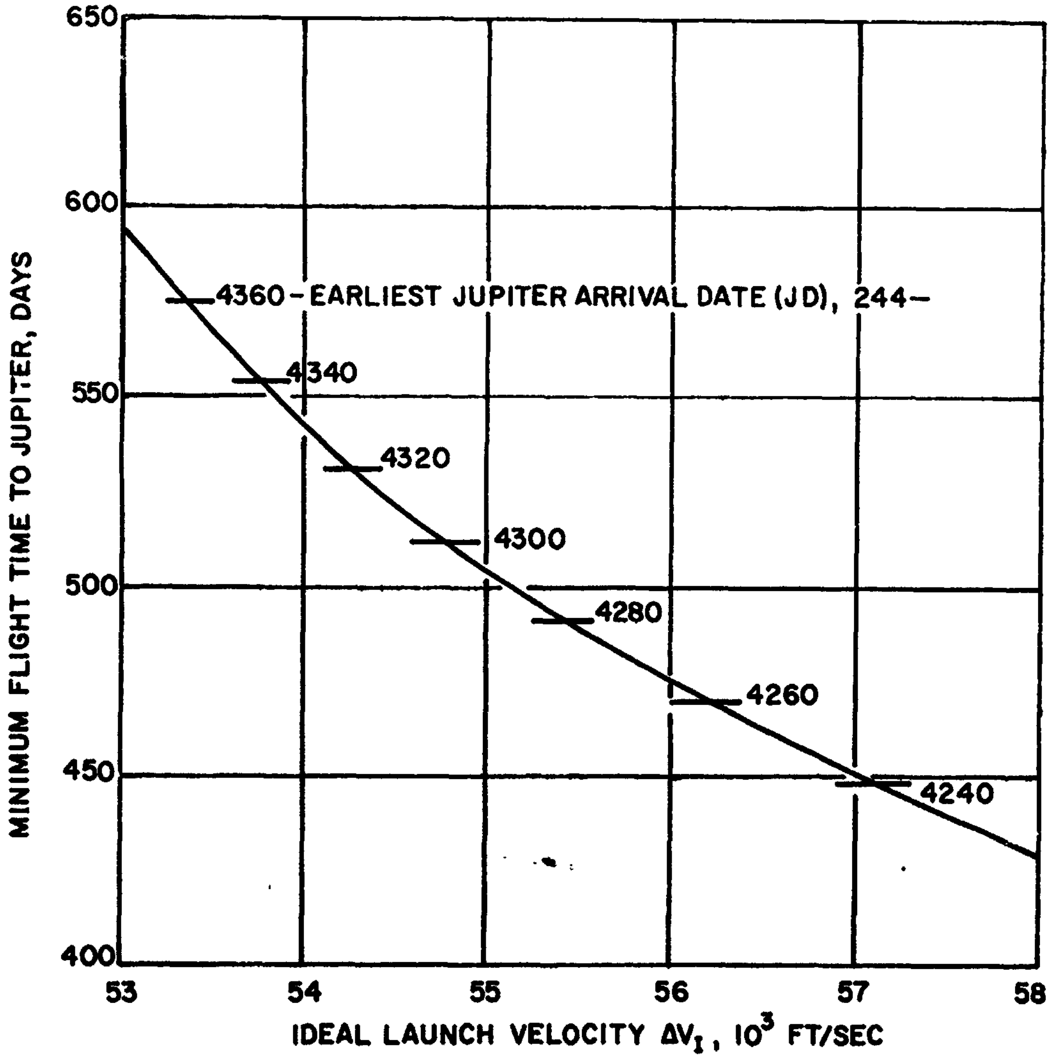

FIGURE 2.11. MINIMUM FLIGHT TIME TO JUPITER, 1978 GRAND TOUR

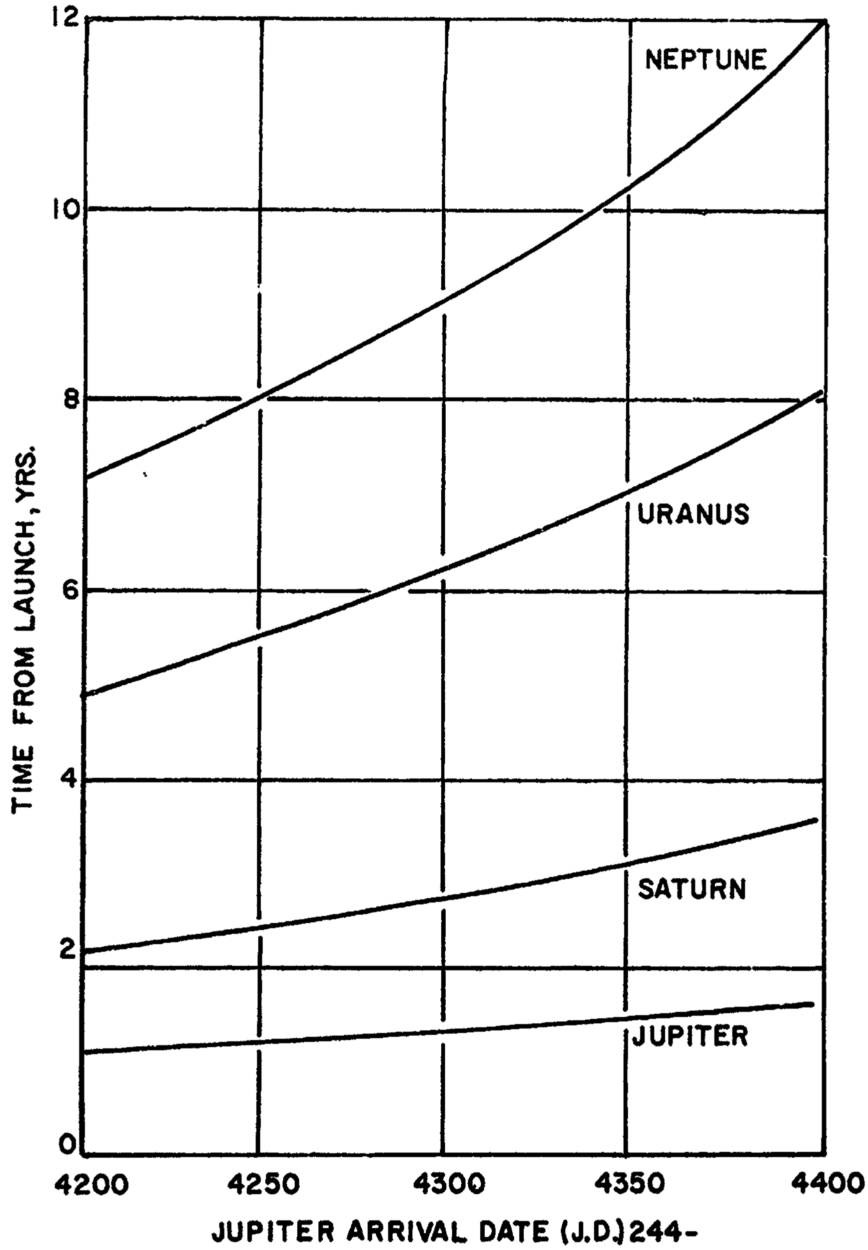

FIGURE 2.12. PLANET ARRIVAL TIMES, 1978 GRAND TOUR

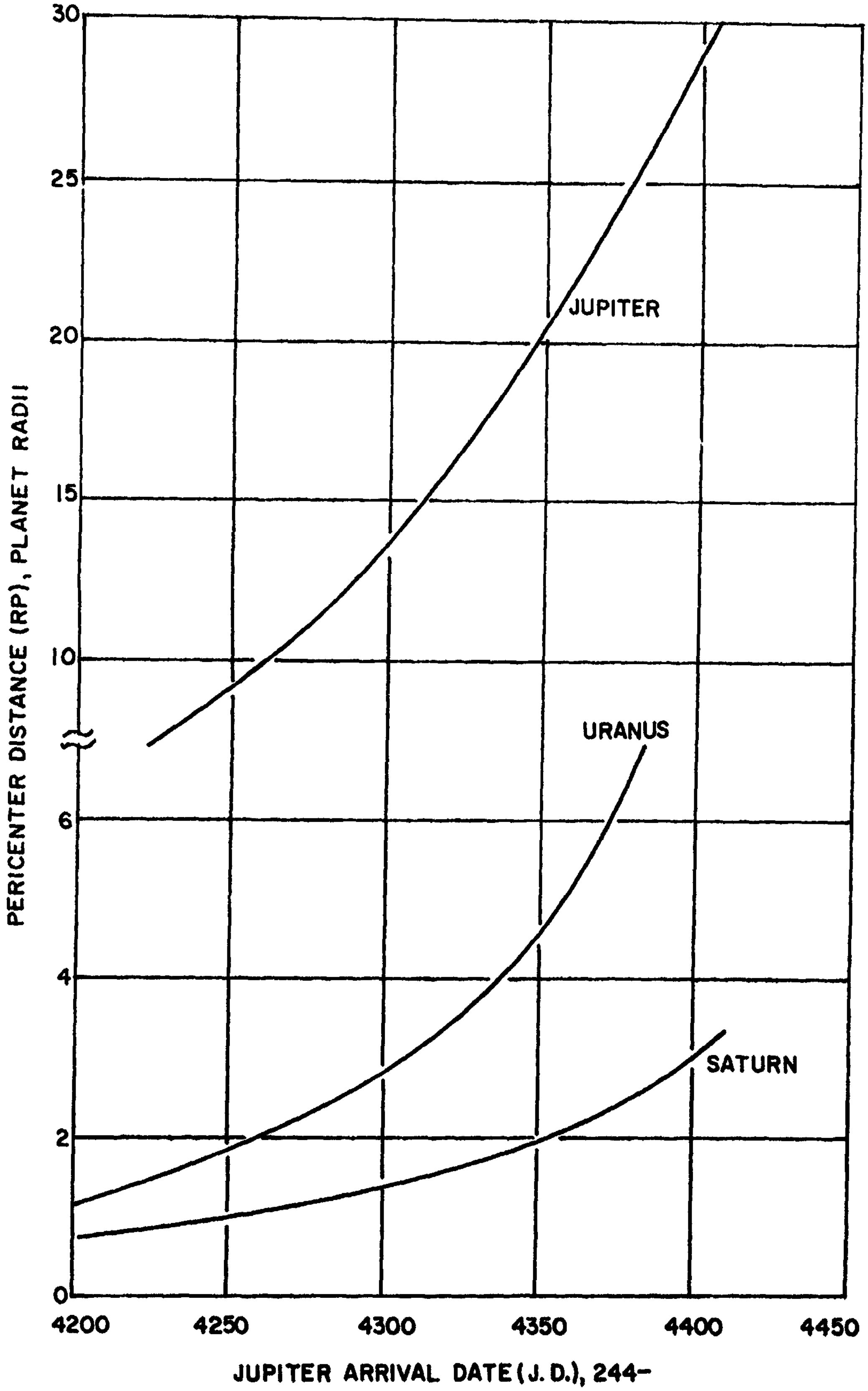

FIGURE 2.13. PLANET CLOSEST APPROACH DISTANCES, 1978 GRAND TOUR.

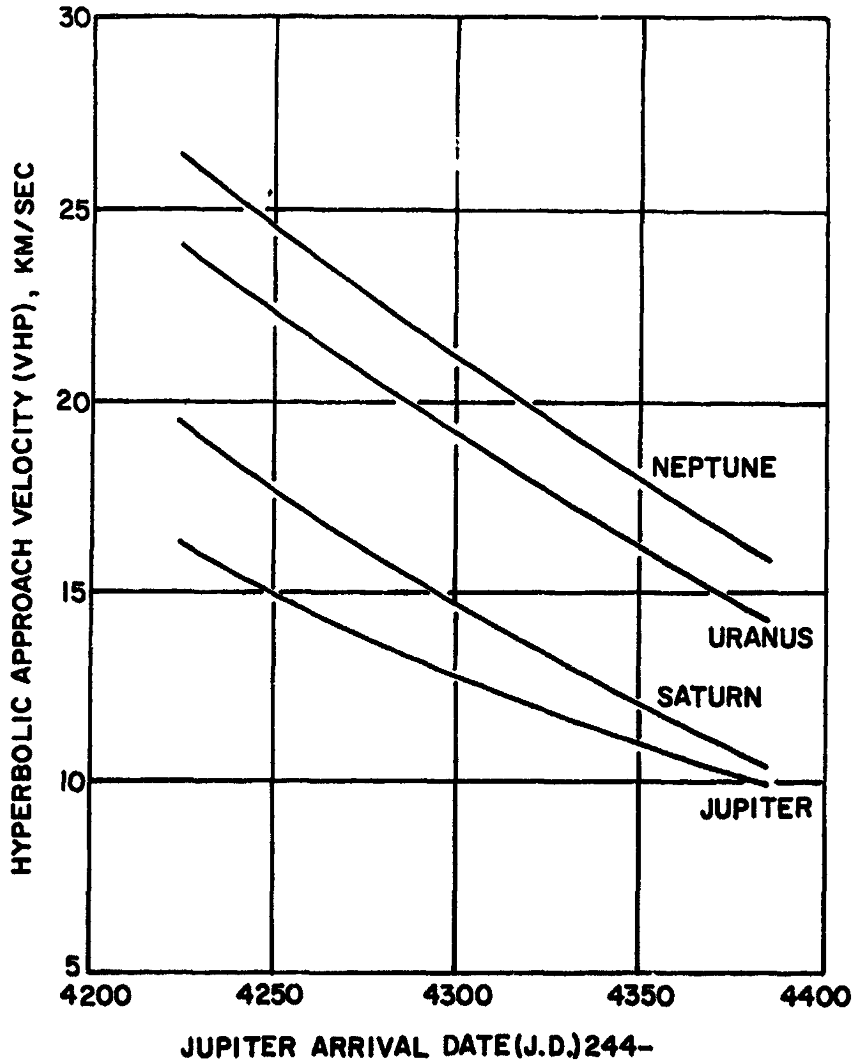

FIGURE 2.14. PLANET ARRIVAL VELOCITY, 1978 GRAND TOUR

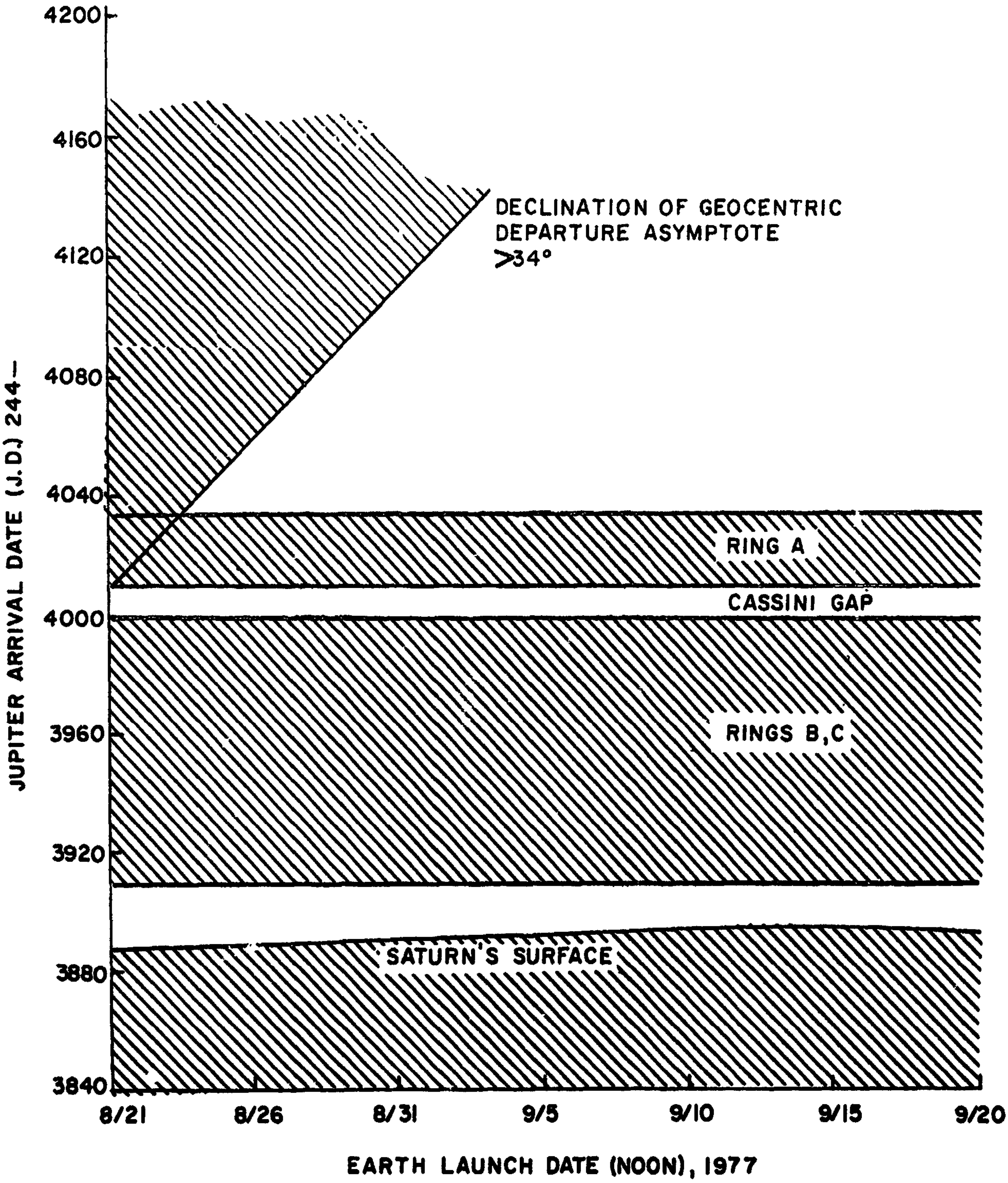

FIGURE 2.15 SATURN'S RINGS AND SURFACE CONSTRAINTS, 1977 GRAND TOUR

Earth launch date. Also shown is the constraint region corresponding to launch declinations greater than 34°. Saturn's surface is the governing "hard" constraint of Grand Tour trajectories in 1977 and 1978. That is, the surface constraint boundary of Jupiter and Uranus lies below that of Saturn. The Cassini Gap between Ring's A and B is about 4000 km wide and offers a potential, but somewhat daring, trajectory selection. Some level of material density below that of the Rings proper is likely to exist in the Cassini Gap.

Figure 2.16 shows the constraint regions imposed by the ± 10 day Earth-planet conjunction bands. In cases where the conjunction bands of two planets overlap, only a single constraint region is shown. For a given planet, the real time difference between successive conjunctions is about one year - approximately the synodic period between Earth and the outer planets. Of course, when projected onto a grid of Jupiter arrival date, this difference contracts for Saturn, Uranus and Neptune. Also, on this grid, the frequency of conjunction is highest for the outermost planet.

Figure 2.17 combines the four constraint conditions and again shows the launch velocity contours. A launch window of about 20 days is thought to be a reasonable requirement for this mission. To minimize the launch velocity spread throughout the window it is desirable that the center

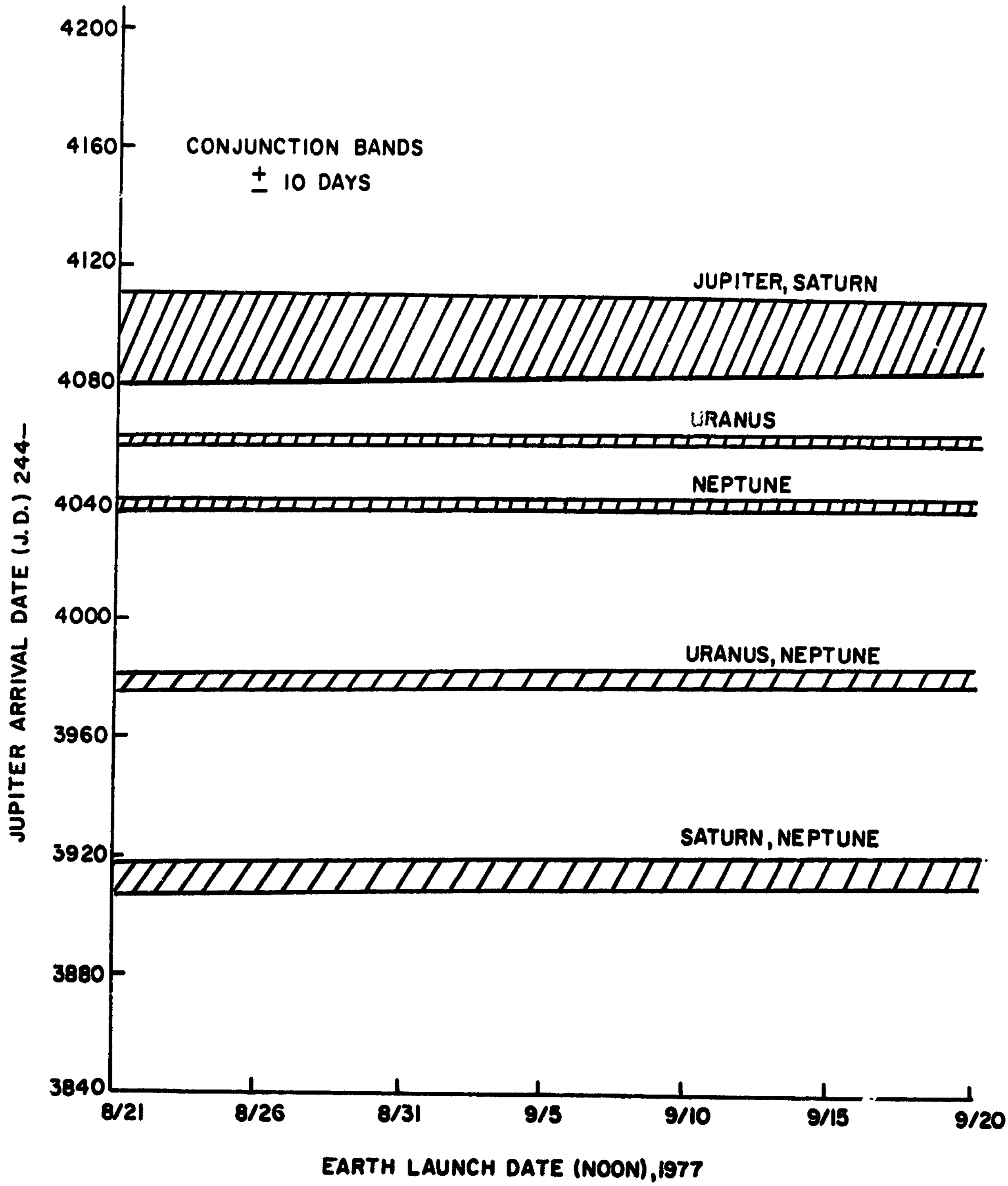

FIGURE 2.16 EARTH-PLANET CONJUNCTION CONSTRAINTS, 1977 GRAND TOUR

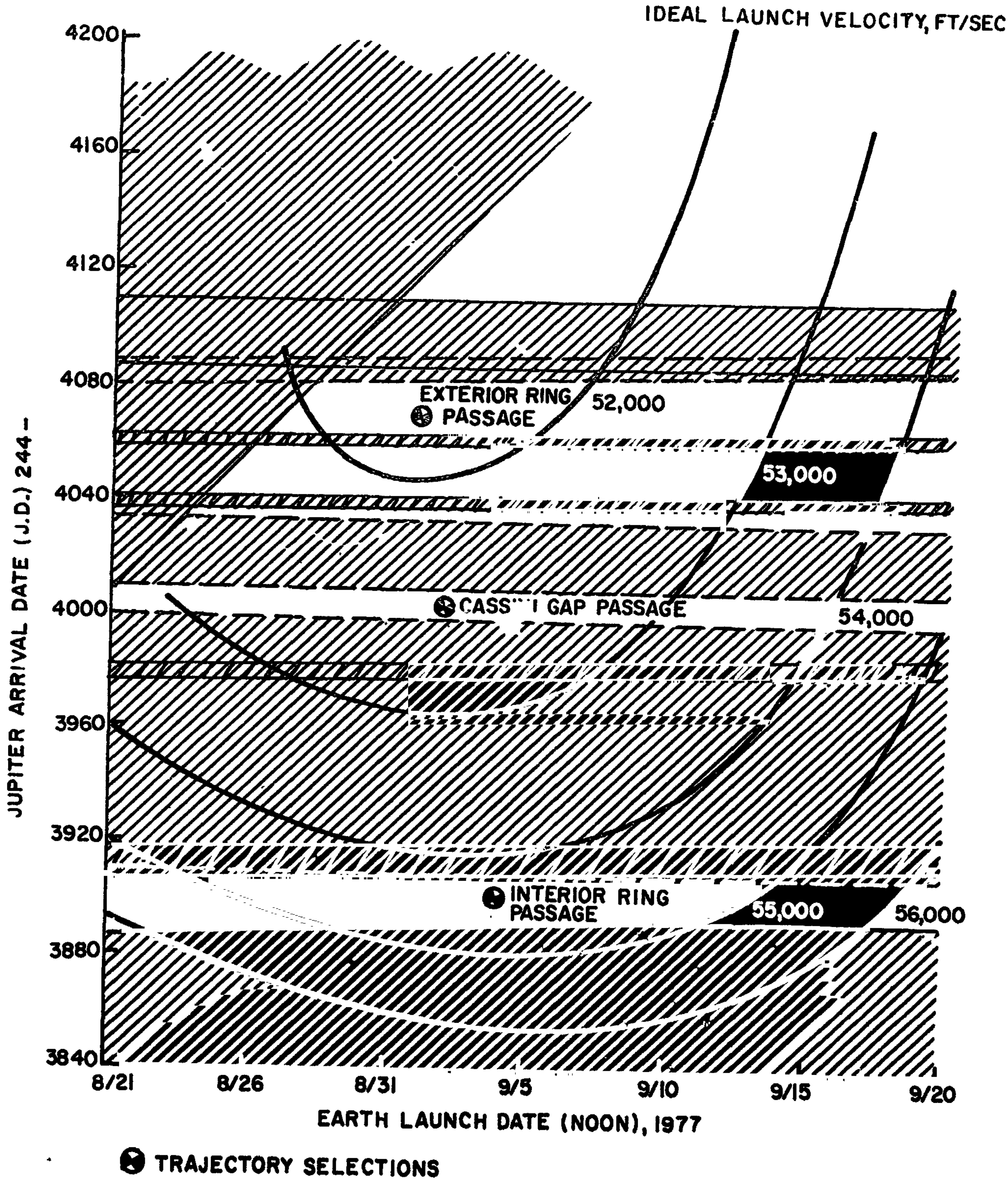

FIGURE 2.17 TRAJECTORY SELECTION GRAPH, 1977 GRAND TOUR

of the window lie near the optimum launch date. Clearly, then, the constraint regions leave little room for selecting trajectories. Two types of trajectories are selected and designated by their principal characteristics:

(1) Exterior Ring Passage - a trajectory passing through the Saturn Ring plane at a distance above the outer Ring boundary.

(2) Interior Ring Passage - a trajectory passing through the Saturn Ring plane at a distance between the surface and the inner Ring Boundary.

A third trajectory selection passing through the Cassini Gap in the Rings is also indicated on the graph. However, because of the unknown material density in the Gap this trajectory could be risky. Since data for this trajectory would be bounded by the other two trajectory types, the Cassini Gap passage will not be considered further in this report.

On the question of Ring density, there is certain to be found some particulate matter outside of the visible boundaries of the Rings. For this reason it is best to choose an Exterior trajectory sufficiently above the visible boundary of Ring A. The trajectory selection shown in Figure 2.17 passes about 20,000 km outside of this boundary.

There remains the task of selecting the Neptune encounter conditions. The selection is made on the basis of the 3 σ guidance error dispersion ellipse such that Earth occultation is obtained but not Canopus occultation. From the guidance analysis, it is estimated that 3 $\sigma_{B \cdot T}$ x 3 $\sigma_{B \cdot R}$ is 45,000 x 39,000 km for the Exterior Ring Passage and 38,000 x 36,000 km for the Interior Ring Passage. Figures 2.18 and 2.19 illustrate the nominal aim point selection for these two trajectories. The selection graphs show the occultation zones of the Earth, Sun and Canopus plotted in target plane coordinates. The occultation boundary (from the exact moment of occultation) has been specified as 0°, 5°, and 20° respectively, for the Earth, Sun and Canopus.

Figures 2.20 to 2.24 illustrate the selection process for the 1978 launch opportunity. Descriptive parameters of the four trajectory selections (1977-E, 1977-I, 1978-E, 1978-I) are listed in Table 2.2. Interior Ring Passages are characterized by faster trip times and closer flyby distances, but require higher launch velocities than the Exterior Ring Passages and also have higher approach velocities. Launches in 1978 allow somewhat shorter trips at the expense of higher launch velocities, but pass Jupiter at much greater distances than do trajectories in 1977. The implication of these comparative characteristics will be more fully discussed in the later sections on guidance, scientific payload selection, and mission requirements.

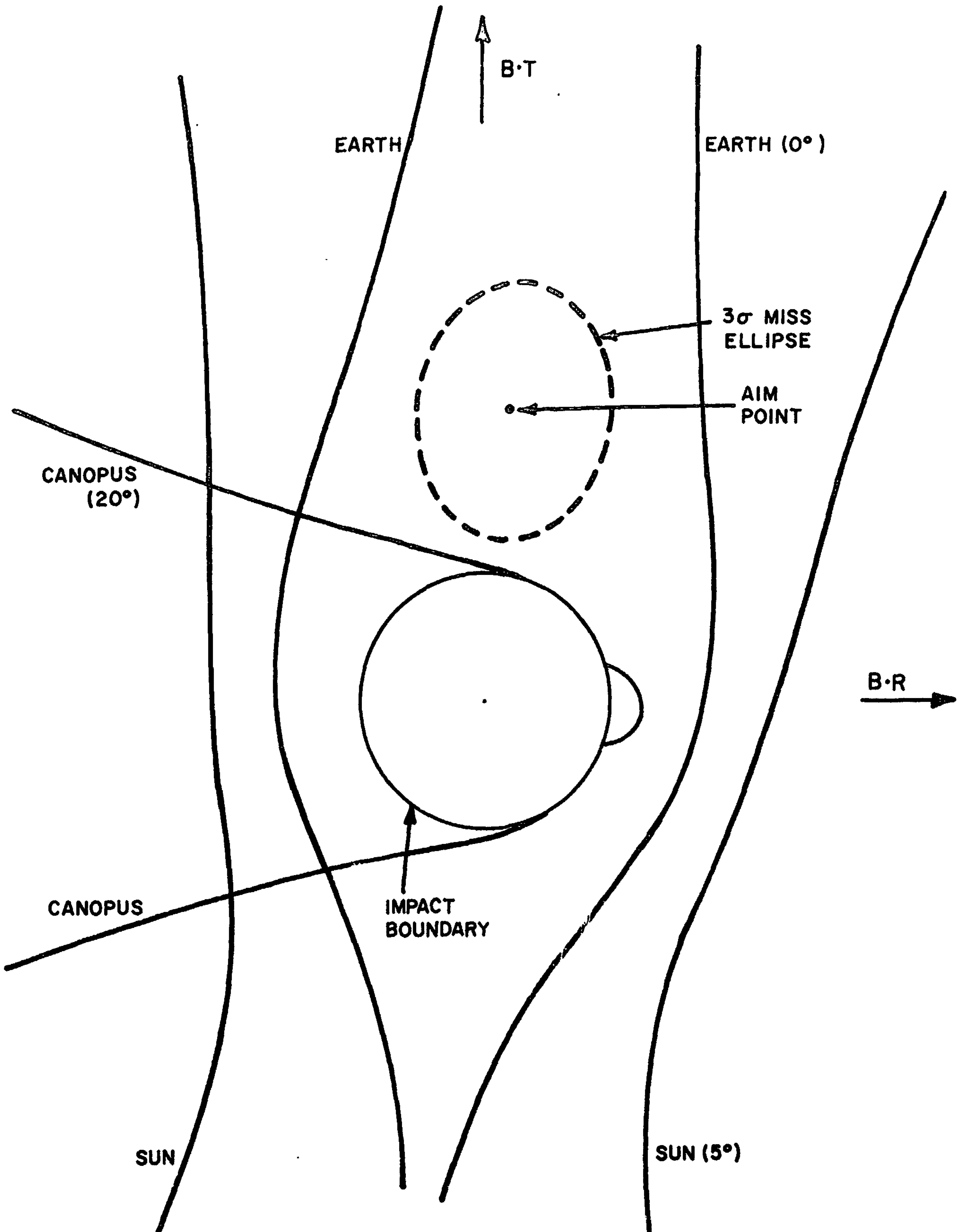

FIGURE 2.18. OCCULTATION ZONES AND TRAJECTORY SELECTION FOR NEPTUNE ENCOUNTER, 1977-E GRAND TOUR

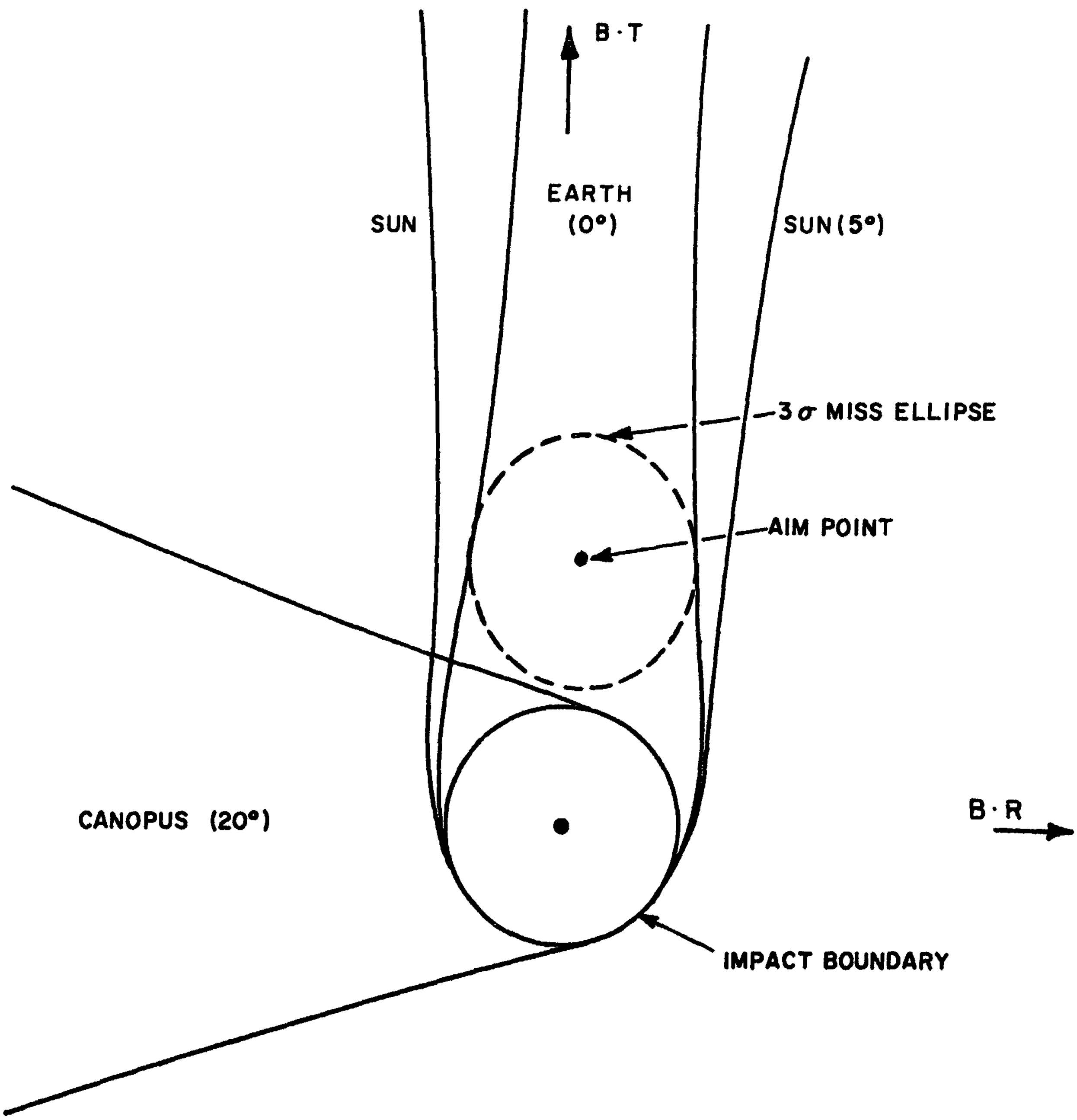

FIGURE 2.19 OCCULTATION ZONES AND TRAJECTORY SELECTION FOR NEPTUNE ENCOUNTER, 1977-I GRAND TOUR.

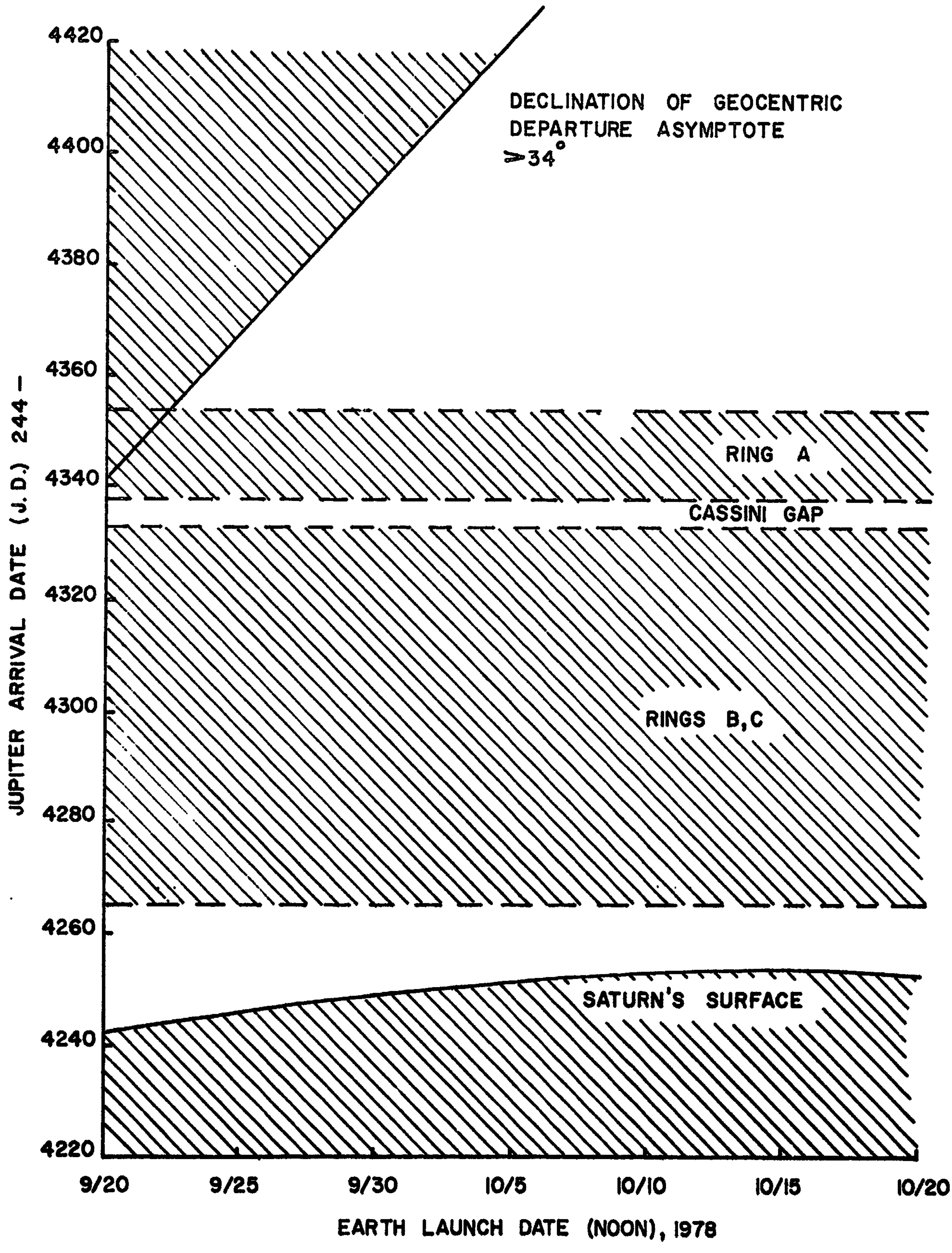

FIGURE 2.20 SATURN'S RINGS AND SURFACE CONSTRAINTS, 1978 GRAND TOUR

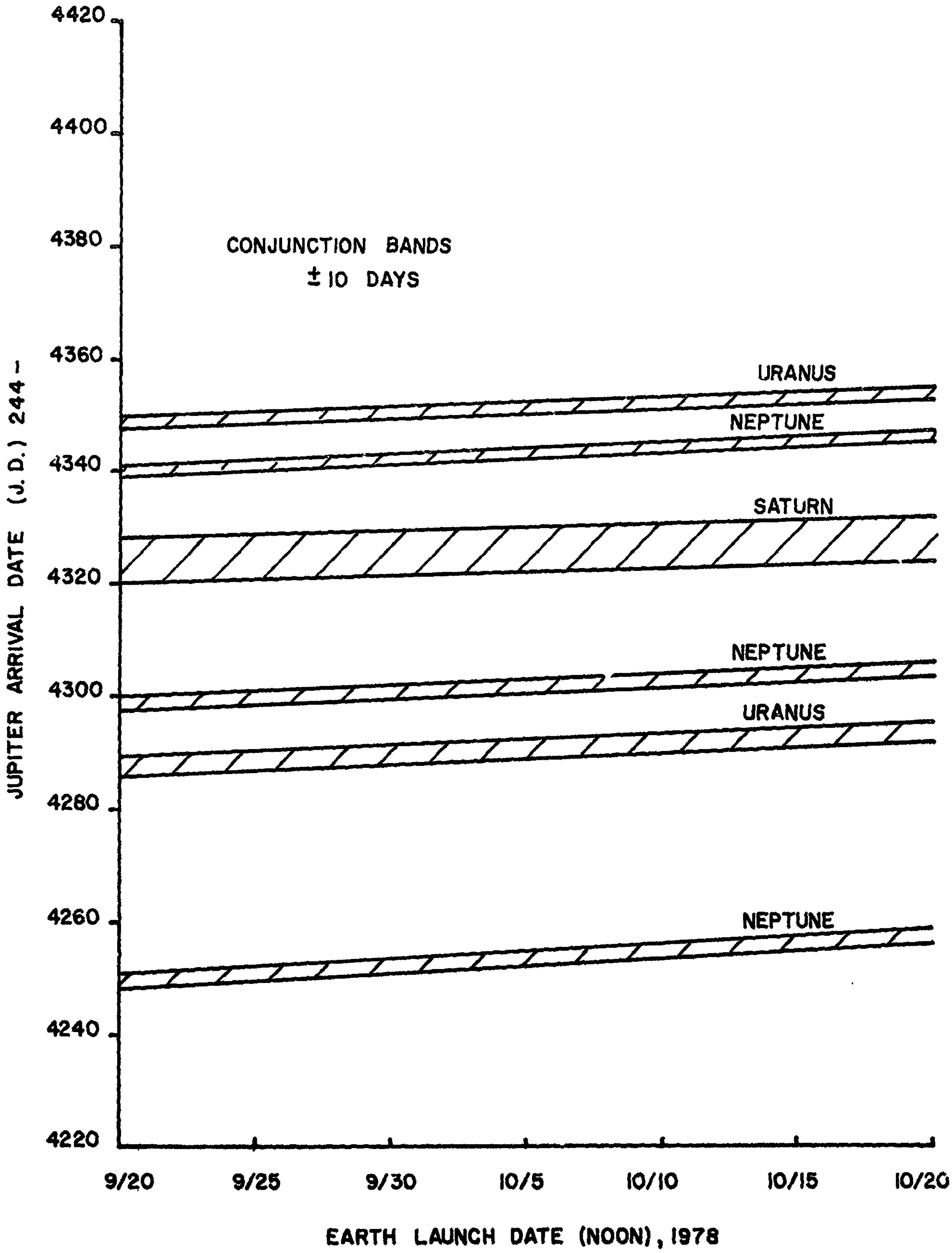

FIGURE 2.21 EARTH-PLANET CONJUNCTION CONSTRAINTS, 1978 GRAND TOUR

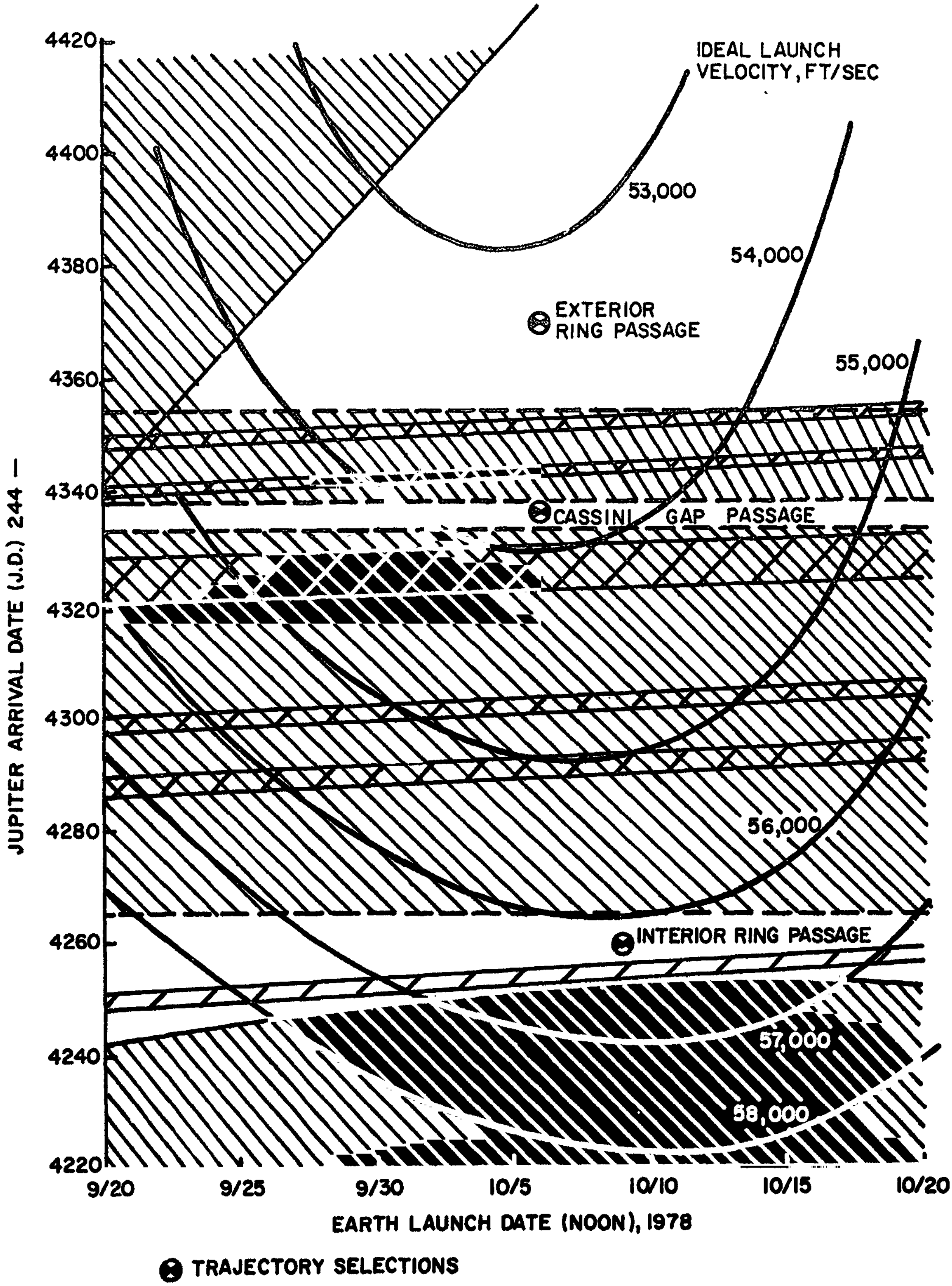

FIGURE 2.22. TRAJECTORY SELECTION GRAPH, 1978 GRAND TOUR

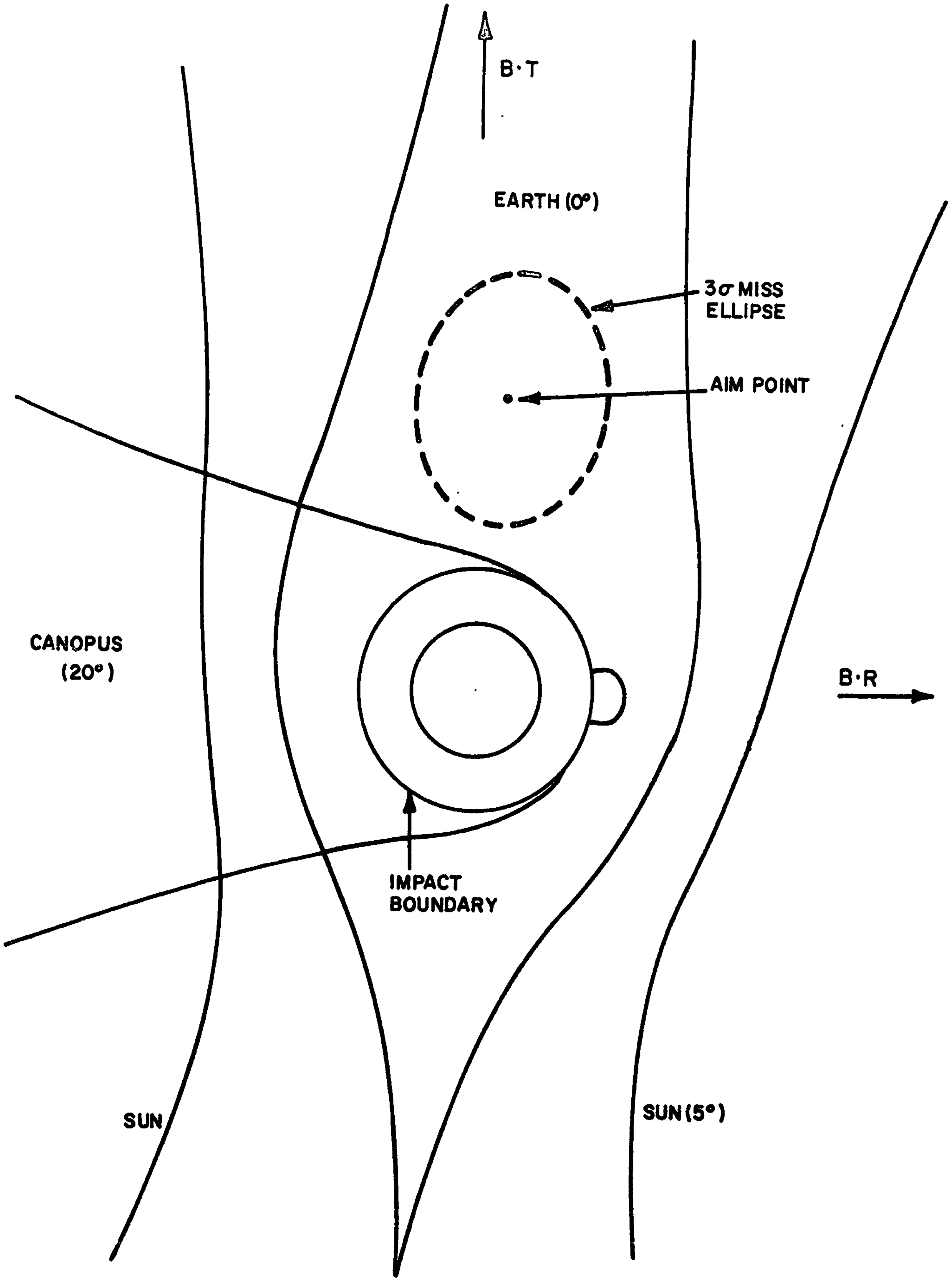

FIGURE 2.23. OCCULTATION ZONES AND TRAJECTORY SELECTION FOR NEPTUNE ENCOUNTER, 1978-E GRAND TOUR.

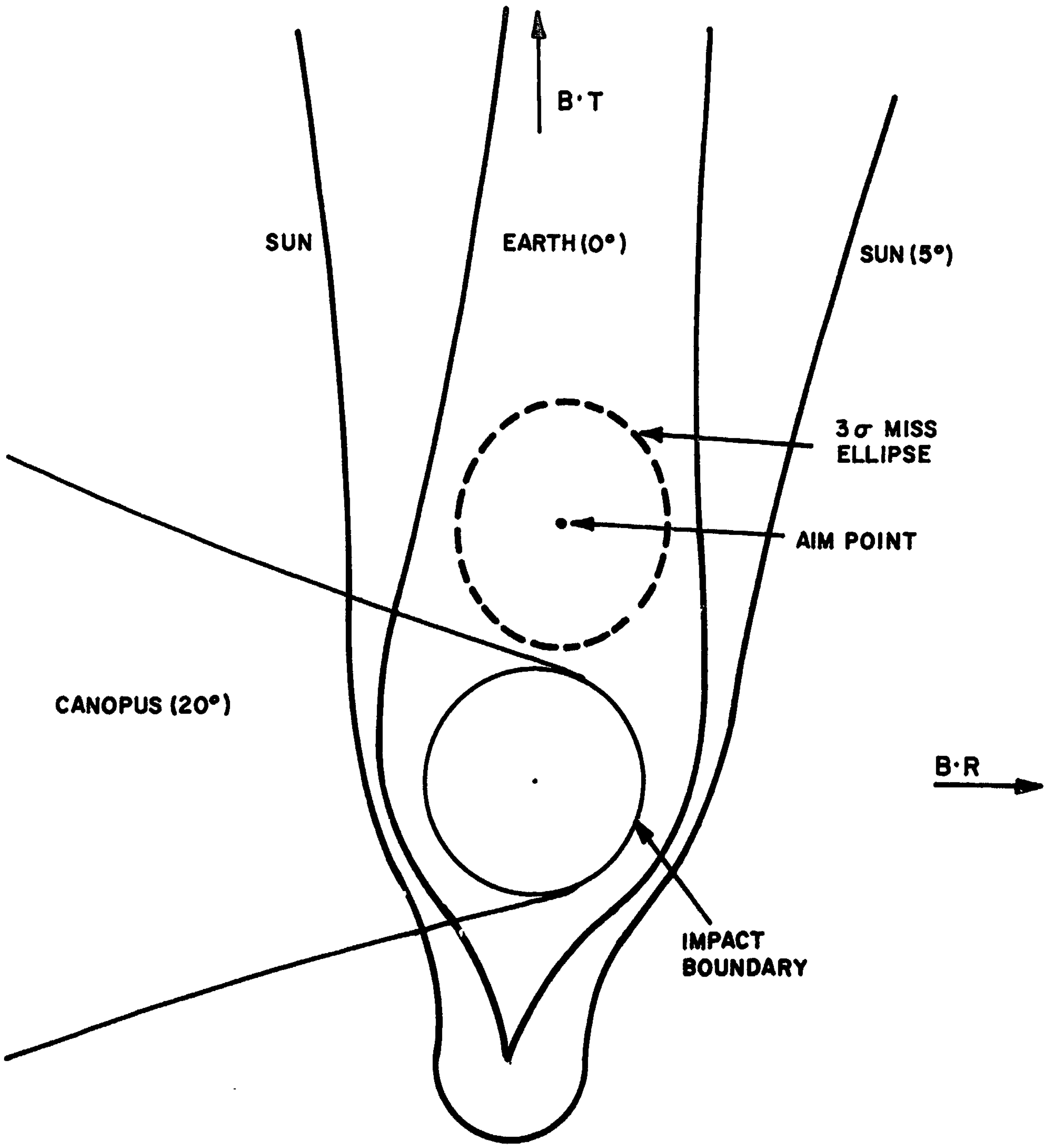

FIGURE 2.24. OCCULTATION ZONES AND TRAJECTORY SELECTION FOR NEPTUNE ENCOUNTER, 1978-I GRAND TOUR.

TABLE 2.2 GRAND TOUR TRAJECTORY SELECTIONS

Trajectory Parameters	Units	1977 Grand Tours: Exterior Ring Passage 1977 - E	1977 Grand Tours: Interior Ring Passage 1977 - I	1978 Grand Tours: Exterior Ring Passage 1978 - E	1978 Grand Tours: Interior Ring Passage 1978 - I
Earth Departure					
Launch Date	¢ Window	Sept. 1, 1977	Sept. 4, 1977	Oct. 6, 1978	Oct. 9, 1978
Ideal Launch Velocity	ft/sec	51,900	54,400	53,200	56,200
Jupiter Encounter					
Flight Time	Days	682	511	582	469
Hyperbolic Velocity	km/sec	7.81	12.16	10.45	14.46
Pericenter Distance	Radii	10.62	4.00	23.55	9.95
Turning Angle	Degree	94.17	97.22	48.27	54.87
Saturn Encounter					
Flight Time	Years	3.98	2.98	3.36	2.53
Hyperbolic Velocity	km/sec	10.69	16.69	11.02	17.02
Pericenter Distance	Radii	2.58	1.056	2.32	1.055
Turning Angle	Degree	85.67	85.76	87.18	84.49
Uranus Encounter					
Flight Time	Years	8.40	6.37	7.53	5.71
Hyperbolic Velocity	km/sec	14.74	21.22	15.08	21.61
Pericenter Distance	Radii	5.58	1.80	5.85	1.98
Turning Angle	Degree	18.56	25.85	17.17	23.20
Neptune Encounter					
Flight Time	Years	11.94	9.05	11.00	8.32
Hyperbolic Velocity	km/sec	16.54	23.58	16.82	23.89
Pericenter Distance	Radii	3.43	2.93	3.43	2.93
Turning Angle	Degree	27.34	17.56	25.91	16.59

Table 2.2

GRAND TOUR TRAJECTORY SELECTIONS (Continued)

Trajectory Parameters		1977 Grand Tours		1978 Grand Tours	
		Exterior Ring Passage 1977-E	Interior Ring Passage 1977-I	Exterior Ring Passage 1978-E	Interior Ring Passage 1978-I
Jupiter Encounter					
Sun Occultation	(5°)	13.3 hrs	2.9 hrs	120.2 hrs	13.6 hrs
Earth Occultation	(0°)	3.9	1.9	6.8	5.0
Canopus Occultation	(20°)	0	0	0	0
Saturn Encounter					
Sun Occultation		2.1	1.1	2.1	1.2
Earth Occultation		1.6	1.0	1.8	1.1
Canopus Occultation		0	0	0	0
Uranus Encounter					
Sun Occultation		3.1	1.1	3.1	1.2
Earth Occultation		0.1	0.9	0	0.8
Canopus Occultation		0	0	0	0
Neptune Encounter					
Sun Occultation		1.7	0.8	1.8	1.3
Earth Occultation		1.0	0.6	1.0	0.9
Canopus Occultation		0	0	0	0

It is of interest to know the variation of trajectory parameters throughout the 20 day launch window. Figures 2.25 and 2.26 show the launch window energy requirements for the 1977 and 1978 Grand Tour. It has been found that planet encounter parameters vary little over the window. This is shown, for example, by Table 2.3 which lists several key parameters of the 1977-E trajectory.

2.6 Planet Encounter Profiles

Several fixed parameters of the planet encounter trajectories have been given in Table 2.2. Since the Grand Tour mission is planet oriented, the time history of certain variables of motion during the encounter phase is of general interest, and is also necessary to the proper selection of scientific payloads. In this section, the dynamical profiles of each planet encounter are illustrated for the 1977-E and 1977-I trajectories.

Profile data was obtained from a computer program (PROFYL) developed for this study. The PROFYL output is of two kinds:

(1) A summary table of the occultations of the Earth, Sun and Canopus, and the crossing of the sub-satellite point over the Sun terminator line. Associated with each of these points is the time and radius of occurrence.

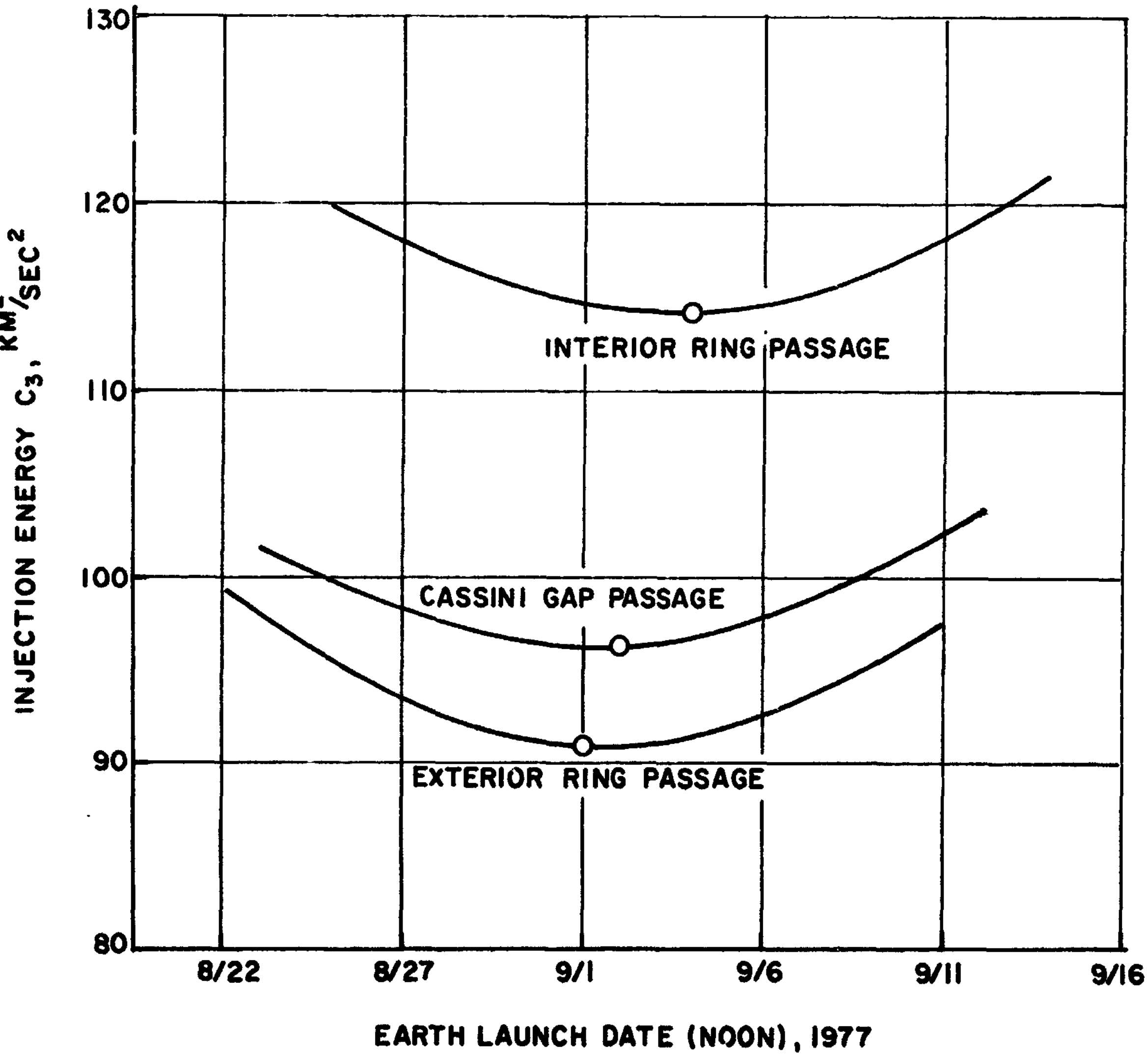

FIGURE 2.25 LAUNCH WINDOW ENERGY REQUIREMENTS, 1977 GRAND TOUR

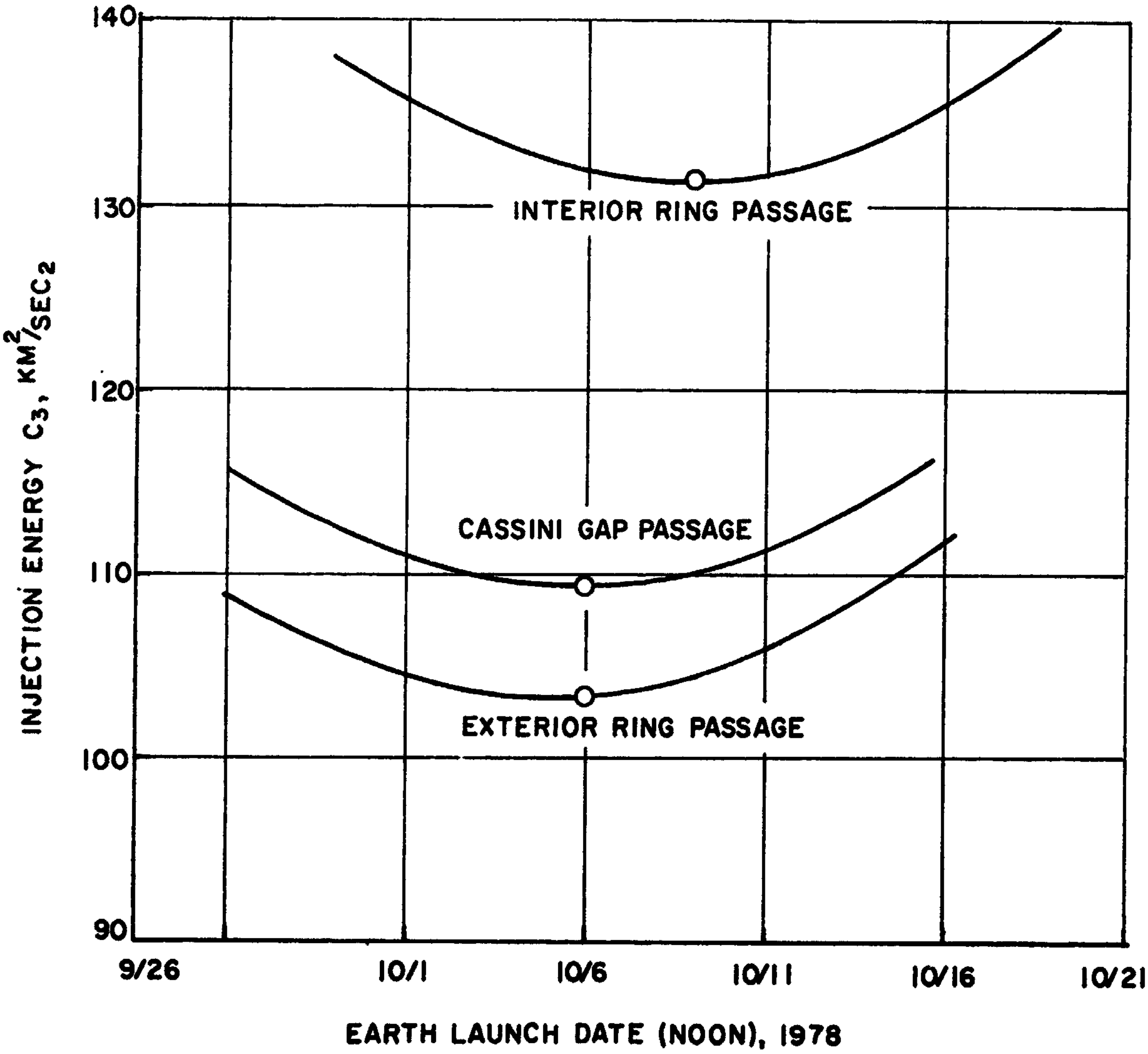

FIGURE 2.26 LAUNCH WINDOW ENERGY REQUIREMENTS, 1978 GRAND TOUR

Table 2.3 PARAMETER VARIABLE ACROSS LAUNCH WINDOW

1977 Exterior Ring Passage

Jupiter Arrival Date = July 15 1979

Trajectory Parameters	Units	Launch Date (Noon)				
		8/22	8/27	9/1	9/6	9/11
Earth Departure						
Ideal Launch Velocity	ft/sec	52,800	52,100	51,900	52,000	52,500
Asymptote Declination	deg	38.0	33.5	30.5	28.2	26.3
Jupiter Encounter						
Flight Time	days	692	687	682	677	672
Hyperbolic Velocity	km/sec	7.79	7.80	7.81	7.83	7.85
Pericenter Distance	radii	10.50	10.60	10.62	10.61	10.58
Saturn Encounter						
Fight Time	years	4.01	4.00	3.98	3.97	3.96
Hyperbolic Velocity	km/sec	10.66	10.67	10.69	10.72	10.74
Pericenter Distance	radii	2.60	2.59	2.58	2.57	2.56
Uranus Encounter						
Flight Time	years	8.45	8.41	8.40	8.38	8.35
Hyperbolic Velocity	km/sec	14.71	14.72	14.74	14.77	14.80
Pericenter	radii	5.62	5.60	5.58	5.55	5.51
Neptune Encounter						
Flight Time	years	12.00	11.98	11.94	11.90	11.87
Hyperbolic Velocity	km/sec	16.50	16.51	16.54	16.57	16.60
Pericenter Distance	radii	3.43	3.43	3.43	3.43	3.43

(2) Position dependent data of selected dynamic variables such as time-to-periapse, altitude, ground speed, etc. True anomaly is used as the independent position variable because of its relative uniformity over different planet encounters.

Graphical presentation of the profile data is given in Figure 2.27 to 2.39 for the 1977-E mission, and in Figures 2.40 to 2.52 for the 1977-I mission. The type of information displayed is as follows:

(1) Pictorial trajectory in plane of motion

(2) Time-to-periapse versus true anomaly

(3) Altitude versus true anomaly

(4) Sun elevation versus true anomaly

(5) Scan rate versus true anomaly

(6) Percent of "visible" hemispheric surface versus true anomaly

(7) Ground trace (latitude, longitude) of sub-satellite point.

Sun elevation refers to the angle of the Sun above the local horizontal at the subsatellite point. Scan rate is the ground speed of the spacecraft with respect to the planet's surface, and hence, includes a component of the planet's rotational velocity. The equator of the planet is the reference plane for the ground trace plots. Here, longitude is a relative coordinate since the zero longitude line is arbitrarily defined at initiation of the PROFYL data sequence.

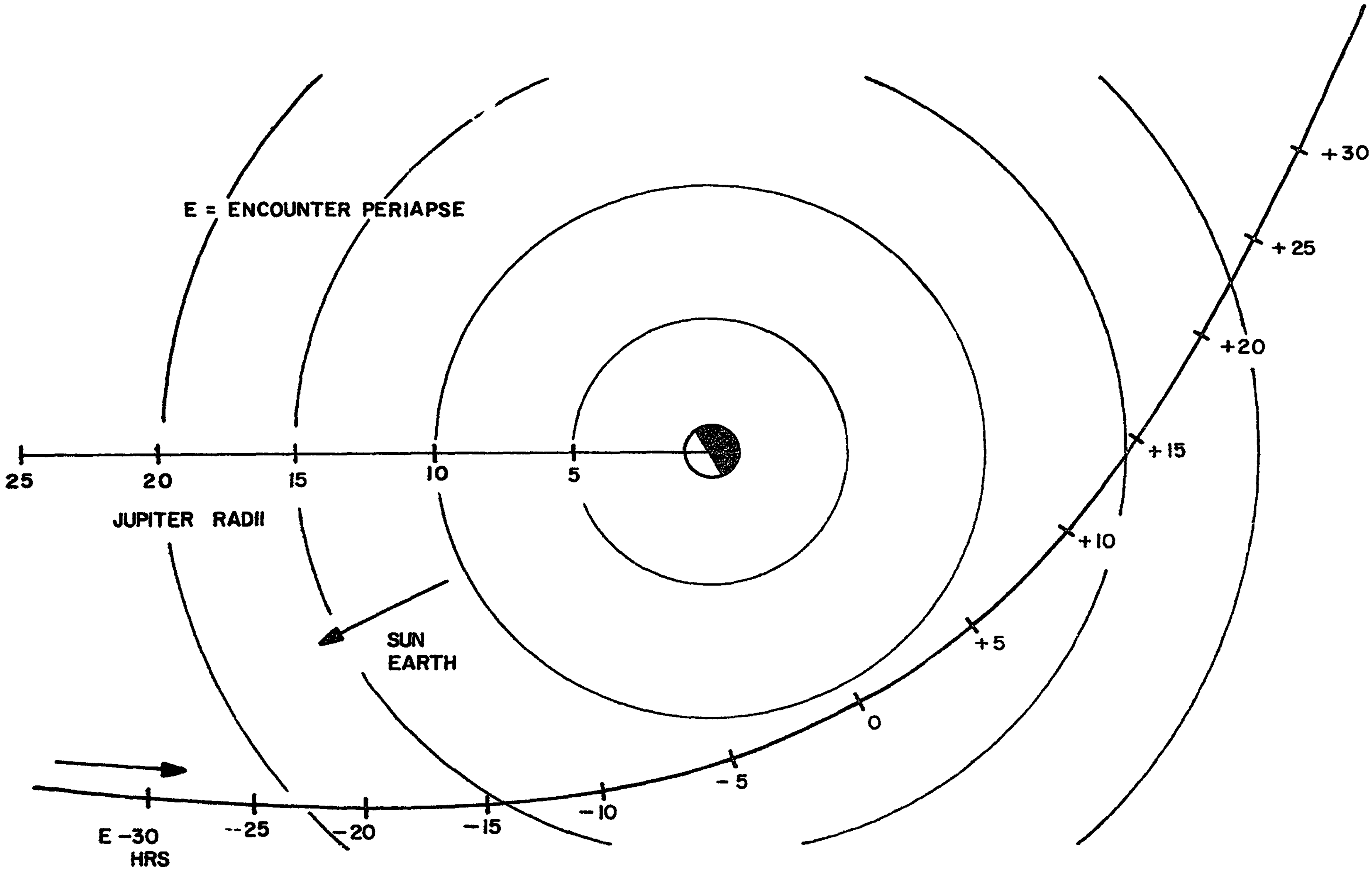

FIGURE 2.27 JUPITER ENCOUNTER TRAJECTORY, 1977-E GRAND TOUR

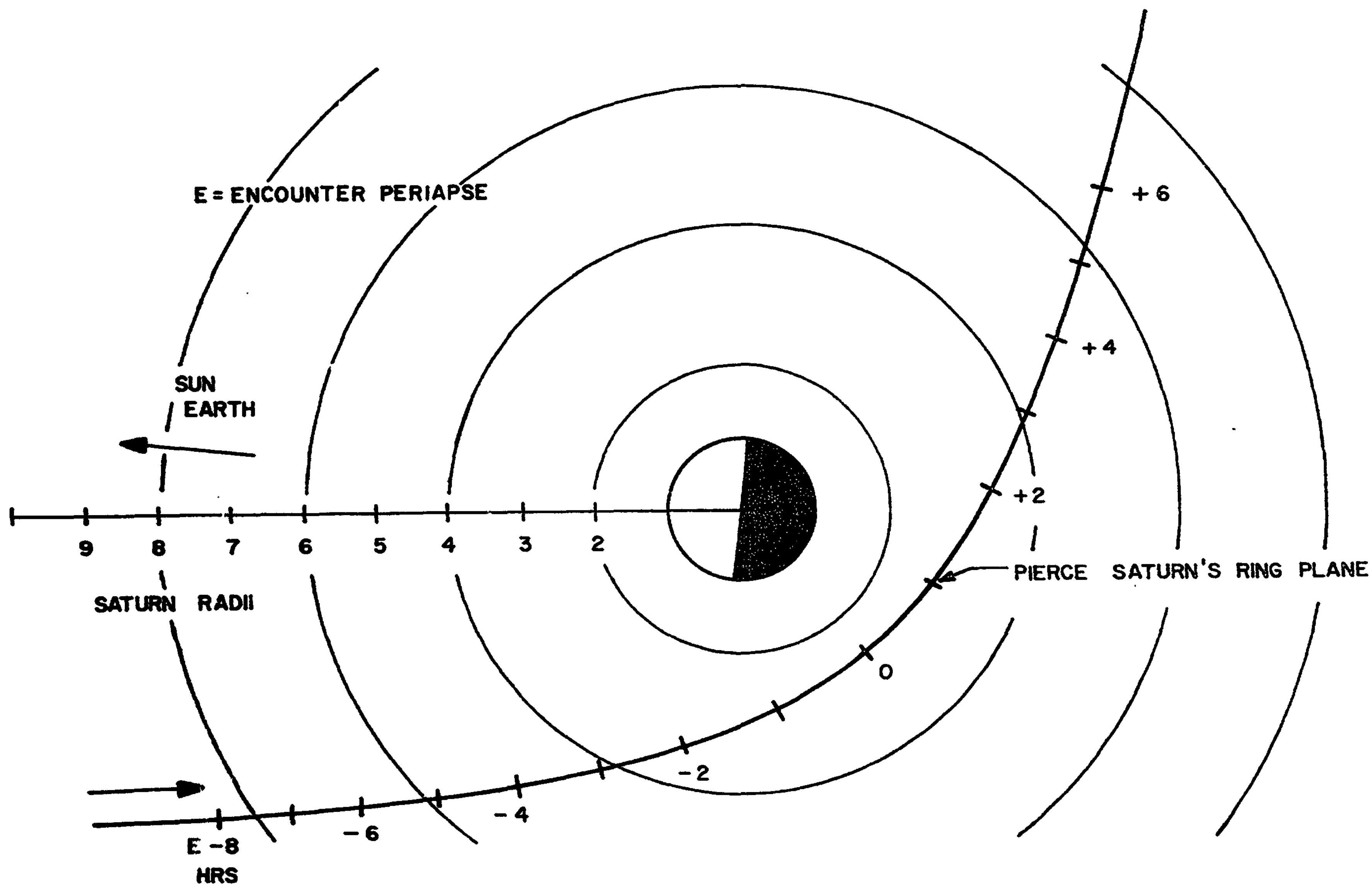

FIGURE 2.28 SATURN ENCOUNTER TRAJECTORY, 1977-E GRAND TOUR

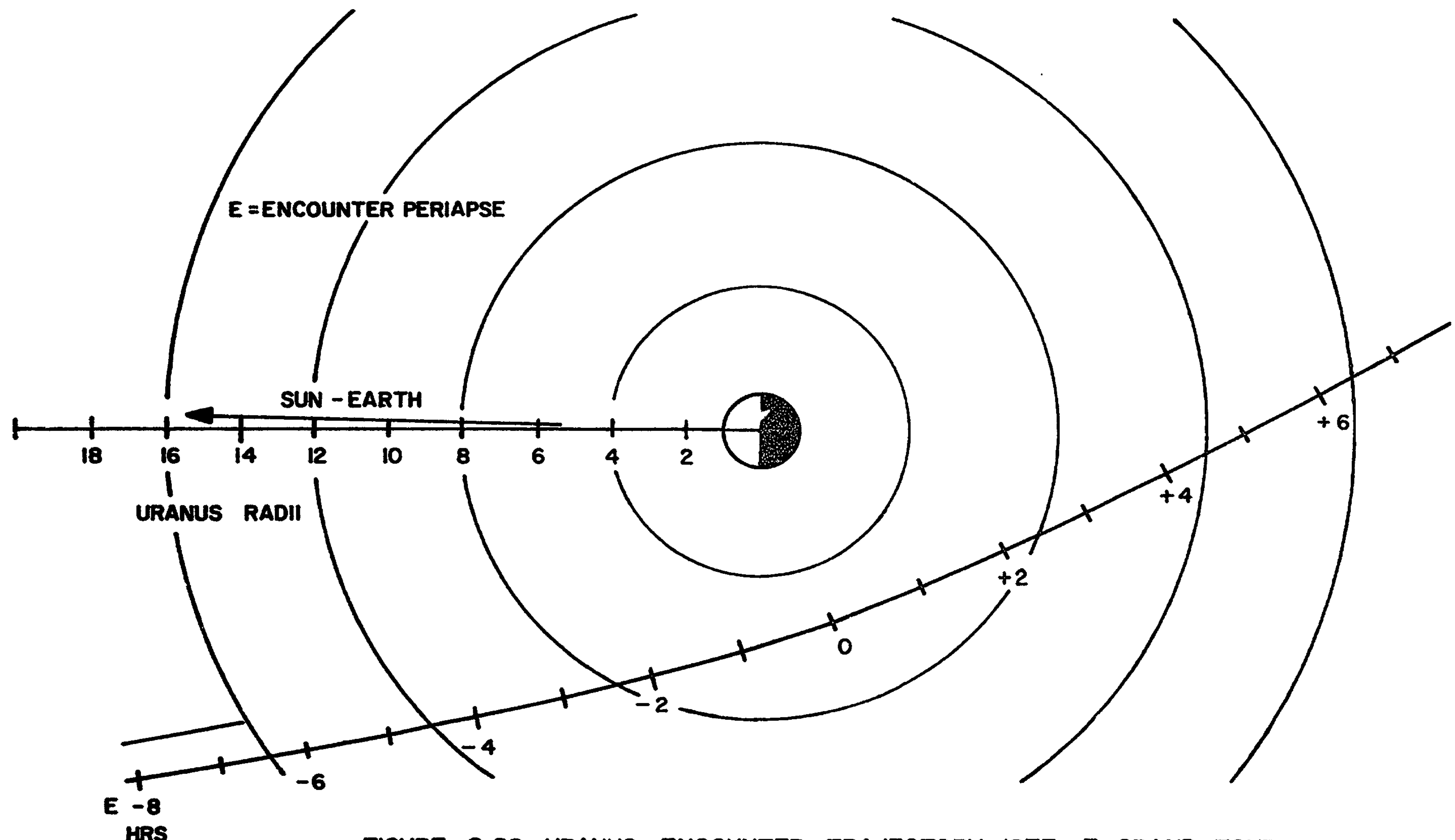

FIGURE 2.29 URANUS ENCOUNTER TRAJECTORY 1977-E GRAND TOUR

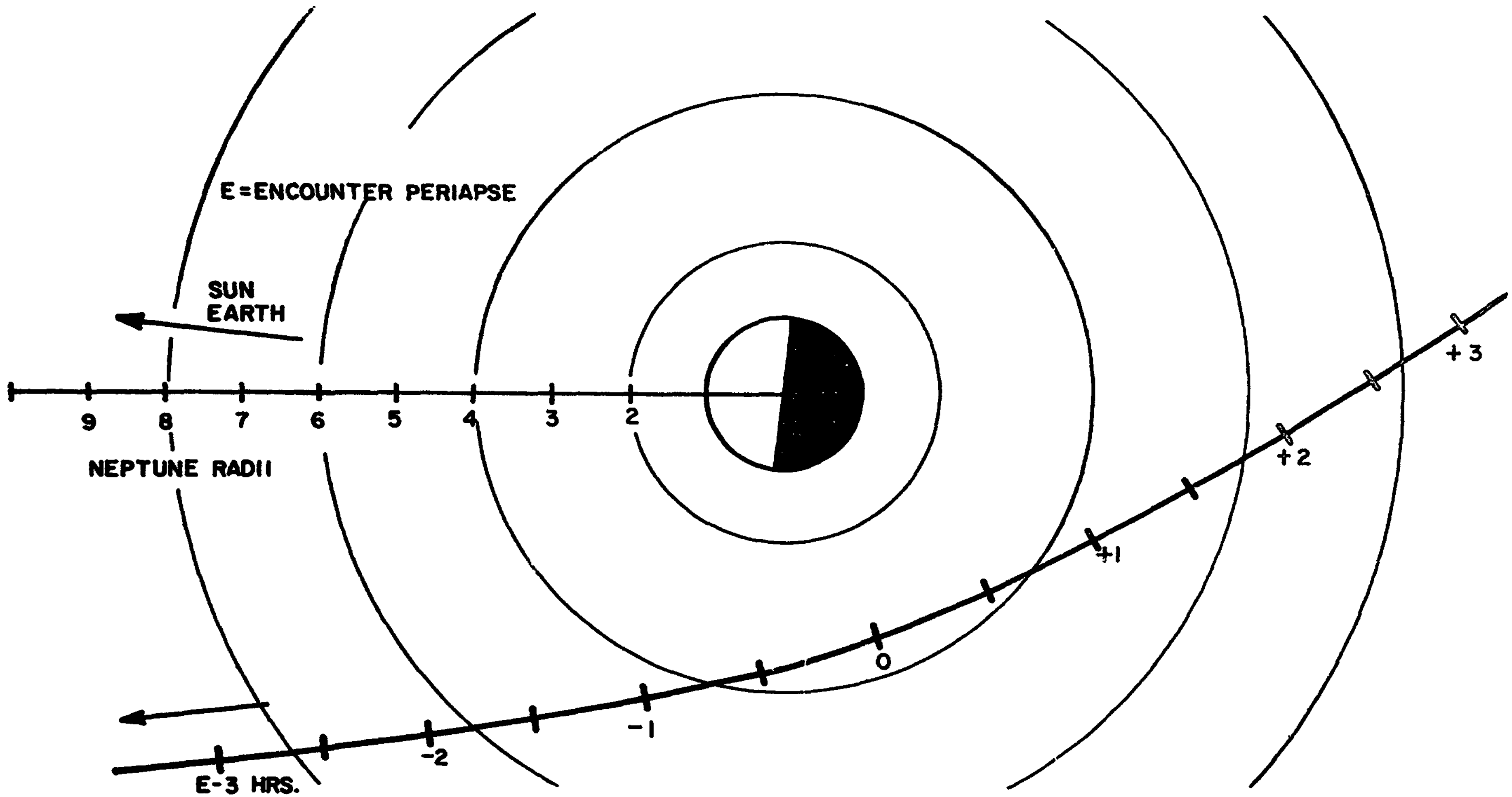

FIGURE 2.30. NEPTUNE ENCOUNTER TRAJECTORY, 1977-E GRAND TOUR

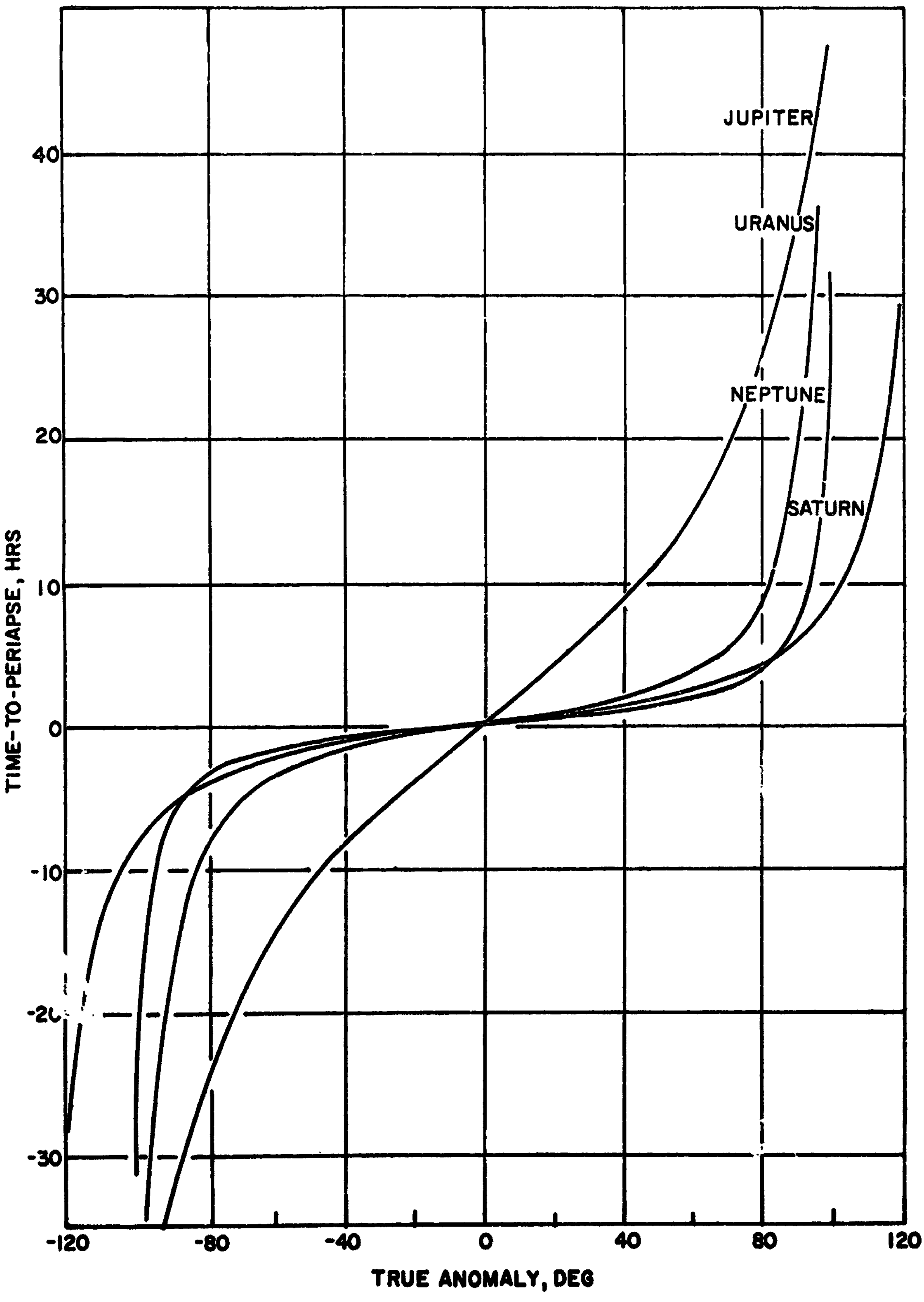

FIGURE 2.31. TIME-TO-PERIAPSE VS. TRUE ANOMALY, 1977-E GRAND TOUR.

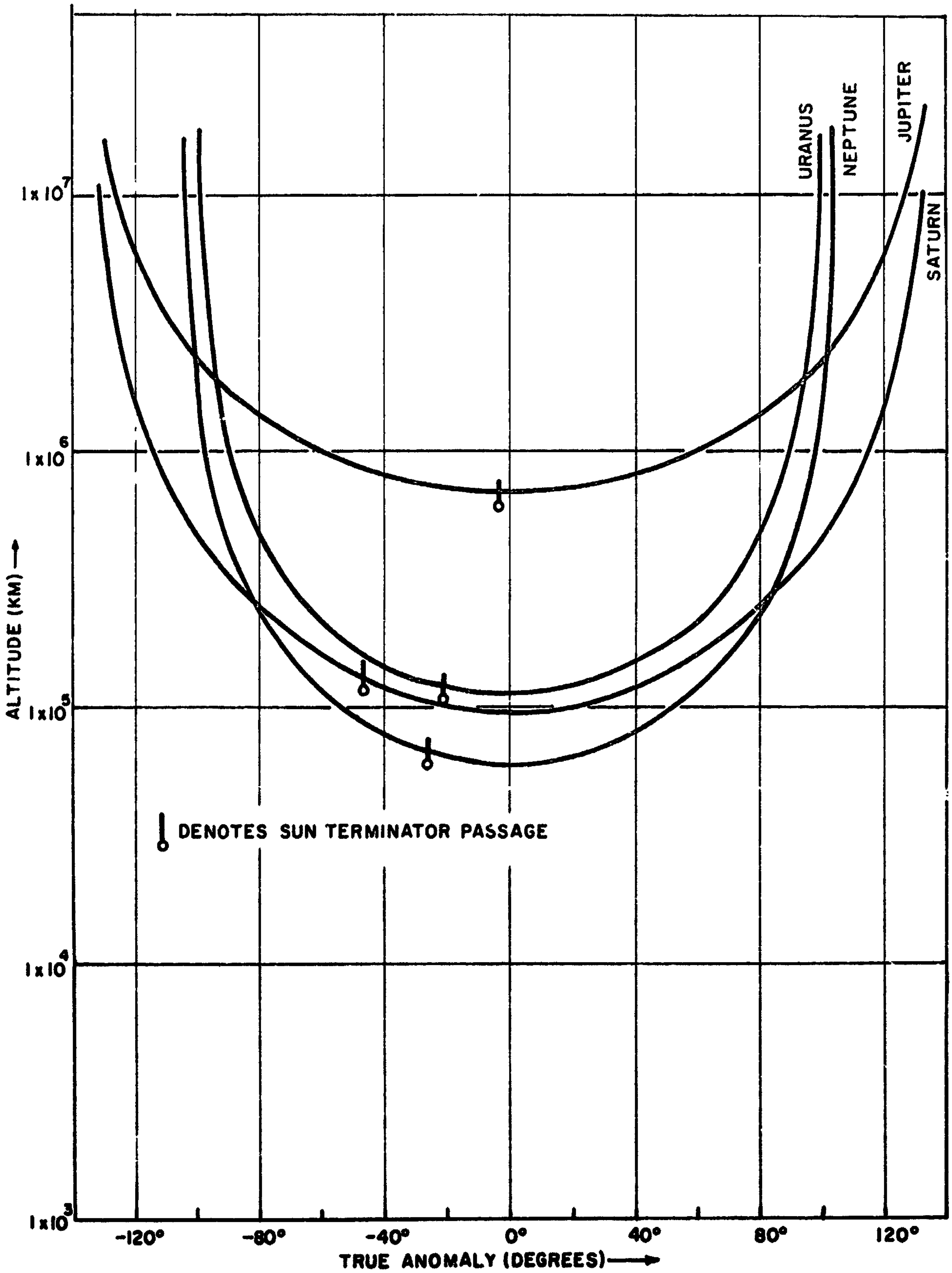

FIGURE 2.32 ALTITUDE VS. TRUE ANOMALY, 1977-E GRAND TOUR

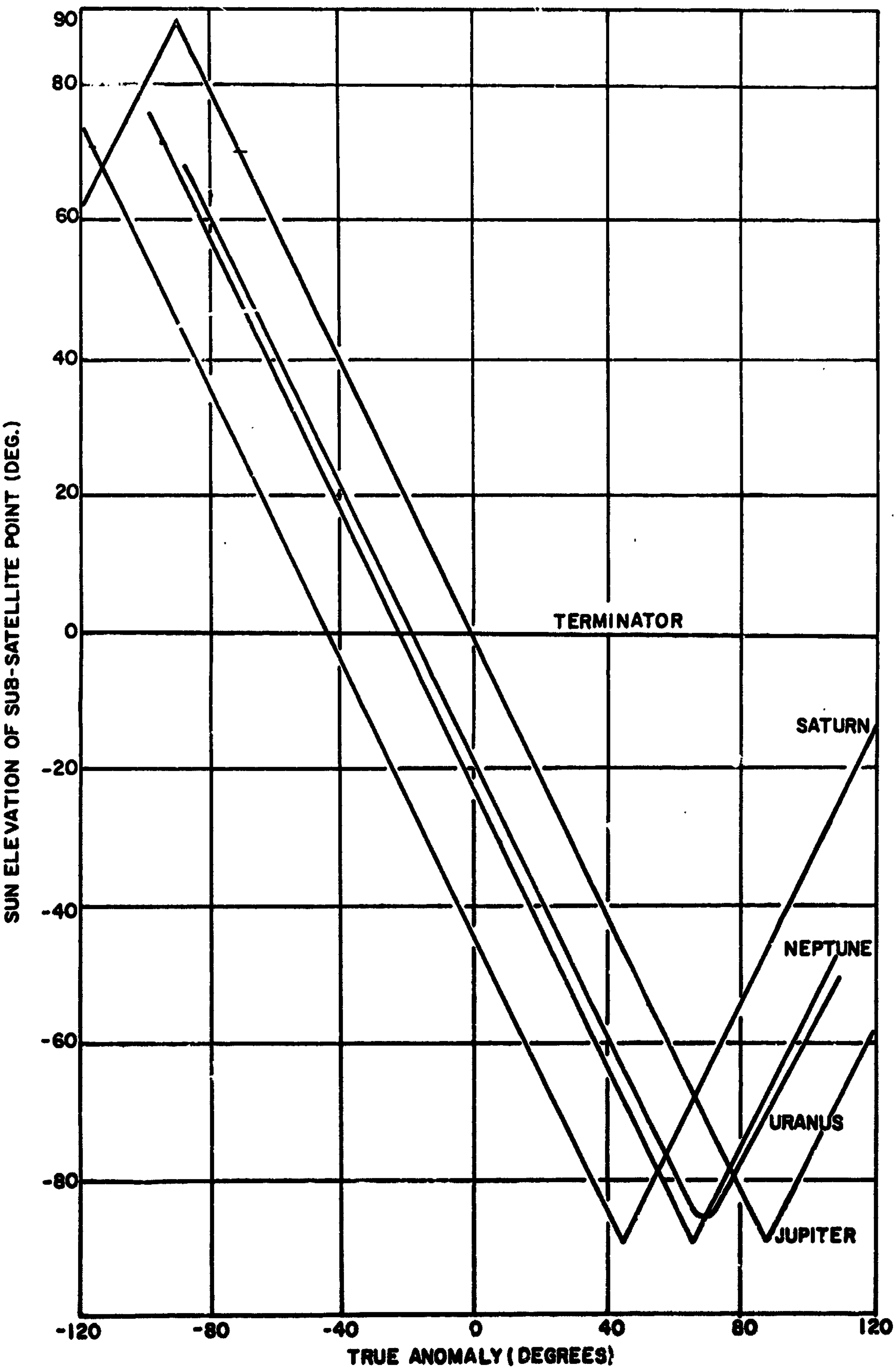

FIGURE 2.33. SUN ELEVATION AT PLANET ENCOUNTERS, 1977-E GRAND TOUR

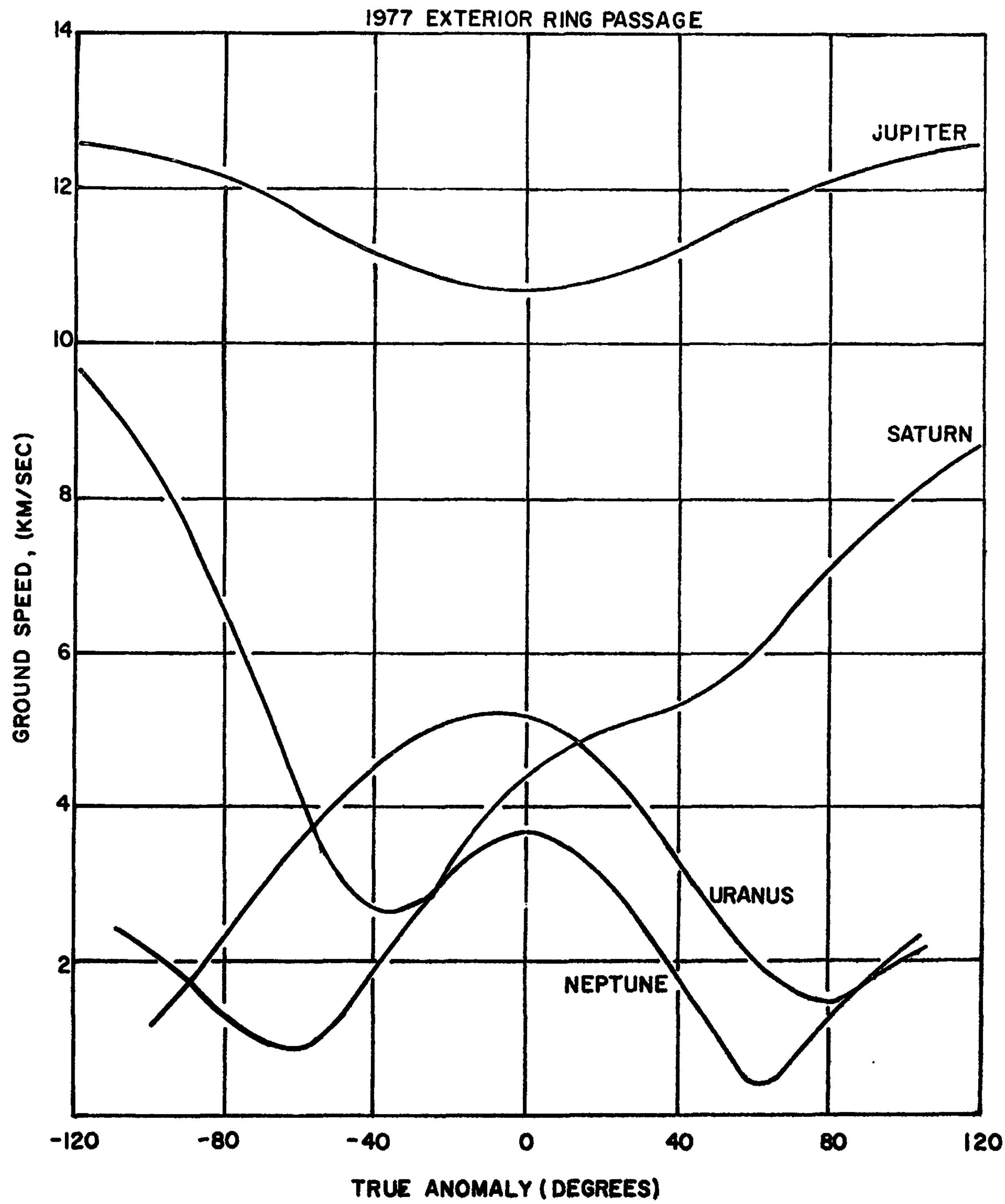

FIGURE 2.34. GROUND SPEED AT PLANET ENCOUNTERS, 1977-E GRAND TOUR

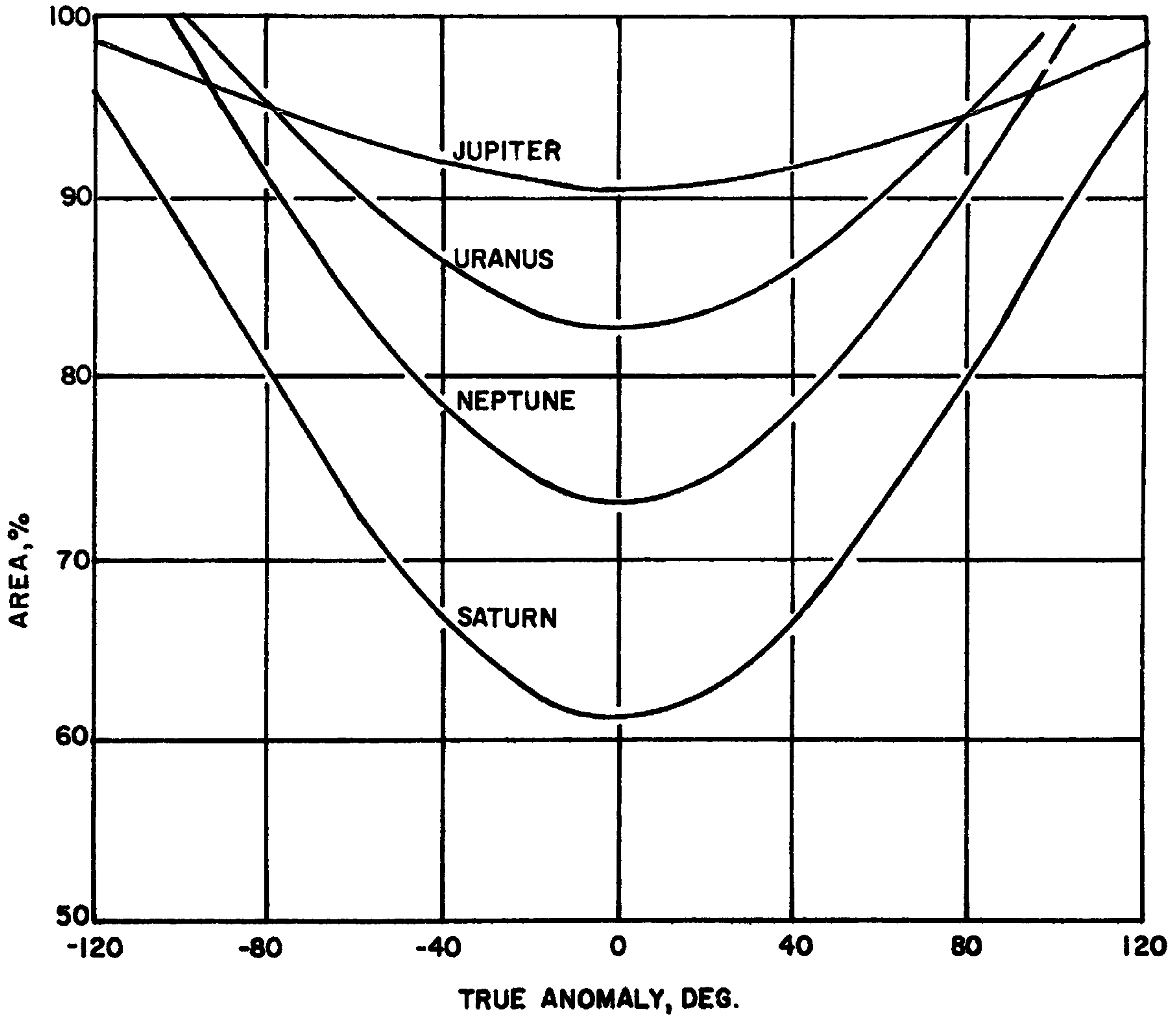

FIGURE 2.35. VISIBLE HEMISPHERIC AREA AT PLANET ENCOUNTERS, 1977-E GRAND TOUR

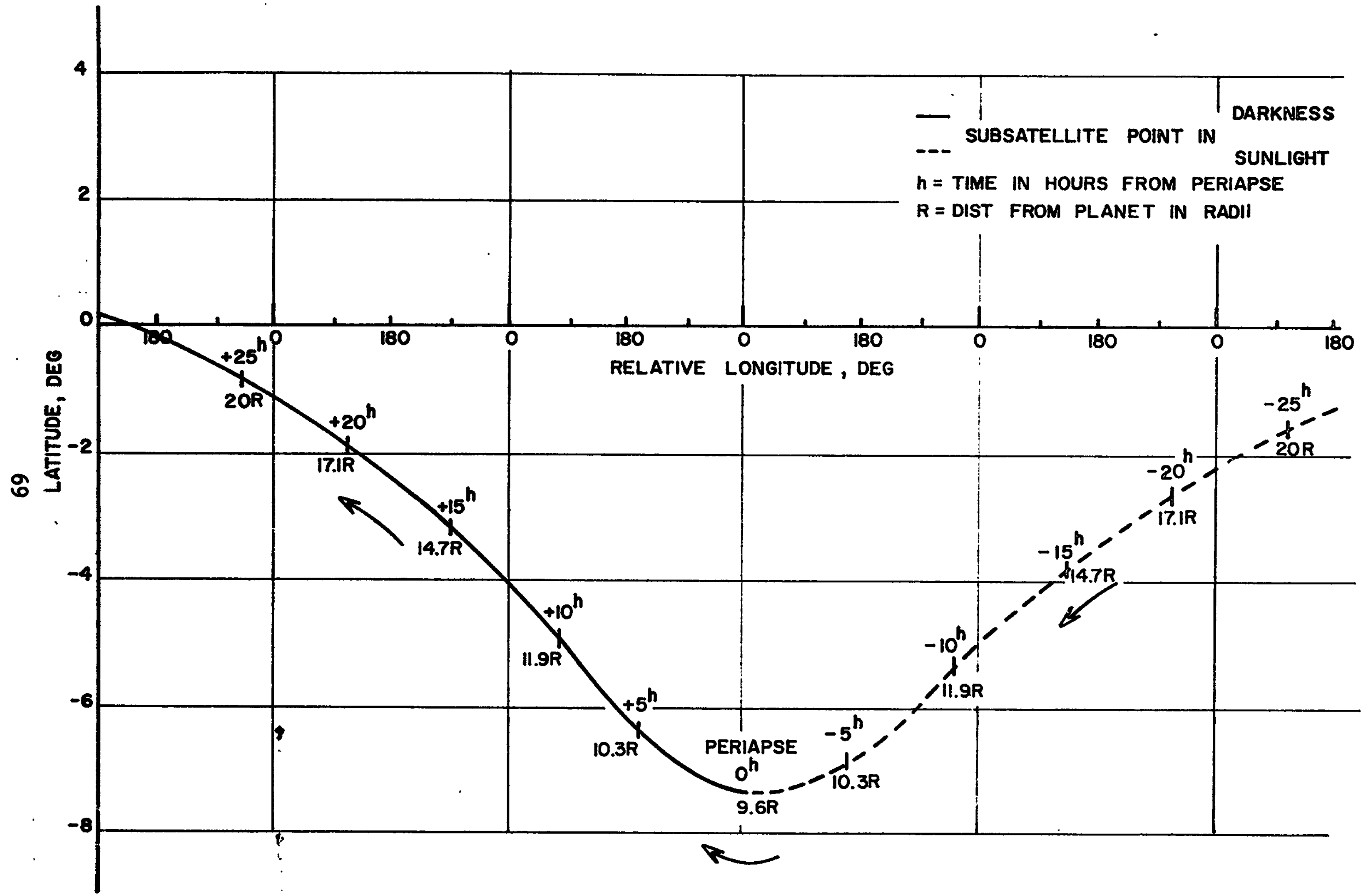

FIGURE 2.36 GROUND TRACE OF JUPITER FLYBY, 1977-E GRAND TOUR

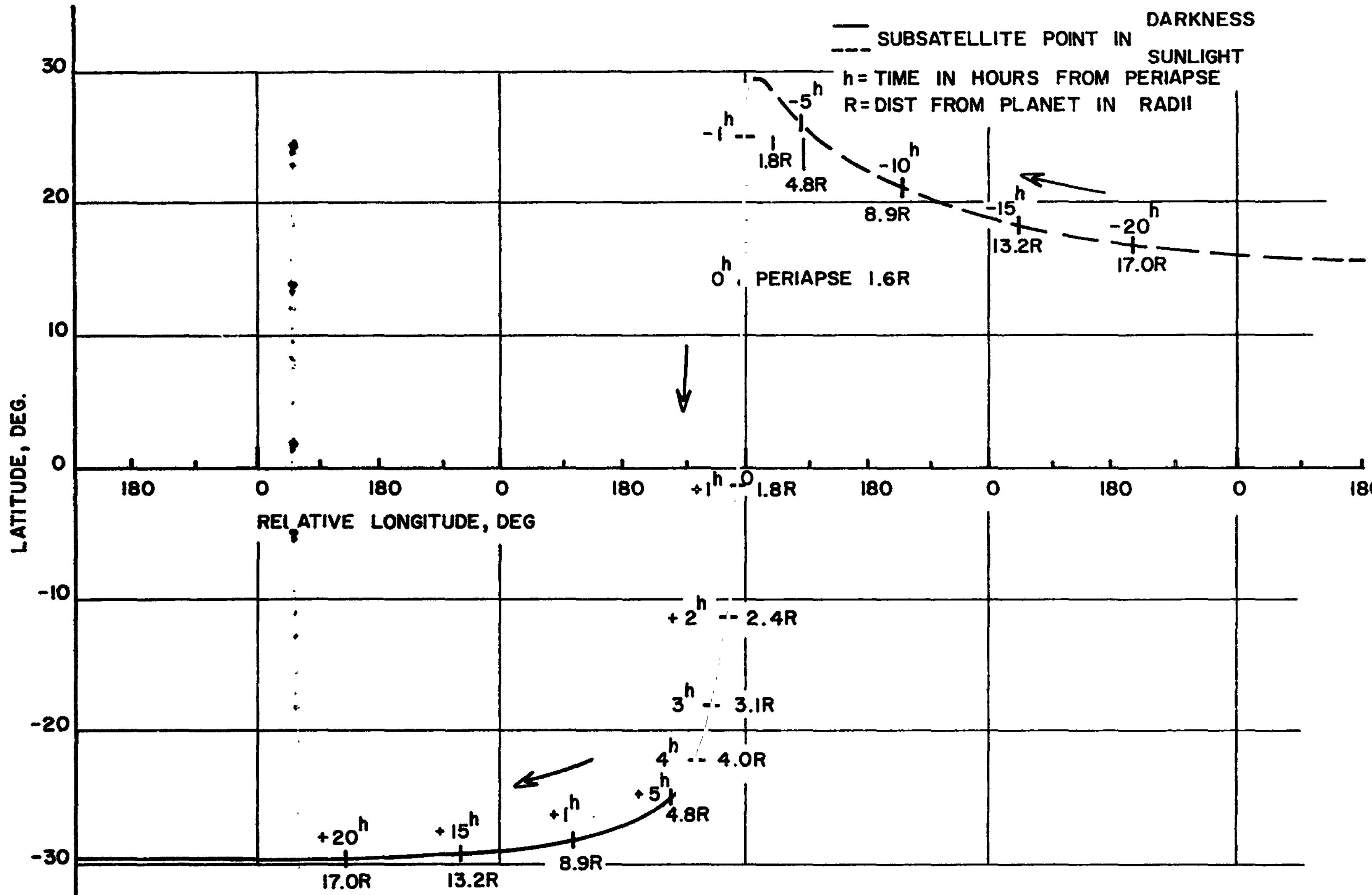

FIGURE 2.37 GROUND TRACE OF SATURN FLYBY, 1977-E GRAND TOUR

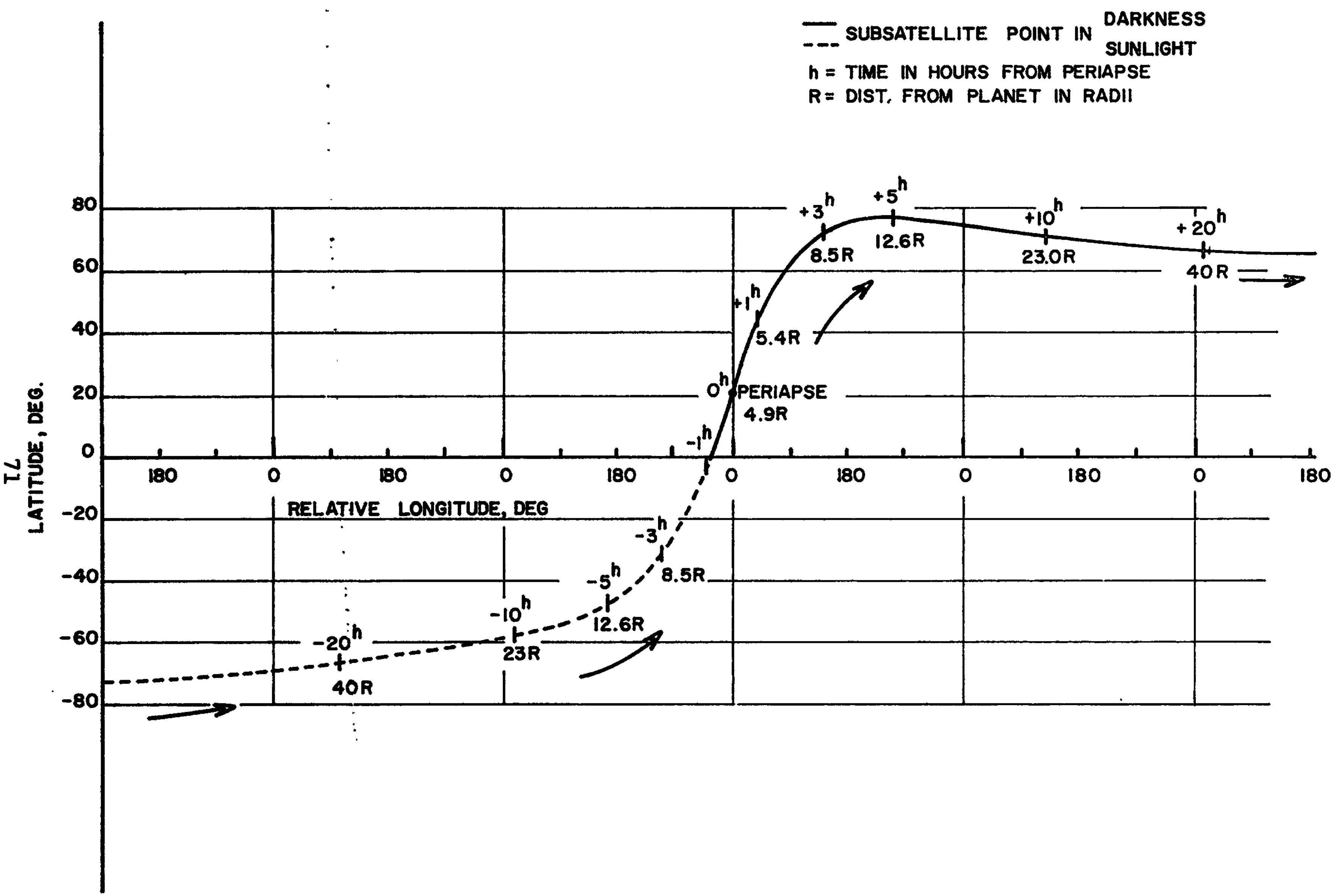

FIGURE 2.38 GROUND TRACE OF URANUS FLYBY, 1977-E GRAND TOUR

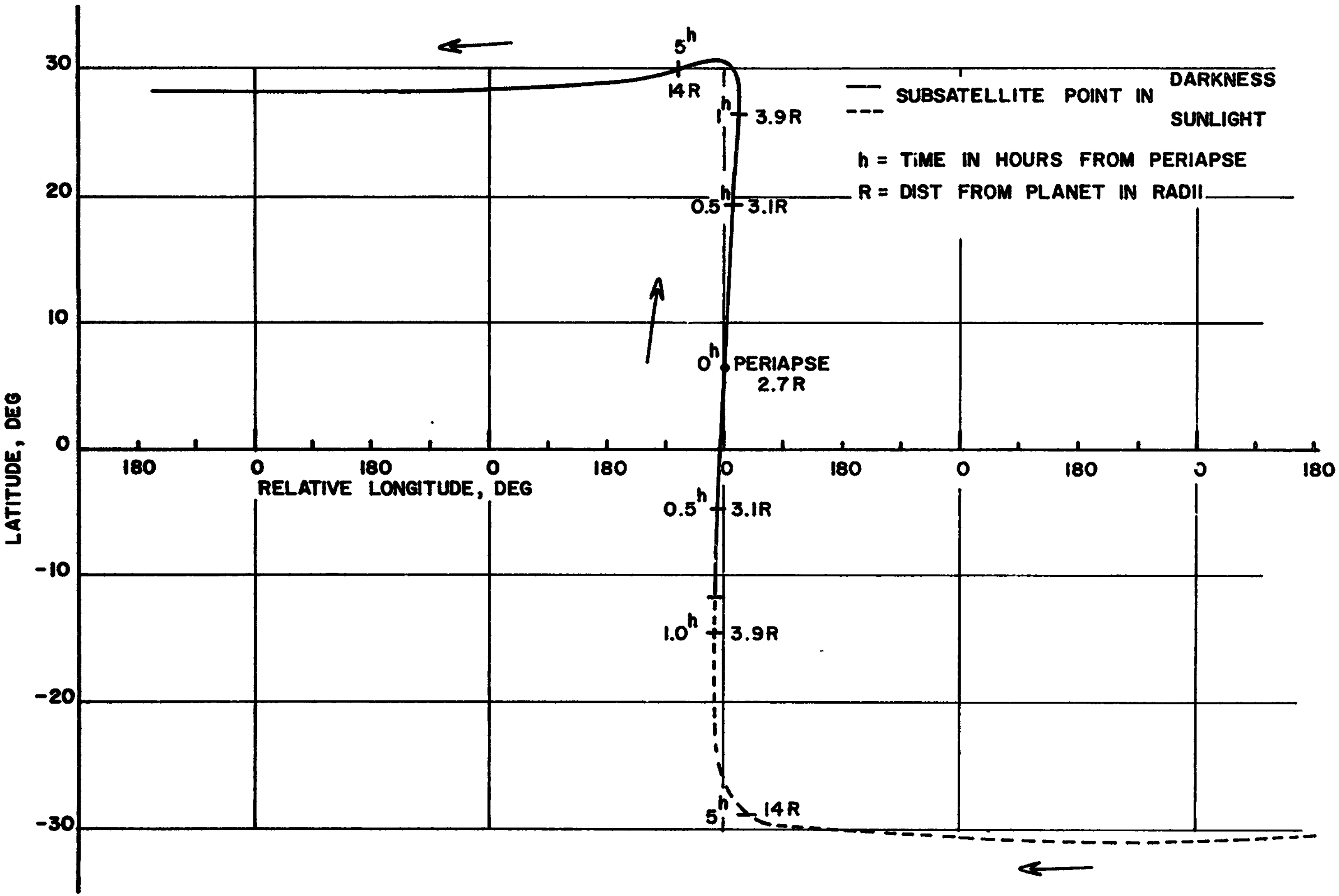

FIGURE 2.39 GROUND TRACE OF NEPTUNE FLYBY, 1977-E GRAND TOUR

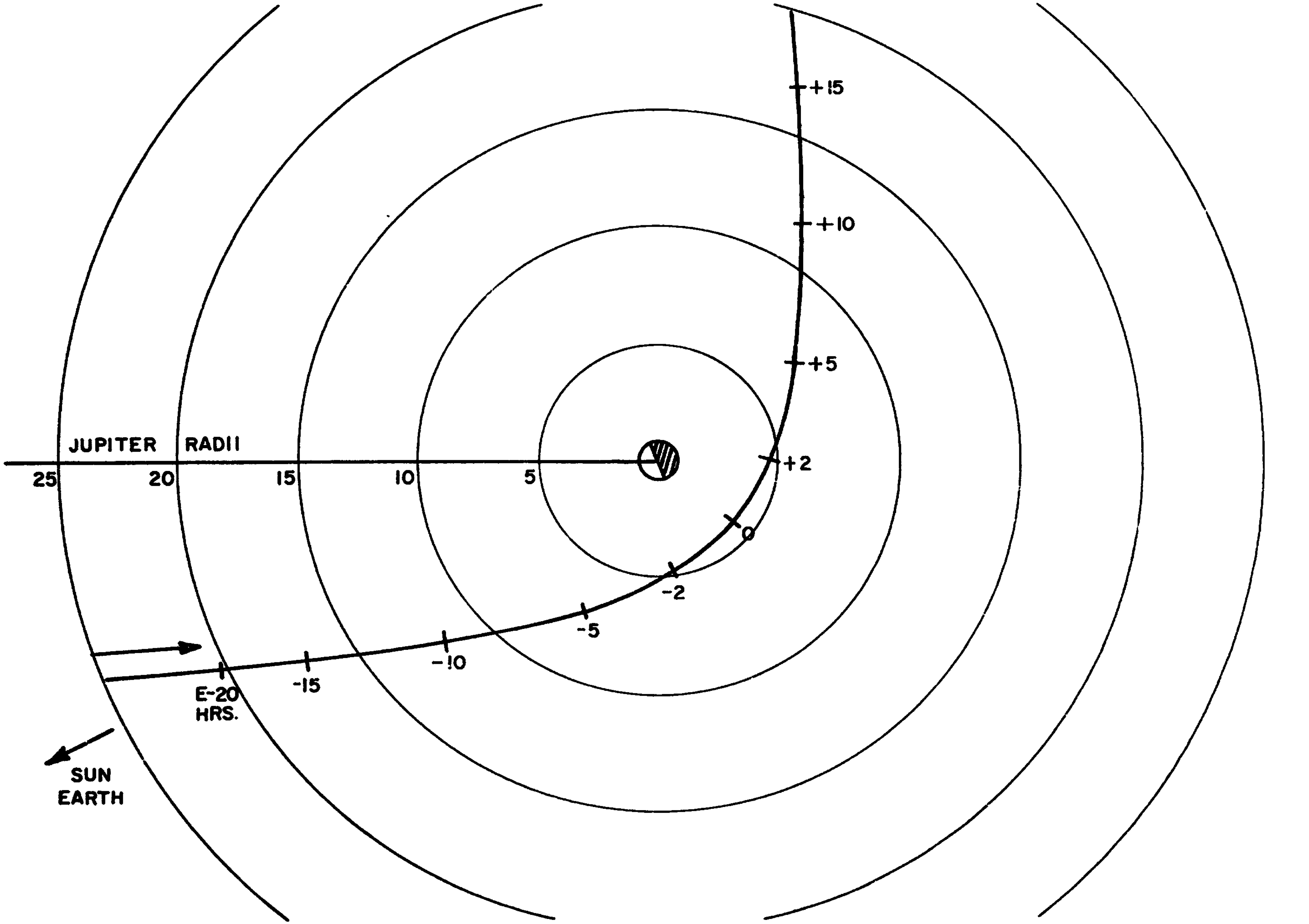

FIGURE 2.40. JUPITER ENCOUNTER TRAJECTORY, 1977-I GRAND TOUR

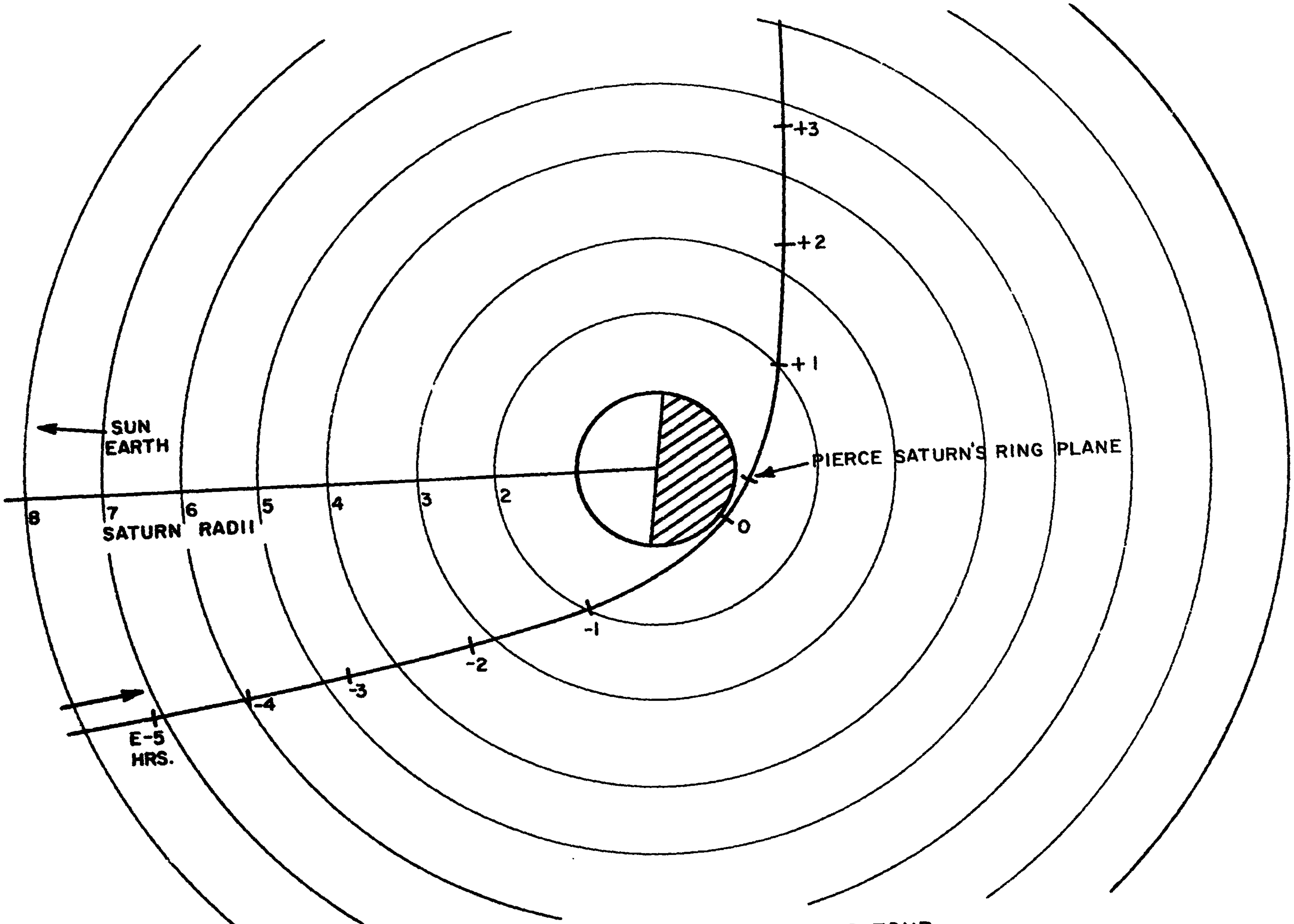

FIGURE 2.41. SATURN ENCOUNTER TRAJECTORY, 1977-I GRAND TOUR

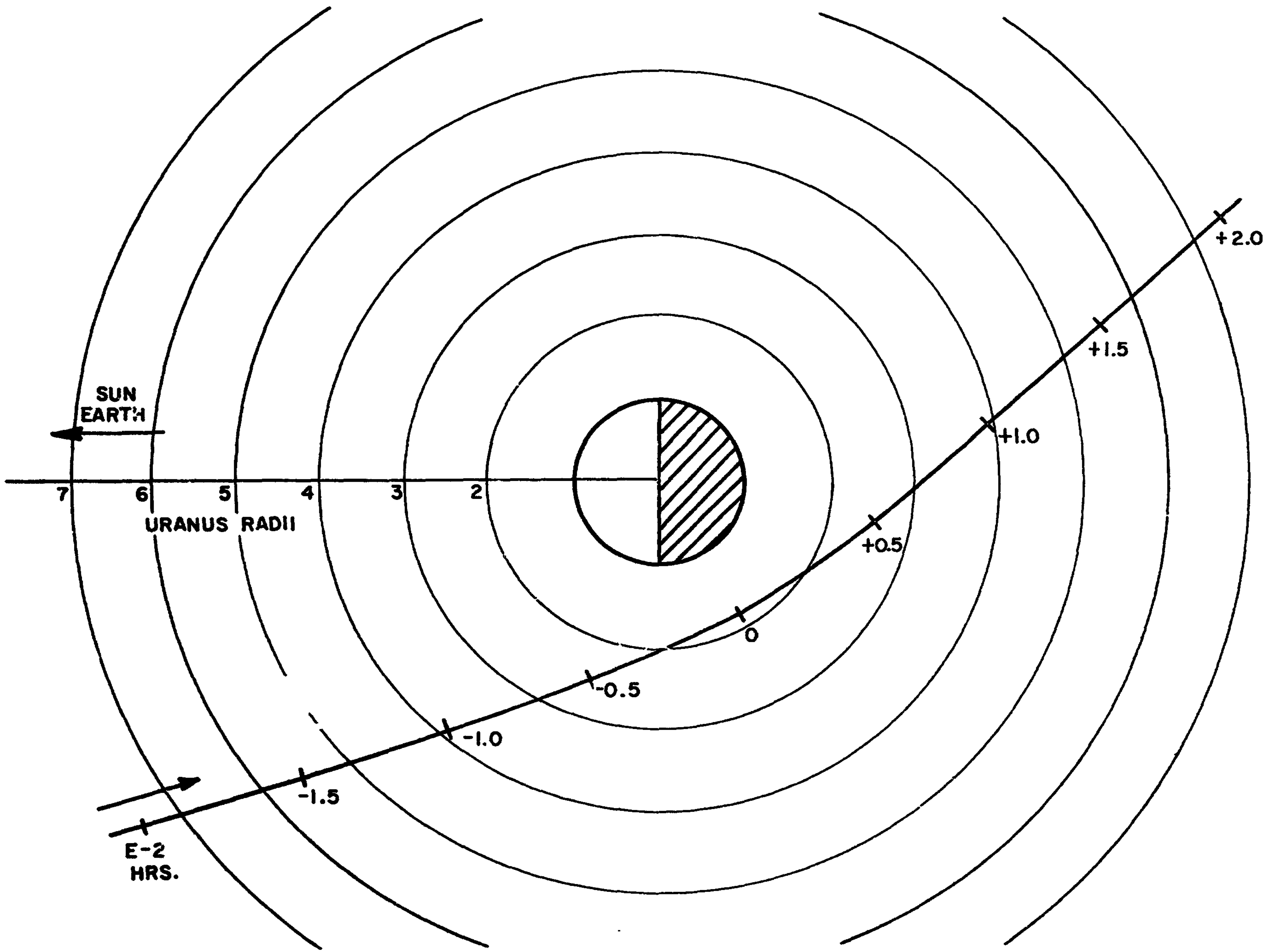

FIGURE 2.42. URANUS ENCOUNTER TRAJECTORY, 1977-I GRAND TOUR

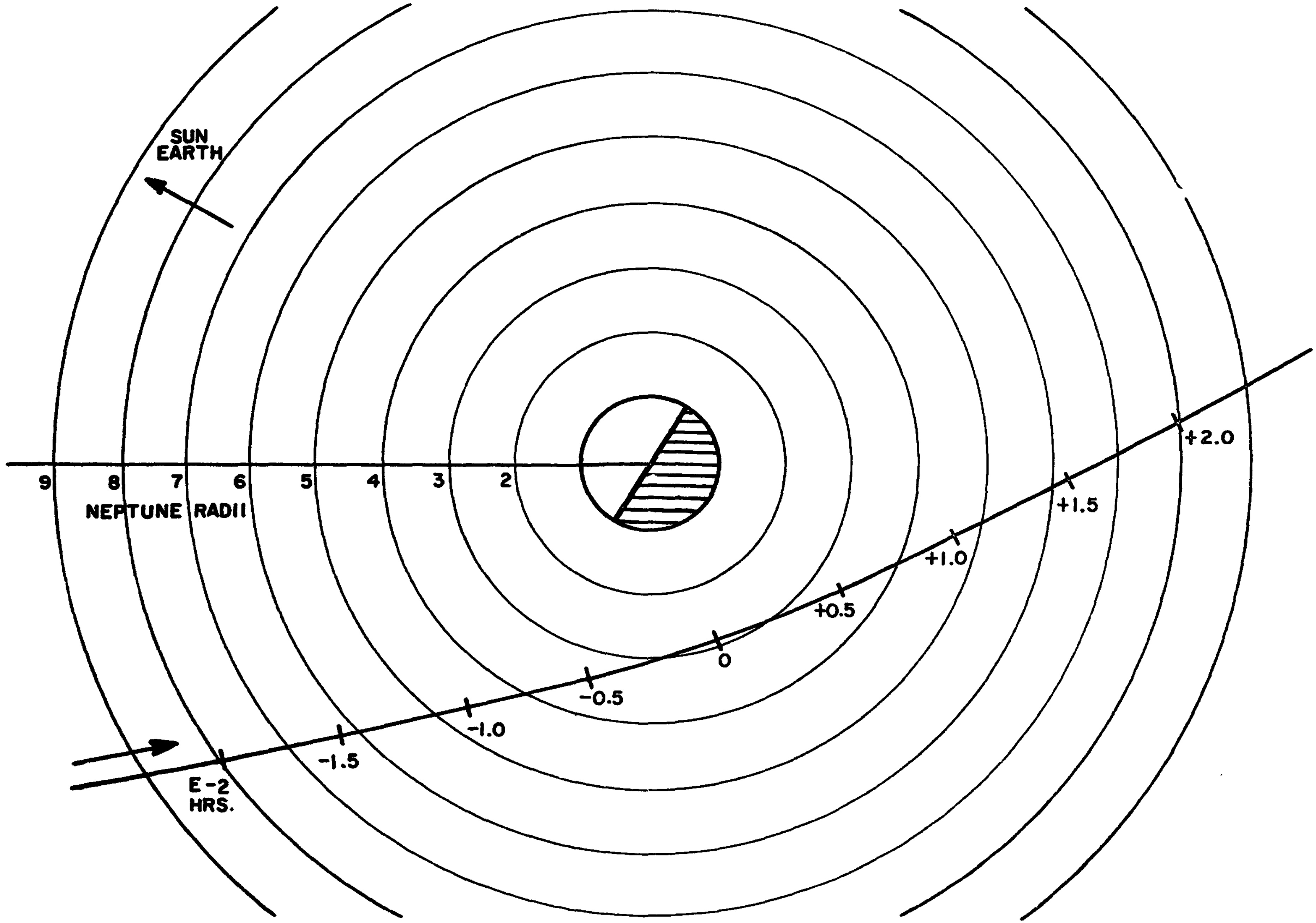

FIGURE 2.43. NEPTUNE ENCOUNTER TRAJECTORY, 1977-I GRAND TOUR

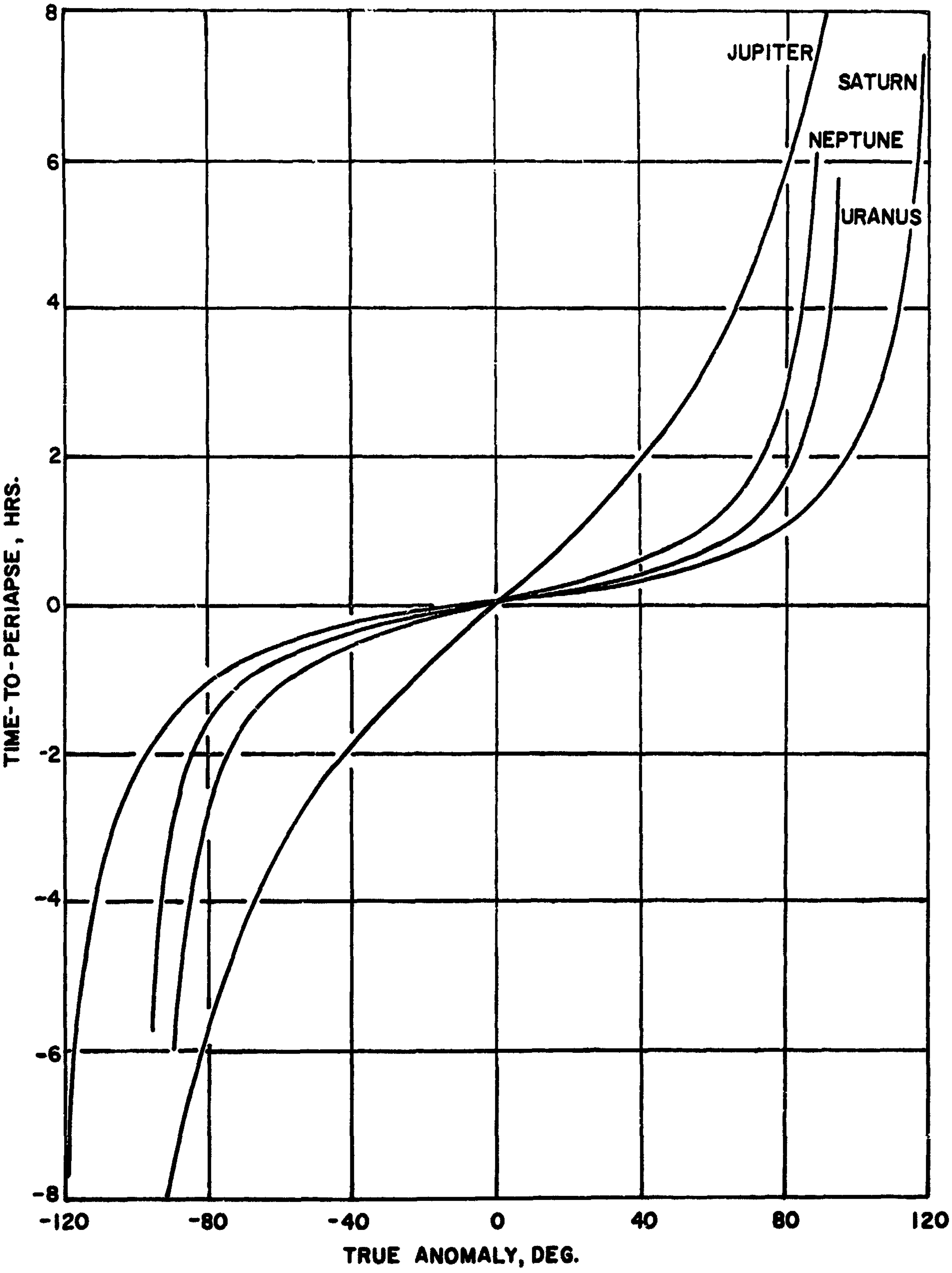

FIGURE 2.44. TIME-TO-PERIAPSE VS. TRUE ANOMALY, 1977-I GRAND TOUR

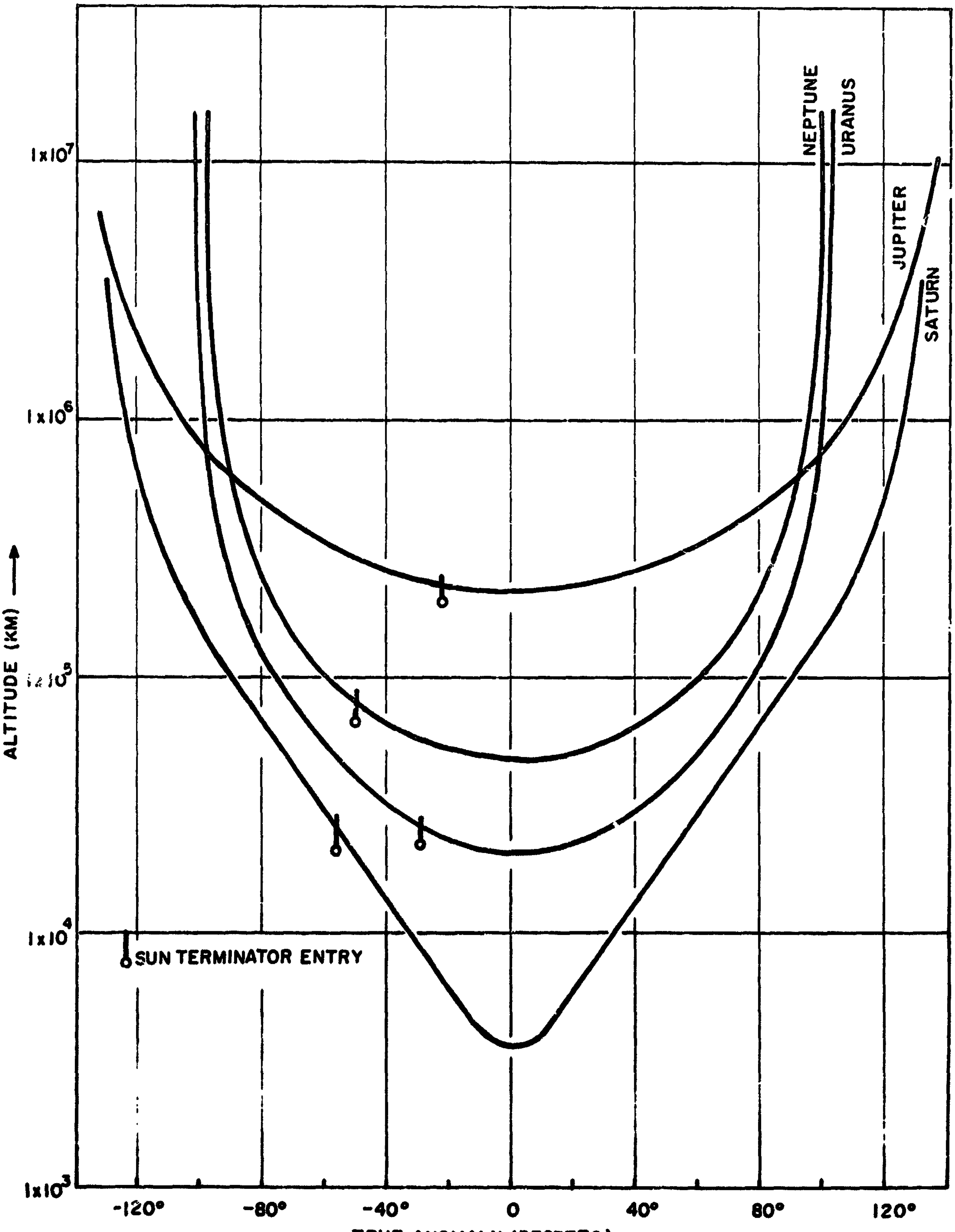

FIGURE 2.45 ALTITUDE VS. TRUE ANOMALY, 1977-I GRAND TOUR

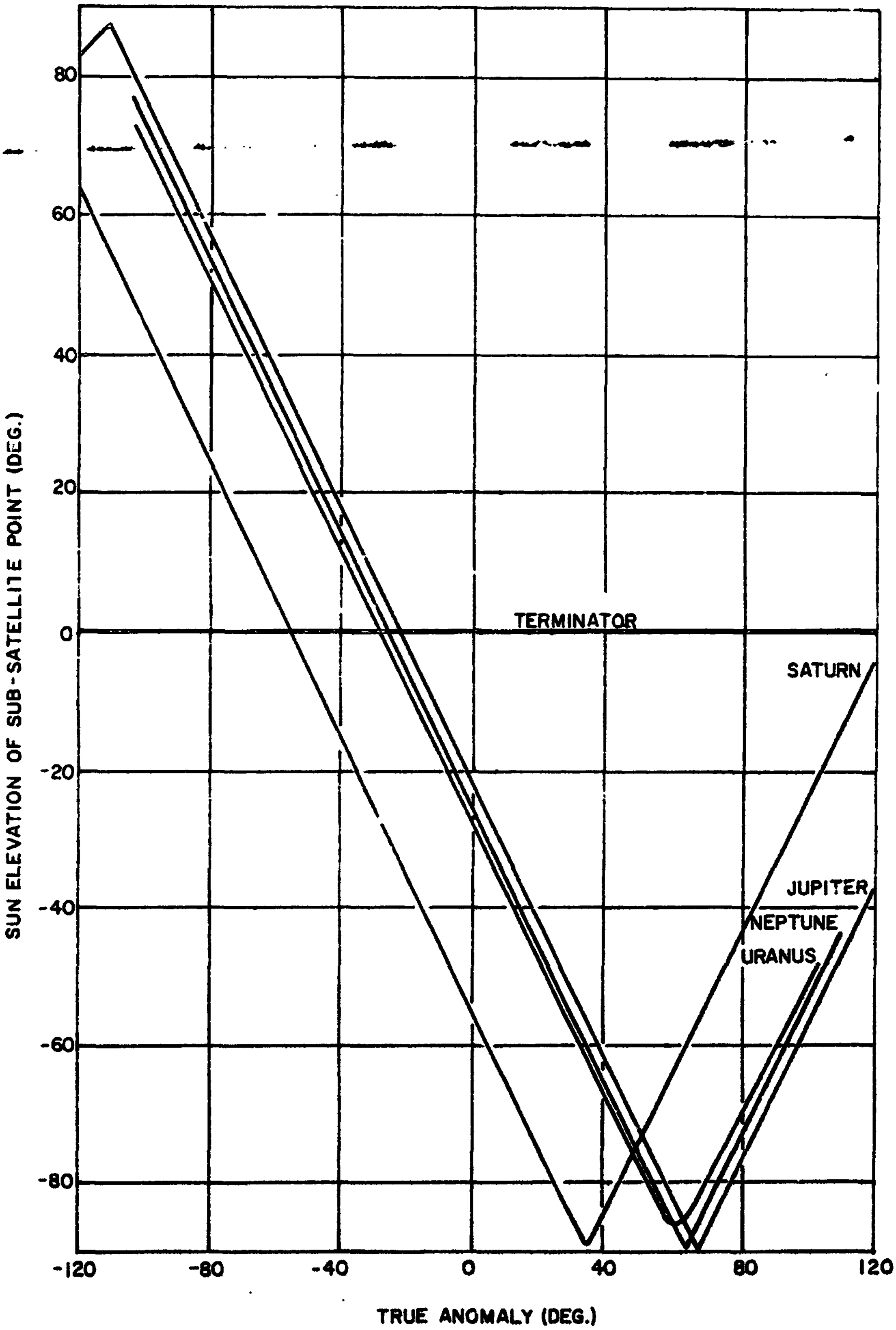

FIGURE 2.46. SUN ELEVATION AT PLANET ENCOUNTERS, 1977-I GRAND TOUR

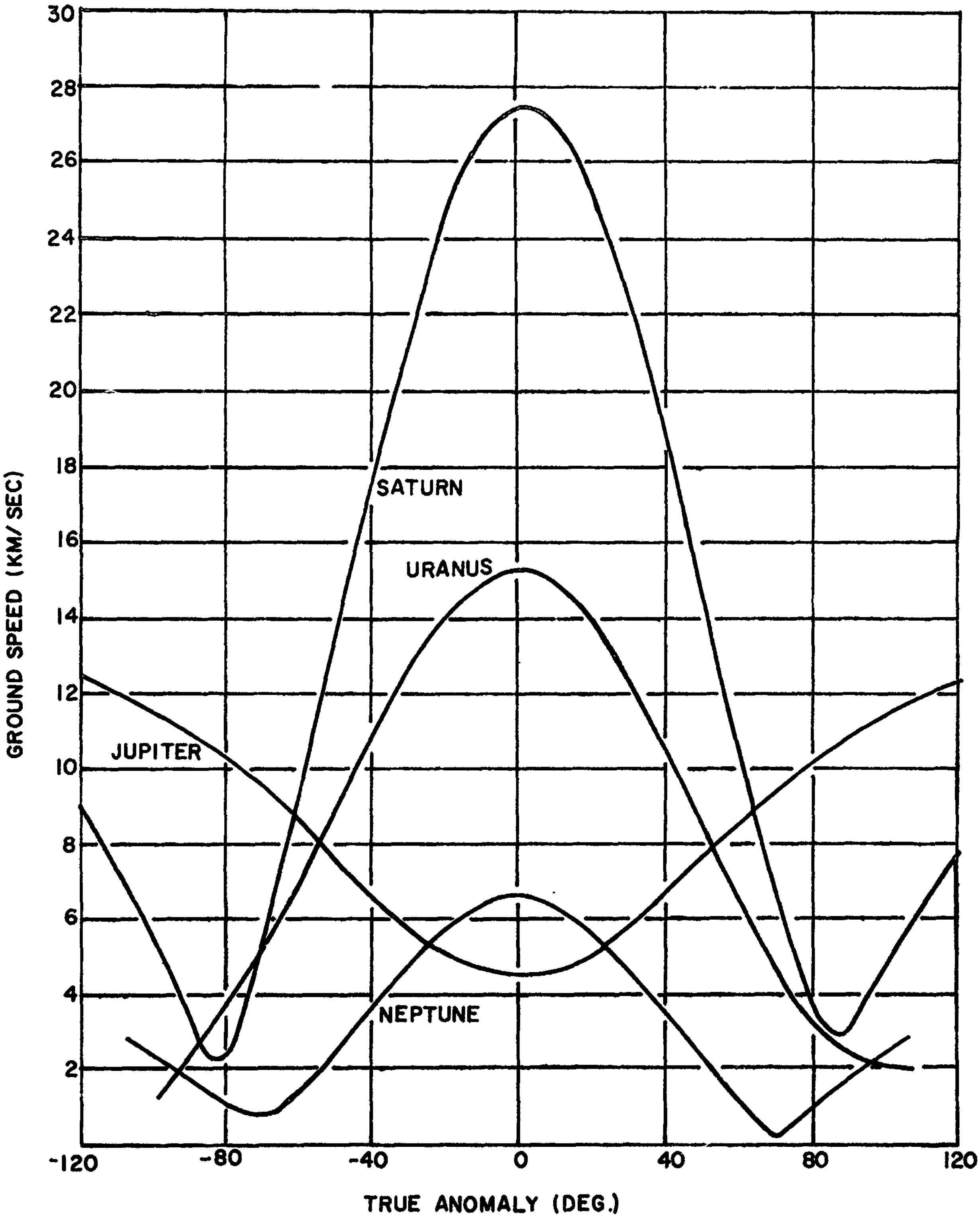

FIGURE 2.47. GROUND SPEED AT PLANET ENCOUNTERS, 1977-I GRAND TOUR

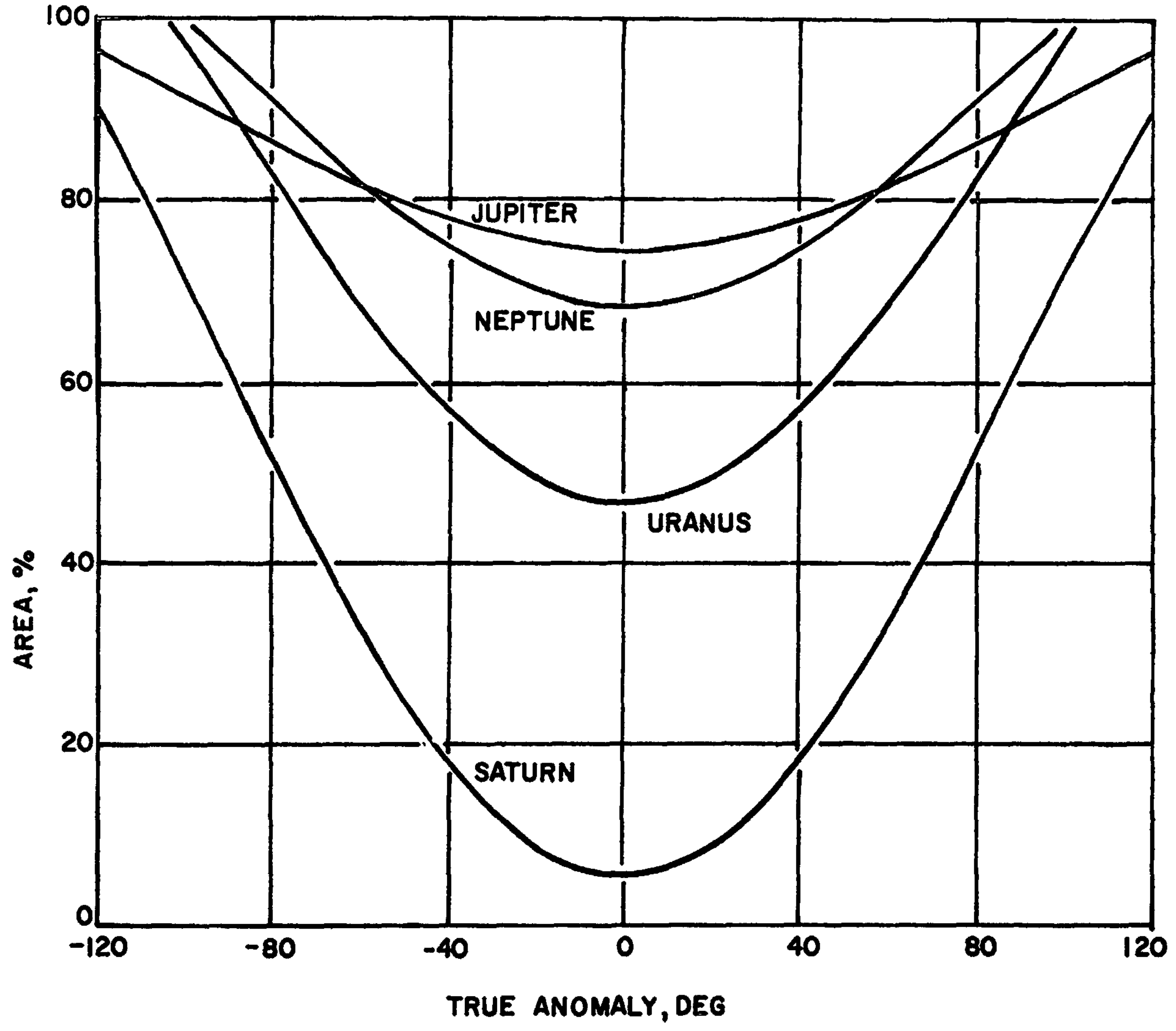

FIGURE 2.48. VISIBLE HEMISPHERIC AREA AT PLANET ENCOUNTERS, 1977-I GRAND TOUR

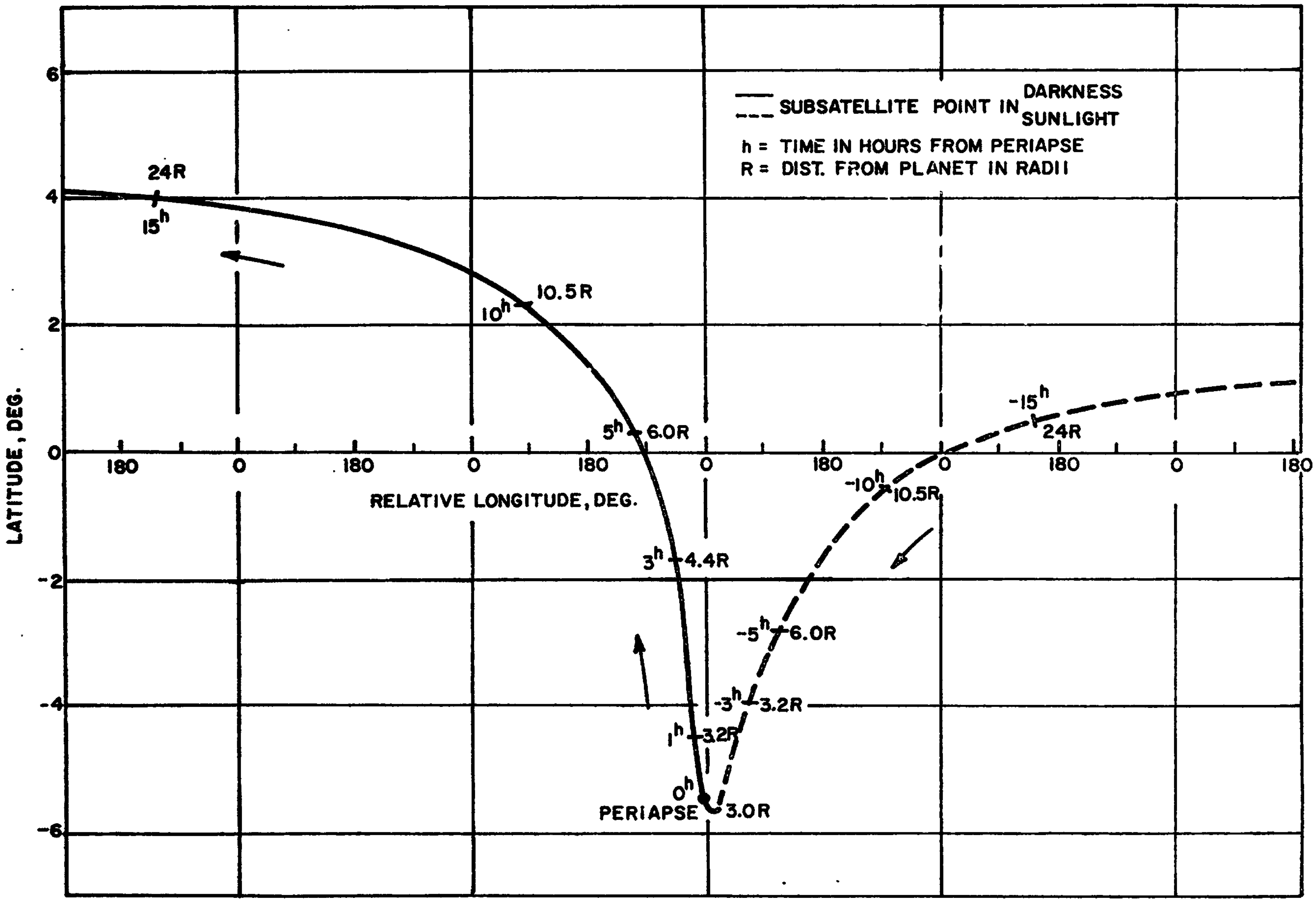

FIGURE 2.49. GROUND TRACE OF JUPITER FLYBY, 1977-I GRAND TOUR

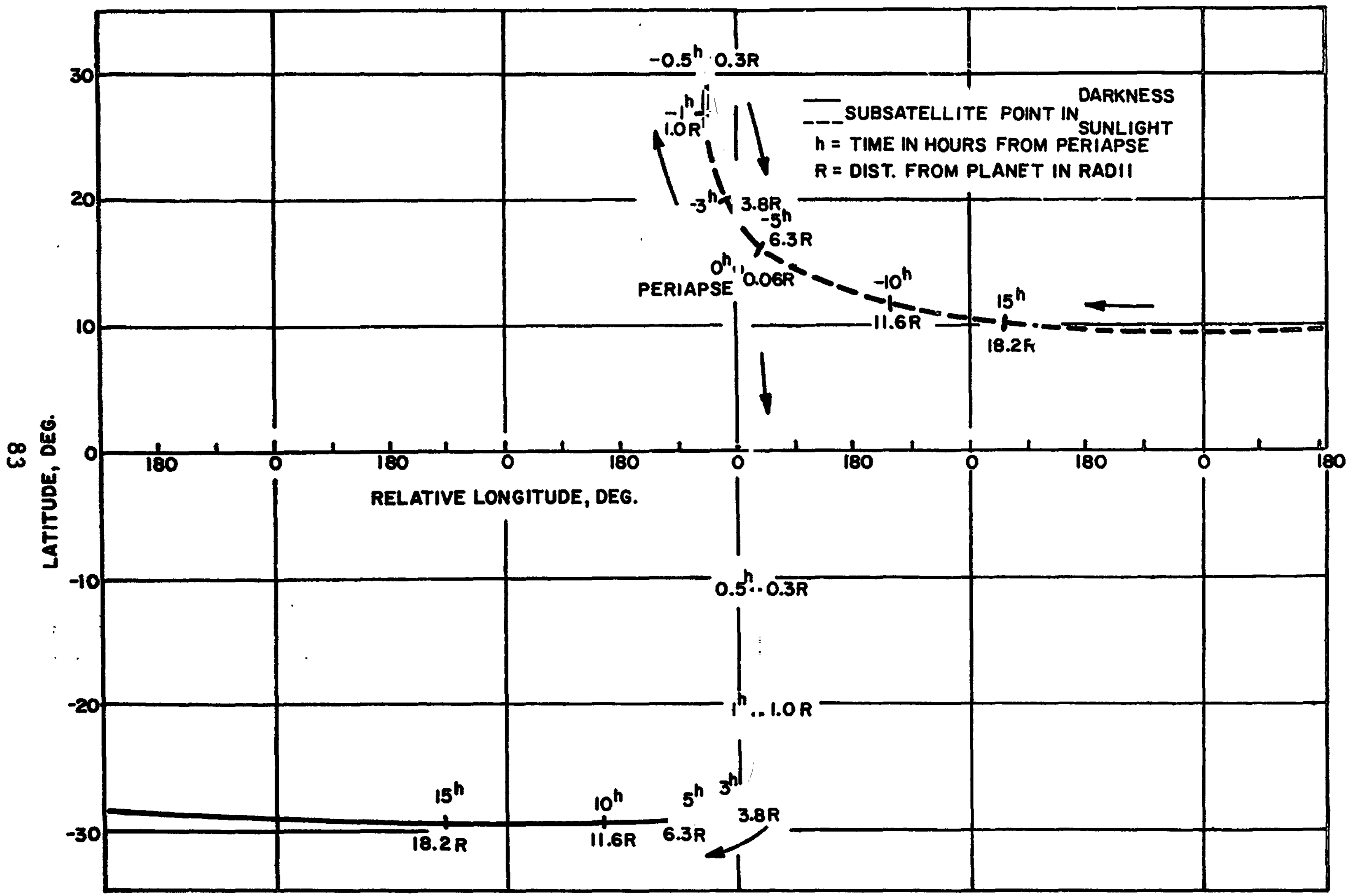

FIGURE 2.50 GROUND TRACE OF SATURN FLYBY, 1977-I GRAND TOUR

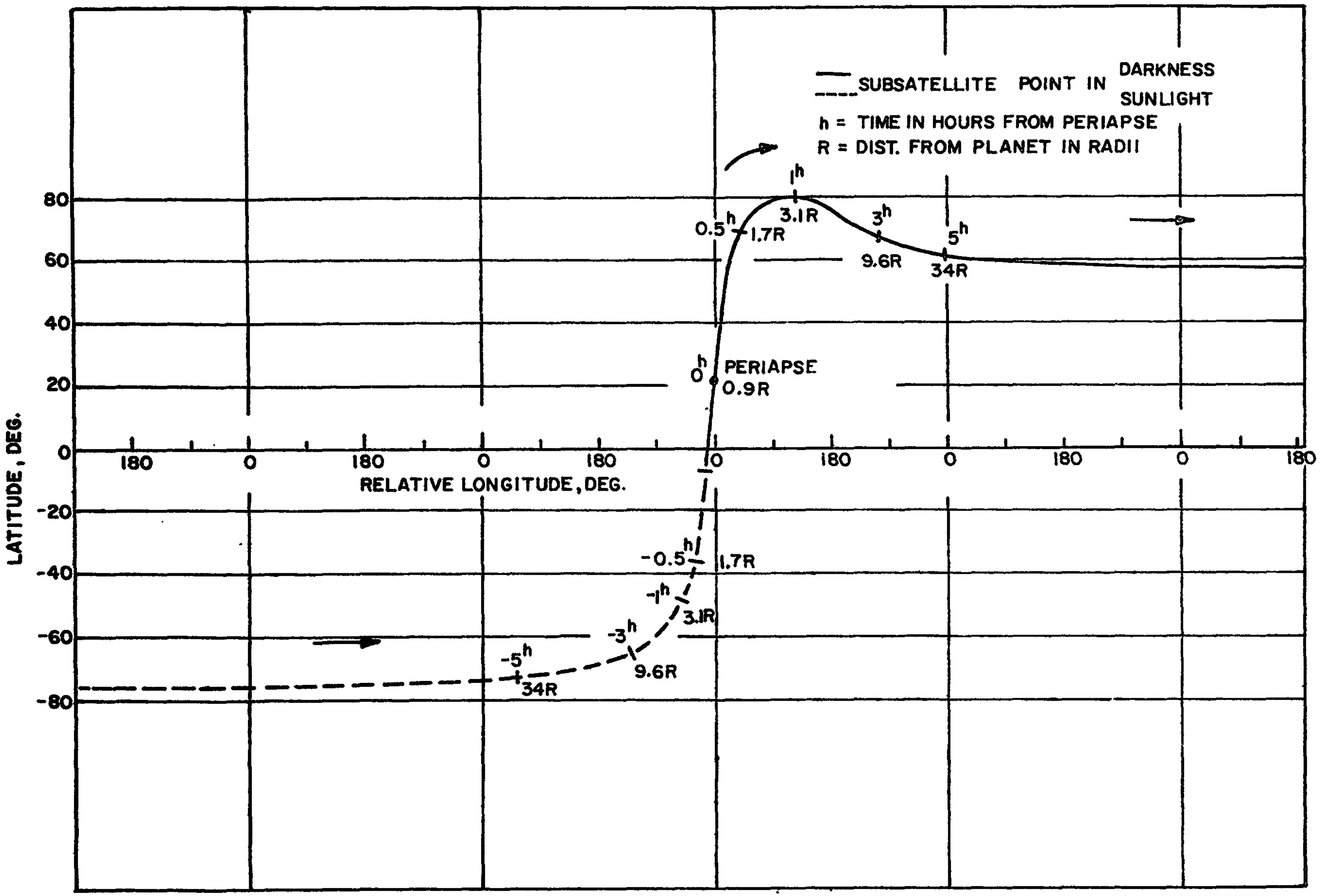

FIGURE 2.51. GROUND TRACE OF URANUS FLYBY, 1977-I GRAND TOUR.

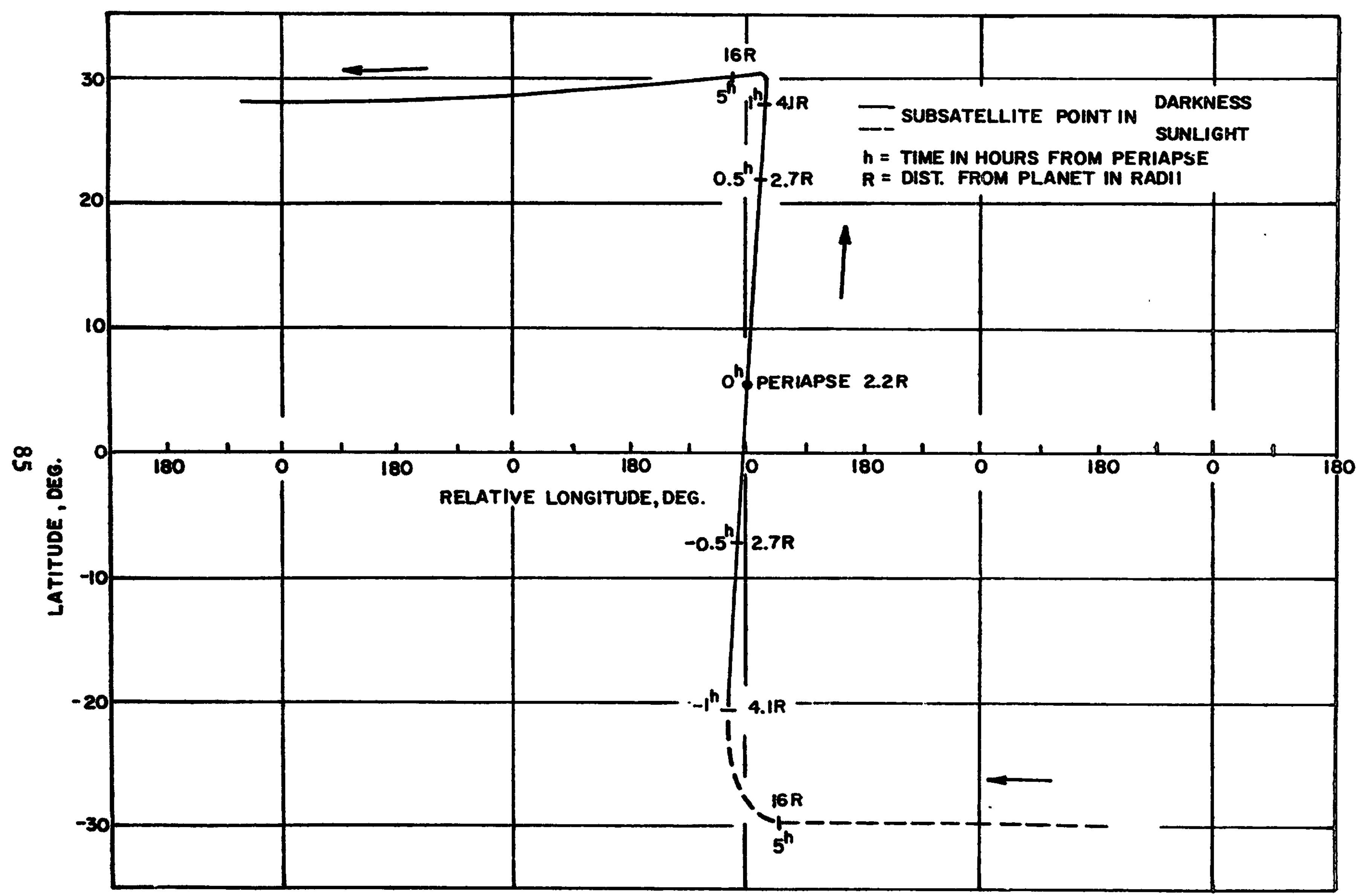

FIGURE 2.52. GROUND TRACE OF NEPTUNE FLYBY, 1977-I GRAND TOUR

SECTION 3

GUIDANCE ANALYSIS AND REQUIREMENTS

By

A. L. Friedlander

3. GUIDANCE ANALYSIS AND REQUIREMENTS

The so-called "free" energy addition and velocity deflection available from an unpowered planetary swingby is, in reality, obtained at some expense to the spacecraft guidance (propulsion) system. Intermittent velocity corrections are required to compensate for a number of trajectory error sources. Since the trajectory error sensitivity is quite severe in the case of the multiple swingby Grand Tour, the guidance considerations are of major importance to the mission designer.

Error sensitivity of the aim points between successive target planets is shown in Table 3.1 for the two trajectory selections in 1977. It is noted that the trajectory passing inside of Saturn's Rings is about 3 to 4 times more sensitive to errors than the trajectory passing outside of the Rings. It may be expected, then, that the Interior Ring Passage Mission will incur a higher guidance ΔV penalty. For either trajectory, it is found that the Saturn-Uranus leg and the Uranus-Neptune leg have nearly the same sensitivity, but that the sensitivity of the Jupiter-Saturn leg is more than an order of magnitude smaller. Accordingly, the ΔV requirement at Jupiter encounter may be expected to have a relatively small contribution to the total ΔV.

As an example of the "astronomical" error that would result if no corrective guidance maneuvers were made, consider the least sensitive of the two trajectories.

TABLE 3.1

GRAND TOUR TRAJECTORY SENSITIVITY

ΔB = ERROR IN AIM POINT AT TARGET PLANE

		1977-E	1977-I	
$\dfrac{\Delta B \text{ SATURN}}{\Delta B \text{ JUPITER}}$	=	400 -	1,100	$\dfrac{\text{KM}}{\text{KM}}$
$\dfrac{\Delta B \text{ URANUS}}{\Delta B \text{ SATURN}}$	=	5,600 -	17,000	$\dfrac{\text{KM}}{\text{KM}}$
$\dfrac{\Delta B \text{ NEPTUNE}}{\Delta B \text{ URANUS}}$	=	4,500 -	20,000	$\dfrac{\text{KM}}{\text{KM}}$

The error at Neptune may be estimated by multiplying together the intermediate sensitivities. Thus,

$$\frac{\Delta B_{Neptune}}{\Delta B_{Jupiter}} \approx 400 \times 5600 \times 4500$$

$$\approx 10^{10} \frac{km}{km}$$

To make matters even worse, the error at Jupiter will certainly be several orders of magnitude greater than 1 km. Clearly, multiple trajectory corrections enroute will be required to insure success of the Grand Tour Mission.

Guidance maneuvers will be specified on both the approach and departure legs of the swingby trajectory at each intermediate planet. Using the Saturn encounter as an example, Figure 3.1 illustrates the guidance policy and the factors of influence. The approach maneuver is necessary to reduce the target errors due to (1) ΔV execution error at the previous planet departure, (2) orbit determination errors at that time, and (3) planet ephemeris errors. The departure maneuver is necessary to compensate for the magnification effects of the gravitational swingby on the orbit determination error which exists at the time of executing the final approach maneuver.

Objectives of the guidance analysis are (1) to obtain an understanding of the guidance problem in terms of its factors of influence, (2) to determine realistic estimates

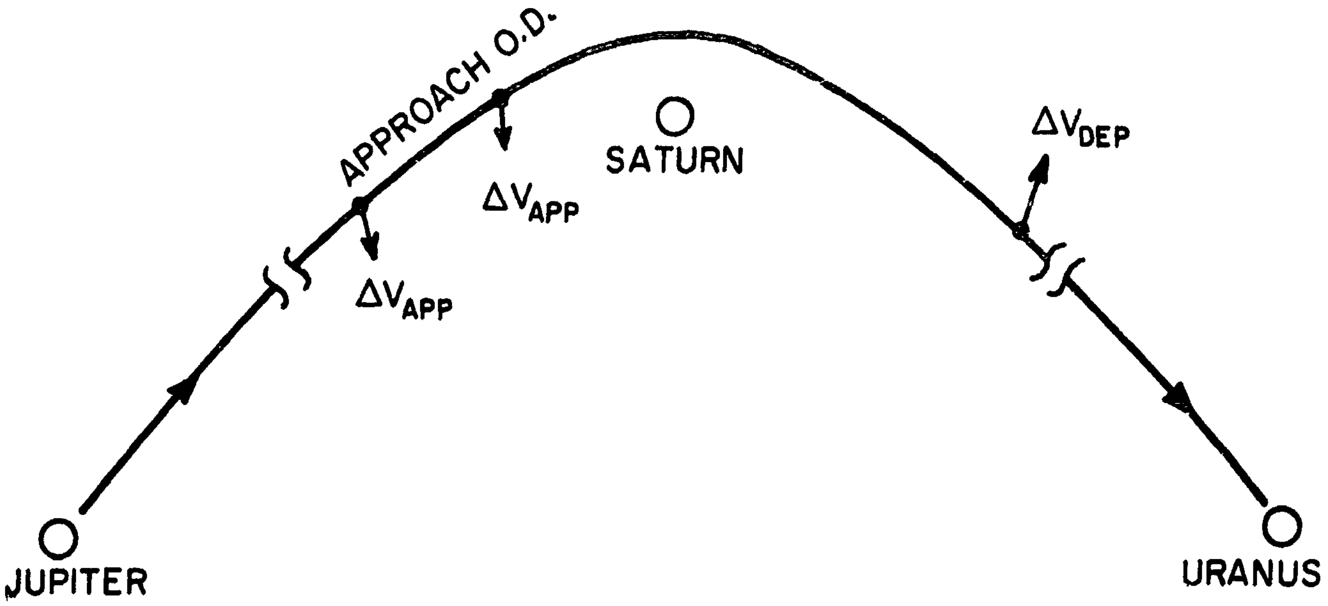

APPROACH MANEUVER: CORRECT SATURN MISS ERROR DUE TO

(1.) ΔV EXECUTION ERROR AT JUPITER DEPARTURE

(2.) ORBIT DETERMINATION ERROR AT JUPITER DEPARTURE

(3.) SATURN'S EPHEMERIS ERROR

DEPARTURE MANEUVER: CORRECT URANUS MISS ERROR DUE TO

(1.) ORBIT DETERMINATION ERROR AT FINAL SATURN APPROACH MANEUVER

APPROACH ORBIT DETERMINATION: ERROR ANALYSIS COMPARING

(1.) EARTH-BASED RADAR TRACKING (DSIF)

(2.) ON-BOARD CELESTIAL TRACKING (PLANET TRACKER)

FIGURE 3.1 ILLUSTRATION OF GUIDANCE MANEUVERS-SATURN ENCOUNTER.

of the spacecraft propulsion system (ΔV) requirements, and (3) to ascertain the tradeoffs available between the ΔV requirements, the method and accuracy of orbit determination, and the trajectory selection. Standard methods of differential trajectory correction and statistical covariance analysis are employed in deriving the guidance results. A comparison is made of two instrumentation systems for planet approach orbit determination, namely, Earth-based radar tracking and on-board celestial tracking.

3.1 Orbit Determination Analysis

For a given trajectory selection, the guidance ΔV requirement is most dependent upon the accuracy of orbit determination of the spacecraft relative to the swingby planets. This is so because the departure maneuvers, especially at Saturn and Uranus, are found to be the largest contributors to the total ΔV. A major phase of the present study was therefore concerned with obtaining reasonable estimates of the orbit determination errors.

At planet approach (sphere of influence), the a priori uncertainty in the miss vector is due to the planet ephemeris error and the error remaining after tracking the spacecraft throughout the previous midcourse phase. Reduction of the a priori uncertainty can be accomplished by continued tracking during the approach phase. The degree of reduction attainable will depend upon the type of tracking system employed and upon the instrumentation errors. Two such systems are postulated for study. The first is Earth-based radar tracking (e.g., DSIF) which is currently the only system in actual use for deep space probes. It is assumed that Earth-based tracking will be the primary or only technique used during midcourse tracking of the Grand Tour. The data type assumed is sampled doppler, or, equivalently, range-rate measurements. Any improvement in orbit determination by continued radar tracking during planet approach must rely on the inherent trajectory kinematics, i. e., the effect of gravitational bending as reflected in the doppler residuals. Generally, this effect is not very significant at large range from the planet.

The second tracking model assumes an on-board celestial system, e.g., sun sensors, a Canopus tracker and a planet tracker. It is likely that the sun sensors and Canopus tracker will be on-board in any case for attitude control purposes through the flight. The additional instrument then is the planet tracker which would be operational only in the planetocentric region. The celestial data types are the directional angles of the planet as seen from the spacecraft. In contrast to Earth-based tracking, the on-board system need not rely on the gravitational bending effect since direct reference is made to the planet. This offers the potential for more accurate orbit determination earlier in the approach phase.

With reference to Figure 3.2, two separate computer programs were developed to evaluate the performance of each tracking system. In each case, the trajectories are modeled as hyperbolic conics, analytical partial derivatives are derived from the conic formulas, and the motion and measurement variables are referred to the planetocentric STR coordinate frame. Since the various error sources are best described in a statistical manner, the approach taken is to compute the error covariance matrix associated with estimating the target parameters. Optimal statistical filtering of the tracking data is assumed for the analysis. Both the Kalman filter and Weighted Least-Squares algorithms (for covariance computation) are available as options to each program. It was found that each algorithm gives approximately the same results. Generally, however, the Kalman approach was used for celestial tracking, and the Least-Squares approach was used for radar tracking. Further details of the analytical basis for the two programs are given elsewhere (Friedlander 1967) and (Gates 1964).

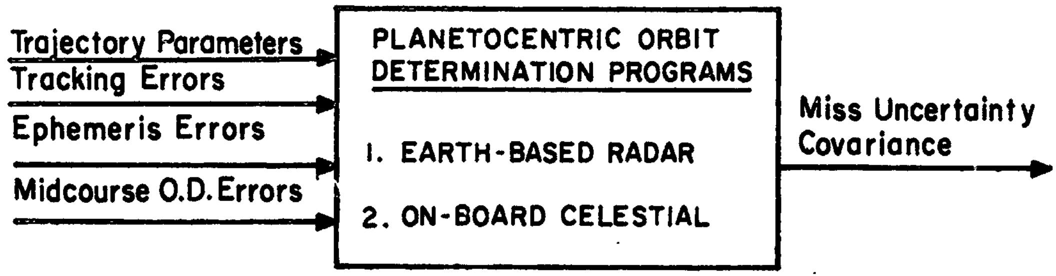

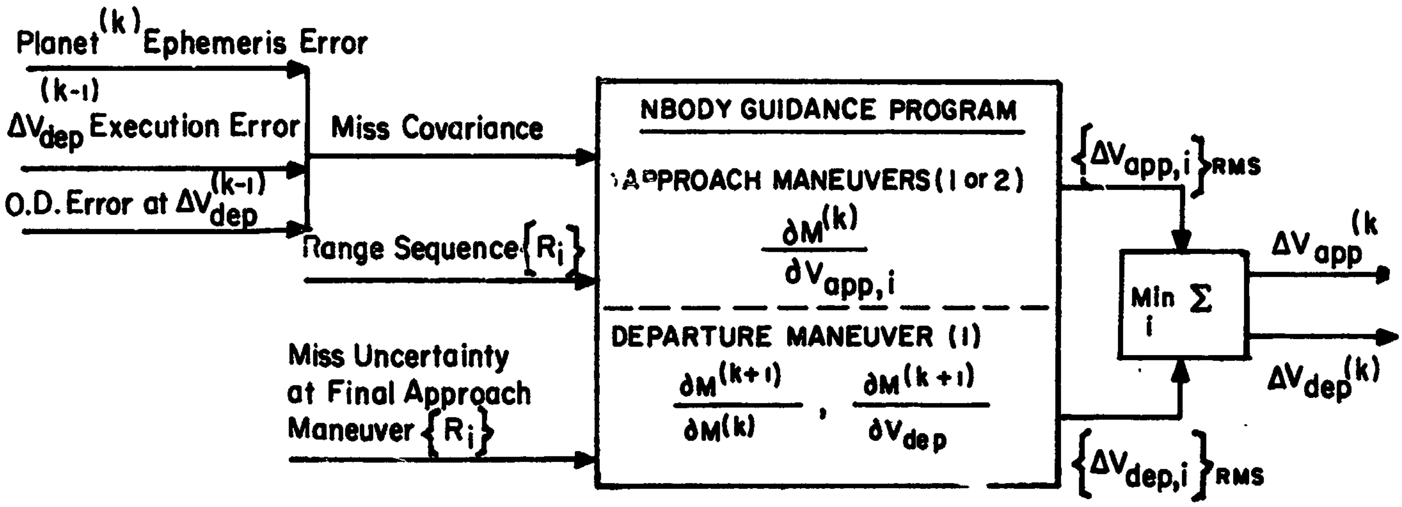

FIGURE 3.2 METHOD OF GUIDANCE ANALYSIS

3.2 Trajectory Correction Analysis

The NBODY Guidance Program illustrated in Figure 3.2 is simply a set of subroutines of the Targeting Program which compute the necessary partial derivative matrices along the nominal trajectory legs, and also the covariance matrices of the guidance maneuvers. The mapping matrix between target planes of the form $\partial \underline{m}_2/\partial \underline{m}_1$ is constructed by finite difference quotients as part of the targeting scheme. All other mapping matrices are obtained by integrating the first-order-variational equations of position and velocity.

The first guidance maneuver would take place several days after launch to compensate for the injection errors in position and velocity. If Λ_{xo} denotes the 6 x 6 covariance matrix of injection errors, then the error covariance matrix mapped to the Jupiter target plane is

$$\Lambda_{m_{10}} = \left[\frac{\partial \underline{m}}{\partial \underline{x}_o}\right] \Lambda_{x_o} \left[\frac{\partial \underline{m}}{\partial \underline{x}_o}\right]^T \tag{3.1}$$

Then, for the first guidance maneuver,

$$\Lambda_{\Delta V_1} = \left[\frac{\partial \underline{m}}{\partial \underline{v}_1}\right]^{-1} \Lambda_{m_{10}} \left[\frac{\partial \underline{m}}{\partial \underline{v}_1}\right]^{-1^T} \tag{3.2}$$

It should be noted that all guidance maneuvers correct the inpact parameters $\Delta\underline{B} \cdot \underline{T}$, $\Delta\underline{B} \cdot \underline{R}$ and the time of encounter ΔT_e. Hence, complete freedom in the magnitude and direction of the velocity correction is assumed. At this point it will be expedient to consider the general case of the approach and departure maneuvers at the k-th planet.

The effect of maneuver execution errors are considered important only for the planet departure maneuvers. This is because the time available to propagate these errors during planet approach is small in comparison to the mid-course times. The execution model assumed is a spherically distributed error proportional to the RMS magnitude of the maneuver. Thus, for the planet departure maneuver the execution covariance is

$$\Lambda_{\epsilon x}^{(k-1)} = \sigma_{\epsilon x}^2 \, \overline{\Delta V}_{dep}^{2\,(k-1)} \cdot I \tag{3.3}$$

$$\overline{\Delta V}_{dep}^{2\,(k-1)} = \text{Trace } \Lambda_{\Delta V, dep}^{(k-1)} \tag{3.4}$$

where I is a 3 x 3 identity matrix. The effect of the execution errors is mapped to the next planet by

$$\Lambda_{m,ex}^{(k)} = \left[\frac{\partial \underline{m}^{(k)}}{\partial \underline{v}_{dep}^{(k-1)}} \right] \cdot \Lambda_{\epsilon x}^{(k-1)} \left[\frac{\partial \underline{m}^{(k)}}{\partial \underline{v}_{dep}^{(k-1)}} \right]^T \tag{3.5}$$

The uncertainty in determining the spacecraft velocity just prior to the departure maneuver contributes a target error covariance $\Lambda_{m,OD}^{(k)}$ which is found by mapping similar to Eq. (3.5). Now, adding the ephemeris error of the target planet, the total error to be corrected by the approach maneuver is

$$\Lambda_{m}^{(k)} = \Lambda_{m,ex}^{(k)} + \Lambda_{m,OD}^{(k)} + \Lambda_{m,eph}^{(k)} \tag{3.6}$$

The approach maneuver is evaluated at a sequence of ranges $\{R_i\}$ from the planet beginning at about the sphere of influence. The maneuver covariance is given by

$$\Lambda_{\Delta V,app}^{(k)} = \left[\frac{\partial \underline{m}^{(k)}}{\partial \underline{v}_{app}^{(k)}}\right]^{-1} \Lambda_{m}^{(k)} \left[\frac{\partial \underline{m}^{(k)}}{\partial v_{app}^{(k)}}\right]^{-1\,T} \tag{3.7}$$

For the same range sequence, the approach orbit determination error covariance $P_{OD}^{(k)}$ is mapped into target errors at the next planet,

$$\Lambda_{m}^{(k+1)} = \left[\frac{\partial \underline{m}^{(k+1)}}{\partial \underline{m}^{(k)}}\right] P_{OD}^{(k)} \left[\frac{\partial \underline{m}^{(k+1)}}{\partial \underline{m}^{(k)}}\right]^{T} \tag{3.8}$$

and the departure maneuver covariance is computed from

$$\Lambda_{\Delta V,dep}^{(k)} = \left[\frac{\partial \underline{m}^{(k+1)}}{\partial \underline{v}_{dep}^{(k)}}\right]^{-1} \Lambda_{m}^{(k+1)} \left[\frac{\partial \underline{m}^{(k+1)}}{\partial \underline{v}_{dep}^{(k)}}\right]^{-1\,T} \tag{3.9}$$

It is assumed that the departure maneuver is made at the planet's sphere of influence.

Finally, an approximate optimization of the maneuvers at each planet is accomplished by finding that R_i which results in a minimum sum of the approach and departure velocity corrections (RMS values). The individual maneuver RMS values are then taken corresponding to the optimal R_i. If two approach maneuvers are allowed, the first is made at R_1 which is about 50 x 10^6 km from the planet. Then, the second maneuver must correct the approach orbit determination error at that point i.e., $P_{OD}^{(k)}$ (R_1). Substituting this new value for $\Lambda_m^{(k)}$ in Eq. (3.7), the second maneuver is evaluated at the remaining points R_2, R_3,... R_N.

The previous Eqs. (3.8) and (3.9) describe how errors in the arrival conditions at one planet are propagated to the next, and determine the planet departure maneuver necessary to correct these errors. Since mere substitution of numerical values for the partial derivative matrices would contribute little to a basic understanding of the problem, it would be helpful to describe the error sensitivity by analytical expressions. Such expressions may be derived using the conic formulas of the hyperbolic encounter.

To simplify the problem, it is assumed that the departure maneuver nulls the error in the departure hyperbolic velocity vector. The encounter time error is neglected since its effect is small in comparison to errors in b and θ. From Eqs. (2.3) to (2.10), the sensitivity of the departure velocity may be expressed as

$$\frac{\partial \underline{V}_{h2}}{\partial b} = \frac{V_h^3\,(1-\cos\Psi)}{\mu}\left[\sin\Psi\ \underline{S} + \cos\Psi\ \cos\theta\ \underline{T} + \cos\Psi\ \sin\theta\ \underline{R}\right] \tag{3.10}$$

$$\frac{\partial \underline{V}_{h2}}{b\partial\theta} = \frac{V_h\ \sin\Psi}{b}\left[\sin\theta\ \underline{T} - \cos\theta\ \underline{R}\right] \tag{3.11}$$

Since we have assumed $\Delta V_{dep}^2 \approx \Delta\underline{V}_{h2} \cdot \Delta\underline{V}_{h2}$,

$$\Delta V_{dep}^2 \approx \left[\frac{\partial \underline{V}_{h2}}{\partial b} \cdot \frac{\partial \underline{V}_{h2}}{\partial b}\right]^2 (\Delta b)^2 + \left[\frac{\partial \underline{V}_{h2}}{b\partial\theta} \cdot \frac{\partial \underline{V}_{h2}}{b\partial\theta}\right]^2 (b\Delta\theta)^2$$

$$= \left[\frac{V_h^3\ (1-\cos\Psi)}{\mu}\right]^2 (\Delta b)^2 + \left[\frac{V_h\ \sin\Psi}{b}\right]^2 (b\Delta\theta)^2$$

Using Eq. (2.6), the bracketed terms above are found to be equal. Therefore, the departure maneuver is equally sensitive to in-plane and out-of-plane error components of $\underline{B}$ (actually, the orbit determination errors)

$$\Delta V_{dep} \approx \left(\frac{V_h \sin\Psi}{b}\right) \left[(\Delta b)^2 + (b\Delta\theta)^2\right]^{1/2} \qquad (3.12)$$

From Table (2.1), it is seen that the parenthetical sensitivity factor in Eq. (3.12) is much larger for the Interior Ring Passage trajectories. Also, this factor is generally smallest for the Jupiter swingby and largest for the Uranus swingby. Taking the 1977-I mission as an example, the maneuver sensitivity at Jupiter, Saturn and Uranus is, respectively, 16, 113 and 165 m/sec per 1000 km.

An approximate analytical expression for the approach maneuver may be derived quite simply. Assume that the approach maneuver is made at a range R >> b, and that this maneuver nulls the two error components of $\underline{B}$ but neglects the error in encounter time. Then, for a field-free space approximation

$$\Delta V_{app} \approx \frac{V_h}{R} \left[(\Delta b)^2 + (b\Delta\theta)^2\right]^{1/2} \qquad (3.13)$$

which shows the maneuver sensitivity to be inversely proportional to range. Equations (3.12) and (3.13) are very useful in checking and interpreting the numerical results obtained from Eqs. (3.7) to (3.9).

3.3 Results of Guidance Analysis

Table 3.2 lists the various error sources considered in this study. Items 3, 4 and 5 contribute directly to trajectory errors (perturbations), whereas the remaining terms contribute to trajectory uncertainty via the orbit determination process. Midcourse disturbances due to solar pressure uncertainties and attitude control gas leaks are found to have a relatively small effect for this mission. The injection accuracy assumed is typical of a Centaur upper stage launch vehicle. It is noted, however, that injection errors have a small effect on the total ΔV requirements of this mission. The maneuver execution error of 1% is perhaps somewhat conservative for a post-1975 attitude control system. Planet ephemeris errors of 0.2 sec arc in latitude and longitude are representative of the best astrometric observations from Earth. The data noise and station location errors assumed for radar tracking represent the projected improvement in the DSIF accuracy (JPL Series, SPS Vol. III). Optical sensor errors assumed for the on-board tracking mode are typical of such systems currently under development (Barone 1967). The designation "a priori" in Table 3.2 means initial values of error sources which are also being estimated along with the miss vector. For example, the gravitational constant uncertainty is greatly reduced during the radar tracking mode. Compensation for the data bias is also effective as on-board observations are accumulated.

TABLE 3.2 ASSUMED ERROR SOURCES (RMS VALUES)

1.	PLANET EPHEMERIS (A Priori)		
	Latitude, Longitude	0.2 sec arc	
	Radial Distance	R_p (AU) x 200 km	
2.	PLANET GRAVITATIONAL CONSTANT (A Priori)		
	0.1%		
3.	MIDCOURSE DISTURBANCES		
	Solar Pressure	5% Uncertainty	Negligible
	Gas Leaks	10^{-10} m/sec^2	Effect
4.	INJECTION ACCURACY		
	Position	10 km	
	Velocity	16 m/sec	
5.	MANEUVER EXECUTION ERROR		
	1% Spherically Distributed		
6.	EARTH-BASED RADAR TRACKING		
	Data Samples	480 sec	
	Data Noise	0.005 m/sec	
	Station Location	3 m	
7.	ON-BOARD CELESTIAL TRACKING		
	Data Samples	2 hrs	
	Data Noise	6 sec arc	
	Data Bias	200 sec arc (A Priori)	
	Planet Center - Finder Bias	0.3% Planet Diameter (A Priori)	

3.3.1 Orbit Determination Errors

The error analysis was applied to each of the four trajectory selections. On-board planet tracking was found to be superior to Earth-based radar tracking in determining the miss components at each planet. The only exception to this is the Jupiter approach where the in-plane miss uncertainty, σ_b, is less in the case of radar tracking. A comparison of the two tracking modes for the 1977-I Grand Tour is shown in Figures 3.3 to 3.8. The RMS uncertainties of the in-plane and out-of-plane miss components are plotted as a function of range to the planet beginning at the initial data acquisition range of 50 x 10^6 km. It is noted that celestial tracking is effective in reducing the uncertainties in both miss components, whereas radar tracking information is rather insensitive to the out-of-plane component.

Taking the Uranus encounter as a worst case comparison, it is seen that radar tracking yields little or no reduction of the initial uncertainty until the range decreases to about 2 x 10^6 km. At this point the gravitational bending effect becomes more pronounced. Even then, the out-of-plane component remains poorly determined until nearer closest approach. In contrast, celestial tracking yields an early and continuing reduction of the miss uncertainty. For example, at a range of 25 x 10^6 km, $b\sigma_\theta$

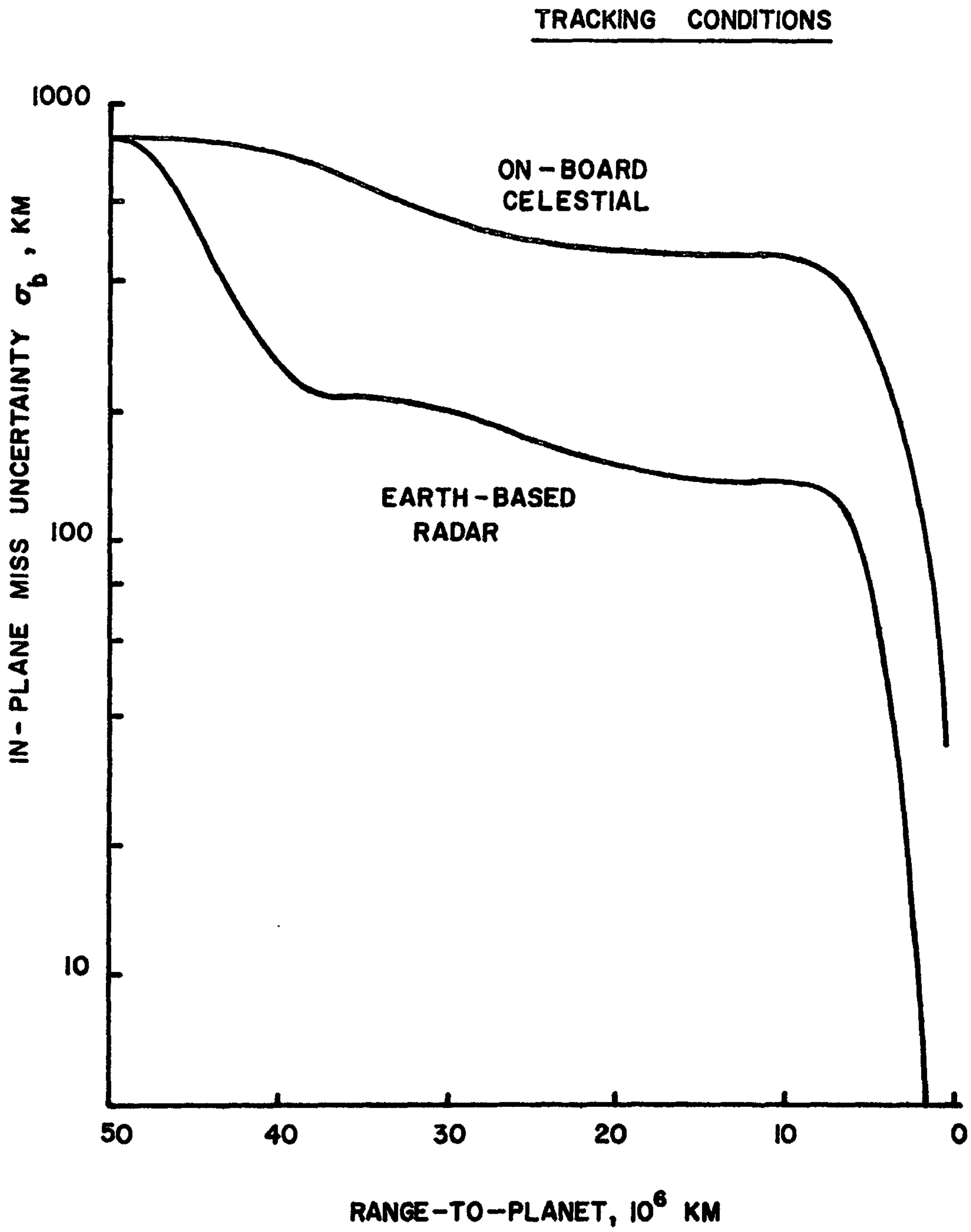

FIGURE 3.3 IN-PLANE MISS UNCERTAINTY FOR JUPITER APPROACH ORBIT DETERMINATION, 1977-I GRAND TOUR

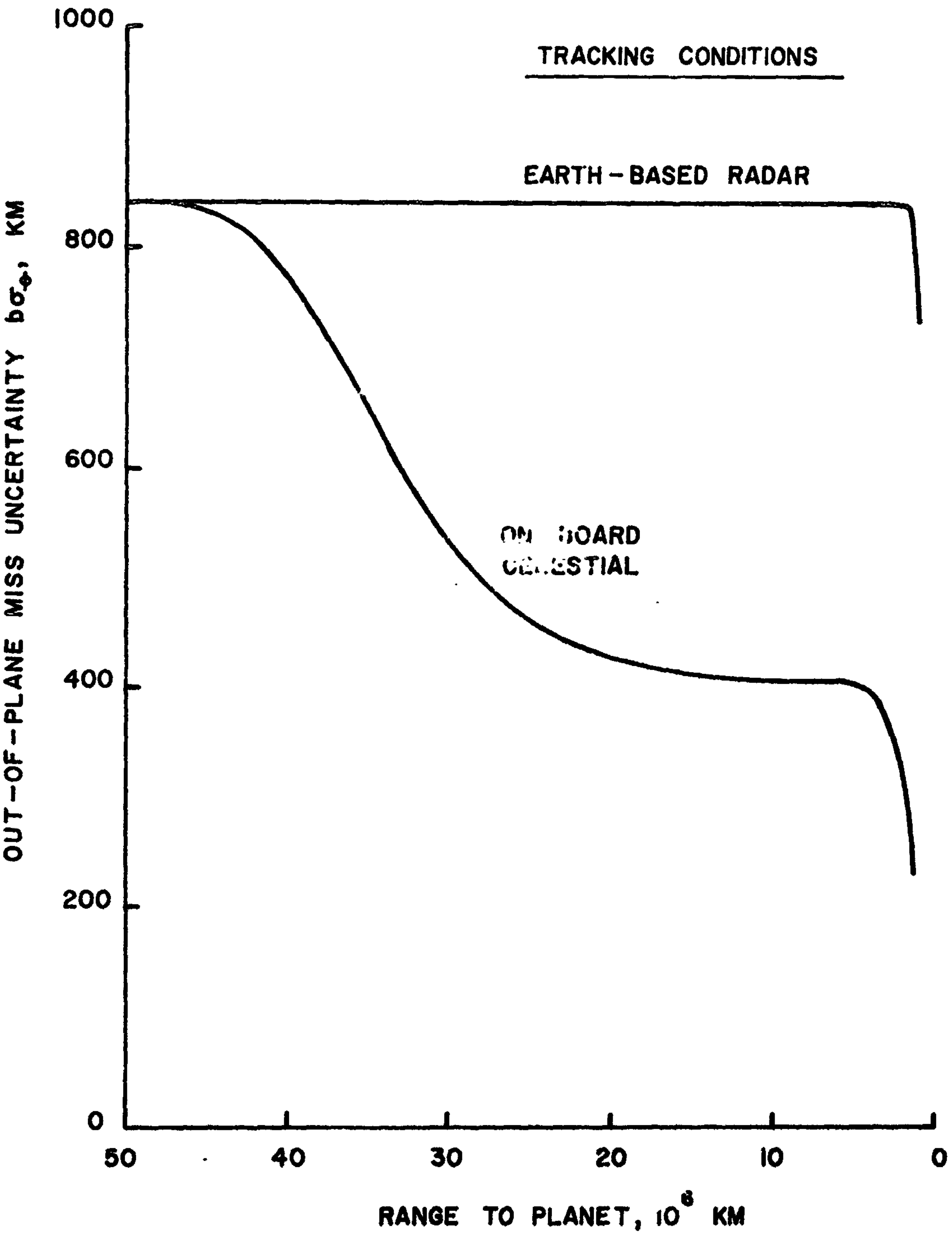

FIGURE 3.4 OUT-OF-PLANE MISS UNCERTAINTY FOR JUPITER APPROACH ORBIT DETERMINATION, 1977-I GRAND TOUR

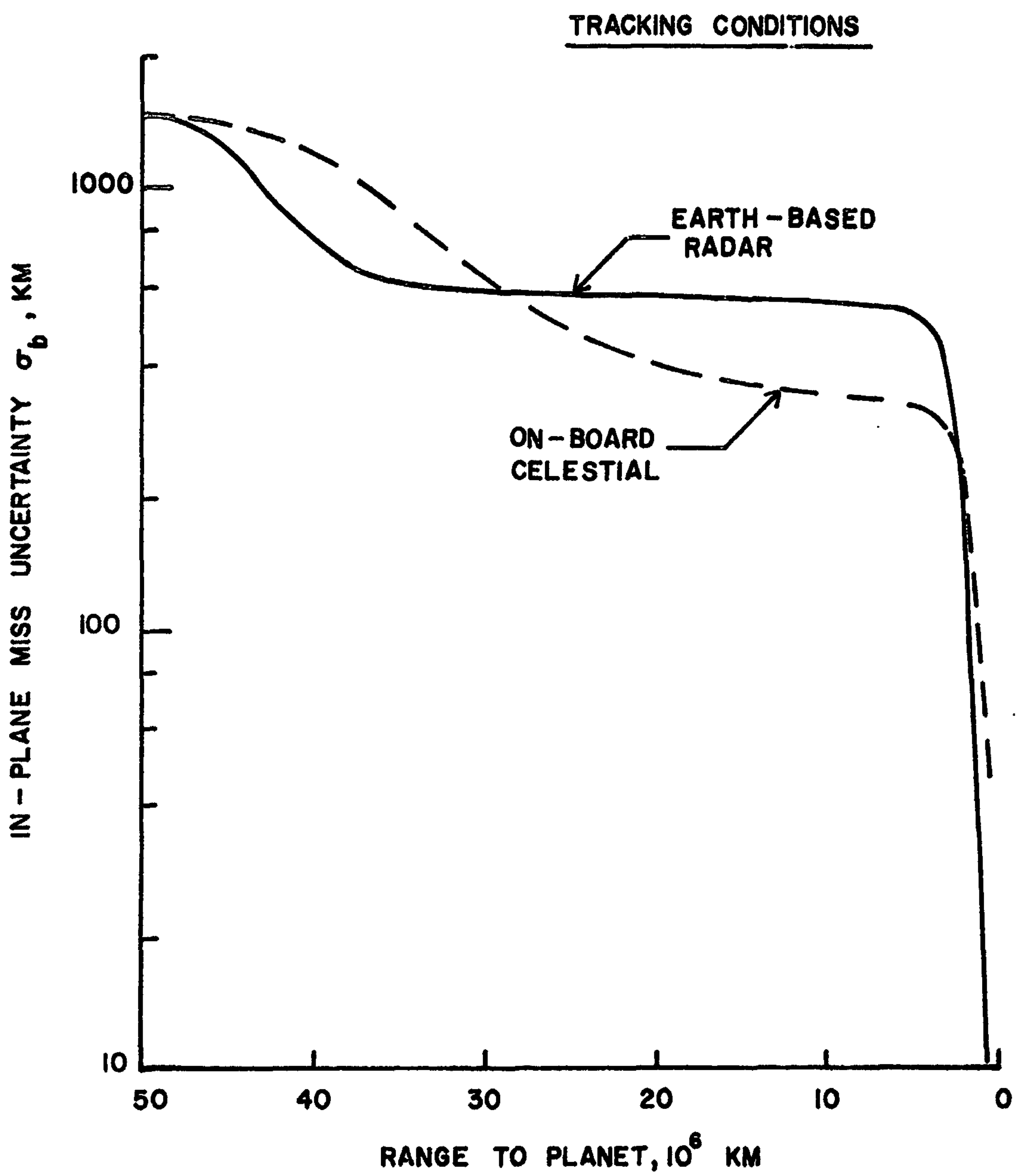

FIGURE 3.5 IN-PLANE MISS UNCERTAINTY FOR SATURN APPROACH ORBIT DETERMINATION, 1977-I GRAND TOUR

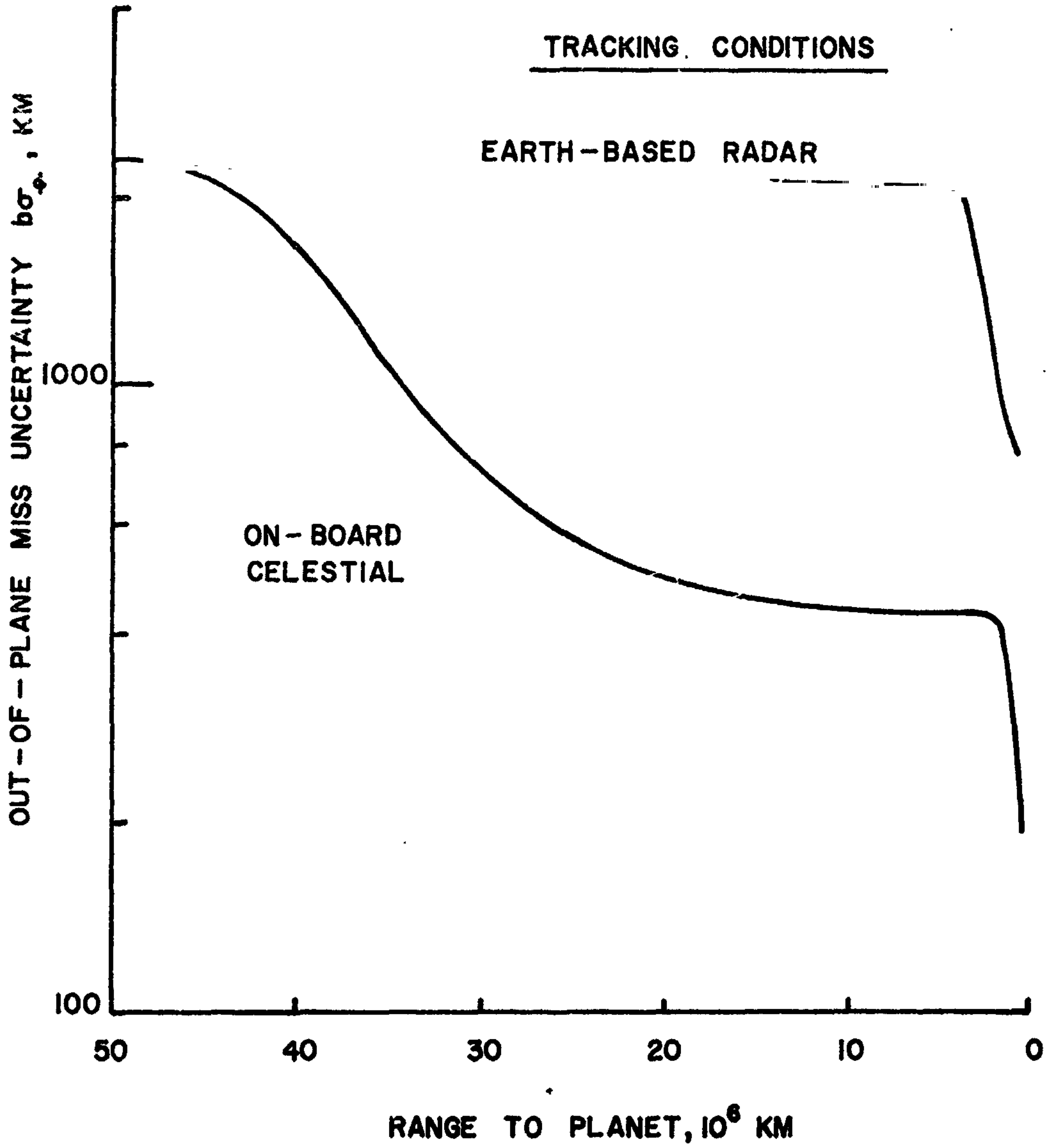

FIGURE 3.6 OUT-OF-PLANE MISS UNCERTAINTY FOR SATURN APPROACH ORBIT DETERMINATION, 1977-I GRAND TOUR

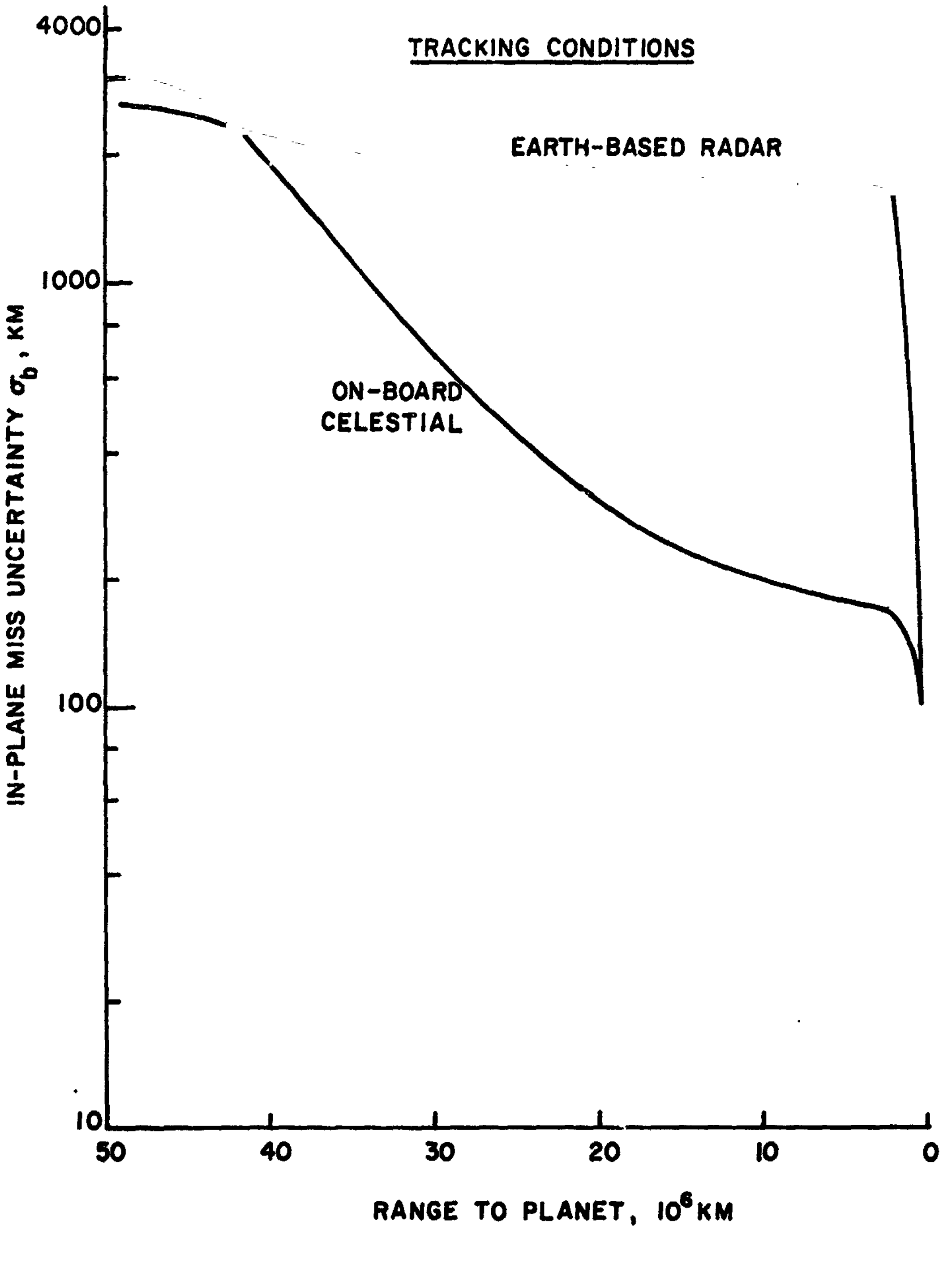

FIGURE 3.7 IN-PLANE MISS UNCERTAINTY FOR URANUS APPROACH ORBIT DETERMINATION, 1977 - I GRAND TOUR.

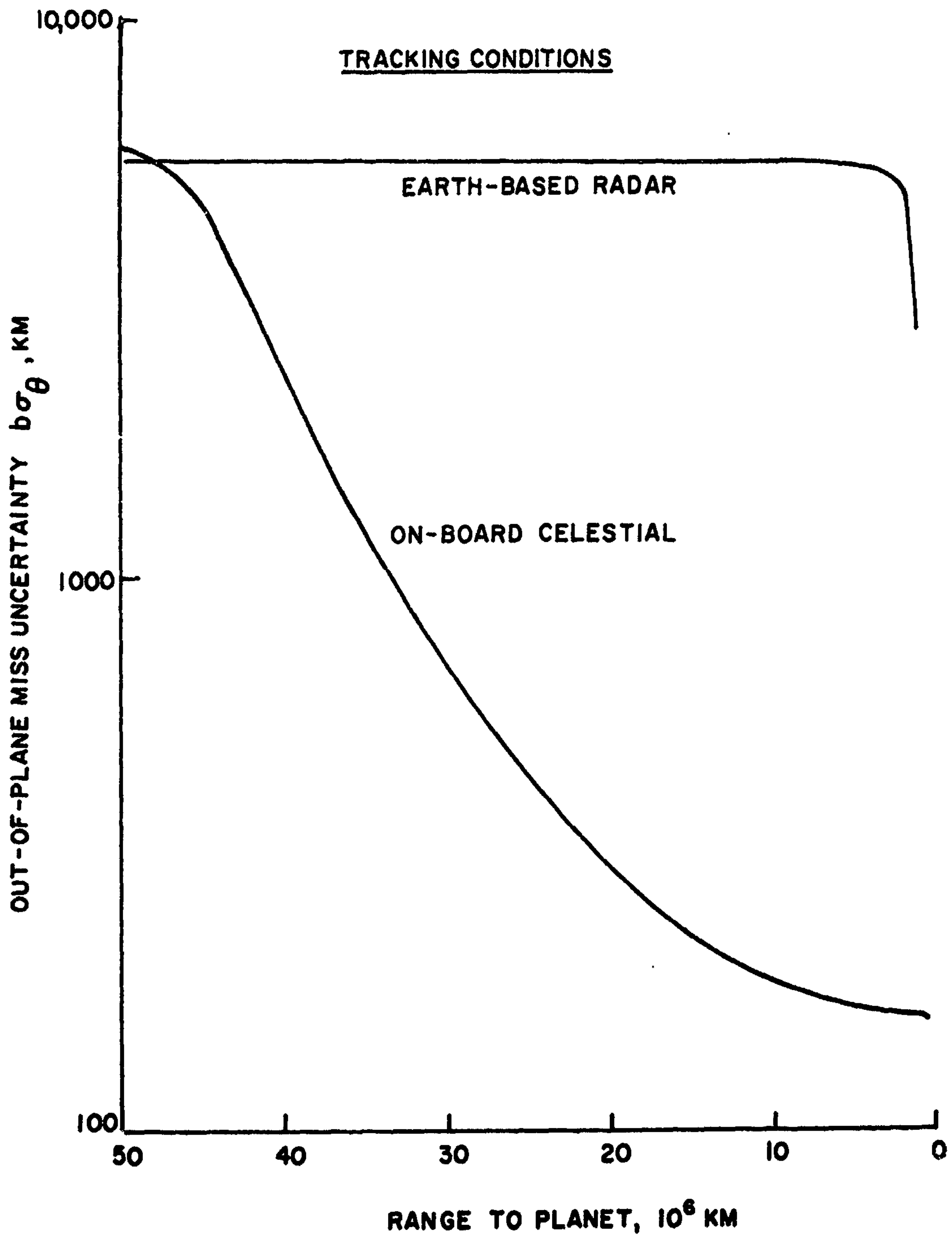

FIGURE 3.8 OUT-OF-PLANE MISS UNCERTAINTY FOR URANUS APPROACH ORBIT DETERMINATION, 1977 - I GRAND TOUR

is 5600 km for radar tracking but only 440 km for celestial tracking. At a range of 10^6 km, the respective uncertainties are 2800 km and 160 km.

Earth-based radar tracking gives better results in estimating the encounter time and the planet's gravitational constant. This is shown for each of the planets in Figures 3.9 and 3.10.

3.3.2 Scheduling of Guidance Maneuvers

As a result of the orbit determination characteristics, the ΔV cost of guidance for the Grand Tour can be quite sensitive to the times at which the planet approach maneuvers are made. The opportunity for minimizing the total ΔV requirement by appropriately scheduling the maneuvers cannot afford to be neglected. To illustrate this point, consider the Uranus swingby on the 1977-I mission. Figure 3.11 shows the approach maneuver requirements as a function of planet range. The celestial tracking mode requires a smaller ΔV for a single correction because the approach error is smaller. This simply reflects the better showing of celestial tracking at Saturn; more accurate orbit determination implies a small departure maneuver which in turn implies smaller execution errors. Figure 3.12 compares the two tracking modes for the Uranus depature maneuver. This result reflects the orbit determination accuracy of Figures 3.7 and 3.8.

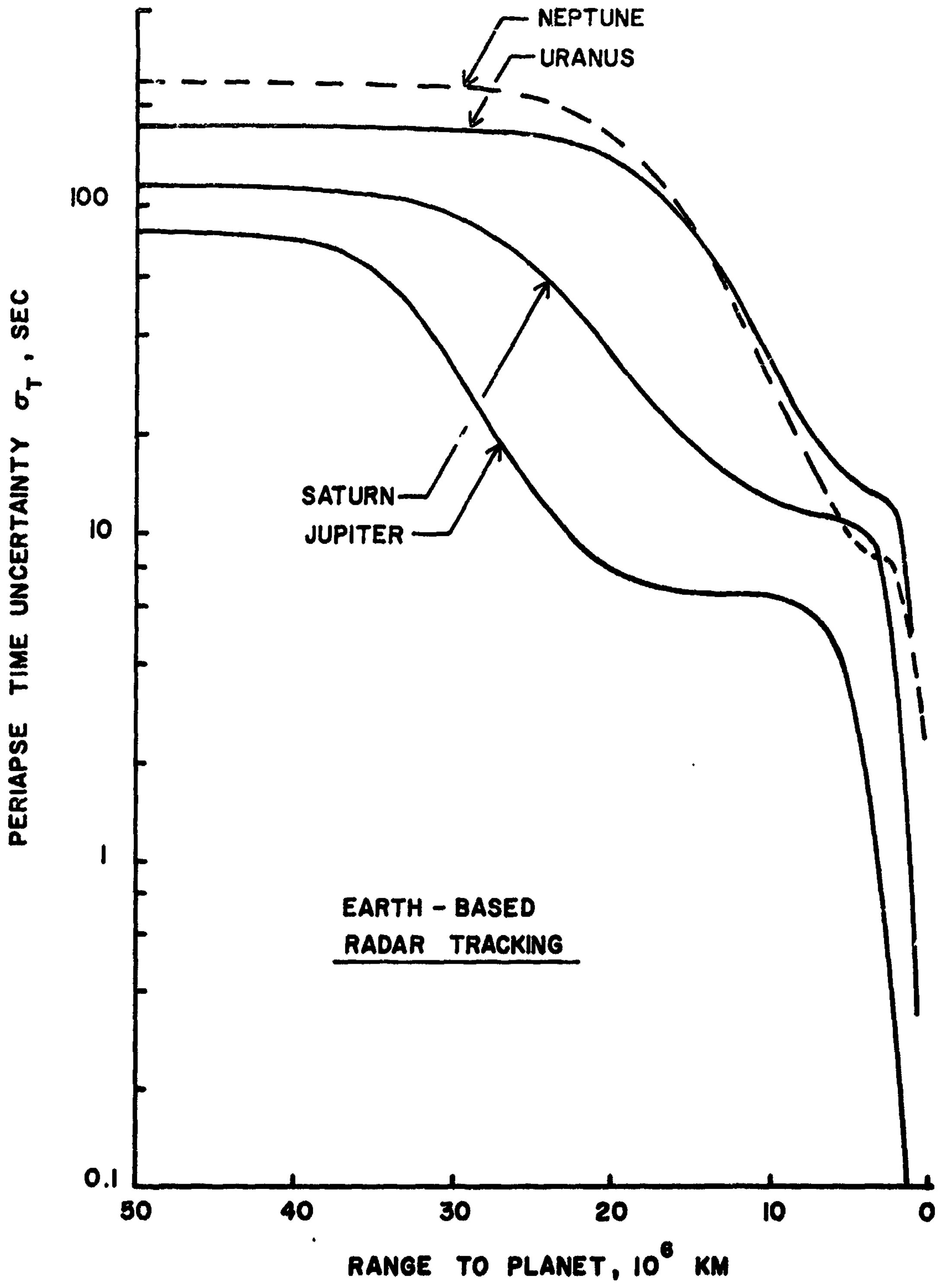

FIGURE 3.9 ENCOUNTER TIME UNCERTAINTY FROM PLANET APPROACH ORBIT DETERMINATION, 1977-I GRAND TOUR

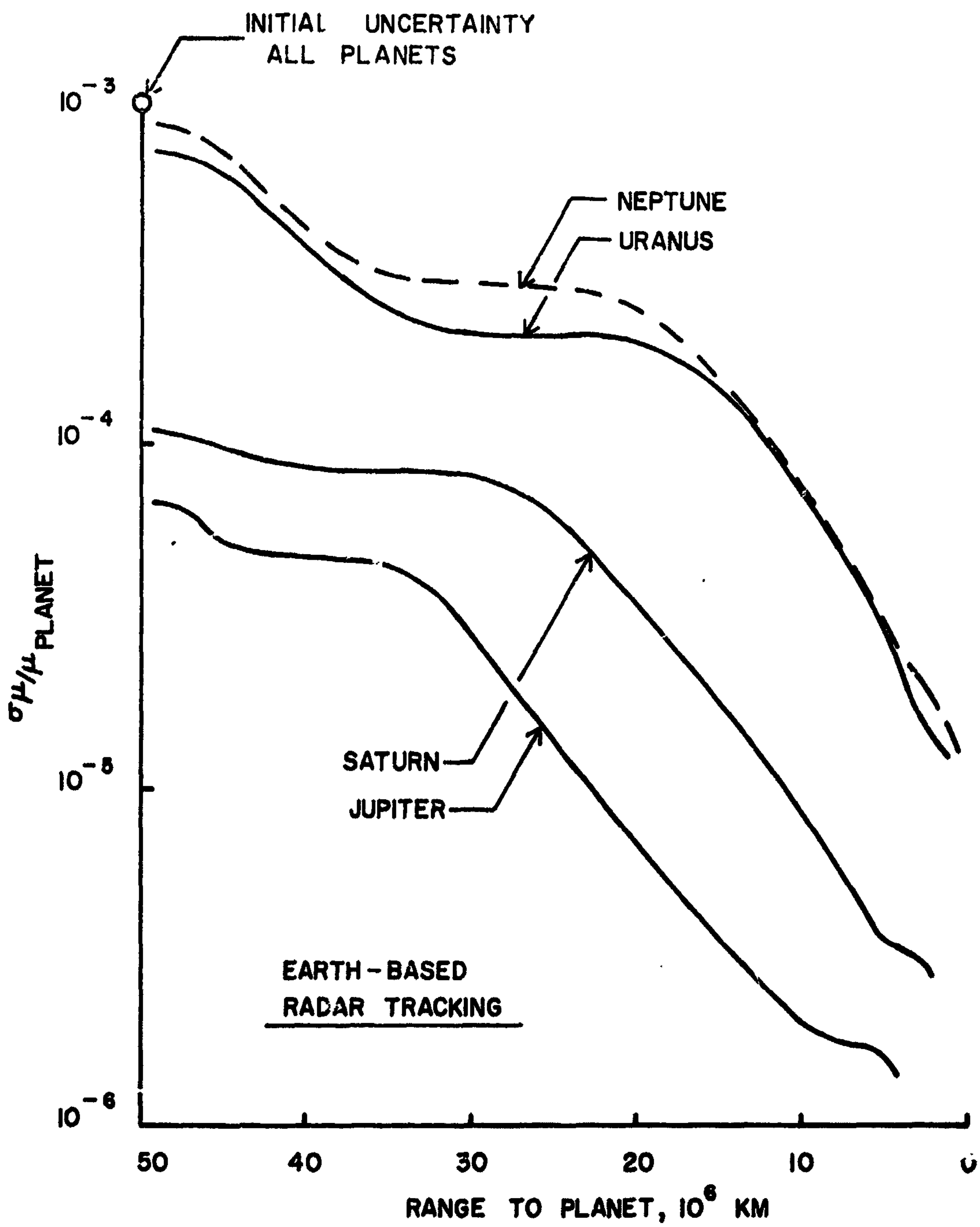

FIGURE 3.10 DETERMINATION OF GRAVITATIONAL CONSTANT (MASS) DURING PLANET SWINGBY, 1977-I GRAND TOUR

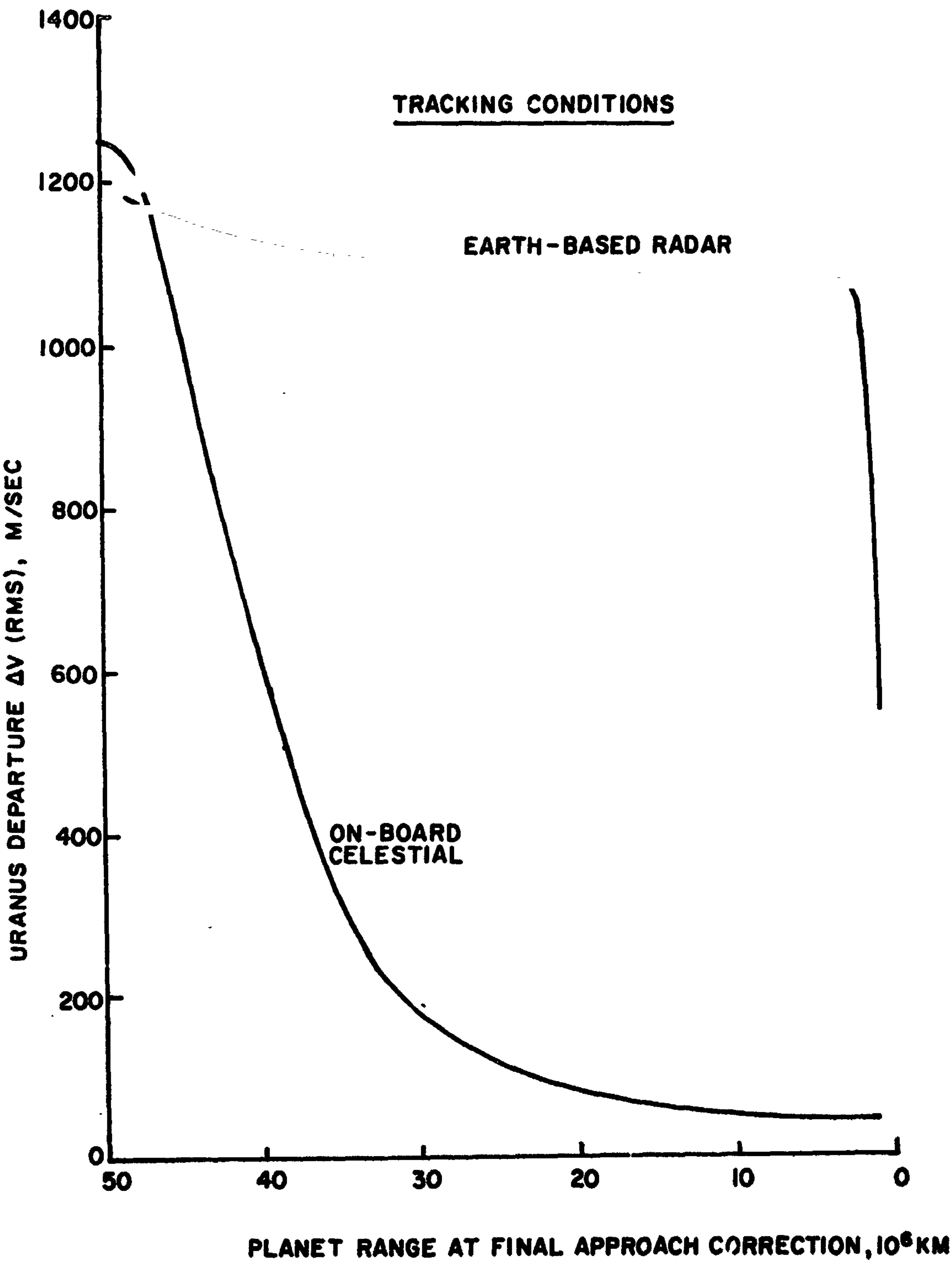

FIGURE 3.11 VELOCITY CORRECTION REQUIREMENT FOR URANUS DEPARTURE, 1977 - I GRAND TOUR

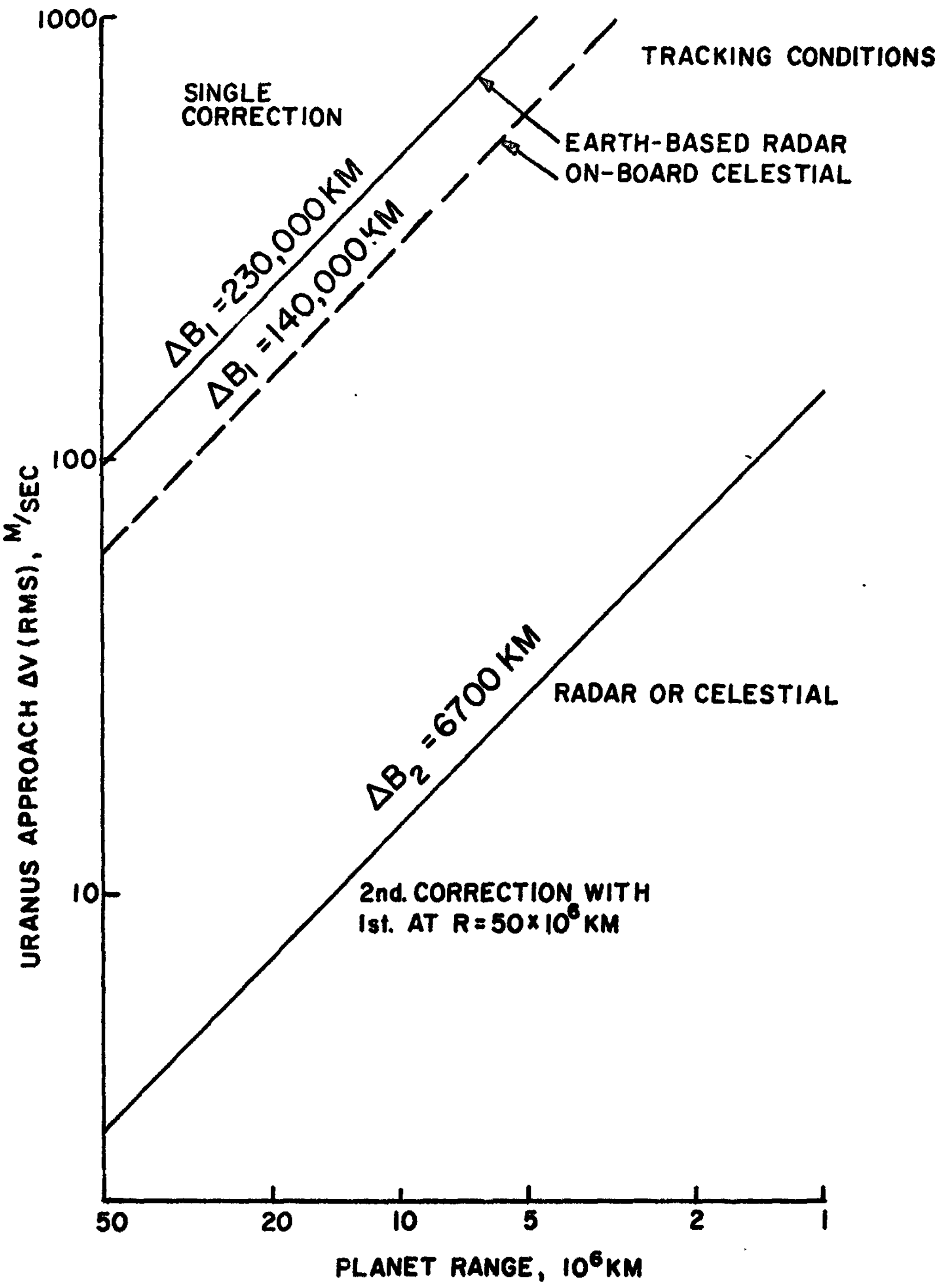

FIGURE 3.12 VELOCITY CORRECTION REQUIREMENT FOR URANUS APPROACH, 1977 - 1 GRAND TOUR

Optimization of the Uranus encounter maneuvers is illustrated in Figure 3.13. If only one approach maneuver were allowed, the minimum mean sum ΔV at Uranus encounter is 1100 m/sec for radar tracking, but only 200 m/sec for celestial tracking. Allowing two approach maneuvers reduces the requirement to 680 m/sec and 110 m/sec, respectively. For the latter case with radar tracking, the best range for the final approach maneuver is about 10^6 km, resulting in RMS values for the Uranus maneuvers of 98, 133 and 549 m/sec. For celestial tracking, the optimal range is about 10×10^6 km, and the RMS values of the maneuvers are 61, 14 and 47 m/sec.

It should be noted that the radar tracking results may be somewhat optimistic since the final approach maneuver is made only 14 hours before encounter (closest approach). The round trip communication time to Uranus is about 5.5 hours. If the maneuver computation and command were Earth-based, this time differential appears to be marginal at best. Even if this were tolerable, the second approach maneuver would increase from 133 m/sec to about 220 m/sec due to the decreased range over the 5.5 hour period. This fact might be kept in mind when interpreting the summary results to be given since these results assume an instantaneous correction capability. In other words, the celestial tracking mode may be even more favorable than is apparent.

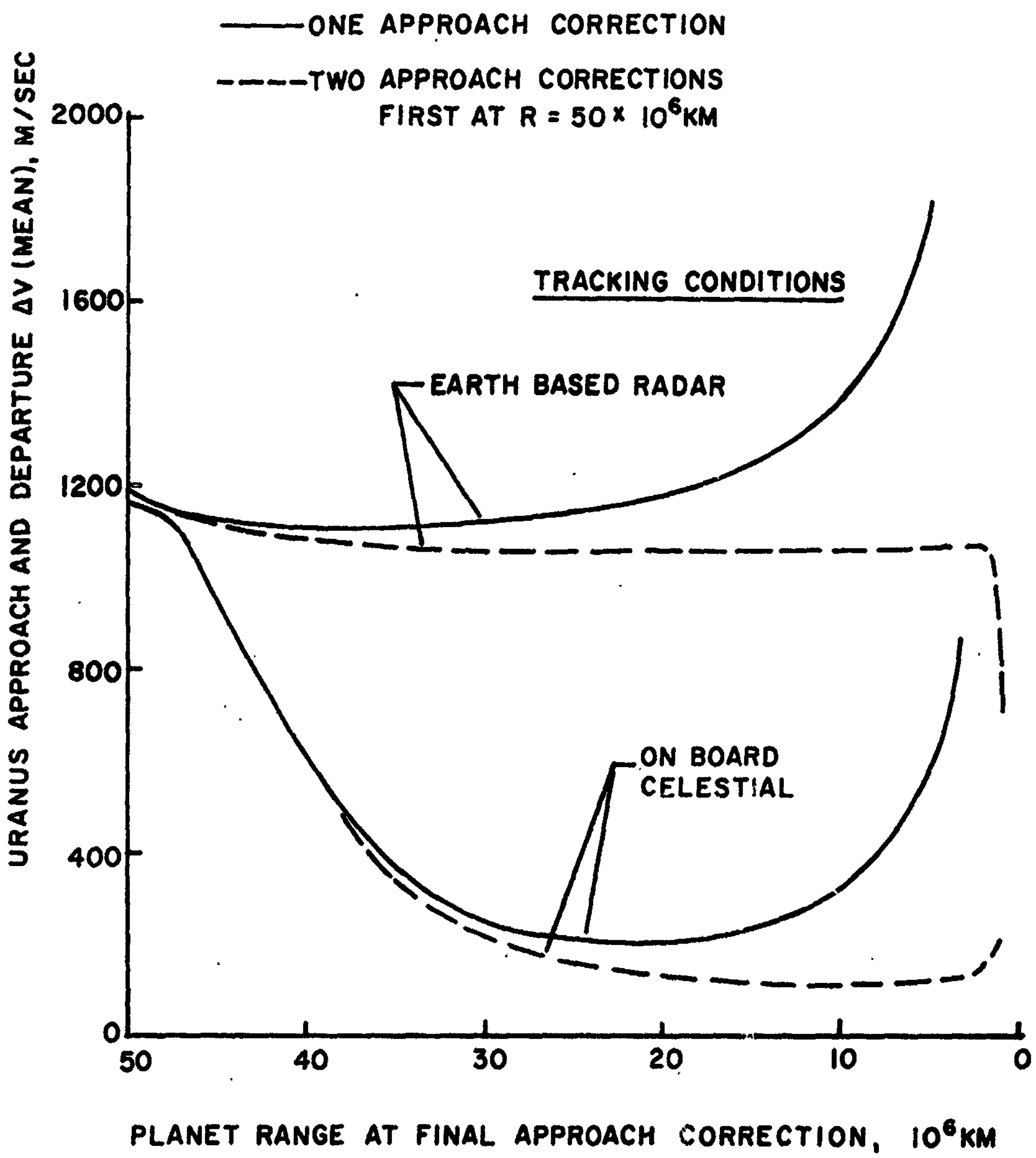

FIGURE 3.13 OPTIMIZATION OF URANUS ENCOUNTER VELOCITY CORRECTION REQUIREMENTS, 1977 - I GRAND TOUR

3.3.3 Summary of ΔV Requirements

Tables 3.3 and 3.4 list the RMS values of the individual guidance maneuvers and the times at which they are made for each of the four trajectory selections and the two tracking modes. These results are obtained by the aforementioned method of minimizing the sum of the approach and departure maneuvers at each planet encounter. The smallest ΔV's are associated with the Jupiter encounter and the largest with the Uranus encounter. Total maneuver requirements are listed in terms of a mean +3 sigma value which is based on a Rayleigh distribution matched to the individual RMS values. The Rayleigh distribution has been found to be an excellent approximation to the actual statistical distribution of ΔV magnitude (Sturms 1966).

The effect of the trajectory selection and the orbit determination tracking mode is summarized by the matrix of total ΔV requirements shown in Table 3.5. In the case of radar tracking, the total ΔV could be as small as 354 m/sec for the 1978-E mission or as high as 1712 m/sec for the 1977-I mission. The large ΔV difference between the Interior Ring Passages of 1977 and 1978 is attributed to larger orbit determination (radar) errors at Saturn and Uranus for the 1977 mission. This is due to differences in planet approach geometry as viewed from the Earth. A comparison of the two tracking modes shows a very

TABLE 3.3 GRAND TOUR ΔV REQUIREMENTS FOR EARTH-BASED RADAR TRACKING

ΔV (RMS), M/SEC

GUIDANCE MANEUVERS	Grand Tour Trajectories			
	1977-E	1977-I	1978-E	1978-I
Post-Earth Injection (I+10d)	13	9	9	9
Jupiter Approach	5 (E-66d)**	4 (E-37d)	3 (E-52d)	4 (E-32d)
Jupiter Departure	10 (E+64d)	29 (E+43d)	7 (E+50d)	19 (E+38d)
1st Saturn Approach	11 (E-15d)	9 (E-34d)	28 (E-5d)	5 (E-34d)
2nd Saturn Approach	———	44 (E-14hr)	———	25 (E-28hr)
Saturn Departure	69 (E+58d)	127 (E+37d)	37 (E+55d)	86 (E+37d)
1st Uranus Approach	48 (E-39d)	98 (E-27d)	25 (E-38d)	63 (E-27d)
2nd Uranus Approach	48 (E-36hr)	133 (E-14hr)	51 (E-36hr)	131 (E-13hr)
Uranus Departure	62 (E+40d)	549 (E+28d)	56 (E+39d)	260 (E+28d)
Uranus-Neptune Midcourse	10	20	10	10
TOTALS (Mean + 3 Sigma)*	450 m/sec	1712 m/sec	354 m/sec	1010 m/sec

*Based on Assumed Rayleigh Distribution for ΔV Maneuvers With Full Correlation Between Approach (k+1) Maneuver and Departure (k) Maneuver.

**E is Time of Encounter.

TABLE 3.4 GRAND TOUR ΔV REQUIREMENTS FOR ON-BOARD CELESTIAL TRACKING

ΔV (RMS), M/SEC

GUIDANCE MANEUVERS	Grand Tour Trajectories			
	1977-E	1977-I	1978-E	1978-I
Post-Earth Injection (I+10d)	13	9	9	9
Jupiter Approach	5 (E-66d)**	7 (E-21d)	5 (E-23d)	6 (E-19d)
Jupiter Departure	10 (E+64d)	20 (E+43d)	4 (E+50d)	11 (E+38d)
1st Saturn Approach	8 (E-20d)	22 (E-10d)	6 (E-13d)	14 (E-10d)
2nd Saturn Approach	———	———	———	———
Saturn Departure	20 (E+58d)	79 (E+37d)	27 (E+55d)	70 (E+37d)
1st Uranus Approach	30 (E-20d)	61 (E-27d)	37 (E-14d)	51 (E-27d)
2nd Uranus Approach	———	14 (E-5d)	———	13 (E-5d)
Uranus Departure	24 (E+40d)	47 (E+28d)	23 (E+39d)	35 (E+28d)
Uranus-Neptune Midcourse	5	5	5	5
TOTALS (Mean + 3 Sigma)*	190 m/sec	428 m/sec	203 m/sec	372 m/sec

*Based on Assumed Rayleigh Distribution for ΔV Maneuvers With Full Correlation Between Approach (k+1) Maneuver and Departure (k) Maneuver.

**E is Time of Encounter.

TABLE 3.5

SUMMARY OF GUIDANCE ΔV REQUIREMENTS
FOR THE GRAND TOUR MISSION

ΔV TOTAL (MEAN + 3 SIGMA)*

TRAJECTORY SELECTION	ORBIT DETERMINATION TRACKING CONDITIONS	
	EARTH-BASED RADAR	ON-BOARD CELESTIAL
1977-E	450 M/SEC	190 M/SEC
1977-I	1712	428
1978-E	354	203
1978-I	1010	372

*BASED ON ASSUMED RAYLEIGH DISTRIBUTION FOR ΔV MANEUVERS WITH PERFECT CORRELATION BETWEEN APPROACH (K+1) MANEUVER AND DEPARTURE (K) MANEUVER.

significant advantage to on-board celestial tracking. In this case, the Interior Ring Passages would require about 400 m/sec, and the Exterior Ring Passages would require only about 200 m/sec.

The ΔV's listed in Table 3.5 are indicative of the total propellant loading of a spacecraft. For example, assuming a propellant specific impulse of 235 seconds, the propellant loading corresponding to 190 m/sec is 8% of the spacecraft weight. The propellant loading corresponding to 1712 m/sec is 53%.

3.3.4 Guidance Accuracy

On the question of guidance accuracy, either tracking mode should provide adequate control of the flyby trajectories at each planet for purposes of the scientific experiments to be carried out. Approach guidance accuracy data for the 1977-I Grand Tour is listed in Table 3.6. Figures 3.14 to 3.17 illustrate the miss dispersions before and after the approach maneuvers. The most severe guidance accuracy requirement of any of the Grand Tour Missions occurs at Saturn on the Interior Ring Passage trajectory. Here, the spacecraft must pass between the surface and the inner Ring boundary. Figure 3.16 shows that the 3σ miss dispersion for either tracking mode meets the accuracy requirement.

TABLE 3.6 GUIDANCE ACCURACY FOR 1977 - I GRAND TOUR

	EARTH-BASED RADAR		ON-BOARD CELESTIAL	
	σ_b	$b\sigma_\theta$	σ_b	$b\sigma_\theta$
JUPITER[1]	260 km	840 km	500 km	470 km
SATURN[1]	90	880	370	390
URANUS[1]	750	2800	180	190
NEPTUNE[2]	13,000	12,000	13,000	12,000

1. Corresponds to Errors at Final Approach Maneuver.
2. Assumes No Neptune Approach Maneuver. If necessary, this error can be reduced by a factor of 2 or 3 by making a late correction on the Uranus - Neptune trajectory leg. The ΔV cost should be under 10 m/sec.

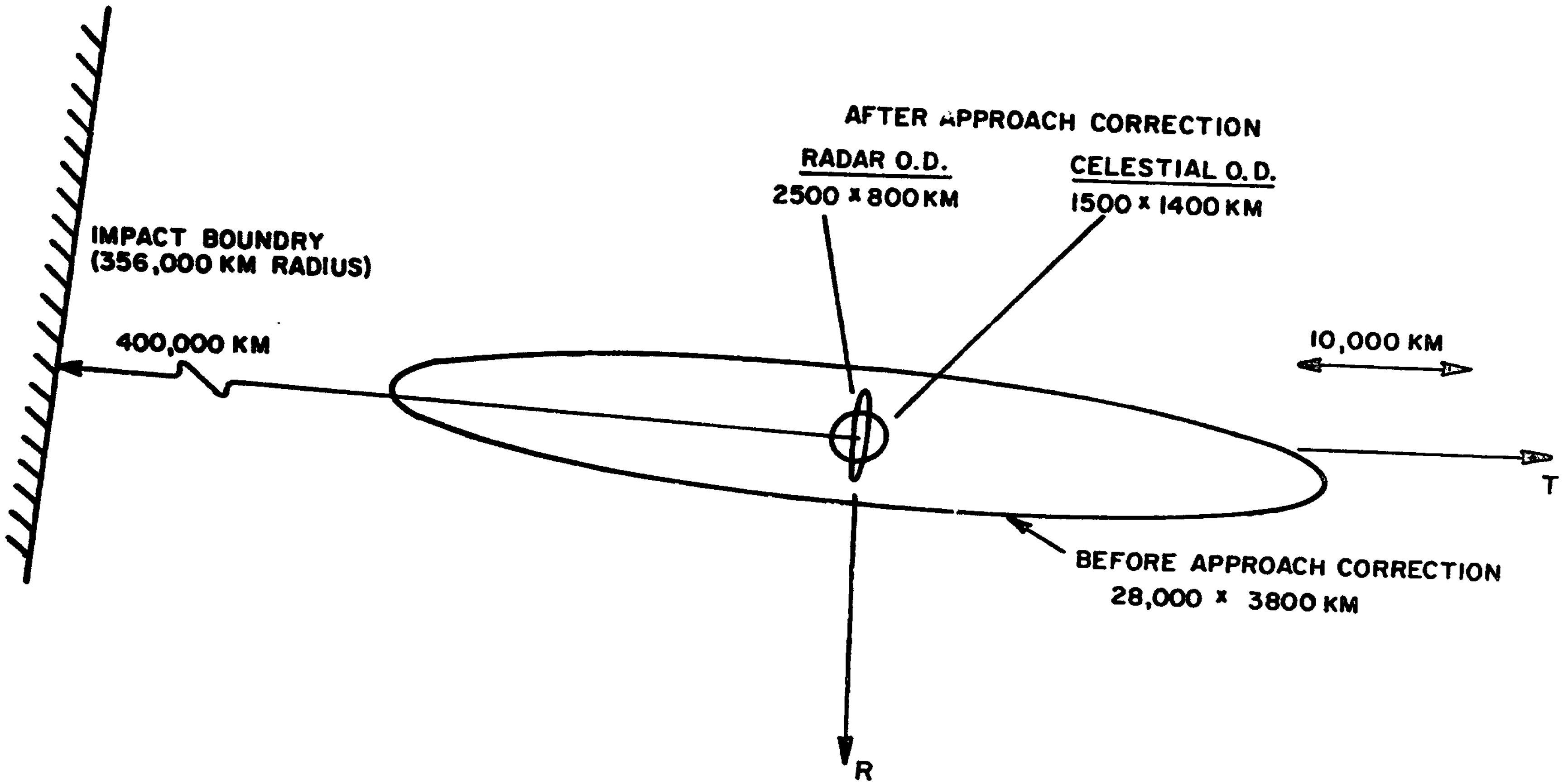

FIGURE 3.14 3σ MISS ELLIPSES FOR JUPITER ENCOUNTER, 1977-I GRAND TOUR

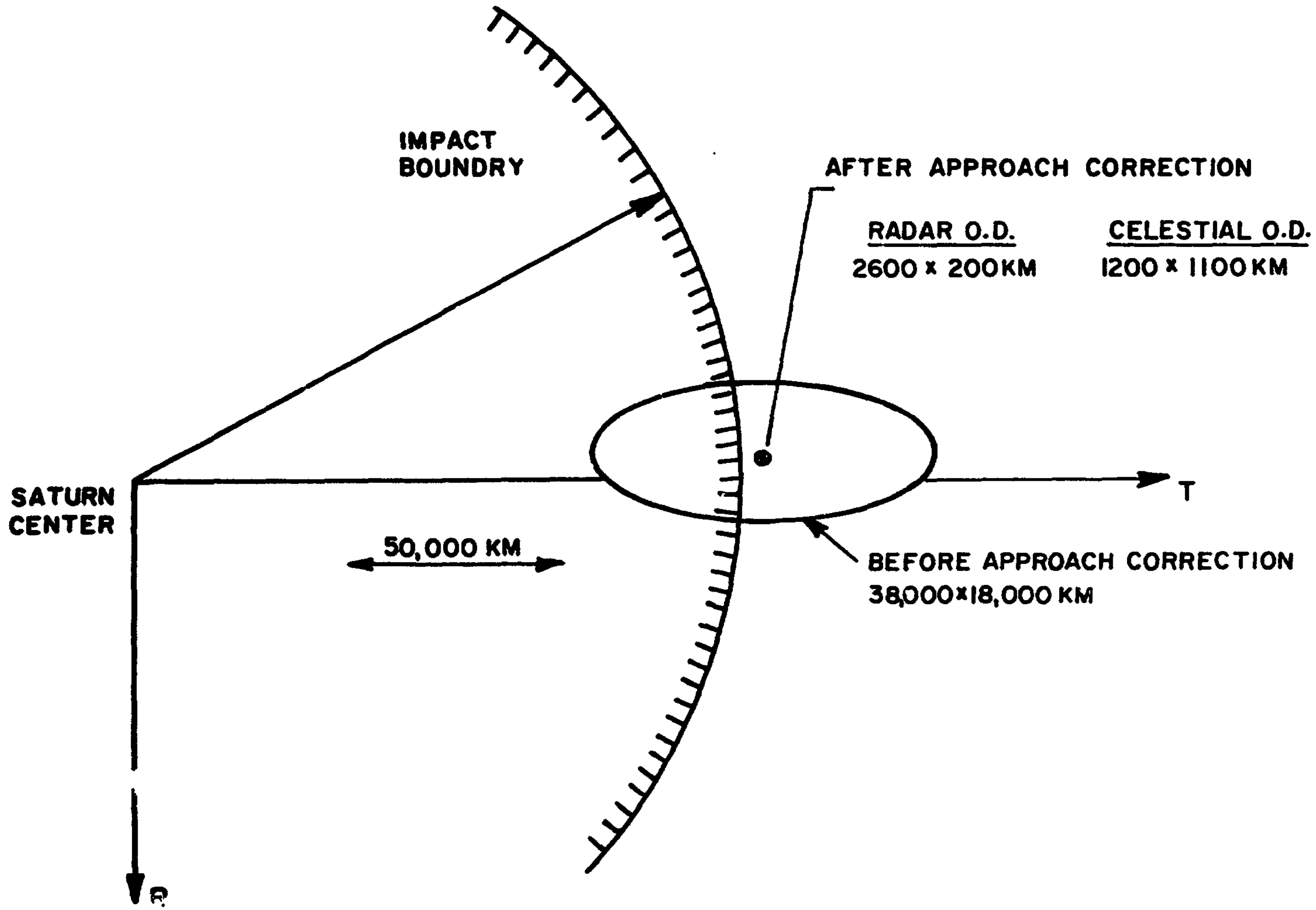

FIGURE 3.15 3σ MISS ELLIPSES FOR SATURN ENCOUNTER, 1977-I GRAND TOUR

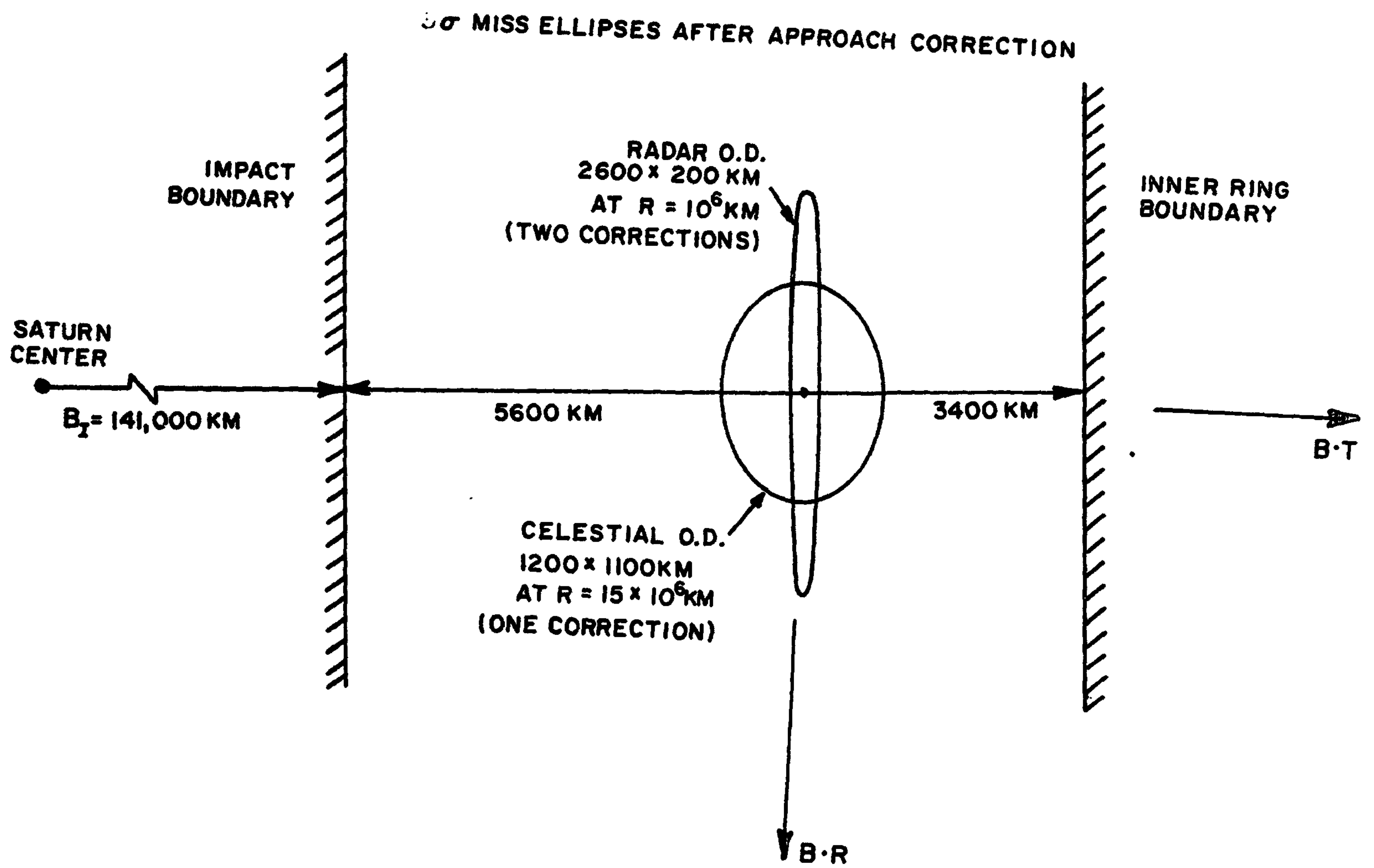

FIGURE 3.16 SATURN APPROACH GUIDANCE ACCURACY, 1977 - I GRAND TOUR

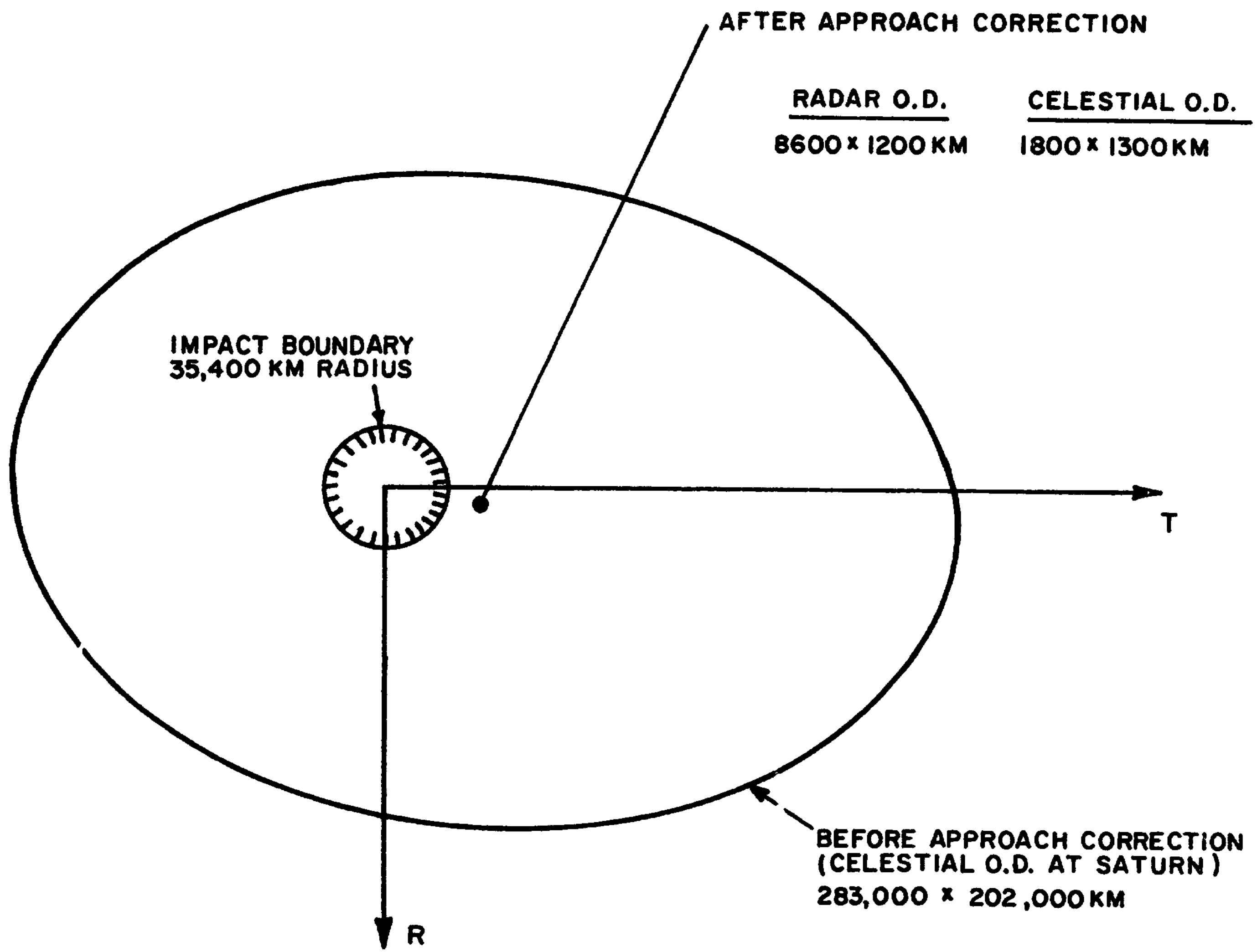

FIGURE 3.17 3σ MISS FOR URANUS ENCOUNTER, 1977-I GRAND TOUR

3.3.5 Guidance Analysis Summary

From the results of the guidance analysis, the following summary remarks may be made:

1. Although the guidance requirements of the Grand Tour Mission are much more severe than current planetary missions, they are not beyond the capability of the present or projected state-of-the-art. Multiple guidance maneuvers are necessary to meet the mission requirements. For each planetary swingby, one or two approach maneuvers and one departure maneuver will suffice. A total of 8-10 maneuvers would be required.

2. The orbit determination process, whether Earth-based radar or on-board celestial tracking, must extent well into the planetary approach phase at Saturn and particularly at Uranus. From the standpoint of guidance accuracy, either tracking mode should be adequate for purposes of the scientific experiments to be carried out.

3. "Interior Ring Passage" missions have a significantly higher guidance ΔV requirement than "Exterior Ring Passage" missions.

4. The largest ΔV contribution occurs at the Uranus encounter. The importance of this result is that if a problem of fuel depletion occurs at this late stage in flight, only the Neptune encounter need be sacrificed. In other words, for a multiple target mission, it is desirable that the

large ΔV corrections occur late rather than early in the flight in order to enhance the probability of mission success for a fixed fuel load.

5. In the interest of minimizing the guidance ΔV requirements, a strong case is made for having an on-board planet tracking capability. This is particularly true for the most sensitive Interior Ring Passage mission. With on-board tracking the largest total ΔV requirement is about 400 m/sec. This is to be compared with 1700 m/sec if Earth-based tracking alone were employed. However, if the 1978 Exterior Ring Passage mission were selected, the advantage of on-board tracking is reduced somewhat. In this case the ΔV requirements are about 200 m/sec for on-board tracking and 350 m/sec for Earth-based tracking.

SECTION 4

EVALUATION OF THE SCIENTIFIC OBJECTIVES

Compiled By

K. L. Uherka

Contributors

A. B. Binder
J. C. Jones
D. L. Roberts
K. L. Uherka

4. EVALUATION OF THE SCIENTIFIC OBJECTIVES

The detailed trajectory and guidance analyses of Sections 3 and 4 have clearly illustrated the possibility of a multiple outer planet mission which utilizes gravity assist at each target. The ultimate worth or usefulness of such a mission depends on the value of the scientific data that is obtained from measurements. Since the opportunities for a Grand Tour mission encountering all four Jovian planets are rare, occurring approximately every 179 years, it is of the utmost importance that the most effective use is made of the payload capabilities. Therefore it is highly desirable that the selection of scientific experiments for the mission payload be based on a systematic and logical methodology.

The selelection methodology, to be useful, should result in a relative "value" being placed on different scientific experiments so that they can be ranked according to their value of importance. This allows experiments and experiment packages to be selected on the basis of highest values. The worth or value of any experiment depends upon its measurement data, and the percentage contribution that these measurements make toward fulfilling the total scientific goals and objectives of exploration for the outer planets. Hence, a complete methodlogy for mission payload selection must also include a scheme for evaluation and ordering of both the basic science objectives, and the measurables that are of interest.

Section 4.1 below is devoted to the methodology that has been developed by ASC/IITRI to determine the science objectives and measurables that are relevant to the overall scientific goal of Examination of the Jovian Planets and Interplanetary Space. The evaluation scheme and logic used to obtain relative values for the scientific objectives is discussed in Section 4.2. The methodology used to determine the value and priority order of actual spacecraft instrumentation (based on their capability to fulfill the scientific objectives) is covered in Section 5, along with the selection criteria used to obtain mission payloads.

4.1 Methodology for Science Selection

The first step in the science evaluation is to obtain a complete listing of the scientific objectives for which measurement data is desirable. To insure completeness, the method of approach starts with a definition of the broad overall Goal of Exploration, which is then further subdivided into subgoals called Exploration Regimes. The Exploration Regimes are more specific than the Goal and also define the scope encompassed by the original goal. The scope of the Exploration Regime subgoals are then further clarified by an additional level of detail which are called Regime Categories. The Regime Categories are then defined by a natural breakdown into Category Objectives, which in turn are subdivided into

Objective Measurables. The Objective Measurables represent the final level of detail and they are directly related to measurable quantities (an example of an Objective Measurable would be "to measure the NH_3 abundance in a planetary atmosphere").

Figure 4.1 illustrates the systematic breakdown of a Goal into succcessive levels of detail. It should be emphasized that each level of breakdown as a whole is entirely equivalent to its previous level. It is felt that the methodology adopted there is general in nature and its logical framework is valuable in that it reduces to a minimum any possibility of overlooking important mission science requirements.

The present study is concerned with a mission to the four outer planets, and thus the Goal of Exploration can be taken quite generally as: Examination of the Jovian Planets and the Interplanetary Medium. The detailed breakdown of this goal is shown in Figure 4.2. The first 3 levels of breakdown into Exploration Regimes, Regime Categories and Category Objectives are shown in the illustration, while the results for detailed Objective Measurables are given in the Figures of Section 4.2. The breakdown shown in the block diagram of Figure 4.2 was strongly influenced by the recommendations of the Space Science Board of the National Academy of Sciences (SSB 1966), in that the emphasis is

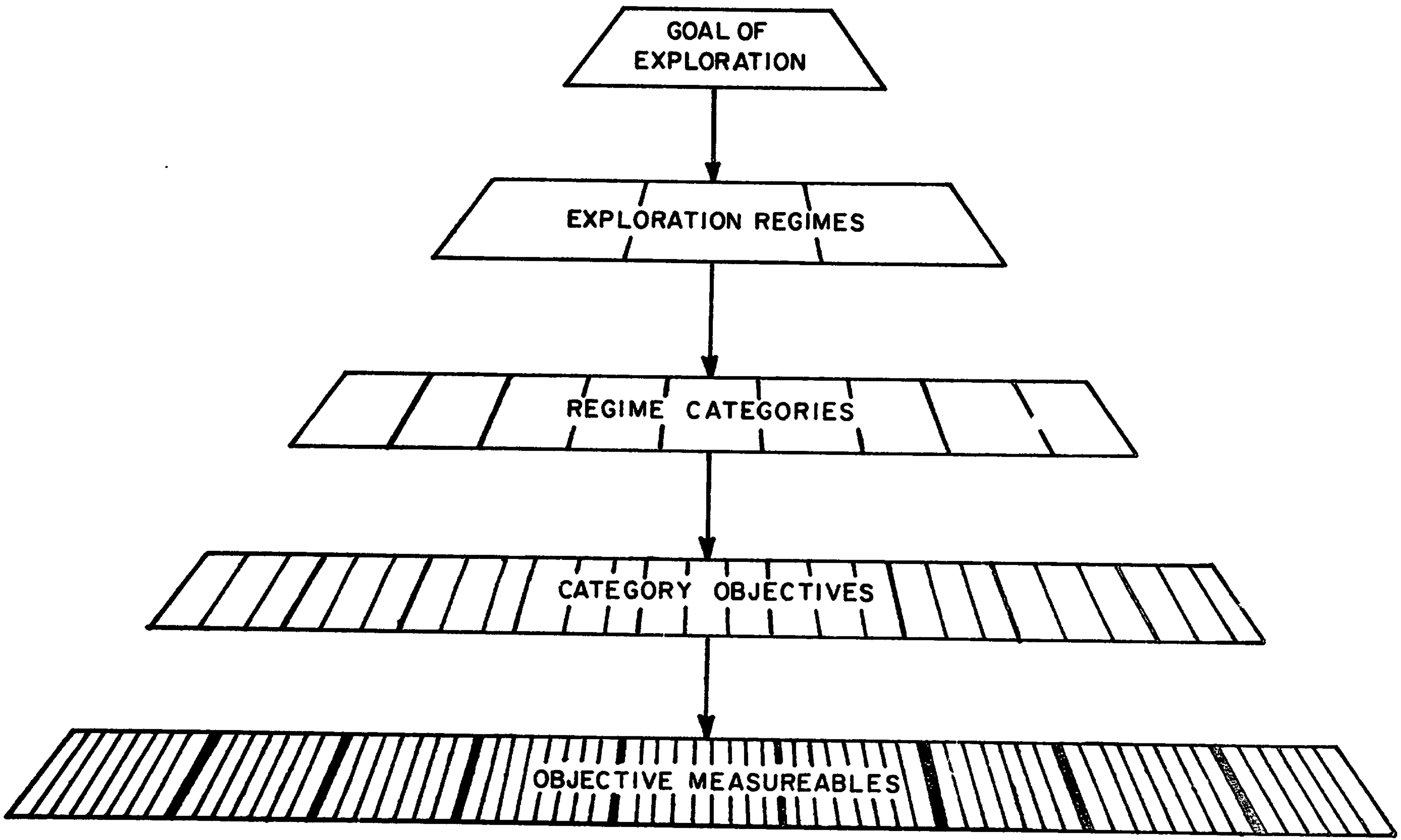

FIGURE 4.1. EVALUATION OF SCIENTIFIC OBJECTIVES

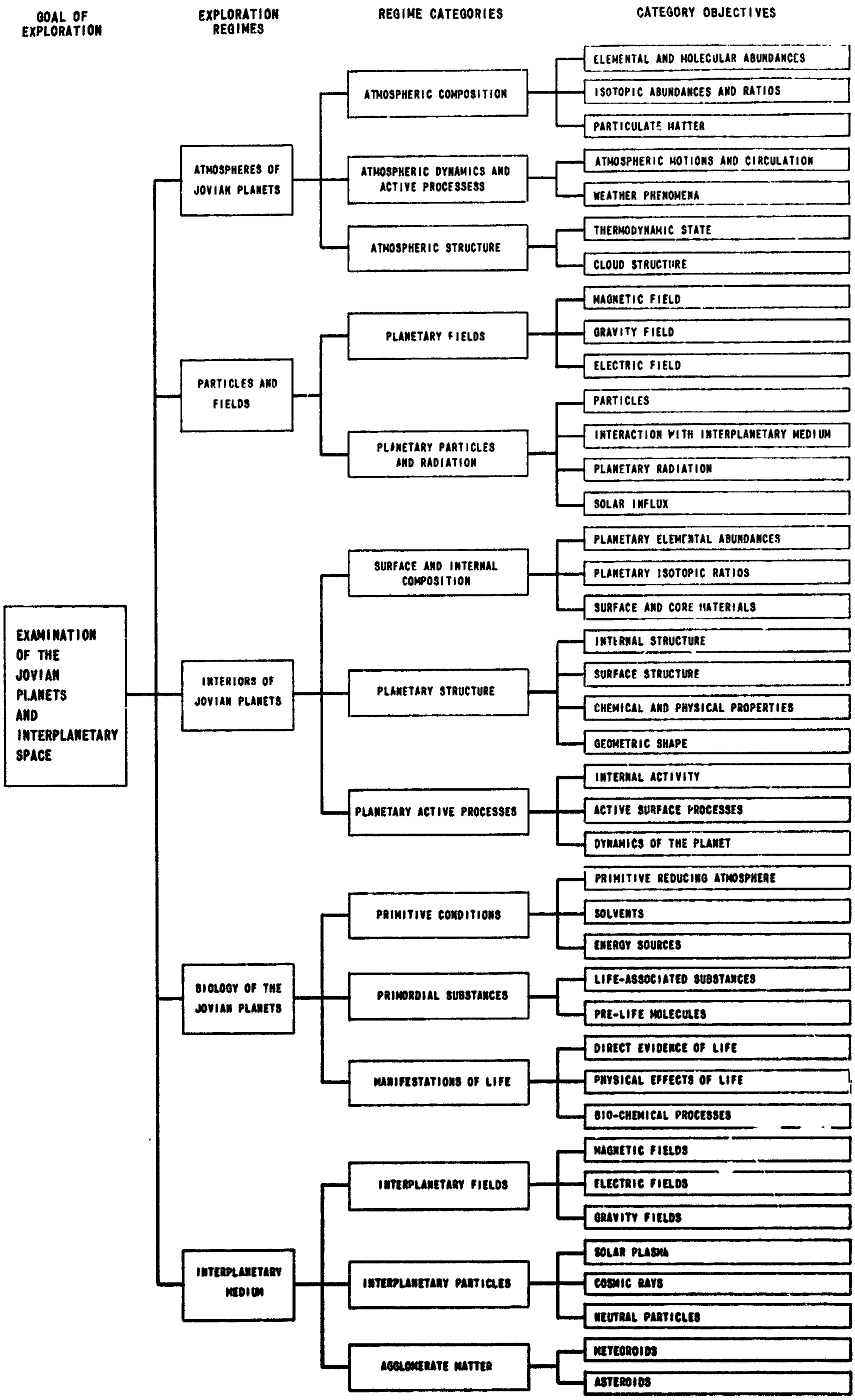

Figure 4.2 DETAILED DEVELOPMENT OF OBJECTIVES FROM GOAL

placed on those factors of scientific exploration which have a bearing on the origin and evolution of the solar system and on life.

4.2 Evaluation of Science Objectives

The format that was developed in the previous section to establish the consecutive levels of detail for the exploration goal can be utilized as a basis for numerical evaluation and priority ordering of the science objectives. As mentioned previously, spacecraft instrumentation can then be evaluated and given a priority that is based on the ability of the instrument to fulfill the scientific requirements.

Numerical evaluation is accomplished by assigning an arbitrary value (such as unity or 1000) to the Goal of Exploration, and then determining the appropriate percentage of this value that is contributed by each Exploration Regime. Similarly, the worth of each individual Exploration Regime can be apportioned among its Regime Categories in terms of relative percentages. Continuing in this fashion, the fractional contributions of the Category Objectives to their individual Regime Categories can be determined. A complete rationale thus results in which each level of the science breakdown is evaluated in terms of the percentage value that it contributes toward fulfilling the next higher level from which it was derived.

The evaluation results corresponding to the first three levels of Figure 4.2 are shown in Figure 4.3. The percentage values shown were obtained through discussion and judgement by a group of scientists and consultants. The Exploration Regime of "Atmospheres of Jovian Planets" was judged to encompass 30% of the total science attributable to the Goal of Exploration because of the nature of the Jovian planets with their massive atmospheres and the fact that it is not known whether a truly definable surface even exists (Michaux, 1967). The science value of Particles and Fields was estimated to be about 22% of the overall goal because of its importance in the origin and present evolutionary state of the outer planets. The remaining percentage contribution to the overall Goal was divided equally among the other three Exploration Regimes as shown in Figure 4.3.

The same procedure was used to estimate the percentage contribution that the Regime Categories make towards fulfilling the science requirements of the particular Exploration Regimes from which they were derived. For example, the first three Regime Categories listed in Figure 4.3 were judged to respectively contribute 42%, 33%, and 25% of the value attributable to the Regime of Atmospheres of Jovian Planets. The higher percentage value given to Atmospheric Composition was chosen on the basis of the important role that elemental, molecular and isotopic abundances play in theories relevant

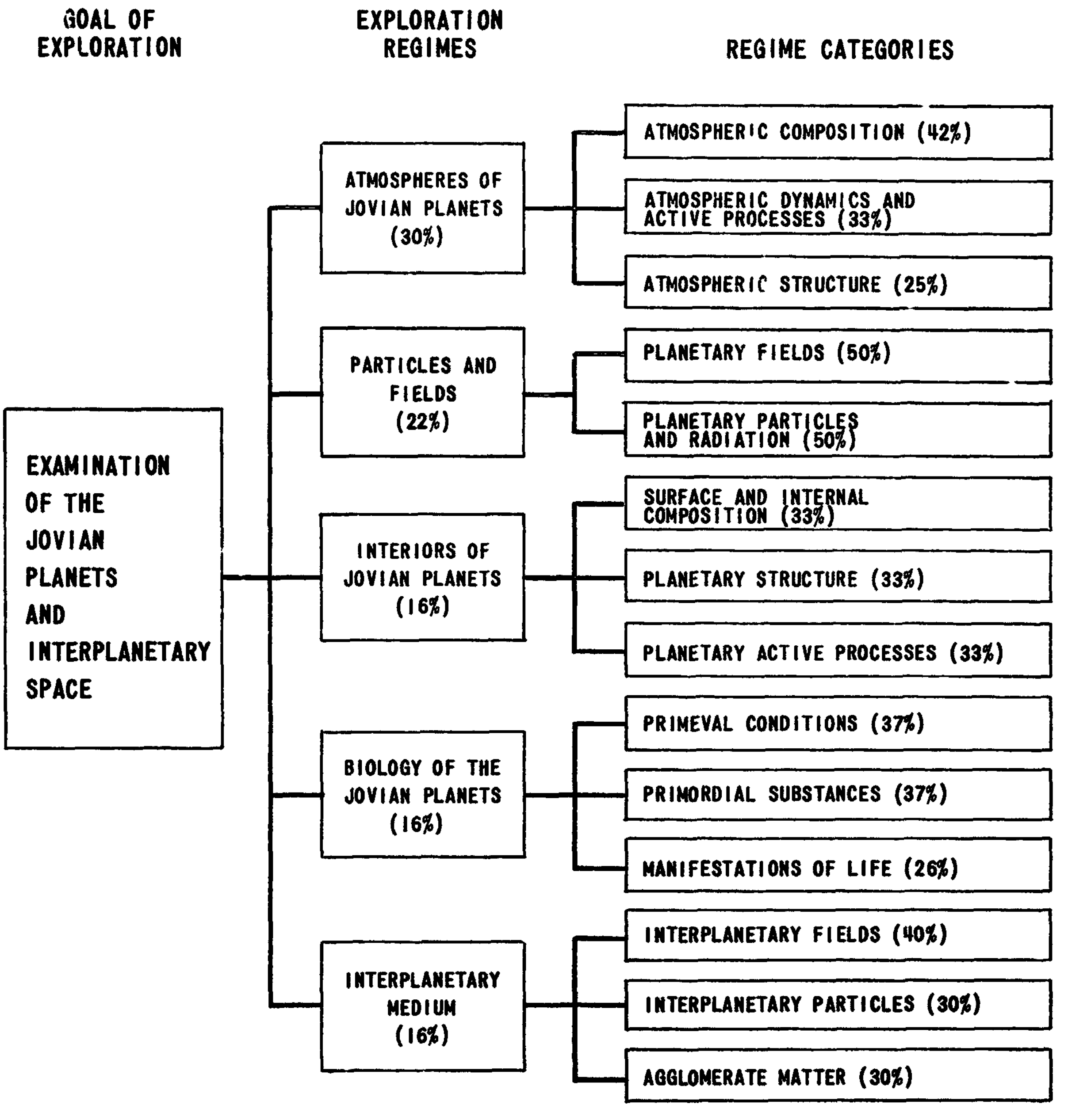

Figure 4.3 SCIENCE EVALUATION OF CATEGORIES RELATIVE TO GOAL

to the origin and evolution of the solar system (e.g., Cameron 1962). Similarly, Atmospheric Dynamics and Active Processes were judged slightly more important than Atmospheric Structure (33% versus 25%) because of the importance of atmospheric circulation and weather phenomena in understanding the past and present evolutionary processes which shape a planet's history.

The breakdown and evaluation of each Regime Category of Figure 4.3 are shown in Figures 4.4 through 4.17. These figures illustrate the detailed breakdown into Category Objectives, which in turn are elucidated by their Objective Measurables as shown. The percentage contribution of each Regime Category to its Exploration Regime (see Figure 4.3) is reiterated in the first title block of each figure. The remainder of each block diagram is devoted to the science details leading to the Objective Measurables, which are then followed by estimates for relative worth. The percentages given in parenthesis under the "Relative Value" column represent the judgement value or worth of each Category Objective relative to its Regime Category. This relative value has been divided among the four outer planets in proportion to their individual importance in relation to the science data pertaining to each Category Objective and the associated Objective Measurables. This planetary portion of the relative Category Objective Value is given in the last

SCIENCE EVALUATION FOR CATEGORY OF ATMOSPHERIC COMPOSITION

The block diagram illustrates the approach used for the detailed development of Objective Measurables for the specific Regime Category of Atmospheric Composition. The numerical values in parentheses give the percentage worth that a given level contributes to the next higher level preceding it. Thus Atmospheric Composition contributes 42% of the total worth attributable to Atmospheres of the Jovian Planets (see Figure 4.3).

The Regime Category has three Category Objectives, which in turn are further subdivided into the relevant measurable quantities called Objective Measurables. The Objective Measurables shown within the brackets of Figure 4.4 are based on present estimates as to what elements, isotopes, and aspects of particulate matter are of paramount importance in understanding the composition of the Jovian planets. Thus the abundances of hydrogen, helium and ammonia rank high in scientific interest (Opik 1962), while their relative worth would be reduced for the terrestrial planets. On the basis of the importance of the defining Objectives Measurables to theories concerning the origin and evolution of the solar system, the relative worths for the Category Objectives of Elemental and Molecular Abundances and Isotopic Abundances and Ratios were judged to be approximately equal to 38% of the total Regime Category value. Particulate Matter was judged to have a slightly lower science value (24%) as shown.

The last column of the block diagram shows how the relative percentage value for each Category Objective was divided up or apportioned among the four outer planets. In general, Jupiter is taken to be of greatest importance because of its unique characteristics and almost star-like mass. Scientific knowledge pertaining to Saturn's composition was estimated to be intermediate in value relative to that of Jupiter and the lower worth of Uranus and Neptune. The exception to the above is Particulate Matter, where all planets were judged to contribute equally.

Regime Category	Category Objectives	Objective Measurables	Relative Value	Planetary Portion of Relative Value
Atmospheric Composition (42%)	Elemental and Molecular Abundances	1. H and H_2 2. He 3. NH_3 4. CH_4 5. H_2O 6. O, O_2 and O_2 7. N and N_2 8. Ne 9. CO and CO_2 10. Xe, A , etc. 11. H_2s And Other Compounds 12. Mean Molecular Weight	(38%)	Jupiter - 16% Saturn - 10% Uranus - 6% Neptune - 6%
	Isotopic Abundances and Ratios	1. H^1/H^2 2. He^3/He^4 3. C^{12}/C^{13} 4. A^{40}/A^{38} 5. Li^6/Li^7 6. B^{10}/B^{11}	(38%)	Jupiter - 17% Saturn - 9% Uranus - 6% Neptune - 6%
	Particulate Matter	1. Aerosol Composition 2. Crystal Composition 3. Radiative and Scattering Properties 4. Spatial Variations of Particulates	(24%)	Jupiter - 6% Saturn - 6% Uranus - 6% Neptune - 6%

Figure 4.4

SCIENCE EVALUATION FOR CATEGORY OF ATMOSPHERIC COMPOSITION

SCIENTIFIC EVALUATION FOR CATEGORY OF ATMOSPHERIC DYNAMICS AND ACTIVE PROCESSES

The block diagram of Figure 4.5 illustrates the logical division of Atmospheric Dynamics and Active Processes into the two Category Objective subdivisions of Atmospheric Motions and Circulation, and Weather Phenomena. The first Category Objective includes all large scale and more or less permanent atmospheric activity as denoted by the Objective Measurables shown in brackets. Weather phenomena includes the more localized and short duration processes such as precipitation, lightning and cyclone activity.

The worth of each level of detail relative to its preceding level is indicated by the percentages in parenthesis. The larger relative value (60%) was attributed to Atmospheric Motion and Circulation because of its greater importance to the overall dynamical activity which establishes the present evolutionary tendancies of the planet. Scientific knowledge of the short duration activity attributable to Weather Phenomena thus contributes the remaining 40% of the total worth.

The portion of the relative Category Objective value that was given to each planet is shown in the last column. Jupiter was apportioned the largest share because of the observed atmospheric activity on this planet (e.g., Hide 1966), a detailed knowledge of which would contribute greatly to our knowledge of atmospheric processes and present evolutionary trends.

Regime Category	Category Objectives	Objective Measurables	Relative Value	Planetary Portion of Relative Value
Atmospheric Dynamics and Active Processes (33%)	Atmospheric Motions and Circulation	1. Scale of Global Circulation Cycles 2. Global Wind Speeds 3. Cloud Formation Rates 4. Differential Cloud Belt Velocities 5. Convective Cells and Turbulence 6. Anomolous Activity (Red Spot, etc.)	(60%)	Jupiter - 25% Saturn - 15% Uranus - 10% Neptune - 10%
	Weather Phenomena	1. Nature of Precipitation Cycles 2. Seasonal Variations 3. Precipitation Rates 4. Thunderstorm and Lightning Activity 5. Cyclone Formations 6. Atmosphere Surface Interactions	(40%)	Jupiter - 13% Saturn - 9% Uranus - 9% Neptune - 9%

Figure 4.5

SCIENCE EVALUATION FOR CATEGORY OF ATMOSPHERIC DYNAMICS AND ACTIVE PROCESSES

SCIENCE EVALUATION FOR CATEGORY OF ATMOSPHERIC STRUCTURE

The Regime Category of Atmospheric Structure was judged to be the smallest contributor in relative value (25%) of those Regime Categories which comprised the Exploration Regime of Atmospheres of Jovian Planets (see also Figure 4.3). This value reasoning was based on the fact that, while Atmospheric Structure is important in defining the present state of a planetary body, it was not judged to be as important as Atmospheric Composition and Dynamics are in their contributions to our knowledge concerning the origin and evolution of the solar system.

The sub-levels of Atmospheric Structure are Thermodynamic State and Cloud Structure, which were judged to contribute an equal portion (i.e. 50%) of the relative value. These sub-levels are further clarified by their Objective Measurables as outlined in Figure 4.6. Jupiter, because of its large mass and unique characteristics, was apportioned the greater share of the relative value. Saturn was also judged more important than Uranus and Neptune in regard to Cloud Structure. This judgement was based on the value of understanding the observed cloud belt system, which is not known to exist on the two outer-most of the Jovian planets.

Regime Category	Category Objectives	Objective Measurables	Relative Value	Planetary Portion of Relative Value
Atmospheric Structure (25%)	Thermodynamic State	1. Temperature Profile 2. Density Profile 3. Pressure Profile 4. Moisture Content 5. Thermal Balance 6. Horizontal Temperature Gradients 7. Thermal Anomalies	(50%)	Jupiter - 17% Saturn - 11% Uranus - 11% Neptune - 11%
	Cloud Structure	1. Extent of Global Coverage 2. Vertical Structure and Number of Cloud Layers 3. Physical Properties 4. Belt and Band Properties	(50%)	Jupiter - 18% Saturn - 14% Uranus - 9% Neptune - 9%

Figure 4.6

SCIENCE EVALUATION FOR CATEGORY OF ATMOSPHERIC STRUCTURE

SCIENCE EVALUATION FOR CATEGORY OF PLANETARY FIELDS

Figure 4.7 shows the logical breakdown of Planetary Fields into its relevant Category Objective levels of Magnetic, Gravity and Electric Fields. The measurable quantities of major interest for each of these levels are specified under the Objective Measurables column of Figure 4.7.

Scientific knowledge concerning magnetic fields was judged to be far more important than a detailed understanding of gravity or electric fields, and thus was apportioned 75% of the worth attributable to the Category of Planetary Fields. This high relative worth was based on the importance of understanding how magnetic fields originate and evolve in planetary bodies, particularly for the rapidly rotating planetary systems under investigation. A further consideration is the role of the magnetosphere in permitting biological evolution through its shielding of energetic solar particles. Data concerning gravity fields was estimated to be of greater value than that for electric fields (i.e., 20% versus 8% relative value), since the latter is of secondary origin arising from interactions between the atmospheric motions, magnetic fields and the solar flux.

The Jovian planets were judged to contribute equal shares in fulfilling the scientific data for each of the three Category Objectives, as shown by the final bracketed information in the block diagram of Figure 4.7.

Regime Category	Category Objectives	Objective Measurables	Relative Value	Planetary Portion of Relative Value
Planetary Fields (50%)	Magnetic Field	1. Magnetic Field Intensity 2. Magnetic Field Direction 3. Long Term Field Variations 4. Magnetic Bursts 5. Paleomagnetism	(72%)	Jupiter - 18% Saturn - 18% Uranus - 18% Neptune - 18%
	Gravity Field	1. Gravitational Acceleration 2. Temporal Variations 3. Tidal Components of Satellites 4. Satellite Pertubations	(20%)	Jupiter - 5% Saturn - 5% Uranus - 5% Neptune - 5%
	Electric Field	1. Electric Field Density 2. Electric Field Direction 3. Temporal Variations 4. Ionospheric Ring Currents 5. Radiation Belt Currents	(8%)	Jupiter - 2% Saturn - 2% Uranus - 2% Neptune - 2%

Figure 4.7

SCIENCE EVALUATION FOR CATEGORY OF PLANETARY FIELDS

SCIENCE EVALUATION FOR CATEGORY OF PLANETARY PARTICLES AND RADIATION

The block diagram in Figure 4.8 illustrates the detailed breakdown for Planetary Particles and Radiation into more descriptive Category Objectives and the final Objective Measurables level of detail. It is seen that the methodology developed in the present study allows a systematic development of the science requirements through the Category Objectives of: (1) Particles, which encompasses both radiation belt phenomena and meteors; (2) interaction with the Interplanetary Medium, for which the science goal is to understand the shock front resulting from the magnetosphere-solar wind interaction; (3) Planetary Radiation includes all energy emission from a planet; and (4) Solar Influx covers the energy input to the planet from the sun.

The Particles objective was judged to have the highest value (36%) relative to fulfilling the science requirements of the overall Regime Category. This judgement was based on the need for a better understanding of radiation belts and their particle interactions so that a comparison of this science data with that of the Earth can be used as a basis for theoretical studies. Jupiter and Saturn were judged to be more important than Uranus and Neptune for the Category Objective because of the intense radiation belt activity on Jupiter and the planetary ring particulates of Saturn.

The second and third Category Objectives considered in Figure 4.8 were estimated to have similar relative values (28% and 24%) with each planet, except Jupiter, sharing equal portions of the relative values. Jupiter was an exception for Planetary Radiation and judged slightly more important than the other planets because of its observed decimeter and decameter radiation (Gordon and Warwick, 1967). The objective of Solar Influx was attributed the lowest relative value (12%) because the energy influx can be determined adequately from a knowledge of the solar constant and existing radiation laws.

Regime Category	Category Objectives	Objective Measurables	Relative Value	Planetary Portion of Relative Value
Planetary Particles and Radiation (50%)	Particles	1. Mass of Radiation Belt Particles 2. Charge of Radiation Belt Particles 3. Distribution of Radiation Belt Particles 4. Energy of Radiation Belt Particles 5. Particle Reaction Rates 6. Size and Distribution of Meteors and Micro-meteorites 7. Planetary Ring Particulates	(36%)	Jupiter - 11% Saturn - 11% Uranus - 7% Neptune - 7%
	Interaction with Interplanetary Medium	1. Flow Pattern of Solar Wind 2. Configuration of Shock Front 3. Particle Interactions in Shock Zones 4. Extent of Magnetosphere Tail 5. Neutral Sheet Structure	(28%)	Jupiter - 7% Saturn - 7% Uranus - 7% Neptune - 7%
	Planetary Radiation	1. Emitted IR Radiation 2. Decimeter Emission 3. Decameter Emission 4. Temporal Variation of Emission 5. Extent and Nature of Airglow 6. Extent and Nature of Aurora 7. Emission Characteristics of Anomalous Regions 8. Existence of Whistlers	(24%)	Jupiter - 9% Saturn - 5% Uranus - 5% Neptune - 5%
	Solar Influx	1. Incident Solar γ-Rays 2. Incident Solar X-Rays 3. Incident Solar UV, Visible and IR Radiation 4. Incident α-particles, protons and electrons 5. Cosmic Rays	(12%)	Jupiter - 3% Saturn - 3% Uranus - 3% Neptune - 3%

Figure 8

SCIENCE EVALUATION FOR CATEGORY OF PLANETARY PARTICLES AND RADIATION

SCIENCE EVALUATION FOR CATEGORY OF SURFACE AND INTERNAL COMPOSITION

The Exploration Regime of Interiors of Jovian Planets has Regime Categories of Surface and Internal Composition, Planetary Structure, and Planetary Active Processes (see Figure 4.3). Each of these three sub-levels was judged to contribute equally (33%) to their Exploration Regime. The further development of the Surface and Internal Composition category is given in Figure 4.9.

As in the case for Atmospheric Composition (see Figure 4.4), an equally high relative science value (38%) was attributed to both elemental abundances and isotopic ratios. This judgment relates to the basic importance that elemental and isotopic variations play in present theories regarding the origin and evolution of our solar system. The bracketed data in the right-hand column of Figure 4.9 shows that Jupiter and Saturn were assigned the largest portions of the relative values attributed to Planetary Elemental Abundances and Isotopic Ratios. This judgment was based on the massive size of these two planets, which for Jupiter's case borders on that of a small star, and the importance of establishing the interior composition of these two giants. This knowledge would contribute greatly to our understanding of the origin and development of large planetary systems. Uranus and Neptune were judged to be equal, but of less importance in the above context.

The last Category Objective, Surface and Core Materials, covered in Figure 4.9 includes the relevant compositional data other than the basic elemental and isotopic abundances. This science data is valuable in establishing the present state of the outer planets, and the relative value was apportioned equally among them.

Regime Category	Category Objectives	Objective Measurables	Relative Value	Planetary Portion of Relative Value
Surface and Internal Composition (33%)	Planetary Elemental Abundances	1. Carbon 2. Oxygen 3. Silicon 4. Magnesium 5. Sulfur 6. Iron 7. H and He 8. Others	(38%)	Jupiter - 16% Saturn - 10% Uranus - 6% Neptune - 6%
	Planetary Isotopic Ratios	1. O^{18}/O^{16} 2. S^{32}/S^{34} 3. C^{13}/C^{12} and C^{14}/C^{12} 4. Others	(38%)	Jupiter - 17% Saturn - 9% Urnaus - 6% Neptune - 6%
	Surface and Core Materials	1. Mineralogy 2. Lithology 3. Hydrocarbons 4. H_2O Phases 5. Metallic and Liquid H_2 6. NH_3 and CH_4 Phases 7. Organic Compounds 8. Metallic Core Materials	(24%)	Jupiter - 6% Saturn - 6% Uranus - 6% Neptune - 6%

Figure 4.9

SCIENCE EVALUATION FOR CATEGORY OF SURFACE AND INTERNAL COMPOSITION

SCIENCE EVALUATION FOR CATEGORY OF PLANETARY STRUCTURE

The detailed development for the Regime Category of Planetary Structure is outlined in Figure 4.10. The four Category Objective levels include the internal distribution of thermodynamic variables (pressure, temperature, etc.), surface characteristics, relevant chemical and physical properties, and the general geometric properties.

A knowledge of the internal structure was judged to be of the greatest value relative to understanding the overall planetary structure. This information on the internal and core regions of the planets is valuable in establishing the formation processes which led to the present state. Again, a greater portion of the 40% relative value can be attributed to Jupiter (13% versus 9% for each of the other Jovian planets) because of its unique status in the solar system.

The Category Objectives of Surface Structure, and Chemical and Physical Properties were judged to be close in their relative values (28% and 20% respectively). The Category of Geometric Shape was ranked lowest in relative value since its Objective Measurables, while being of general interest, do not contribute greatly to understanding the origin and evolution of the planets. Each of the Jovian planets was judged to contribute an equal portion to the relative value of the last three Category Objectives of Figure 4.10.

Regime Category	Category Objectives	Objective Measurables	Relative Value	Planetary Portion of Relative Value
Planetary Structure (33%)	Internal Structure	1. Density Distribution 2. Phase Change Discontinuities 3. Temperature Distribution 4. Spatial Extent of Core Region	(40%)	Jupiter - 13% Saturn - 9% Uranus - 9% Neptune - 9%
	Surface Structure	1. Existence of a Definable Surface 2. Physical State (solid or liquid) 3. Structure of Features 4. Surface Elevations 5. Surface Appearance 6. Layering and Contacts of Solid Features	(28%)	Jupiter - 7% Saturn - 7% Uranus - 7% Neptune - 7%
	Chemical and Physical Properties	1. Surface Pressure and Temperature 2. Electrical and Magnetic Properties 3. Thermal Properties 4. Radiative Properties 5. Particle Sizes and Texture 6. Hardness and Consolidation 7. Chemical Reaction Rates	(20%)	Jupiter - 5% Saturn - 5% Uranus - 5% Neptune - 5%
	Geometric Shape	1. Average Radius 2. Surface Elevation with Respect to Datum 3. Center of Mass 4. Planetary Mass and Mass Distribution	(12%)	Jupiter - 3% Saturn - 3% Uranus - 3% Neptune - 3%

Figure 4.10

SCIENCE EVALUATION FOR CATEGORY OF PLANETARY STRUCTURE

SCIENCE EVALUATION FOR CATEGORY OF PLANETARY ACTIVE PROCESSES

The breakdown of Planetary Active Processes into its sub-levels is shown in Figure 4.11. The three Category Objective levels include internal phenomena, active surface processes and general dynamical activity. The Objective Measurables define in detail the measurable phenomena that are of interest and also illustrate the characteristics which constitute the total of each Category Objective level.

Since it is not known whether or not a definable surface even exists on the Jovian planets, the traditional surface activity usually associated with the terrestrial planets, such as topographic changes and faulting, may not be present. For this reason, the Internal Activity objective was ranked considerably higher than Active Surface Processes in its relative value. Thus Internal Activity was judged to contribute about 64% to the overall value of the Regime Category of Planetary Active Processes. The high relative value of Internal Activity is further exemplified through the importance of interior processes in establishing the present and future evolutionary trends of planetary bodies. A larger portion of the worth for this Category Objective was attributed to Jupiter than to the other planets, because of its massive size and the associated core activity that is expected to exist (such as the core dynamo effect necessary to produce the observed magnetic field).

The relative contribution of Active Surface Processes was estimated as 24% of the total, in contrast to only 12% for Dynamics of the Planet. This judgment was based on the fact that the first of these two Category Objectives is valuable in estimating the present evolutionary trends, while additional information on the latter would not be as significant in its contribution towards understanding the origin and evolution. For these two Category Objectives, an equal fraction of the total relative value was attributed to each of the Jovian planets.

Regime Category	Category Objectives	Objective Measurables	Relative Value	Planetary Portion of Relative Value
Planetary Active Processes (33%)	Internal Activity	1. Core Circulation and Currents 2. Extent of Internal Energy Sources 3. Regions of Anomalous Heat Flow 4. Internal Faulting, Expansion, etc.	(64%)	Jupiter - 19% Saturn - 15% Uranus - 15% Neptune - 15%
	Active Surface Processes	1. Mass Movement and Topographic Changes 2. Volcanism 3. Faulting, Folding, etc. 4. Erosional Processes 5. Telluric Currents 6. Seismic Waves 7. Incident Radiaton and Particle Flux	(24%)	Jupiter - 6% Saturn - 6% Uranus - 6% Neptune - 6%
	Dynamics of the Planet	1. Rotation Period 2. Tidal Variations 3. Polar Wandering	(12%)	Jupiter - 3% Saturn - 3% Uranus - 3% Neptune - 3%

Figure 4.11

SCIENCE EVALUATION FOR CATEGORY OF PLANETARY ACTIVE PROCESSES

SCIENCE EVALUATION FOR CATEGORY OF PRIMEVAL CONDITIONS

The worth for the Exploration Regime of Biology of the Jovian planets was assessed as 37% being contributed by a knowledge of Primeval Conditions, 37% by Primordial Substances, and 20% by Manifestations of Life (see Figure 4.3). The first two Regime Categories were judged to be the most important because exobiology of the outer planets, if it exists, is believed to be in a primitive state. The probability for finding evidence for living organisms is small, and thus the Manifestations of Life category was taken to be of slightly lower value.

Figure 4.12 shows the breakdown of Primeval Conditions into its Category Objectives, which were taken as Primitive Reducing Atmosphere, Solvents, and Energy Sources. Further elucidation is then given through their Objective Measurables. The three Category Objectives under consideration were judged to contribute equally in fulfilling the science requirements for the overall Regime Category. The reason for this is that a reducing atmosphere, solvents and suitable energy sources are all deemed necessary for the initiation of life-producing processes.

The planetary portions of the Category Objective relative values (given by the bracketed data in the last column of Figure 4.12) were assigned with Jupiter having the highest weight, Saturn second, and with Uranus and Neptune each having an equal but smaller contribution. The reasoning for this evaluation was based on the warmer temperature (hence, a more suitable biological environment) of the nearer of the Jovian planets, and the fact that liquid solvents and energy sources are thought to be more readily available on Jupiter and Saturn.

Regime Category	Category Objectives	Objective Measurables	Relative Value	Planetary Portion of Relative Value
Primeval Conditions (37%)	Primitive Reducing Atmosphere	1. Abundance of H 2. Abundance of CH_4 3. Abundance of NH_3 4. Abundance of HCN and HF 5. Relative Percentages of Oxidizing Constituents	(33%)	Jupiter - 10% Saturn - 9% Uranus - 7% Neptune - 7%
	Solvents	1. Abundance of Liquid H_2O 2. Abundance of Liquid NH_3 3. Other Polar Molecule Liquids	(33%)	Jupiter - 10% Saturn - 9% Uranus - 7% Neptune - 7%
	Energy Sources	1. Number and Intensity of Lightning Discharges 2. Intensity of Solar UV Radiation 3. Surface Dynamo Currents 4. Other Energy Sources	(33%)	Jupiter - 10% Saturn - 9% Uranus - 7% Neptune - 7%

Figure 4.12

SCIENCE EVALUTION FOR CATEGORY OF PRIMEVAL CONDITIONS

SCIENCE EVALUATION FOR CATEGORY OF PRIMORDIAL SUBSTANCES

Primordial Substances include all biological ingredients necessary for the development of life or that are associated with life. The Category Objectives and their measureable phenomena are shown in the block diagram of Figure 4.13.

Since Life-Associated Substances are more indicative of biological life development than are Pre-Life Molecules, the first Category Objective of Figure 4.13 was estimated to contribute about twice the value of Pre-Life Molecules in fulfillment of the scientific knowledge necessary for understanding the Regime Category associated with Primordial Substances. Therefore the relative values were taken to be 67% and 33% as shown.

As discussed for the previous Regime Category of Primeval Substances (see Figure 4.12), the relative values were apportioned among the planets on the basis of Jupiter having highest priority, Saturn second, and then followed by Uranus and Neptune. These results are shown in the last column of Figure 4.13.

Regime Category	Category Objectives	Objective Measurables	Relative Value	Planetary Portion of Relative Value
Primordial Substances (37%)	Life-Associated Substances	1. Proteins 2. Enzymes 3. Carbohydrates 4. Nucleic Acids 5. Lipids 6. DNA, Etc.	(67%)	Jupiter - 21% Saturn - 18% Uranus - 14% Neptune - 14%
	Pre-life Molecules	1. Organic Carbon Compounds 2. Amino acids 3. Purines 4. Other Complex Organic Molecules	(33%)	Jupiter - 10% Saturn - 9% Uranus - 7% Neptune - 7%

Figure 4.13

SCIENCE EVALUATION FOR CATEGORY OF PRIMORDIAL SUBSTANCES

SCIENCE EVALUATION FOR CATEGORY OF MANIFESTATIONS OF LIFE

The final Regime Category to be considered under the Exploration Regime for Biology of the Jovian Planets is Manifestations of Life, the detailed development of which is shown in Figure 4.14.

The value judgments were such that Direct Evidence of Life contributes more than half of the total worth attributable to the overall Regime Category under consideration . This judgment follows logically from the fact that detection of actual life-forms far outweighs the importance of sensing secondary effects which may or may not be actually associated with living substances. The relative value of detecting phenomena such as growth or the possible reproduction of a substance was estimated at about 26%, while a 20% value relative to the overall Regime Category was attributed to processes associated with biochemical activity.

Jupiter with its warmer environment, due to its proximity to the sun, is judged to sustain a higher probability of supporting biological life forms. Thus a greater portion of the relative value for each of the Category Objectives was given to Jupiter than to the other planets. Similarly, Saturn was judged to have a higher weight than Uranus and Neptune with their frigid environments. These results are tabulated in the last column of Figure 4.14.

Regime Category	Category Objectives	Objective Measurables	Relative Value	Planetary Portion of Relative Value
Manifestation of Life (26%)	Direct Evidence of Life	1. Presence of Cells 2. Presence of Micro-organism 3. Presence of Flora 4. Presence of Fauna 5. Presence of Fossils 6. Presence of Artifacts	(54%)	Jupiter - 20% Saturn - 14% Uranus - 10% Neptune - 10%
	Physical Effects of Life	1. Growth 2. Movement 3. Optical Activity 4. Reproduction	(26%)	Jupiter - 9% Saturn - 7% Uranus - 5% Neptune - 5%
	Biochemical Processes	1. Gas Exchange (CO_2, O_2, etc.) 2. pH Changes 3. Eh Changes 4. Heat Generation 5. Anaerobic Metabolic Processes	(20%)	Jupiter - 7% Saturn - 5% Uranus - 4% Neptune - 4%

Figure 4.14

SCIENCE EVALUATION FOR CATEGORY OF MANIFESTATIONS OF LIFE

SCIENCE EVALUATION FOR CATEGORY OF INTERPLANETARY FIELDS

The exploration science associated with the interplanetary medium has been classified according to the Regime Categories of: Interplanetary Fields, Interplanetary Particles, and Agglomerate Matter. The value judgments pertaining to the above were given in Figure 4.3, with Interplanetary Fields being judged slightly more important than the other two categories. This value judgment was based on the need for a better understanding of magnetic fields, their origin, and the role they played in the early history of the solar system.

The Category Objectives for Interplanetary Fields are shown in Figure 4.15, along with the more descriptive level of Objective Measurables. As mentioned above, knowledge concerning the structure and variations of the magnetic fields in interplanetary space is of prime importance as an aid to understanding the past and present evolutionary history of the solar system. Thus the relative value for Magnetic Fields has been set at 84% in contrast to the 8% values for Electric and Gravity Fields.

The planetary portion of the relative Category Objective values was based on the importance of the regions of interplanetary space located between the outer planets. Thus the planetary portions of the relative values that are indicated for Jupiter, Saturn, Uranus, and Neptune refer respectively to distance intervals of 1 to 5 AU, 5 to 10 AU, 10 to 20 AU, and 20 to 100 AU from the sun. As shown in the last column of Figure 4.15, each of the four intervals was judged as being equally important in their fractional contribution toward fulfilling the science requirements.

Regime Category	Category Objectives	Objective Measurables	Relative Value	Planetary Portion of Relative Value
Inter-planetary Fields (40%)	Magnetic Fields	1. Magnetic Field Vector 2. Spatial Variations of Field 3. Temporal Fluctuations 4. Interaction Between Solar and Galactic Fields 5. Effect of Solar Field Reversals	(84%)	Jupiter(1-5AU) - 21% Saturn(5-10AU) - 21% Uranus(10-20AU) - 21% Neptune(20-100AU)-21%
	Electric Fields	1. Electric Field Vector 2. Spatial Variations of Field 3. Induced Currents in Interplanetary Medium 4. Influence of Solar Activity	(8%)	Jupiter(1-5AU) - 2% Saturn(5-10AU) - 2% Uranus(10-20AU) - 2% Neptune(20-100AU)- 2%
	Gravity Fields	1. Gravitational Acceleration 2. Spatial Variations 3. Planetary Pertubations 4. Gravity Gradient through Asteroid Belt	(8%)	Jupiter(1-5AU) - 2% Saturn(5-10AU) - 2% Uranus(10-20AU) - 2% Neptune(20-100AU)- 2%

Figure 4.15

SCIENCE EVALUATION FOR CATEGORY OF INTERPLANETARY FIELDS

SCIENCE EVALUATION FOR CATEGORY OF INTERPLANETARY PARTICLES

The science breakdown into the various levels of detail for the Regime Category of Interplanetary Particles is illustrated in the block diagram of Figure 4.16. The Category Objective of Solar Plasma was judged to contribute 56% to the total science value needed for an understanding of Interplanetary Particles. This value was based on the important role that the solar wind plays throughout the solar system, such as its capability to sweep any stationary particles out of the solar system and also its influence on rearranging the interplanetary magnetic field configuration.

The Category Objective of second importance is Cosmic Rays, since they offer a vital means of comparing the energy spectrum of energetic particles which have both solar and galactic sources. The four regions of interplanetary space (as indicated in the last column of Figure 4.16) were estimated to be of equal importance in their contributions towards fulfilling the relative values associated with the objectives of Solar Plasma and Cosmic Rays.

The interplanetary elements and particles are generally considered to be in a completely ionized state. At some distance from the sun, perhaps beyond the outer-most planet, the solar radiation and plasma will not be sufficient to completely excite the gaseous medium. Thus, scientific knowledge of neutral elements (particularly hydrogen) is of importance in assessing the degree of interaction between the solar system plasma and the neutral hydrogen of interstellar space. Though the exact transition region is uncertain, a greater portion of the relative value for Neutral Particles has been attributed to the outer regions of the solar system (i.e., 10 to 100 AU as shown in Figure 4.16).

Regime Category	Category Objectives	Objective Measurables	Relative Value	Planetary Portion of Relative Value
Inter-planetary Particles (30%)	Solar Plasma	1. Hydrogen Abundance 2. Density and Energy Flux of p^+ 3. Density and Energy Flux of e^- 4. Density and Energy Flux of α-particles 5. Density and Energy Flux of heavy ions 6. Isotopic Ratios 7. Average Density, Pressure and Kinetic Temperature Distribution 8. Velocity Vector of Solar Wind 9. Momentum and Energy of Solar Wind 10. Influence of Solar Flares 11. Intensity Variations of Solar Electromagnetic Radiation	(56%)	Jupiter(1-5AU) - 14% Saturn(5-10AU) - 14% Uranus(10-20AU) - 14% Neptune(20-100AU) 14%
	Cosmic Rays	1. Relative Abundance of Cosmic Ray Protons, α-particles, and heaver nuclei 2. Energy Spectrum of Solar Component 3. Energy Spectrum of Galactic Component 4. Spatial and Temporal Flux Variations	(32%)	Jupiter(1-5AU) - 8% Saturn(5-10AU) - 8% Uranus(10-20AU) - 8% Neptune(20-100AU) 8%
	Neutral Particles	1. Radial Position at which Solar Plasma merges into the Neutral Interstellar Medium 2. Nature and Dimensions of Transition Region 3. Abundance of Neutral Hydrogen and Other Constituents	(12%)	Jupiter(1-5AU) - 1% Saturn(5-10AU) - 2% Uranus(10-20AU) - 4% Neptune(20-100AU) 5%

Figure 4.16

SCIENCE EVALUATION FOR CATEGORY OF INTERPLANETARY PARTICLES

SCIENCE EVALUATION FOR CATEGORY OF INTERPLANETARY AGGLOMERATE MATTER

Agglomerate matter that is of interest for the multiple outer planet mission includes the two Category Objectives of Meteoroids and Asteroids. Figure 4.17 outlines the relevant Objective Measurables which fully define the extent of these objectives.

The relative values for Meteoroids and Asteroids were judged to be 60% and 40% respectively, in their importance to the science requirements of Agglomerate Matter. The higher value for Meteoroids was based on their more universal dispersion throughout the solar system, and also on the importance of correlating Earth based data with that for other parts of the solar system. For this reason, the relative value for this category objective was apportioned equally among the four intervals situated between 1-5 AU, 5-10 AU, 10-20 AU, and 20-100 AU from the sun. All of the Asteroid science value was naturally assigned to the 1 to 5 AU region where the asteroid belt is located.

Regime Category	Category Objectives	Objective Measurables	Relative Value	Planetary Portion of Relative Value
Agglomerate Matter (30%)	Meteoroids	1. Compostion of Interplanetary Dust 2. Density Distribution of Interplanetary Dust 3. Particle Sizes of Interplanetary Dust 4. Composition of Meteoroids 5. Density and Size Distribution of Meteoroids 6. Spatial Variations of Meteoroid Flux in Solar System	(60%)	Jupiter(1-5AU) - 15% Saturn(5-10AU) - 15% Uranus(10-20AU)- 15% Neptune(20-100AU)-15%
	Asteroids	1. Asteroid Density Distribution 2. Asteroid Composition 3. Asteroid Sizes and Mass 4. Effective Temperature of Asteroids 5. Velocity and Energy Distribution of Asteroids	(40%)	Jupiter(1-5AU) - 40% Saturn(5-10AU) - 0% Uranus(10-20AU)- 0% Neptune(20-100AU)- 0%

Figure 4.17

SCIENCE EVALUATION FOR CATEGORY OF INTERPLANETARY AGGLOMERATE MATTER column of the figures. The reasoning used in the value judgements is discussed on the title pages opposite to each of Figures 4.4 through 4.17 at the end of this section.

While the numerical percentages that have been assigned in Figures 4.4 through 4.17 are subjective, it is felt that they are fairly representative of judgement values within the scientific community at the present time. In addition, the systematic approach used readily allows a logical mechanism for re-evaluation if new data or priorities are brought to light. It was for this reason, in order to facilitate any re-evaluation necessary, that the worth value at each level of the science breakdown was stated in terms of the percentage contribution relative to the level immediately preceding it, in contrast to having the percentage contribution at each level related directly to the original Goal of Exploration.

The summary results for the science evaluation of Figures 4.3 through 4.17 are given in Table 4.1. The table shows the computed value for each level of science relative to the overall Goal of Exploration. For convenience, the total goal value was taken to be equal to 1000. The number values given represent the portion of the 1000 value that is attributable to each Exploration Regime, Regime Category, and Category Objective. As an example, the total value relative to the overall goal for the Category Objective of Cloud Structure

GOAL OF EXPLORATION	VALUE	EXPLORATION REGIME	VALUE RELATIVE TO GOAL	REGIME CATEGORY	VALUE RELATIVE TO GOAL	CATEGORY OBJECTIVE	PLANETARY VALUE OF CATEGORY OBJECTIVE RELATIVE TO GOAL				TOTAL VALUE RELATIVE TO GOAL
							JUPITER	SATURN	URANUS	NEPTUNE	
EXAMINATION OF THE JOVIAN PLANETS AND INTERPLANETARY SPACE	1000	ATMOSPHERES OF JOVIAN PLANETS	300	ATMOSPHERIC COMPOSITION	126	ELEMENTAL AND MOLECULAR ABUNDANCES	20	12	8	8	48
						ISOTOPIC ABUNDANCE AND RATIOS	21	11	8	8	48
						PARTICULATE MATTER	7.5	7.5	7.5	7.5	30
				ATMOSPHERIC DYNAMICS AND ACTIVE PROCESSES	99	ATMOSPHERIC MOTION AND CIRCULATION	25	15	10	10	60
						WEATHER PHENOMENA	12	9	9	9	39
				ATMOSPHERIC STRUCTURE	75	THERMODYNAMIC STATE	13	8	8	8	37
						CLOUD STRUCTURE	14	10	7	7	38
		PARTICLES AND FIELDS	220	PLANETARY FIELDS	110	MAGNETIC FIELD	20	20	20	20	80
						GRAVITY FIELD	5.5	5.5	5.5	5.5	22
						ELECTRIC FIELD	2	2	2	2	8
				PLANETARY PARTICLES AND RADIATION	110	PARTICLES	12	12	8	8	40
						INTERACTION WITH INTERPLANETARY MEDIUM	8	8	8	8	32
						PLANETARY RADIATION	11	5	5	5	26
						SOLAR INFLUX	3	3	3	3	12
		INTERIORS OF JOVIAN PLANETS	160	SURFACE AND INTERNAL COMPOSITION	53	PLANETARY ELEMENTAL ABUNDANCES	9	6	3	3	21
						PLANETARY ISOTOPIC RATIOS	9	5	3	3	20
						SURFACE AND CORE MATERIALS	3	3	3	3	12
				PLANETARY STRUCTURE	53	INTERNAL STRUCTURE	6	5	5	5	21
						SURFACE STRUCTURE	4	4	4	4	16
						CHEMICAL AND PHYSICAL PROPERTIES	2.5	2.5	2.5	2.5	10
						GEOMETRIC SHAPE	1.5	1.5	1.5	1.5	6
				PLANETARY ACTIVE PROCESSES	53	INTERNAL ACTIVITY	10	8	8	8	34
						ACTIVE SURFACE PROCESSES	3	3	3	3	12
						DYNAMICS OF THE PLANET	2	2	2	2	8
		BIOLOGY OF THE JOVIAN PLANETS	160	PRIMEVAL CONDITIONS	59	PRIMITIVE REDUCING ATMOSPHERE	6	5	4	4	19
						SOLVENTS	7	5	4	4	20
						ENERGY SOURCES	7	5	4	4	20
				PRIMORDIAL SUBSTANCES	59	LIFE-ASSOCIATED SUBSTANCES	13	11	8	8	40
						PRE-LIFE MOLECULES	6	5	4	4	19
				MANIFESTATIONS OF LIFE	42	DIRECT EVIDENCE OF LIFE	9	6	4	4	23
						PHYSICAL EFFECTS OF LIFE	4	3	2	2	11
						BIO-CHEMICAL PROCESSES	3	2	1.5	1.5	8
		INTERPLANETARY MEDIUM	160	INTERPLANETARY FIELDS	64	MAGNETIC FIELDS	13.5	13.5	13.5	13.5	54
						ELECTRIC FIELDS	1.3	1.3	1.2	1.2	5
						GRAVITY FIELDS	1.3	1.3	1.2	1.2	5
				INTERPLANETARY PARTICLES	48	SOLAR PLASMA	6.5	6.5	6.5	6.5	26
						COSMIC RAYS	4	4	4	4	16
						NEUTRAL PARTICLES	.5	1	2	2.5	6
				AGGLOMERATE MATTER	48	METEOROIDS	7.3	7.3	7.2	7.2	29
						ASTEROIDS	19	0	0	0	19

Table 4.1 SUMMARY RESULTS FOR OVERALL SCIENCE EVALUATION

is found from the relative percentage values of Figures 4.3 and 4.6 to be given by (.50) x (.25) x (.30) x (1000) = 38. The portion of each of the total Category Objective values that is attributable to the individual planets is also tabulated in Table 4.1.

SECTION 5

PAYLOAD SELECTION

Compiled by

K. L. Uherka

Contributors

A. B. Binder
L. Golden
H. Goldman
J. C. Jones
D. L. Roberts
K. L. Uherka

5. PAYLOAD SELECTION

The selection of actual instrumentation and the consequent payload to be used for the multiple outer planet mission could be based on a variety of criteria. Some of the relevant factors include: scientific worth of the measurements, national prestige, weight and/or power requirements of the instrument packages, economic considerations, and so forth. Factors such as national prestige are difficult to assess, and as a consequence the present study will be limited to a certain extent. This limitation is self-imposed in that the purpose of this investigation is to develop a spacecraft instrument selection methodology based principally on the science requirements, in an attempt to formulate a logical scheme that can be used as a guide in determining the final payload.

Section 5.1 of this Section is devoted to the methodology used for the selection of instruments for the flyby mission to the Jovian planets. The final selection criteria is based on the capability of a particular instrument to fulfill the science objectives discussed in the previous chapter, but subject to various constraints such as: the requirement to increase present knowledge by an order of magnitude, compatability of instruments with flyby missions, weight requirements, and trajectory profile restrictions.

Section 5.2 is devoted to a discussion of the types of instrumentation that are considered and their role in fulfilling the science requirements. The actual worth evaluation of measurement techniques for a 1977 mission passing exterior to the rings of Saturn is covered in Section 5.3. Section 5.4 concludes the chapter with a presentation of the selected payloads.

5.1 Methodology for Payload Selection

The basic thesis of the present study is to outline a logical framework through which spacecraft instrumentation can be selected on the basis of their contributions to science. The chart of Figure 5.1 illustrates the general flow of ideas that has been developed to evaluate spacecraft instrumentation. As a first step, values of scientific objectives and measurables relative to the overall exploration goal were established in the previous chapter. The evaluation scheme sought to place the major emphasis on those scientific objectives that contributed the most to our understanding of the origin and evolution of the solar system through examination of the Jovian planets. Using these results as the basic foundation, the next step is to determine what measurement techniques would, when operating remotely in a flyby mode, be capable of obtaining useful scientific data relative to the science requirements.

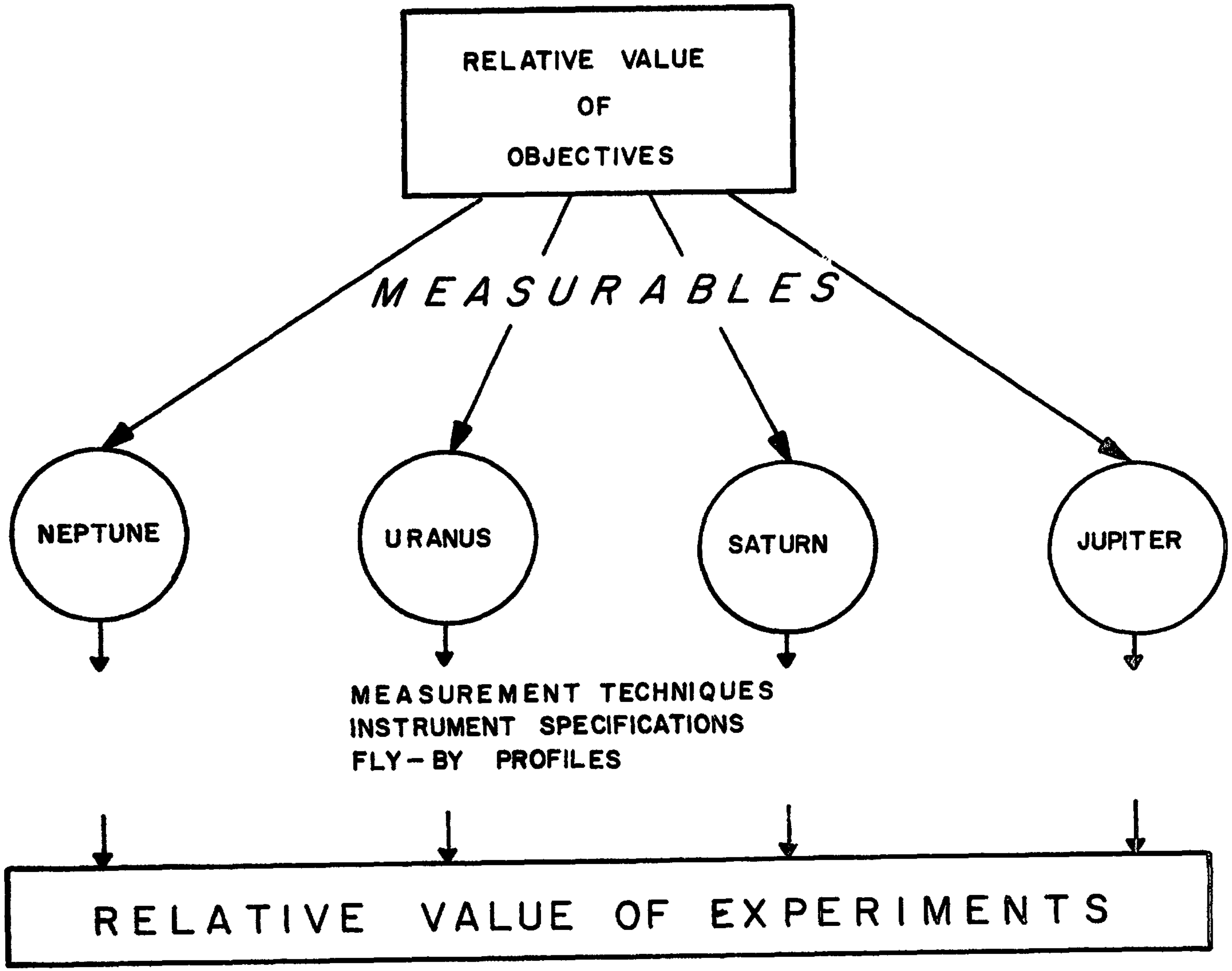

FIGURE 5.1
FLOW DIAGRAM FOR EVALUATION AND SELECTION OF SPACECRAFT EXPERIMENTS

The applicable flyby measurement techniques that were selected are shown in Table 5.1, along with a summary presentation of the Category Objectives that were developed from the original Goal of Exploration. It should be noted that the measurement techniques are those which were judged to be most effective in obtaining data relative to the Objective Measurables that were presented for each Category Objective level in Figures 4.4 through 4.17. The designation of "Not Applicable" under the right-hand column for Measurement Techniques in Table 5.1 indicates those objectives for which present remote sensing techniques were deemed inadequate to increase our present knowledge significantly. Also, it should be noted that only those techniques that were considered most appropriate for a flyby mission to the outer planets have been considered. As an example, while spectrometery is an applicable technique for the Category Objective of Atmospheric Elemental and Molecular Abundance, it was omitted because narrow band photometry provides a simpler means of measurement and can provide adequate data for the initial mission to the Jovian planets under consideration. The next generation of missions would undoubtedly require the more sophisticated techniques of spectrometry measurements. The Occulation Data technique for this same Category Objective pertains only to the determination of the mean molecular weight (See Objective Measurables Column of Figure 4.4). Similar reasoning and judgement was

GOAL OF EXPLORATION	EXPLORATION REGIME	REGIME CATEGORY	CATEGORY OBJECTIVE	APPLICABLE FLYBY MEASUREMENT TECHNIQUES FOR MULTIPLE OUTER PLANET MISSION
EXAMINATION OF THE JOVIAN PLANETS AND INTERPLANETARY SPACE	ATMOSPHERES OF JOVIAN PLANETS	ATMOSPHERIC COMPOSITION	ELEMENTAL AND MOLECULAR ABUNDANCES	PHOTOMETRY AND OCCULTATION DATA
			ISOTOPIC ABUNDANCE AND RATIOS	PHOTOMETRY
			PARTICULATE MATTER	POLARIMETRY, PHOTOMETRY AND RADAR
		ATMOSPHERIC DYNAMICS AND ACTIVE PROCESSES	ATMOSPHERIC MOTION AND CIRCULATION	TELEVISION AND RADIOMETRY
			WEATHER PHENOMENA	RADIOMETRY
		ATMOSPHERIC STRUCTURE	THERMODYNAMIC STATE	RADIOMETRY AND OCCULTATION DATA
			CLOUD STRUCTURE	TELEVISION
	PARTICLES AND FIELDS	PLANETARY FIELDS	MAGNETIC FIELD	MAGNETOMETER
			GRAVITY FIELD	TRAJECTORY DATA
			ELECTRIC FIELD	NOT APPLICABLE
		PLANETARY PARTICLES AND RADIATION	PARTICLES	μ-METEORITE AND COSMIC RAY DELECTORS AND ION AND TRAPPED PART. PACKAGE
			INTERACTION WITH INTERPLANETARY MEDIUM	PLASMA PROBE, MAGNETOMETER AND ION. CHAMBER AND TRAPPED PART. PACKAGE
			PLANETARY RADIATION	PHOTOMETRY AND RADIOMETRY
			SOLAR INFLUX	PLASMA PROBE AND COSMIC RAY DETECTOR
	INTERIORS OF JOVIAN PLANETS	SURFACE AND INTERNAL COMPOSITION	PLANETARY ELEMENTAL ABUNDANCES	NOT APPLICABLE
			PLANETARY ISOTOPIC RATIOS	NOT APPLICABLE
			SURFACE AND CORE MATERIALS	NOT APPLICABLE
		PLANETARY STRUCTURE	INTERNAL STRUCTURE	NOT APPLICABLE
			SURFACE STRUCTURE	ADAR
			CHEM. AND PHYSICAL PROPERTIES	N.. APPLICABLE
			GEOMETRIC SHAPE	TELEVISION AND OCCULTATION DATA
		PLANETARY ACTIVE PROCESSES	INTERNAL ACTIVITY	NOT APPLICABLE
			ACTIVE SURFACE PROCESSES	NOT APPLICABLE
			DYNAMICS OF THE PLANET	TELEVISION
	BIOLOGY OF THE JOVIAN PLANETS	PRIMEVAL CONDITIONS	PRIMITIVE REDUCING ATMOSPHERE	NOT APPLICABLE
			SOLVENTS	PHOTOMETRY
			ENERGY SOURCES	RADIOMETRY
		PRIMORDIAL SUBSTANCES	LIFE-ASSOCIATED SUBSTANCES	PHOTOMETRY
			PRE-LIFE MOLECULES	PHOTOMETRY
		MANIFESTATIONS OF LIFE	DIRECT EVIDENCE OF LIFE	NOT APPLICABLE
			PHYSICAL EFFECTS OF LIFE	NOT APPLICABLE
			BIO-CHEMICAL PROCESSES	NOT APPLICABLE
	INTERPLANETARY MEDIUM	INTERPLANETARY FIELDS	MAGNETIC FIELDS	MAGNETOMETER PACKAGE
			ELECTRIC FIELDS	NOT APPLICABLE
			GRAVITY FIELDS	TRACKING DATA
		ATOMIC PARTICLES	SOLAR PLASMA	PLASMA PROBE
			COSMIC RAYS	COSMIC RAY DETECTOR
			NEUTRAL PARTICLES	MARS SPECTROMETER
		AGGLOMERATE MATTER	METEOROIDS	μ-METEOROID DETECTOR
			ASTEROIDS	μ-METEOROID DETECTOR

Table 5.1 APPLICABLE MEASUREMENT TECHNIQUES BASED ON SCIENCE REQUIREMENTS

used to select the other measurement techniques given in Table 5.1.

The general techniques of Table 5.1 are, of course, directly associated with actual or contemplated spacecraft instrumentation. An understanding of the capabilities of these instruments is required in order to assess their ability to fulfill, either completely or partially, the desired science objectives. Thus, the measurement techniques, along with a knowledge of the remote sensing potential of the associated spacecraft instruments provide a means for evaluating the worth of a particular instrument. This worth is directly related to that portion of the Objective Measurables of a particular Category Objective (see Section 4) for which the instrument yields useful scientific data. Of course, if a particular measurement contributes data that applies to more than one Category Objective level, the overall worth of the instrument in question is increased accordingly. The ultimate value and priorty of any individual instrument will thus depend both on the magnitude of the pure science value of an Category Objective (see Table 4.1) for which it yields data and on the total number of Category Objectives for which it is applicable. This summation feature of the present evaluation scheme provides a highly desirable and logical approach for assessing the full worth of an instrument, and contributes greatly towards the effective utilization of spacecraft capabilities.

Although the general evaluation scheme appears to be more or less straight forward, there are several constraints which must be considered and accounted for. First of all, there is the fact that a certain amount of scientific data, particularly in the case of Jupiter, is presently available. Thus, for a spacecraft measurement to have full value, it should yield information which increases knowledge beyond its present extent. As a result, an evaluation contraint was adopted which states that: "for a particular instrument to have value it must provide scientific data that is an order of magnitude better than the data which is presently available." This constraint, of course, is planet dependent and was treated as such in the evaluations. Perhaps the major evaluation variable is the influence of the trajectory profiles at each planet. For example, the data from an instrument such as TV which depends on factors such as ground resolution and reflected sunlight, depends critically on the spacecraft altitude during encounter as well as on the amount of time spent over the daylight hemisphere.

The methodology for the final instrument evaluation scheme which evolved is illustrated by Figure 5.2. The first step indicates the science evaluation performed in the previous chapter, in which the relative value of each science objective was determined for each planet. The next step was to select the applicable flyby measurement techniques that are best

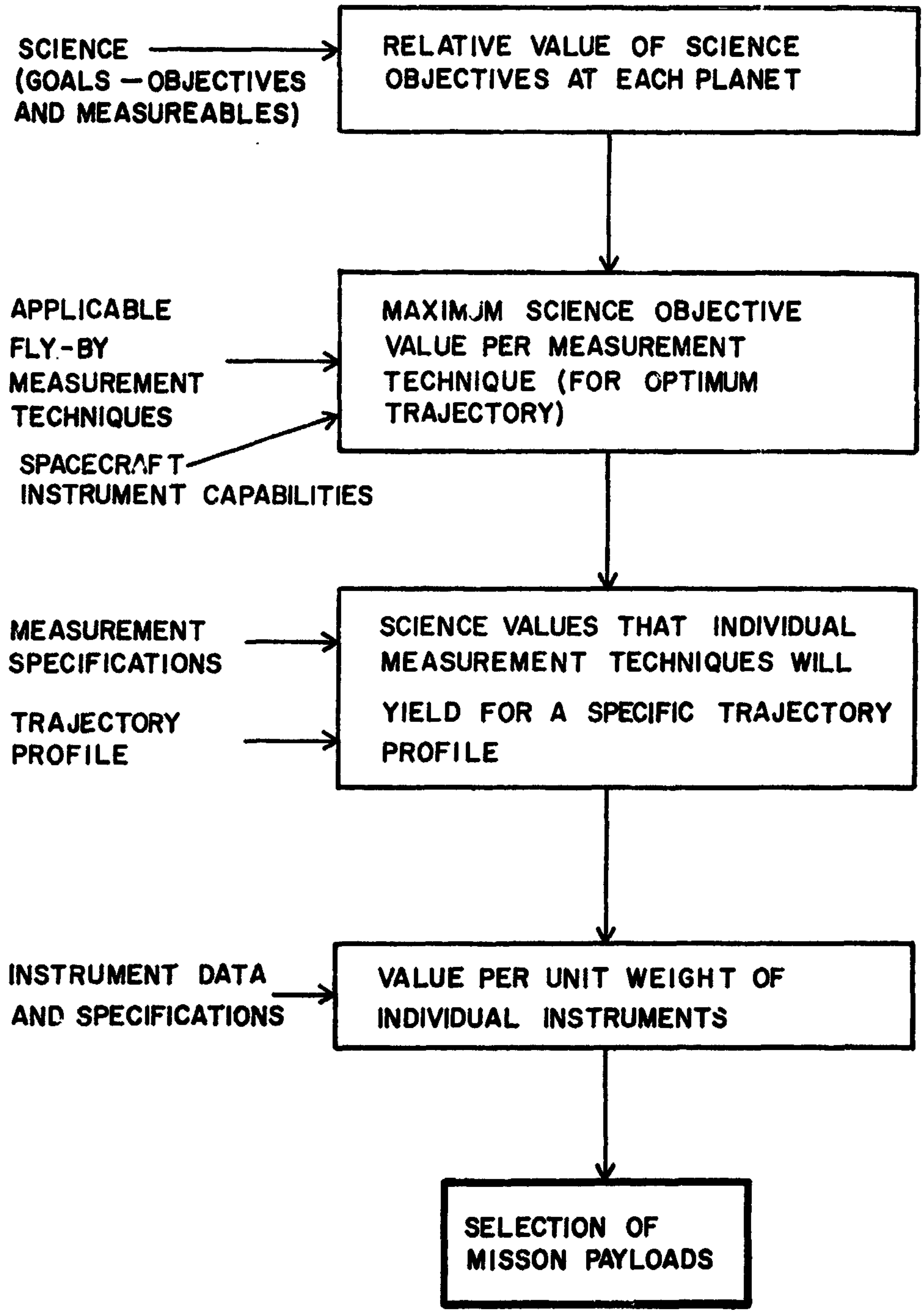

FIGURE 5.2 METHOD FOR EVALUATION AND SELECTION OF PAYLOAD

suited for obtaining scientific data relative to the Category Objectives and their Objective Measurables, the results of which were shown in Figure 5.1. Using this information, along with a knowledge of the capabilities of the related spacecraft instruments that are discussed in the next section (5.2), it will be possible in Section 5.3 to estimate the maximum science value that the data of any particular instrument could yield. This step in the evaluation scheme is indicated by the second block of Figure 5.2, and indicates the percentage of the Category Objective values that a particular instrument could fulfill under ideal conditions (assuming an increase of present knowledge by an order of magnitude and an optimum trajectory profile).

The third step in the evaluation scheme is to assess the influence of the various constraints due to non-optimum fly-by profiles, illumination conditions, resolution requirements, etc., for each planet. The assessment is accomplished by round-table discussion and analysis by a qualified group of scientists and engineers. This step then, represented by the third block of Figure 5.2, effectively results in the determination of a "degradation factor" at each planet and for each trajectory opportunity under consideration (see Sections 2 and 3). The final result is a new relative value for each instrument that is less than or equal to the previous optimum value for the case of ideal conditions. The detailed evaluation results for the 1977 opportunity with an exterior passage around Saturn's outer-most ring (designated as: 1977-E) are given in Section 5.3.

The final phase in the payload selection involves priority ordering of the spacecraft instruments. This can be accomplished by introducing the weight of the spacecraft instruments as an additional factor to be used in the selection criteria. Since the total payload weight for a given space vehicle is limited due to fuel requirements, etc., it is logical that, given two instruments with the same relative value, the instrument having the least weight should have first priority on the spacecraft since this allows for the possibility of additional instruments and hence a higher total value for the final payload (for a given payload weight). Thus using the instrument specifications of Section 5.2, the value per unit weight of each individual instrument can be determined. These results along with the recommended mission payloads are presented in Section 5.4.

5.2 Description of Instrumentation

The following section describes briefly the types of instruments which were tabulated in Table 5.1 as possibilities for a Grand Tour Mission. Several are very similar to existing spacecraft instruments, but some are beyond the present state-of-the-art of spacecraft technology.

In each case the mode of operation and any critical facts concerning the instrument's inclusion in a mission payload have been outlined. Also, a summary of the important specifications is presented in Table 5.2.

5.2.1 Meteoroid Detector - This instrument is of the dielectric/acoustic type similar to that flown on the Mariner spacecraft. It consists of an aluminum acoustic plate with a crystal microphone on one side, and overcoated on both sides with an evaporated dielectric capacitance. The dielectric capacitors provide directional information of impacts and in addition have a detecting threshold at least one order of magnitude below that of the microphone. A threshold detection limit of momentum $\leq 10^{-6}$ dynes-sec is desired for the dielectric capacitor and assuming particle velocities x 10 kms/sec, this gives a mass detection threshold $\leq 10^{-12}$ gms.

A momentum spectrum is produced by pulse height analysis of the acoustic impact signals, the range being x 10^{-5} dyne-sec to $\sim 10^{-3}$ dyne sec.

The instrument could be operated continuously throughout the mission, the mean rate of data acquisition would be nominal except during passage through the Asteroid Belt and in the region of Saturn's rings. At these times the data rate required is ~ 1 bit/sec. Data from the detector consists of an accumulated count of the total number of microphone impacts, and for each impact a pulse height

Table 5.2

SUMMARY OF SPECIFICATIONS FOR APPLICABLE FLYBY INSTRUMENTATION

No.	Instrument	Wts. (lb)	Power (watts)	Data Rate Cruise	Data Rate Encounter	Comments	Refs.
1	Meteoroid Detector	2.1	0.4	Nominal	Nominal	----	1
2	Magnetometer Package	10	8	1 bps	1 bps	----	2,3
3	Cosmic Ray Detector	2.6	0.6	Nominal	Nominal	----	1,4,5
4	Plasma Probe	6.4	3	3 bps	3 bps	----	1,6,7
5	Ion and Trapped Particle Package	4.9	1	1 bps	1 bps	----	1,8
6	Polar./Phot. Package	5	2	----	10 bps	light side planet only	9
7	IR-μ wave Radiometer	10	5	----	1 bps	light and dark side	3,10
8	R. F. Detector	5	5	----	1 bps	light and dark side	11
9	TV #2 (low resol.)	10	10	----	10^4 bps	light side only (30 frames)	1
10	Narrow band UV Photometers	10/15	5	----	1 bps	view exosphere	12,13
11	Occulation (2 freq.)	20	10	----	1 bps	ingress and egress	14
12	Absorption Photometers	20	5	----	1 bps	light side only	13
13	Mass Spectrometer	10	5	1 bps	1 bps		15
14	Airglow/Aurora Phots.	8	2	----	1 bps	dark side only	13
15	TV #1 (high resol.)	30	20	----	10^4 bps	light side (30 frames)	1
16	Radar	20	20	----	1 bps	light and dark side	16,17
17	IR-μ wave Rad. (high res.)	20	10	----	10^2 bps	light and dark side	18

Table 5.2 (Continued)

SUMMARY OF SPECIFICATIONS FOR APPLICABLE FLYBY INSTRUMENTATION

References:

1. "Mariner Mars 1964 Project Report: Scientific Experiments," R. K. Sloan, JPL Technical Report 32-883 (1968).
2. "Scientific Experiments for Ranger 1 and 2," JPL Technical Report 32-56 (1961).
3. "Mariner - Venus 1962: Final Project Report," NASA-SP-59 (1965).
4. "Cosmic Radiation Helium Spectrum Below 90 MeV per Nucleon Measured on IMP-1 Satellite," C. Y. Fan et al., J.G.R., 70, 3515 (1965).
5. "Cosmic Ray Telescope," NASA New. Release No. 65-117-D (1965).
6. "The Orbiting Geophysical Observatories," G. H. Ludwig, Space Sci. Rev., 2 175 (1963).
7. "Plasma Probe Instrumentation on Explorer X," H. S. Bridge, et al., Space Research III, John Wiley & Sons, Inc. (1963).
8. "An Automatic Ionization Chamber," H. V. Neher, Rev. Sci. Insts., 24, 99, (1953).
9. "Infrared Filter Wedge Spectrometer Instrument for Nimbus 'D' Satellite", ITT Industrial Labs., ITTIL 67-1034.
10. "Mariner Spacecraft," NASA News Release No. 62-182 (1963).
11. "Cosmic Noise Measurements from 1960 Eta 1 at 3.8 Me/s", Molozzi and Tyas, Nature, 190, 616 (1961).

Table 5.2 (Continued)

SUMMARY OF SPECIFICATIONS FOR APPLICABLE FLYBY INSTRUMENTATION

References (Continued)

12. "Ultraviolet Emissions Observed Near Venus from Mariner V," C. A. Barth et al., Science, 158, 1675, (1967).

13. "The Injun III Satellite," B. J. O'Brien et al., State Univ. Iowa, Report No. SUI 62-24 (1962).

14. "Venus Radio Occultation Measurements," A. Kliore et al., Mariner Standord Group, Science, 158, p. 1678 and p. 1688, (1967).

15. "A Double-Focussing Magnetic Mass Spectrometer for Satellite Use," C. A. Reber and L. G. Hall, NASA-TN-D-3211 (1966).

16. "Scientific Experiments for Ranger 3,4 & 5," Technical Report No. 32-199, JPL, October 1962.

17. "Surveyor I Mission Report," JPL Technical Report No. 32-1023.

18. "The Nimbus I Meteorological Satellite," W. Nordberg and H. Press, Bull. Amer. Meteor. Soc., 45, 684, (1964).

analysis of the microphone impulse, a direction indication from the capacitance detectors, and the total number of capacitance impacts between each microphone impact.

5.2.2 Magnetometer Package - The range of the magnetic field strength to be measured during the mission extends from ~ 1 gamma in the interplanetary medium to ~ 5 gauss (1 gauss = 10^5 gamma) in the vicinity of Jupiter. To cover this range two types of magnetometer are included.

For measurements of the interplanetary field, which is approximately 3 gamma, with an accuracy ~ 0.05 gamma, a Rubidium vapor magnetometer could be used. By subjecting the vapor cell to fields produced by a system of Helmholtz coils, both the magnitude and the direction of the interplanetary field can be measured in the range 0.05 - 100 gammas. For planetary field measurements, in the range 100 gamma - 5 gauss, a triaxial fluxgate magnetometer could be used.

The vapor magnetometer should operate throughout the mission at a measurement rate ~ 1 per min., corresponding to a data rate ~ 0.2 bits/sec. During planet encounters both instruments may be in use simultaneously, giving a data rate ~ 1 bit/sec.

5.2.3 Cosmic Ray Detector - In order to monitor the flux and the approximate energy distribution of cosmic rays a simple charged particle telescope of the type flown on IMP-1 and Mariner IV is desirable. This consists of three gold-silicon barrier layers, surface area 2 cm^2, spaced by aluminum and platinum absorbers, producing an angle of acceptance of 45°. By a combination of coincidence counting and pulse height analysis of the signals from each barrier layer, discrimination between protons, alpha particles and electrons is obtained and the energy range of each type can be estimated. Incident protons are detected within the energy ranges 0.8 - 15 Mev, 15 - 80 Mev, and 80 - 190 Mev; alpha particles within energy ranges 3 - 60 Mev, 60 - 280 Mev and $\geq$ 280 Mev. In addition electrons with energy > 0.2 Mev are detected by the first barrier layer only.

5.2.4 Plasma Probe - A Faraday Cup type probe was selected to measure the flux density and energy spectrum of the positive particles of the Solar plasma. The present threshold sensitivity of this type of instrument is 10^{-13} amp/cm^2, corresponding to fluxes 5.10^5 parts/cm^2/sec. This is approximately two orders of magnitude lower than the average flux at 1 AU and therefore equal to the expected flux at distances 10 AU. Thus the present threshold sensitivity must be reduced by at least an order of magnitude or the collecting area increased by an order of magnitude, to be effective at distance > 10 AU on the Grand Tour Mission.

The energy range of analysis available with this type of instrument is 10 eV to 10 keV, divided into 10 energy ranges. Measurements should be made in three directions as in the Mariner IV instrument, in order to find the vector of the Solar plasma. Taking the three measurements at approximately 20 sec. intervals, yields a mean data rate 3 bits/sec which is continuous throughout the mission.

5.2.5 Ionization and Trapped Particle Package - Three types of particle detectors are included in this package to measure the solar cosmic rays and energetic electrons in the interplanetary medium and to determine the spatial distribution, energy spectra and particle types of any trapped radiation belts which may exist at any of the outer planets.

A total-ionization chamber, consisting of a thin wall aluminum sphere filled with argon gas and containing a quartz fiber electrometer, provides an integrated value for the total amount of ionizing radiation. The wall thickness would be designed to allow gas ionization only by electrons with energy > 1 Mev, protons with energy > 10 Mev and alpha particles with energy > 40 Mev. Further energy and particle type discrimination is achieved using Silicon diode type detectors and Geiger-Muller tubes, both of which detect individual particle impacts.

The silicon surface barrier diode is essentially insensitive to electrons and by amplitude discrimination of the output pulse, at least two levels of proton detection can be obtained. The proton energy ranges monitored can therefore be designed as Mev < E < 10 Mev and < E < 4 Mev using a single detector.

The energy range of the Geiger-Muller tube is determined largely by the thickness and material of the entrance window. By suitable choice of e entrance windows of G-M tubes, electron energies > 40 keV and proton energies > 0.5 Mev can be divided into several regions.

The ionization chamber is essentially an omni-directional detector except where it is shielded by the spacecraft, the angles of acceptance of G.-M. tubes and Si diode, however, are determined by the metal shielding in front of the window. Thus angular distribution information can be obtained by orientating the detecting in different directions with respect to the stabilized spacecraft. Since the detectors are inherently event counters, and will operate continuously throughout the mission, the data rate will vary over several orders of magnitude, due to solar flare events and passage through any planetary radiation zones.

5.2.6 Polarization and Photometry Package - This instrument operates only at planetary encounters, viewing the solar illuminated disk. If pointed at the planet center, it can provide albedo and polarization data for almost all phase angles from 0-180°. Ten wide-band wavelength regions are desired in order to cover the entire UV-IR range. In addition, the incorporation of two polaroid filters is needed to determine the polarization.

As visualized, the instrument consists of a single photo-multiplier and collecting optics giving a spatial resolution of 1/00 of the planetary disk. Spectral and polarization discrimination is provided by two rotating filter wheels operated in series. One wheel carries ten wide band-pass filters and the other, two polaroid windows and an open aperture. Thus each measurement consists of 30 data points, using all combinations of filters and windows. Measurements are required at least every 5° change in phase angle, and in order to obtain maximum possible coverage, a total of 300 measurements are required at each planet.

5.2.7 IR-Microwave Radiometer - A radiometer with a number of pass-bands in the wavelength range 2μ - 1 mm can provide data on the thermal emission of the planets. The instrument operates during planet encounter, on both the light and dark sides, with a spatial resolution of 1/00 of the planets disk. Five detection bands in the region 2μ - 1 mm would be satisfactory, each sensitive to 1/10°K changes in the planetary emission.

Complete thermal mapping of each planet is possible during a flyby with 300 measurements, i.e., 1500 data points, taken over a period $\leq$ 3 hours. The instrument should be bore-sighted with the TV cameras for visual identification, and a facility to preprogram examination of a particular interesting area on a planet would be desirable.

5.2.8 R.F. Detector - A radio frequency noise detector operating in the wavelength range 1 - 10 meters is required to indicate the presence of electrical discharges within the planetary atmospheres. Although lightning discharges have a peak energy output at $\sim$100 meters, other noise sources could predominant at wavelengths other than 1 - 10 meters. At Jupiter in particular, the decameter radio bursts and the absorption of an ionosphere (if present) preclude noise detection at λ > 10 meters and since the energy spectrum of lightning discharges decreases rapidly with decreasing wavelength, the most useful wavelength range is 1 - 10 meters.

5.2.9 Low Resolution Television - The instrument envisioned here is similar to that flown on Mariner IV, consisting of a small Cassegrain reflecting telescope and an electrostatic vidicon camera. The field of view required is 1.5 deg., the number of lines per frame = 1000, and a small number of interchangeable wide band filters would add spectral information to the images. Assuming values of closest approach corresponding to the 1977 Exterior Ring passage, this would give spatial resolutions ranging from $\sim$ 500 kms to $\sim$50 kms at Jupiter and from 50 kms to $\sim$ 5 kms (at the terminator) at Saturn, Uranus and Neptune. This is a satisfactory resolution at the latter planets for a study of cloud structure and atmospheric motion. However, at Jupiter, although it is almost an order of magnitude better than present ground-based resolution, it is not sufficient for the particular measurables of concern. The instrument is therefore given a lower value at Jupiter than at Saturn, Uranus and Neptune.

Operation of the instrument begins when the whole planet occupies an appreciable fraction of the frame size, and such pictures can be used to determine the geometric shape. A minimum of 30 pictures per planet are desired, giving a data total $\sim 2.10^8$ bits/planet.

5.2.10 Abundance Photometers - Approximately seven photomultiplier tubes and narrow band-pass filters are needed to measure exospheric mission lines in the UV-visual and hence obtain the exospheric abundance ratios. The required field of view for each detector is $\sim 5°$, in the direction perpendicular to the Sun-spacecraft line. The filter band-passes would each be set at an expected emission line of H, He, O, N, A, or Ne, one further detector at a spectral position of no emission is required to differentiate between scattered and emitted radiation.

The instrument operates at a distance of ~10 planet radii before and after, and during this time ~ 100 data points/channel would be taken.

A further three detectors, two with very narrow band-passes filters at the spectral location of the isotopes of H and He and one as a monitor of scattered light, will provide information on the isotopic ratios of hydrogen and helium in the exosphere.

5.2.11 Occulation - Transmission of data from the spacecraft during occulation can provide a single frequency determination of the atmospheric occulation profile. However, experimental data transmitted in this time would be lost, at least in part. Hence the method of obtaining atmospheric and ionospheric occulation profiles will be to use a multi-channel radio receiver on the spacecraft tuned to at least two frequencies in the S-band region. This will receive and record transmissions from Earth which are then partially processed and retransmitted to Earth after planet encounter. Since the atmospheres of the outer planets are very thick, large changes of frequency, phase and amplitude of the radio signals may be expected, therefore operation in a transponder mode by the spacecraft would create very complex data without any increase in scientific value.

5.2.12 Narrow Band Absorption Photometers -

Two photomultipliers each with a narrow band-pass filter, can be used to measure the absorption band of a particular atmosphereic neutral gas component. One filter should be positioned at the wavelength of an absorption band of the component to be detected and the other positioned in the continuum adjacent to the band. Five such pairs of detectors operating in the UV to IR spectrum are required to measure absorptions in the reflected solar radiation from the planet arising from CH_4, NH_2, H_2O, H_2 and He for example. A further two pairs can be included to measure absorption arising from life-associated molecules (assuming such absorptions have been identified).

The instrument should be planet-centered, with a spatial resolution < 1/10 disk and operate at encounter, viewing the illuminated disk. A total of ~ 30 measurements are needed and the total data acquired would be ~ 3000 bits.

5.2.13 Mass Spectrometer - A neutral mass spectrometer uses electrostatic and magnetic deflection techniques to separate ions created by ionization (of the neutral atoms) within the instrument. The desired instrument is a simipler version of the type flown on Explorer 17 for the same purpose, when neutral density measurements were made of He, O, N, O_2, N_2, and H_2O. The instrument should operate throughout the entire mission, taking measurements at a maximum rate of 1/min. and thus the data rate is $\leq$ 0.1 bits/sec.

5.2.14 Airglow Photometers - Four photomultiplier tubes and narrow band-pass filters in the UV-visible region can be used to measure atmospheric airglow and auroral emission on the dark side of the planets. The instrument should be planet-centered, with a field of view $\sim 5°$ and should operate only beyond the terminator. A minimum of 30 data points per detector are required to scan the planets dark side, giving at minimum 1000 bits per planet.

5.2.15 High Resolution Television - This instrument utilizes the same type of electrostatic vidicon camera as the low resolution system but will include a larger telescope, (estimated diameter $\geq$ 10 cms). The field of view required is $\simeq$ 0.15 deg and the camera should be located within the frame of the low resolution system. With 1000 lines/frame, this gives a resolution at Jupiter ranging from ~ 50 km to ~ 5 km (at the terminator). At Saturn, Uranus and Neptune, however, the spatial resolution ranges from ~ 5 km to ~ 500 km. This is too small for the study of cloud structure and atmospheric motion and hence the value of the instrument is reduced at these planets. A minimum of one high resolution image for each low resolution image is required; the total amount of data for this camera is then $\sim 2 \times 10^8$ bits per planet.

5.2.16 Radar - An active radar system comprising a transmitter and receiver on the spacecraft is required to locate particulate matter in the planetary atmosphere or a surface below the atmosphere. A minimum of two wavelengths are desirable in the range of 10 cm to 1 meter. The instrument can operate on both light and dark sides at a measurement rate of ~ 1 pulse/min. The present state of knowledge of the Outer Planets makes this very much a search mode experiment since even the existence of planet surfaces is not proven. At the present time there does not appear to be an active radar system with reasonable power and weight specifications to perform this function.

5.2.17 High Resolution Radiometer - A high resolution radiometer operating at several wavelengths in the range 2μ - 1 mm with a spatial resolution ~ 10 km is judged to be capable of mapping local thermal cells in the planetary atmospheres. With an angular resolution ~ 0.005 deg., the spatial resolution at Jupiter is $\geq$ 100 kms and at Saturn, Uranus and Neptune, $\geq$ 10 kms. Thus the value of the instrument, in achieving the required measurement, is low at Jupiter and high at the other planets.

The instrument can be boresighted with the high resolution television but it should also be capable of making several spaced measurements per TV picture. Also, the radiometer will be operated on both light and dark sides of the planet, a data total ~ 10^6 bits/planet.

5.3 Evaluation of Measurement Techniques

The detailed worth evaluation of applicable flyby instruments is presented in this section using the evaluation methodology that was outlined in Section 5.1 along with the instrument specifications of Section 5.2. The relative worth of any instrument depends principally on its ability to meet measurement specifications at a given planet for a given trajectory. In order to simplify the presentation, the detailed results will be presented only for the 1977-E opportunity discussed in Sections 2 and 3. The relevance to the other mission opportunities will be briefly discussed in the next section.

The results of the evaluation are summarized in Tables 5.3 through 5.8. The first two columns of the tables reiterate the science evaluation of Section 4 for the relevant Regime Categories and their Category Objectives. Those Category Objectives for which no applicable flyby measurement technique was indicated in Table 5.1 have been omitted from further consideration. The third column titled "Applicable Flyby Instrument" lists the instruments which were judged most appropriate for an initial mission to the Jovian planets, the selection of which was based on the discussions of the previous sections.

INSTRUMENT EVALUATION FOR THE CATEGORY OF ATMOSPHERIC COMPOSITION

The first two columns of Table 5.3 reiterate the science breakdown and the relative value percentages that resulted from the evaluation scheme of Chapter 4 (see also Figure 4.4 and Table 5.1). The flyby instruments that are applicable for each Category Objective level are listed in the center column of the table.

The fourth column gives the value judgment for the maximum percentage value that the scientific data of each instrument, under optimum flyby conditions, could possibly contribute towards fulfilling the science requirements of the relevant Category Objective. These science requirements are determined by the Objective Measurables as were specified in Figure 4.4. For example, Emission UV Photometers were judged as capable of providing 20% of the scientific knowledge desired for Elemental and Molecular Abundances and 5% for Isotopic Abundances as a result of narrow-band photometeric studies of airglow, auroral emission, etc. For the case of Particulate Matter, the value judgment indicated that a combined instrument package utilizing polarimetry, wideband UV-IR photometry and radar was capable as a group of providing 100% of the total value attributable to the objective, assuming optimum conditions.

The last four columns of Table 5.3 indicate whether or not the maximum instrument value was attainable at the individual planets during the 1977-E opportunity. For several of the cases shown, the contributions of the instruments at the planet Jupiter were judged to be less than the maximum value because the large miss distances reduce the resolution obtainable at this planet. Also for Particulate Matter, the projected radar technology was estimated to be capable of yielding only about one-half (or 15%) of the desired information.

Table 5.3

INSTRUMENT EVALUATION FOR THE CATEGORY OF ATMOSPHERIC COMPOSITION

Regime Category	Category Objectives	Applicable Flyby Instrument	Maximum Value (%) of Instrument Relative to Objective	Planetary Value of Instrument Relative to Objective for 1977-E Trajectory			
				Jup.	Sat.	Uran.	Nept.
Atmospheric Composition (42%)	Elemental and Molecular Abundances (38%)	1. Narrow Band Emission UV Photometer #1	20%	20%	20%	20%	20%
		2. Absorption UV-IR Photometer	8%	8%	8%	8%	8%
		3. Occulation Data	25%	8%	17%	25%	25%
	Isotopic Abundances & Ratios (38%)	1. Narrow Band Emission UV Photometer #2	5%	5%	5%	5%	5%
	Particulate Matter (24%)	1. Polarimeter } Package	50%	45%	50%	50%	50%
		2. UV IR Photometer } Package	20%	18%	20%	20%	20%
		3. Radar	30%	15%	15%	15%	15%

INSTRUMENT EVALUATION FOR THE CATEGORIES OF ATMOSPHERIC DYNAMICS AND ACTIVE PROCESSES AND ATMOSPHERIC STRUCTURE

The science brekdown, the corresponding relative values given in Figures 4.5 and 4.6, and the applicable flyby instruments from Table 5.1 are given in the first three columns of Table 5.4. It is seen from the fourth column of the table that applicable instruments are capable of contributing only a small percentage of the total value associated with the Category Objectives of Atmospheric Motion and Weather Phenomena. These value judgments were based on the premise that a full understanding of atmospheric dynamics could only be obtained through the data of atmospheric probes and in situ measurements, in contrast to the remote sensing capabilities of flyby instruments. On the other hand, the maximum value that can be obtained from the instruments applicable for the measurables of Thermodynamic State and Cloud Structure constitutes a considerable portion of the science worth available. This conclusion follows directly from the fact that measurables such as cloud features are readily detected by remote means.

The final columns of Table 5.4 give the revised instrument percentage value at each planet, after assessment of the trajectory profiles and other constraints discussed in the text. As an example, the use of television to obtain data on Atmospheric Motions and Circulation was judged to be severely hampered by the short encounter times for which sunlight was available. For the case of cloud structure, the 40% maximum value available through low resolution TV was reduced to 8% at Jupiter because the data would not be significantly better than Earth based results. For the high resolution TV system the maximum 40% value was judged to be applicable for the Jupiter profile, but was reduced for the other planets because the data would give much more detail than is desired for a satisfactory interpretation of the cloud features, at least for the case of a first mission.

Table 5.4

INSTRUMENT EVALUATION FOR THE CATEGORIES OF ATMOSPHERIC DYNAMICS AND ACTIVE PROCESSES AND ATMOSPHERIC STRUCTURE

Regime Category	Category Objectives	Applicable Flyby Instrument	Maximum Value (%) of Instrument Relative to Objective	Planetary Value of Instrument Relative to Objective for 1977-E Trajectory			
				Jup.	Sat.	Uran.	Nept.
Atmospheric Dynamics and Active Processes (33%)	Atmospheric Motion and Circulation (60%)	1. TV #1 and #2	10%	3%	3%	2%	2%
		2. IR-μ-wave Radiometer #2	5%	1/2%	5%	5%	5%
	Weather Phenomena (40%)	1. R. F. Detector	5%	5%	5%	5%	5%
Atmospheric Structure (25%)	Thermo-Dynamic State (50%)	1. Occulation Data	--	--	--	--	--
		2. IR-μ-wave Radiometer #1	30%	30%	30%	30%	30%
	Cloud Structure (50%)	1. TV (High Res.) #1	40%	40%	12%	10%	10%
		2. TV (Low Res.) #2	40%	8%	40%	40%	40%

INSTRUMENT EVALUATION FOR CATEGORY OF PLANETARY PARTICLES AND RADIATION

Table 5.5 illustrates the results of the science and instrument evaluations for the Regime Category of Planetary Particles and Radiation. The applicable flyby instruments as deduced from the results of Sections 5.1 and 5.2 are given in the third column, which is then followed by the maximum percentage value that the instrument was judged to be capable of providing. This maximum instrument value represents the percentage of the total Category Objective value that the instrument could provide under ideal conditions. The values given in Table 5.5 are a result of value judgments that were made in relation to the estimated capability of the instrument data to provide new knowledge concerning the Objective Measurables given in Figure 4.8.

The final planetary percentage values of the instruments have in almost all cases been judged as equal to the maximum values that could be expected. The reason for this is the fact that the trajectory profiles at the planets have a relatively minor influence on the worth of particles and fields experiments, in contrast to the high degree of influence for many other types of experiments.

Table 5.5

INSTRUMENT EVALUATION FOR CATEGORY OF PLANETARY PARTICLES AND RADIATION

Regime Category	Category Objectives	Applicable Flyby Instrument	Maximum Value (%) of Instrument Relative to Objective	Planetary Value of Instrument Relative to Objective for 1977-E Trajectory			
				Jup.	Sat.	Uran.	Nept.
Planetary Particles and Radiation (50%)	Particles (36%)	1. -meteorite Detector	10%	10%	10%	10%	10%
		2. Cosmic Ray Detector	10%	10%	10%	10%	10%
		3. Ionization Chamber and Trapped Particle Det.	30%	30%	30%	30%	30%
	Interaction with the Interplanetary Media (28%)	1. Plasma	25%	25%	25%	25%	25%
		2. Magnetometer Package	25%	25%	25%	25%	25%
		3. Ion Chamber and Trapped Part. Det.	25%	25%	25%	25%	25%
	Planetary Radiation (24%)	1. Narrow Band UV Photometer #3	15%	14%	10%	10%	10%
		2. IR Radiometer } Package	20%	20%	20%	20%	20%
		3. -wave Radiometer } Package	15%	15%	15%	15%	15%
	Solar Influx (12%)	1. Plasma Probe ($\alpha + p^t$)	20%	20%	20%	20%	20%
		2. Cosmic Ray Detector	10%	10%	10%	10%	10%

INSTRUMENT EVALUATION FOR THE CATEGORIES OF PLANETARY FIELDS, PLANETARY STRUCTURE, AND PLANETARY ACTIVE PROCESSES

Table 5.6 gives the instrument evaluation results for those science objectives that were presented previously in Figures 4.7, 4.10, and 4.11. As before, only those Category Objectives are considered for which applicable flyby instruments were indicated in Table 5.1. The value judgments show that in general the applicable instruments have a small capability toward fulfilling the total science measurable requirements of their Category Objectives, with the possible exception of the magnetometer package which could yield 30% of the desired data on the planetary Magnetic Field objective.

The only two Category Objectives for which the trajectory profiles and other constraints were judged to reduce the instrument effectiveness below its maximum capabilities were Geometric Shape and Dynamics of the Planet. The value judgments here were based on a study of the available Earth-based data, with the conclusion that some of the measurables were already known to the desired accuracy. This was particularly true for the inner-most of the Jovian planets as shown in the last four columns of Table 5.6.

Table 5.6

INSTRUMENT EVALUATION FOR THE CATEGORIES OF PLANETARY FIELDS, PLANETARY STRUCTURE, AND PLANETARY ACTIVE PROCESSES

Regime Category	Category Objectives	Applicable Flyby Instrument	Maximum Value (%) of Instrument Relative to Objective	Planetary Value of Instrument Relative to Objective for 1977-E Trajectory			
				Jup.	Sat.	Uran.	Nept.
Planetary Fields (50%)	Magnetic Field (72%)	1. Magnetometer	30%	30%	30%	30%	30%
	Gravity Field (20%)	1. Trajectory Data	10%	10%	10%	10%	10%
Planetary Structure (33%)	Surface Structure (28%)	1. Radar	10%	10%	10%	10%	10%
	Geometric Shape (12%)	1. TV #1	15%	5%	9%	15%	15%
		2. Occulation Data	5%	1/2%	3%	5%	5%
Planetary Active Structure (33%)	Dyanmics of the Planet (12%)	1. TV #1	1%	---	1/20%	1/5%	2/5%

INSTRUMENT EVALUATION FOR CATEGORIES OF PRIMEVAL CONDITIONS AND PRIMORDIAL SUBSTANCES

The science evaluation and applicable flyby instruments for the Regime Categories of Primeval Conditions and Primordial Substances are presented in the first three columns of Table 5.7. The principle instrument considered is a narrow-band photometer for the purpose of studying the UV-IR absorption spectra of various molecular constituents (see the Objective Measurable listings of Figures 4.12 and 4.13).

The estimated maximum capability of the Absorption UV-IR Photometer was judged as 70% of the respective Category Objective values as shown in the fourth column of Table 5.7, while RF data on lightning and related phenomena has a maximum relative contribution of 25%. One of the major difficulties is that the absorption spectra associated with Pre-Life Molecules and Life-Associated Substances are very complex, and there is considerable doubt as to whether they can be identified through the background absorption bands of the regular atmospheric constituents on the Jovian planets. The worth evaluation presented in Table 5.7 has been based on the premise that technology development can resolve this problem by the 1977-1978 time frame. In this instance, the planetary value of the instrument at Jupiter was reduced because a sufficient amount of data could be obtained from Earth-based studies on this planet.

Table 5.7

INSTRUMENT EVALUATION FOR CATEGORIES
OF PRIMEVAL CONDITIONS AND PRIMORDIAL SUBSTANCES

Regime Category	Category Objectives	Applicable Flyby Instrument	Maximum Value (%) of Instrument Relative to Objective	Planetary Value of Instrument Relative to Objective for 1977-E trajectory			
				Jup.	Sat.	Uran.	Nept.
Primeval Conditions (37%)	Solvents (33%)	1. Absorption UV-IR Photometer (Disk)	70%	7%	70%	70%	70%
	Energy Source (33%)	1. R. F. Detector (Lighting)	25%	25%	25%	25%	25%
Primordial Substances (37%)	Life-Associated Substances (67%)	1. Absorption UV-IR Photometer	70%	7%	70%	70%	70%
	Pre-Life Molecules (33%)	1. Absorption UV-IR Photometer	70%	7%	70%	70%	70%

INSTRUMENT EVALUATION FOR THE CATEGORIES OF INTERPLANETARY FIELDS, INTERPLANETARY PARTICLES, AND AGGLOMERATE MATTER

Table 5.8 reiterates the science evaluation results that were presented previously in Figures 4.15, 4.16, and 4.17. The applicable flyby instruments are also given along with the value judgment for the maximum percentage value that the instrument data could contribute towards fulfilling the science objectives.

In all cases, except for the Asteroids, the full instrument value is available for each planetary interval. The reason for this, of course, is that the trajectory profiles at each planet have no effect on the instrument worth since the science objectives pertain only to interplanetary space. Since data is desired throughout the solar system, each of the intervals measured from the sun (i.e., 1-5 AU, 5-10 AU, 10-20 AU, and 20-100 AU) was attributed full value. The asteroid belt is located at about 2.8 AU, therefore the meteroid detection for sensing asteroid materials has value only for the 1-5 AU interval as indicated in the planetary value columns of Table 5.8.

Table 5.8

INSTRUMENT EVALUATION FOR THE CATEGORIES OF INTERPLANETARY FIELDS, INTERPLANETARY PARTICLES, AND AGGLOMERATE MATTER

Regime Category	Category Objectives		Maximum Value (%) of Instrument Relative to Objective	Planetary Value of Instrument Relative to Objective for 1977-E Trajectory			
				Jup.	Sat.	Uran.	Nept.
Inter-planetary Fields (30%)	Magnetic Fields (84%)	1. Mag. Package	80%	80%	80%	80%	80%
	Gravity Fields (8%)	1. Tracking Data	80%	80%	80%	80%	80%
Interplanetary Particles (30%)	Solar Plasma (56%)	1. Plasma Probe	80%	80%	80%	80%	80%
	Cosmic Rays (32%)	1. Cosmic Ray Detector	80%	80%	80%	80%	80%
	Neutral Particles (12%)	1. Mass Spectrometer	80%	80%	80%	80%	80%
Agglom-erate Matter (30%)	Meteoroids (60%)	1. -Meteoroid Detector	75%	75%	75%	75%	75%
	Asteroids (40%)	1. -Meteoroid Detector	10%	10%	---	---	---

In Tables 5.3 through 5.8, the column indicating the Maximum Value (%) of Instrument Relative to Objective gives the judgment as to what percentage of the total Category Objective value that a particular instrument could possibly fulfill assuming ideal conditions with an optimum trajectory profile. It should be noted that in most cases the indicated instrument is of such a nature that its scientific data pertains only to some fraction or portion of the total number of Objective Measurables which constitute the Category Objective as listed in the second column. Thus in all cases, no one particular instrument has been judged capable of fulfilling 100% of the science requirement. In fact, in most cases, even the use of several different instruments for the purpose of obtaining data on the measurables of a particular Category Objective was not judged as sufficient to yield a 100% relative value. The reason for this is that complete fulfillment requires the use of probes and in situ measurements in addition to remote sensing data.

The final columns in the tables give the adjusted value for each instrument at each planetary target. This adjusted value corresponds to the 1977-E trajectory profiles that were presented in Section 2. For those cases in which the compatability between the instrument and the trajectory profile at a particular planet was judged to be sufficiently close to an ideal situation, the relative value of the instrument at this point was taken to be equal to the maximum value of the instrument given in the fourth column. For those cases in which the interrelation was not judged to be satisfactory, the instrument value was reduced accordingly to a percentage number somewhat less than the maximum attainable value.

There were many factors which entered into the value judgments associated with the last four columns of Tables 5.3 through 5.8. The trajectory profile data given in Section 2 was perhaps the most critical (see Figures 2.27 through 2.39). The encounter trajectories for the 1977-E opportunity are given respectively for Jupiter, Saturn, Uranus and Neptune in Figures 2.27 through 2.30. These profiles provide data on the distance from the spacecraft to the planet, as well as indicating the time differential (in hours) between periapse and a given position on the trajectory path. Figure 2.31 is a plot of the time differential to periapse as a function of true anomaly for each of the Jovian planets. This data was used in assessing the degree of commonality of the various instruments in regards to the total data acquisition times available at each of the Jovian planets. A plot of altitude versus true anomaly is shown in Figure 2.32, and was used to determine the surface resolutions attainable with individual instruments. The sun elevation profiles of Figure 2.33 was useful in assessing the worth of TV systems and other instruments requiring illumination. Similarly the ground speed traces of the sub-satellite point (see Figure 2.34) were required to determine whether or not those instruments, sensitive to relative motion, could be used at each of the outer planets. The data of Figure 2.35 gives the illuminated area that is visible, and hence the total coverage available from spacecraft TV and related instruments. Finally, the ground traces as a function of latitude and longitude (see Figures 2.36 to 2.39) give the planetary coverage available when data is obtained only at the sub-satellite point.

The profile data discussed above was used along with other information, such as the planetary black-body emission curves of Figure 5.3 and the curves for the incident solar radiation to the upper atmosphere (from which the reflected flux from the planet can be estimated by using published values for the albedo) shown in Figure 5.4, to determine the effectiveness of each instrument in relation to its capability to detect the existing radiation levels, provide adequate spatial resolution, etc.

As a further illustration, the criteria used for judging whether an instrument was capable of providing adequate spatial resolution was based on the fact that present Earth-based telescopes can provide a resolution of about 0.1" of arc in the UV and visual wavelength regions. This corresponds to a linear resolution of approximately 300 km on Jupiter, 620 km on Saturn, 1300 km on Uranus, and 2100 km on Neptune. Thus for those instruments (operating in the UV and visual range) dependent on spatial resolution, the maximum relative

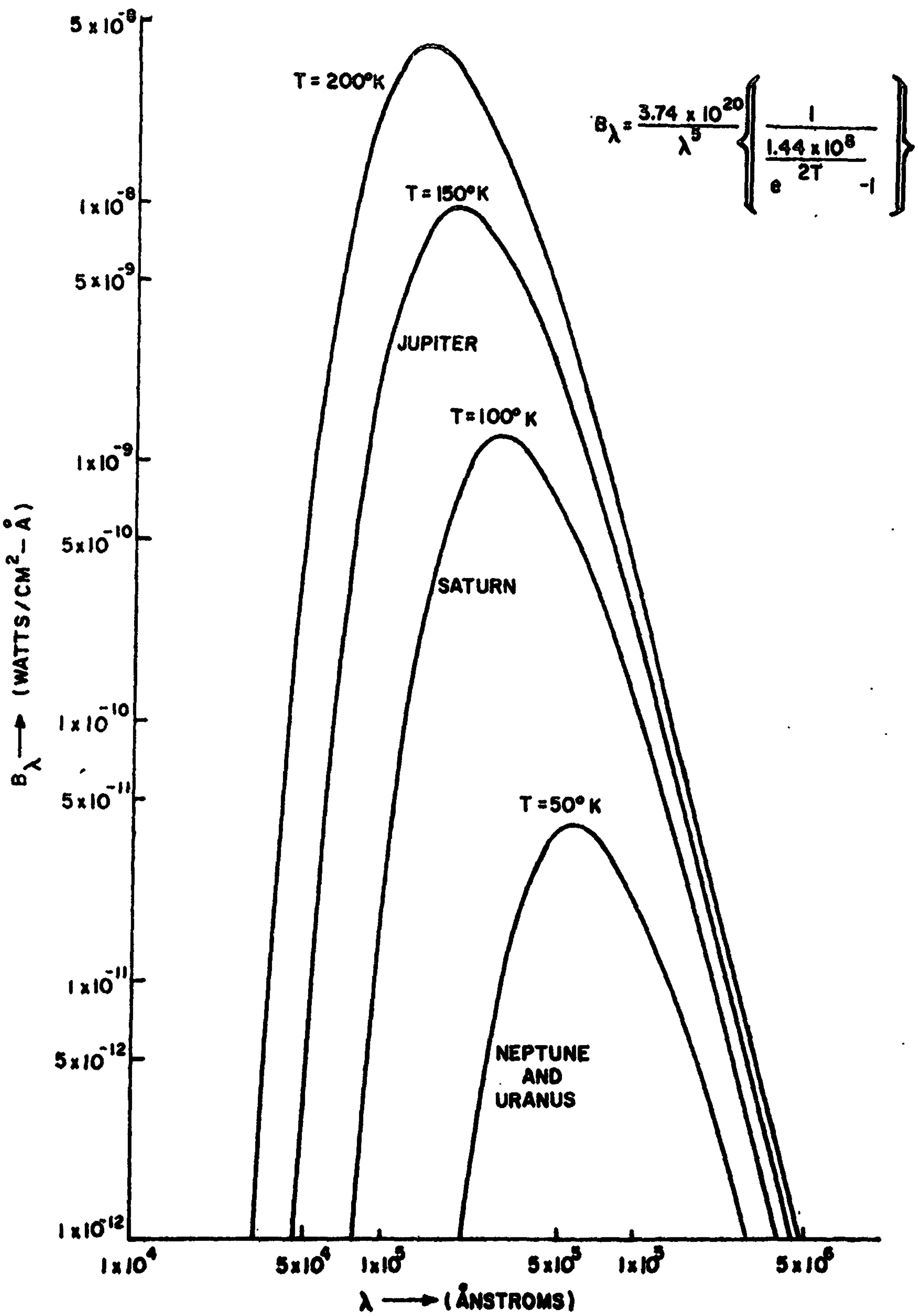

FIGURE 5.3. THEORETICAL BLACK-BODY EMISSION FOR THE JOVIAN PLANETS.

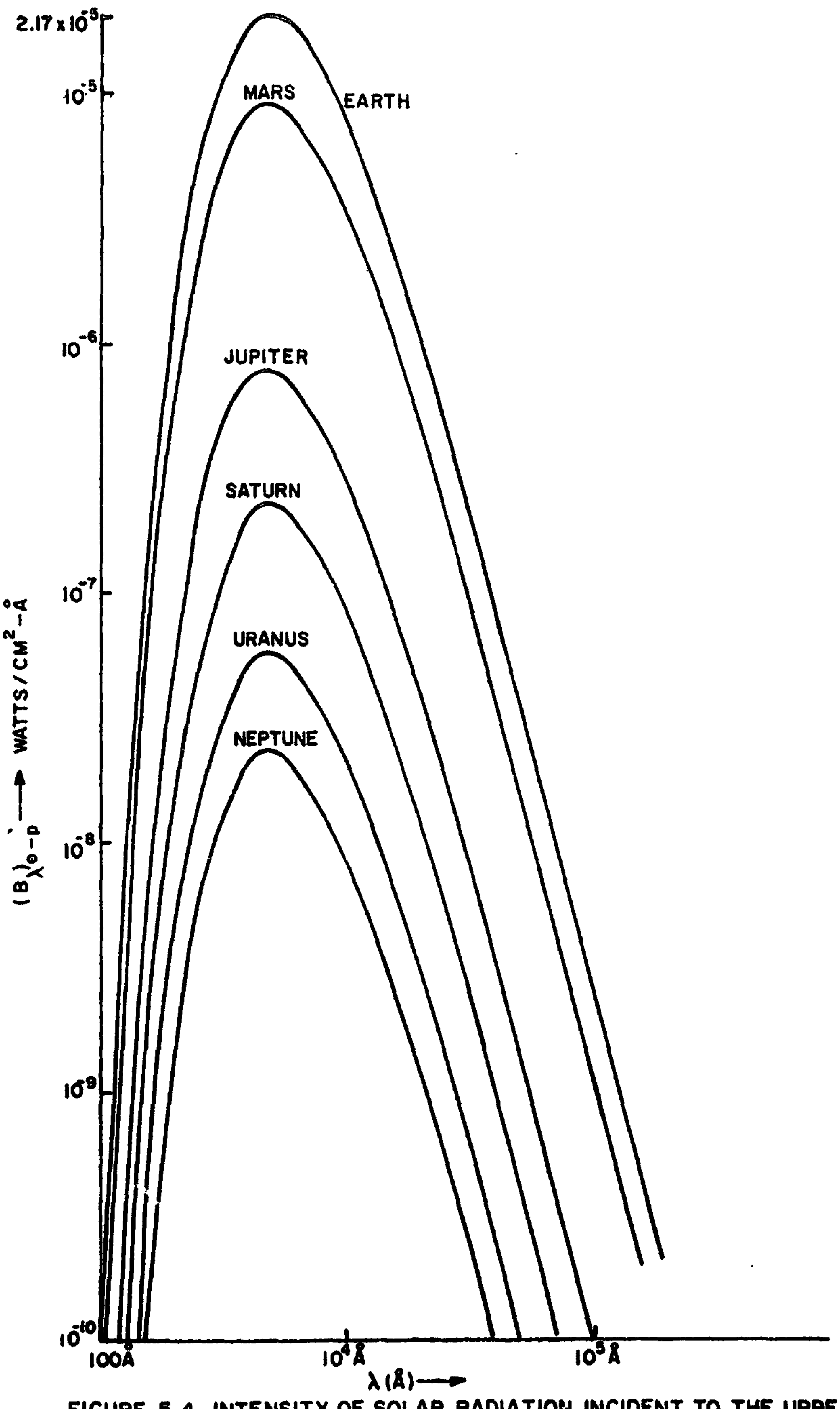

FIGURE 5.4. INTENSITY OF SOLAR RADIATION INCIDENT TO THE UPPER ATMOSPHERES OF THE OUTER PLANETS

value was permissible only if the obtainable resolution was increased by an order of magnitude (i.e., 30, 60, 130, and 210 km resolution respectively for Jupiter, Saturn, Uranus, and Neptune). For the IR and μ-wave regions, the desired resolutions were taken to be about a factor of 10 greater than the limits given above.

The reasoning used in the judgments for the planetary value of the instruments is discussed briefly on the title pages accompanying each of Tables 5.3 through 5.8. It should be emphasized that the percentage value assigned to each instrument is relative to the Category Objective value as was apportioned to the individual planet in Table 4.1.

5.4 Instrument Values

The instrument evaluation results of the previous sections are summarized in Table 5.9. The first column lists the flyby instruments that were considered in Tables 5.3 through 5.8. These instruments are ordered according to their "value per unit weight." The second and third columns of Table 5.9 give respectively a brief description of each instrument and its weight. This data was drawn from Section 5.2 as well as from published literature concerning spacecraft instrumentation.

The "Values" columns of Table 5.9 represent the total value (in arbitrary units) of each instrument at each planet

INSTRUMENT TYPE	INSTRUMENT DETAILS	WEIGHT	VALUES: JUPITER	SATURN	URANUS	NEPTUNE	TOTAL	VALUE/WT	CATEGORY OBJECTIVES
METEOROID DETECTOR	DIELECTRIC/ACOUSTIC $10^{-13} \leftrightarrow 10^{-6}$ gms THRESHOLD 10^{-5} DYNES SEC.	2.1	86	67	62	62	277	124	PARTICLE (PLANETARY); METEROIDS; ASTEROIDS
MAGNETOMETER PACKAGE	$1\gamma \leftrightarrow 500\gamma$ (VAPOR) $500\gamma \leftrightarrow 5G$ (FLUXGATE)	10	190	190	190	190	760	76	PLANETARY FIELDS; INTERACTION WITH I.P. MEDIUM; INTERPLANETARY FIELDS
COSMIC RAY DETECTOR	1-200 Mev/NUCLEON Au/Si DETECTORS (3)	2.6	45	45	41	41	172	66	SOLAR INFLUX; PARTICLE INTERACTIONS; INTERPLANETARY COSMIC RAYS
PLASMA PROBE	$10^{5} \leftrightarrow 10^{9}$ part./cm^{2}/sec. 30ev $\leftrightarrow$ 10 KeV	6.4	76	76	76	76	304	48	PLANETARY SOLAR INFLUX; INTERACTION WITH I.P. MEDIUM; SOLAR PLASMA
IONIZATION AND TRAPPED PARTICLE PACKAGE	G.M. TUBES & Si DIODES PROTONS 0.5 $\leftrightarrow$ 10 Mev ELECTRONS 40 $\leftrightarrow$ 100 KeV	4.9	56	56	44	44	200	41	PARTICLE INTERACTIONS; INTERACTION WITH I.P. MEDIUM
POLARIZATION AND PHOTOMETER PACKAGE	MULTI-COLOR WIDE BAND	5	48	52	52	52	204	41	PARTICULATE MATTER
IR $\leftrightarrow\mu$-WAVE RADIOMETER #1	LOW RESOLUTION	10	76	42	42	42	202	20	THERMODYNAMIC STATE; PLANETARY RADIATION
R. F. DETECTOR	1 - 10m WAVELENGTH (RADIO NOISE)	5	23	17	15	15	70	14	WEATHER PHENOMENA; ENERGY SOURCES (BIOLOGY)
TELEVISION #2	LOW RESOLUTION	10	19	45	30	30	124	12.4	CLOUD STRUCTURE; ATMOSPHERE MOTIONS; GEOMETRIC SHAPE
NARROW BAND PHOTOMETERS #1 & 2	7 CHANNEL UV EMISS. #1 +3 CHANNEL UV EMISS. #2	10 15	40 50	24 30	16 20	16 20	96 120	9.6 8	ELEM. AND MOL. ABUNDANCES; ISOTOPIC RATIOS
OCCULTATION	MULTI-BAND	20	24	31	36	36	127	6	ELEM. AND MOL. ABUNDANCES; THERMODYNAMIC STATE; GEOMETRIC SHAPE
ABSOR. UV $\leftrightarrow$ IR PHOTOMETER	10 CHA [illegible] CHANNELS	28	21	45	34	34	134	5	ELEM. AND MOL. ABUNDANCE; SOLVENTS
MASS SPECTROMETER	ELECTROSTATIC	10	4	8	16	20	48	4.8	INTERPLANETARY NEUTRAL PARTICLES
NARROW BAND PHOTOMETER #3	4 CHANNEL UV-VIS #3	8	15	5	5	5	30	4	PLANETARY RADIATION
TELEVISION #1	HIGH RESOLUTION	30	64	18	11	12	105	3.5	CLOUD STRUCTURE; ATMOSPHERE MOTIONS; GEOMETRIC SHAPE
RADAR	10 cm-1m WAVELENGTH (ACTIVE SYSTEM)	20	17	16	16	16	65	3.3	PARTICULATE MATTER; SURFACE STRUCTURE
IR $\leftrightarrow\mu$-WAVE RADIOMETER #2	HIGH RESOLUTION	20	1	8	5	5	19	1	ATMOSPHERIC MOTION AND CIRCULATION

Table 5.9 RESULTS OF INSTRUMENT EVALUATION FOR 1977-E MULTIPLE OUTER PLANET MISSION

relative to the overall goal of Examination of the Jovian Planets and Interplanetary Space. The values given under each planetary heading indicate the additive worth of each particular instrument at that planet. In other words, the worth values are obtained by summing the individual contributions of an instrument over all of the Category Objectives to which that particular instrument contributed scientific data. Thus for example, at Jupiter, the meteoroid detector had an estimated capability of fulfilling 10% of the total worth attributable to the Category Objective of (planetary) Particles (see Table 5.5), 75% of the worth attributable to Meteoroids and 10% of the worth attributable to Asteroids (see Table 5.8). From the basic science evaluation that was summarized in Table 4.1, it is seen that these Category Objectives had values relative to the overall goal of 12, 7.3 and 19 respectively at Jupiter. The additive worth of the meteoroid detector is thus given by

$$(.1)(12) + (.75)(7.3) + (.1)(19) \simeq 8.6$$

which when multiplied by a factor of 10 (for convenience, all worth values in Table 5.9 have been multiplied by a factor of 10) corresponds to the tabulated result.

It might be noted that, since the original goal was arbitrarily based on a value of 1000 and also the values in Table 5.9 have been multiplied by the factor 10, the worth values given in Table 5.9 are uniformly a factor of 100.

greater than their actual numerical percentage contribution toward the overall Goal of Exploration. The last "Value" column of Table 5.9 gives the total instrument value when summed over all planets. Thus, for example, it is seen that a meteoroid detector is capable of yielding scientific data which contributes about 2.8% of the total knowledge that is desired about the outer portions of the solar system. A magnetometer package, on the other hand, could yield 7.6% of all desired data if operative during the complete mission. The corresponding percentages for the other instruments are evident from Table 5.9.

As indicated in the previous sections, the economics of spaceflight and the usual restrictions on the total permissible payload weight indicate that it is desirable to include instrument weights as a factor in making payload selections. For this reason, the value per unit weight of each instrument type has been calculated using the "total value" and the "weight" indicated in the third column. These results are given in the value/weight column of Table 5.9, and the order of the instrument listing in the table have been based on these ratios. The final column of Table 5.9 is a tabulation of the Category Objectives to which instruments contributed scientific data (see also Tables 5.3 through 5.8). An exception to the above should be noted, in that the value contributions of the Absorption UV-IR Photometer to the Category Objectives of Pre-Life Molecules and Life Associated Substances (see Table 5.7) have been omitted from the computations leading to Table 5.9. The reason for this omission was based on the fact that there are no presently known absorption lines from which measurables such as proteins, amino acids and other complex organic molecules could definitely be identified. If future research provides a means of interpretating these complex spectra when superimposed with the other absorption spectra of the atmospheric contituents, the estimated worth of the absorption photometer would have to be reevaluated.

The major results of the instrument evaluation can be presented in graphical form as shown in Figure 5.5. This graph represents the accumulative scientific value, that is obtained by adding successive instruments to the overall payload, as a function of payload weight. The order for adding each additional instrument was based on the priority selection in accordance with the highest value/weight as given in Table 5.9. Since the slope of each segment of the curve is equal to the value per unit weight of the indicated instruments, the greatest increase in the payload science value occurs for those initial instruments of highest value per unit weight.

Also shown in Figure 5.5 are the payload values for hypothetical missions which terminate first at Jupiter, then Saturn, and also the case for the first three Jovian planets. These curves illustrate clearly the added science

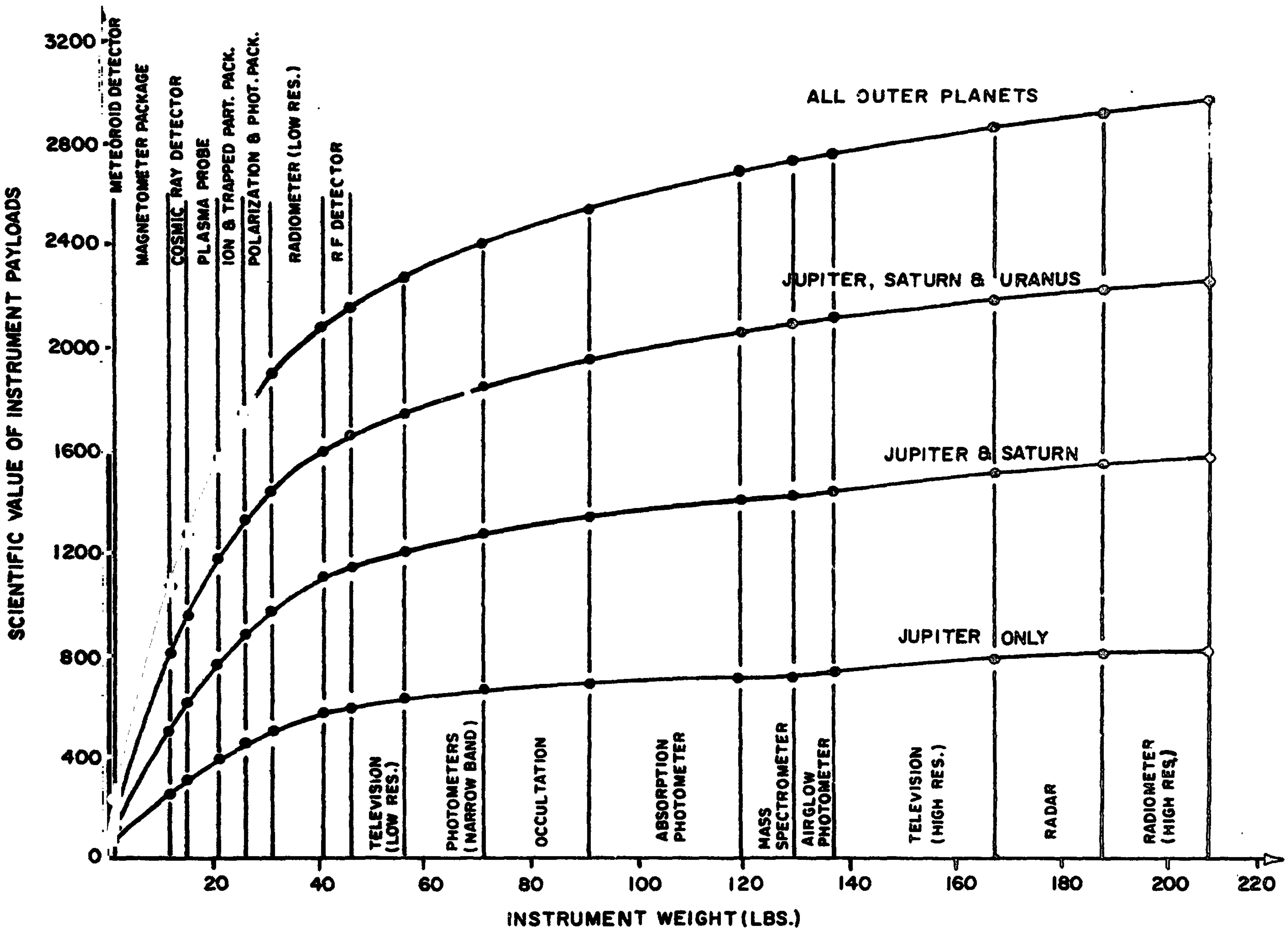

FIGURE 5.5. VALUE OF INSTRUMENT PAYLOADS BASED ON "VALUE PER UNIT WEIGHT".

value between successive encounters is approximately equal. This results from the high degree of commonality between the selected flyby instruments, i.e., the majority of the instruments are of comparative importance at each target planet.

It is clear from Figure 5.5. that, given a fixed payload weight, the instrument package can be readily selected which yields the highest scientific value. Thus for example, for an optimum 26 lb payload would contain only particles and fields experiments (i.e., meteoroid detector, magnetometer package, cosmic ray detector, plasma probe, and the ion and trapped particle package). An optimum 60 lb payload would permit inclusion of a low resolution TV system as a part of its priority instruments. Further discussion associated with payload selections will be covered in Section 6.

The results presented above pertain specifically to the 1977-E mission opportunity to the Jovian planets. It is appropriate at this stage to discuss the evaluation results for the other opportunities that were analyzed in Section 2. Changes in the mission opportunities affect only the final stage of the evaluation scheme in which the influence of the trajectory profiles at each planet was analyzed. Thus, reevaluation for the 1977-I (where "I" denotes passage interior to Saturn's rings), 1978-I, and 1978-E opportunities involves only the planetary instrument percentage values in the last four columns of Tables 5.3 through 5.8. A re-assessment of the instrument weights given in Table 5.9 is also required in some cases in order to compensate for such things as telescopic lens that are necessary to meet the desired constraints on spatial resolution.

A comparison of the 1977-I and 1978-I trajectory profiles showed that the major difference is that the miss distances are almost uniformly greater at each planet for the 1978 opportunity than they were for 1977. Thus the relative instrument value judgements are approximately the same for both cases, although the weights of some instruments (such as TV) must be increased to obtain adequate resolution. On the other hand, a comparison of the 1977-I and 1977-E opportunities showed that the approach distances to the planets are less at each target for the case of the interior ring passage. This change is not particularly significant, except for the case of Saturn, as can be seen from Figures 5.6 and 5.7. It should be noted that it is only on the night-side of Saturn that a very close approach to the surface occurs. Since most of the instruments (whose data and resolution are dependent on spacecraft altitude) operate principally on the sunlit side, the trajectory profiles for Saturn, Uranus, and Neptune in Figure 5.7 are approximately equivalent for the purposes of instrument evaluation. Therefore the relative changes in the spacecraft profiles, between the 1977-E and 1977-I opportunities, are of the same order of magnitude for all of the outer planets. Also the corresponding instrument

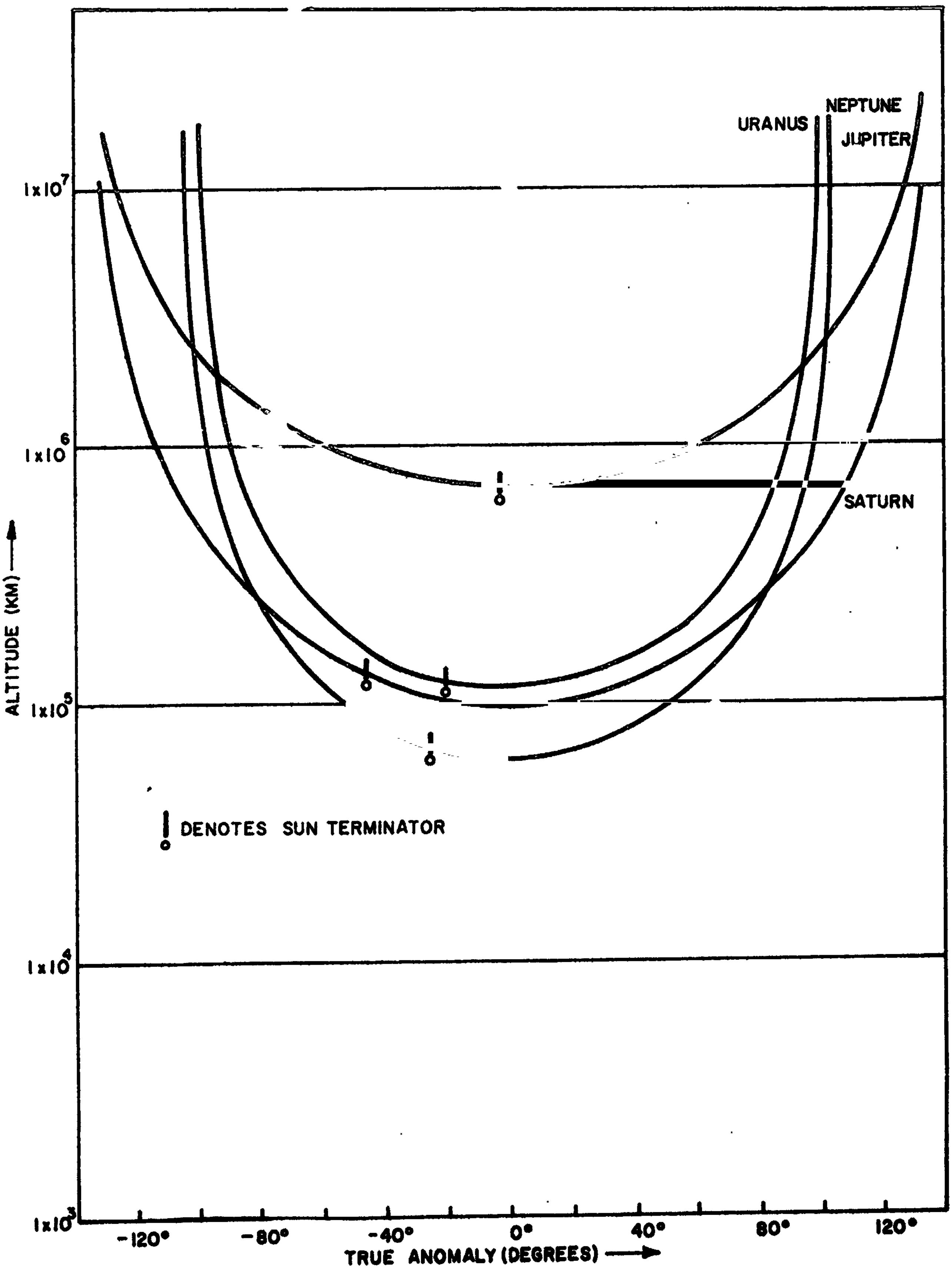

FIGURE 5.6. ALTITUDE VS. TRUE ANOMALY, 1977-E GRAND TOUR

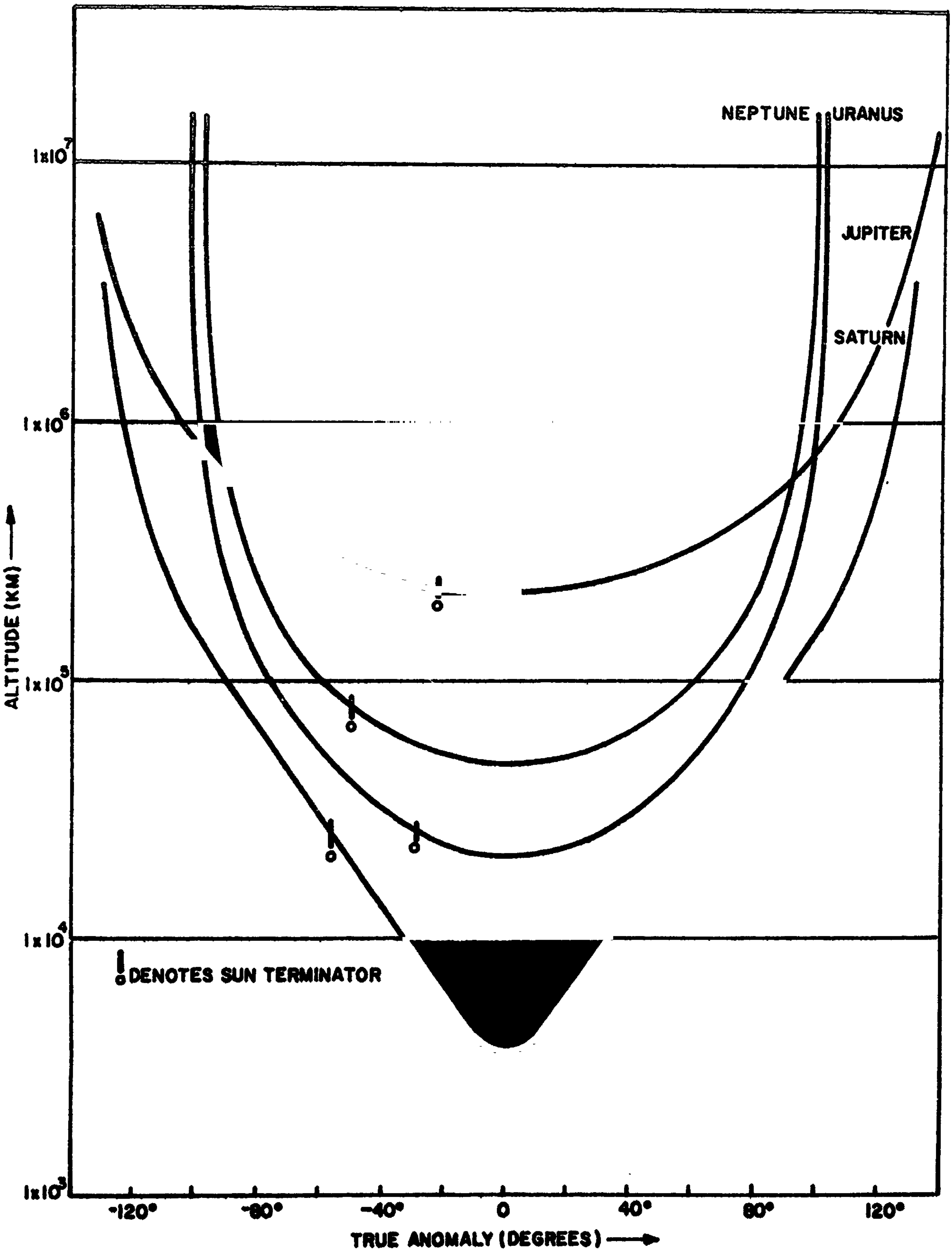

FIGURE 5.7. ALTITUDE VS. TRUE ANOMALY, 1977-I GRAND TOUR.

weights are altered only by a small percentage factor between the 1977-E and 1977-I opportunities.

The net result is that the evaluation results presented for the 1977-E opportunity are also essentially valid for the 1977-I passage. Although the instrument evaluation numbers and the weights are altered slightly in some cases, the general trends and priority orders that were given in Table 5.3 and Figure 5.5 are still valid. The same conclusions apply for a comparison between the 1978-E and 1978-I opportunities. A comparison between a 1977 and 1978 opportunity results in higher weights for many of the instruments in the 1978 mission. However, the general priority trends remain relatively unchanged, in particular the particles and fields instruments retain their highest rank. The remaining possibility involves a trajectory passing through the Cassini gap in Saturn's rings. The evaluation results for this case were intermediate between those for the interior and exterior ring passages. However, this particular mission opportunity was not seriously considered because of the uncertain density of particulates within the gap and their effect on spacecraft survival.

A capsule summary of the accomplishments and conclusions obtained in Sections 4 and 5 can be stated as follows:

1. An effective methodology was developed which resulted in a logical evaluation

scheme for both the pure science objectives and the instrument payloads.

2. The evaluation of the science objectives resulted in the highest priority values being attributed to objectives associated with the atmospheres of the Jovian planets.

3. In contrast, the worth evaluation of applicable flyby instruments gave the highest values to particles and fields experiments. This conclusion was a direct result of the commonality feature of these instruments, in that they contribute knowledge towards Planetary Particles & Fields, as well as to Interplanetary Medium objectives.

4. The scientific value of the instrument payloads per planet are of approximately equal worth. In other words, the additional increment of science value gained as each target is encountered during the outer planet mission is roughly the same for each of the planets. This is true for all payload weights.

5. The exterior and interior Saturn ring passage opportunities for a given year yield trajectory profiles that have nearly equal payload values. Therefore, a choice between the 1977-I and 1977-E opportunities will depend principally on a tradeoff between guidance requirements and spacecraft survival probabilities.

6. The relative instrument values are approximately the same for 1978 opportunities as in 1977, although the instrument weights tend to be slightly higher in 1978. Thus the 1977 opportunities may be favored to those in 1978.

SECTION 6

MISSION REQUIREMENTS FOR THE GRAND TOUR

by

D. L. Roberts

6. Mission Requirements for the Grand Tour

The previous sections have dealt with the three most important problem areas of the Grand Tour Mission, namely trajectory selection, guidance, and experiment evaluation. This section of the report will combine the results of these analyses together with considerations of other, less critical, subsystems, into an assessment of the overall spacecraft weight and the launch vehicle requirements for the mission.

6.1 Payload Selections

The evaluation of scientific experiments, and their ordering in terms of value per pound, as discussed in Section 5, allows scientific payloads to be selected on the basis of their contribution to the mission. It can be noted from the experimental value curves of Figure 5.5 (page 5) that the scientific experiments fall into two major categories. There are a group of particles and field experiments, with high value per lb, which constitute the "steep" part of the curve and there is the "plateau" region of the curve where little value is added per additional pound of experiments. It is the first group of experiments which has been used to define the "minimum" payload for the Grand Tour Mission.

Table 6.1 shows the division of the experiments into four payloads. The term "minimum" is used in the sense that it is felt that any lesser investment in experiments would

	EXPERIMENT	WEIGHT LBS	POWER WATTS	DATA BITS
"MINIMUM"	MICROMETEOROID DETECTOR	2	0.4	NOMINAL
	MAGNETOMETER PACKAGE	10	8	1 bps (CONT.)
	COSMIC RAY DETECTOR	2.5	0.6	NOMINAL
	PLASMA PROBE	6.5	3.0	3 bps (CONT.)
		21	12	$\simeq$ 5 bps
"SMALL"	TRAPPED PARTICLE DETECTOR	5	1.0	10,000 bpp*
	POLARIMETER - PHOTOMETER	5	2	100,000
	IR, μ WAVE RADIOMETER	10	5	10,000
	RF DETECTOR	5	5	10,000
		46	25	5 bps + 10^5 bpp
"MEDIUM"	LOW RES. TV	10	10	2×10^8 bpp
	NARROW UV PHOTOMETERS	15	5	10,000
	OCCULTATION (DUAL FREQU)	20	10	10,000
	ABSORPTION PHOTOMETERS	28	2	1,000
	MASS SPECTROMETER	10	5	NOMINAL
	AIRGLOW PHOTOMETERS	8	5	10,000
		137	57	5 bps + 2×10^8 bpp
"LARGE"	HIGH RES. TV	30	20	2×10^8 bpp
	RADAR (10 cm)	20	20	1,000
	HIGH RES. IR RADIOMETER	20	10	1×10^6
		207	112	5 bps + 4×10^8 bpp

*bpp = BITS PER PLANET

TABLE 6.1 SELECTED SCIENCE PAYLOADS (ACCUMULATIVE) render the mission not worthwhile. A nominal bit rate of five bit per second will be adequate to transmit all the data from these experiments. This payload derives much of its value from the interplanetary phase of the mission. This is shown in Figure 6.1 where there is only a small step increase in value as each planet is intercepted. In truth, this minimum payload would barely justify the complexity of the Grand Tour Mission.

By the ac 'tion of the next four experiments a "small" payload is derived. These four experiments are all planetary oriented and will provide much useful data on each of the outer planets. The position at which to draw the line between one payload and another is never quite clear and has been guided here by consideration of the required data bit rate. Without a TV system, the small payload achieves considerable value as seen in Figure 6.1 but its data requirement is still relatively nominal, i.e., five bits per second throughout the mission and a total of 10^5 bits for the planetary intercepts. The experiment next in importance is indeed the TV system and it adds some 2×10^8 bits at each planetary encounter. However it is also possible to include the next five experiments as well, without adding markedly to the power requirements or bit rate. Therefore the "medium" payload contains the first fourteen experiments and stops just short of the high resolution TV system. The "large" payload contains all the experiments considered in this study. In power and data, it has

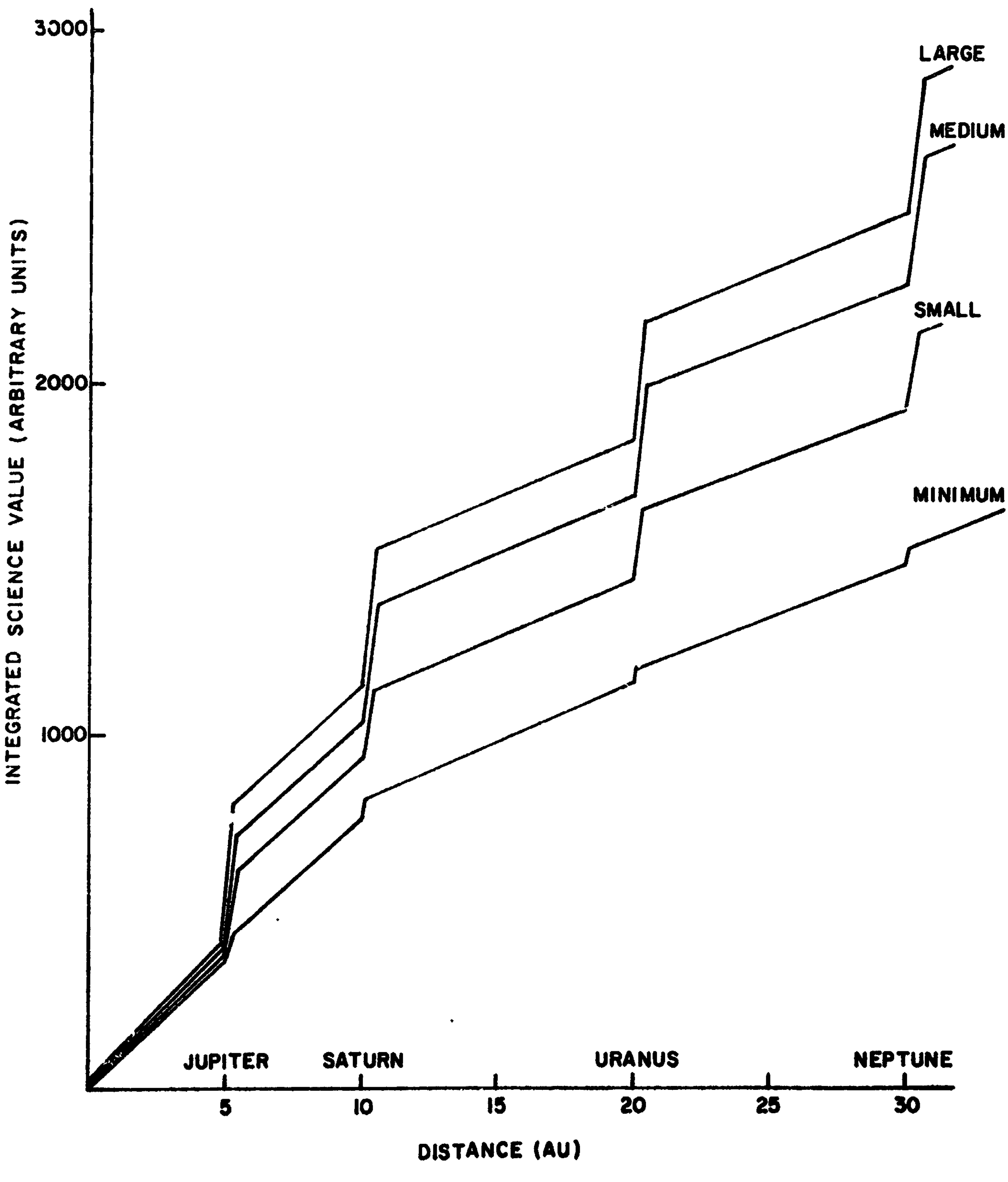

FIGURE 6.1. INTEGRATED SCIENCE VALUE OF PAYLOADS.

approximately twice the requirements of the medium payload. It is heavily planet oriented and from Figure 6.1 it can be seen to make a major scientific contribution at each target.

6.2 Typical Spacecraft Weights

On the basis of selected payloads and the overall guidance requirements, an attempt has been made to estimate the total spacecraft weight to perform the Grand Tour Mission. This leads directly to an estimate of the launch vehicle requirements for the mission. The weight estimates which follow are not based on any specific spacecraft design, conceptual or otherwise. They are extrapolations, on a subsystem weight basis, from other more detailed engineering studies (Goddard 1967, General Dynamics 1966, TRW 1966) and using the Mariner '67 as the technology base.

There are a range of Grand Tour Mission which have different requirements and hence different spacecraft weights. There are four selected trajectories with their associated, and quite distinct, midcourse velocity requirements depending on whether a planet seeker or radar tracking is used. There are four selected payloads each with its own power and data requirements. Rather than select a typical example, a matrix of information is presented which will bound all the variables of the Grand Tour Mission. Table 6.2 shows the way in which the spacecraft weight totals have been built up. This applies to the 1977 E opportunity and includes minimum and medium

SUB SYSTEM	MINIMUM PAYLOAD			MEDIUM PAYLOAD		
		TRACKER	RADAR		TRACKER	RADAR
SCIENCE	MINIMUM	21 LBS	21 LBS	MEDIUM	137 LBS	137 LBS
COMMUNICATIONS 10/20 WATT 8' ANTENNA	20 bps JUP. 24 SAT. 13 UR. 5 NEP.	50	50	400 bps JUP. 150 SAT. 40 UR. 15 NEP.	100	100
POWER	125 WATTS	125	125	250 WATTS	250	250
GUIDANCE	INCLUDING TRACKING	110	230	INCLUDING TRACKING	180	410
ATTITUDE CONTROL	3-AXIS	60	80	3-AXIS	120	160
DATA AND SEQUENCING	5×10^4 BITS STORE	100	100	2×10^8 BITS STORE	150	150
THERMAL CONTROL		40	40		60	60
STRUCTURE AND MISC.	20%	100	110	20%	190	240
ESTIMATED TOTAL WEIGHT		605 LBS	760 LBS		1180 LBS	1500 LBS

TABLE 6.2 SUB-SYSTEM WEIGHT ESTIMATES (1977E)

payloads with either a planet tracker or radar tracking for guidance. The science payload weights are taken directly from Table 6.1.

The communications requirements are calculated somewhat as a compromise. In all cases it is necessary to accommodate the minimum data rate from the furthest target (Neptune) plus sufficient in excess to transmit the planetary data after intercept within a reasonable time. For the "minimum" payload, rates of 20, 24, 13, and 5 bits per second, at the respective planets, are achieved by utilizing an 8 foot diameter spacecraft antenna and a 10/20 watt transmitter. The system uses 20 watts and the 85' DSIF combination out to Jupiter, 10 watts and the 210' DSIF out to Saturn, and 20 watts and the 210' DSIF beyond Saturn. The excess capability at Jupiter, Uranus, and Saturn would make this same communication system suitable for the "small" payload as well. It would then only take approximately 2 hours to transmit the 10^5 bits of planetary data at Jupiter and Saturn, about four hours at Uranus, and about eight hours at Neptune.

The "medium" payload requires a larger communications capability and uses a 20/50 watt transmitter with an 8 foot diameter spacecraft antenna. The 210' DSIF dish and the full 50 watts of power will be required for the data at each intercept, yielding rates of 500, 125, 30, and 13 bits per second, respectively. After intercept with Neptune, it would take some two months to transmit all the data at the rate of

13 bits per second. This is probably inadequate and consideration should be given to increasing the spacecraft antenna diameter beyond 8 feet or to increasing the spacecraft transmitter power. For the interplanetary data the 20 watt transmitter can be used with the 85' DSIF as far as 7 Au and the 50 watt transmitter can be used with the 85' DSIF as far as Saturn. This same transmitting system can be used for the large payload as well but will require about twice the time to transmit all the data after each planetary intercept.

The power requirements for the spacecraft have been assumed as 125 and 250 watts respectively in Table 6.1. These should be adequate to supply all the experimental requirements, the communications system, and the engineering functions of the spacecraft. Slightly larger powers will probably be required for the small and large payloads and values of 150 and 300 watts respectively have been used. In all cases a R.T.G. system was assumed as the sole power supply and specific weights of one pound per watt were used to represent the total subsystem weight including shielding and power conditioning.

The guidance requirements are different for each opportunity, for each payload weight, and for each tracking system. Table 6.3 shows the total guidance subsystem weight estimates for all mission options. In all cases the majority of the weight is invested in the propulsion system. An I_{sp} of 235 seconds has been used in all the calculations and the propulsive mass fractions have been taken from Section IV-F-3

TRAJECTORY	TRACKING SYSTEM	MIDCOURSE DV	SUB-SYSTEM WEIGHT			
			MINIMUM PAYLOAD	SMALL PAYLOAD	MEDIUM PAYLOAD	LARGE PAYLOAD
1977E	ON-BOARD	190 M/SEC	110 LBS	120 LBS	180 LBS	210 LBS
	RADAR	450	230	260	410	540
1977I	ON-BOARD	430	230	255	390	510
	RADAR	1710	1300	1600	2300	2700
1978E	ON-BOARD	200	115	125	190	220
	RADAR	350	155	170	280	330
1978I	ON-BOARD	375	180	195	315	370
	RADAR	1010	550	600	1000	1200

TABLE 6.3 SUBSYSTEM WEIGHT FOR MIDCOURSE GUIDANCE (INCLUDING PROPULSION)

of the Launch Vehicle Estimating Factors (1968). A tracking subsystem weight of 30 pounds was assumed for the planet tracker system and of 10 pounds for the earth based radar tracking system and are included in the table. The overall weight penalty with radar tracking particularly for the inner ring passage missions, is clearly demonstrated in Table 6.3.

The attitude control system weights are a function of the moment of inertia of the spacecraft and hence of its mass and size. Table 6.4 shows the total attitude control subsystem weight estimates (including propellant) for each of the mission options. They are all based on a mission duration of 10 years using nitrogen cold gas in a hard limit cycle, three axis system. The weight estimates are based on the Mariner IV technology. No special contingency has been allowed for passage through the asteroid belt.

The data storage and sequencer subsystem weights are again based on Mariner technology. The subsystem weight for the minimum payload has been estimated at 100 pounds. This has been increased for the larger payloads because of the increased storage requirement and because of the added complexity of the experimental sequences. Weights of 120, 150, and 200 pounds have been allowed for the "small", "medium" and "large" payloads respectively.

The thermal control subsystem has been assumed to be largely passive. Since an RTG system is included, it is assumed that it will be possible to pipe its excess heat

TRAJECTORY	TRACKING SYSTEM	SUBSYSTEM WEIGHT			
		MINIMUM PAYLOAD	SMALL PAYLOAD	MEDIUM PAYLOAD	LARGE PAYLOAD
1977E	ON-BOARD	60 LBS	65 LBS	120 LBS	160 LBS
	RADAR	80	100	160	200
1977I	ON-BOARD	80	100	155	190
	RADAR	250	275	400	500
1978E	ON-BOARD	60	65	120	160
	RADAR	70	85	140	180
1978I	ON-BOARD	75	90	140	180
	RADAR	150	160	250	300

TABLE 6.4 SUBSYSTEM WEIGHT FOR ATTITUDE CONTROL (INCLUDING PROPELLANT)

output to most parts of the spacecraft. Nominal weight allowances of 40, 50, 60, and 80 pounds have been allowed for the thermal control subsystem weight for the four payloads considered. These weights have been assumed not to vary with the opportunity.

The spacecraft's structure has been assumed to absorb 10% of the spacecraft weight. In addition 10% has been added for miscellaneous contigencies which must include redundancy to permit adequate reliability for the 10 year mission duration.

The total spacecraft weight estimates are given in Table 6.5 for all the mission options. They range from 605 lbs for a "minimum" payload mission using the 1977 E opportunity with an onboard planet tracker, to 4900 lbs for the "large" payload mission using the 1977 I opportunity with radar tracking. Table 6.5 also shows the capabilities of four launch vehicles for comparison with the estimated total spacecraft weights. The SLV3X-Center-TE364 can be used only for the 1977 E mission and then its 750 lb capability will only deliver the "minimum" and "small" payloads, with onboard tracking. A 5 segment Titan III D-Centaur is not adequate for the interior ring passage missions. It can be used for all the 1977 exterior opportunities with onboard tracking, and for "medium" payloads with radar tracking. For the 1978 exterior missions, only "medium" and "small" payloads are possible for onboard and radar tracking respectively. The

		SPACECRAFT WEIGHT				LAUNCH VEHICLE CAPABILITY			
MISSION	TRACKING	MINIMUM	SMALL	MEDIUM	LARGE	SLV 3X -CENT-364	TIII D -CENT	TIII D -CENT-BII	TIII F -CENT
1977E	ON BOARD	605	725	1180	1560	750	1900	2200	3300
	RADAR	760	930	1500	1950				
1977I	ON BOARD	760	925	1480	1900	-	-	1450	2000
	RADAR	2270	2750	4060	4900				
1978E	ON BOARD	620	730	1190	1510	-	1250	1700	2500
	RADAR	675	810	1330	1650				
1978I	ON BOARD	720	850	1365	1710	-	-	1000	1200
	RADAR	1250	1300	2330	2850				

TABLE 6.5 COMPARISON OF LAUNCH VEHICLE CAPABILITY WITH SPACECRAFT WEIGHT

addition of a burner II stage makes the Titan III D-Centaur-Burner II launch vehicle adequate for all exterior ring passages. It can also support interior missions in 1977 and 1978 with "small" payloads provided onboard tracking is used. Finally for comparison a seven segment Titan III F-Centaur launch vehicle capability is included but it offers little advantage over the Titan III D-Centaur-Burner II.

If it is contemplated that missions will be attempted at both the 1977 and 1978 opportunities with a common spacecraft design and launch vehicle, then the possible options are quite restricted. These are shown in Table 6.6. The smallest acceptable launch vehicle is a Titan III-Centaur and this will only launch a "medium" payload with onboard tracking, or a "small" payload using radar. The Titan III-D Centaur-Burner II will launch all exterior missions and "small" interior missions with onboard tracking. It should however be re-emphasized that these conclusions are based on weight estimates that are indeed just estimates and have not been derived from a specific spacecraft conceptual design study.

LAUNCH VEHICLE	COMMON PAYLOAD 1977-78			
	EXTERIOR		INTERIOR	
	ON-BOARD	RADAR	ON-BOARD	RADAR
SLV 3X-CENT-TE364	-	-	-	-
TITAN III D-CENT.	MEDIUM	SMALL	-	-
TITAN III D-CENT-BII	LARGE	LARGE	SMALL	-
TITAN III F-CENT	LARGE	LARGE	SMALL	-

TABLE 6.6 LAUNCH VEHICLE CAPABILITY FOR COMMON 1977-78 MISSIONS

SECTION 7

CONCLUSIONS

7. CONCLUSIONS

In advance of a discussion of the conclusions of this study, it is important to reiterate the purpose of the study, which was to provide preliminary data on the major problem areas associated with the Grand Tour Mission concept. The study has therefore concentrated on two major problem areas, guidance and scientific compatability. In both instances it has been shown that the requirements are tractable and that the mission warrants detailed definition and conceptual design effort.

The recommended launch years for the Grand Tour Mission are 1977 and 1978. The alignment of the planets will make five launch years possible (1976 to 1980), and at each opportunity it is possible to go inside or outside the rings of Saturn. A brief analysis has shown a potentially high collision rate if the spacecraft penetrates the rings of Saturn. The 1976 opportunity has been rejected from detailed consideration because it involves a close passage of Jupiter with penetration of the radiation belts. The 1979 and 1980 opportunities have been rejected because of the high launch energy and the exceedingly large miss distance at Jupiter.

The guidance velocity requirements depend critically on the spacecraft tracking system which is used, on the closeness of passing Saturn, and on the launch opportunity. The exterior ring passages are less demanding than the interior passages by a factor of three for radar tracking and a factor of two for on-board planet tracking. From a guidance standpoint the 1977 and 1978 exterior missions are recommended. Using an on-board tracker the total velocity requirements, for the 8 midcourse corrections are 190 meters per second and 203 meters per second respectively.

The study has demonstrated the scientific compatability of all four outer planets. There is a clear need for knowledge of all four targets. Payloads have been assembled, which will contribute significant data on each of the target planets. The minimum useful payload which [illegible] been derived obtains its value from particles and fields measurements mainly in interplanetary space but also to some extent at each target. Its weight is about 20 pounds. Three other typical payloads are developed and all are able to contribute at Jupiter, Saturn, Uranus and Neptune approximately equally, and each can be designed to retain their value and compatability for either interior or exterior passages. The television system has been found to act as a breakpoint in the payload selection. Its very high data requirements mean that it essentially controls the communications subsystem requirements and therefore to some extent also the power, guidance, and attitude control subsystem weights. Its inclusion in the payload means that many, less demanding experiments can also be included without a significant impact on the overall subsystem requirements. "Medium" payload weights in the range of 60 to 130 pounds are recommended.

The total spacecraft weights required for all mission options are in the range from 600 to 4000 lbs. The exterior ring passages are strongly recommended and the appropriate weight range for these is reduced to 600 to 2000 lbs for science payload weights between 20 and 200 lbs. An on-board planet tracker is recommended as the most effective tracking system, further reducing the upper limit of the weight range to 1500 lbs. However, for the exterior passages the differences are such that radar could be used as a backup and only the Neptune intercept would be lost if the on-board system failed.

If it is important that the same spacecraft design and launch vehicle be possible at both opportunities, the minimum vehicle is a Titan III-D-Centaur which has a capability of 1900 lbs in 1977 and 1250 lbs in 1978 for the exterior ring passages.

The recommended missions would utilize the 1977 and 1978 opportunities, use an on-board planet tracker, have a payload in the region of 100 lbs weight, and require a total spacecraft weight of some 1200 lbs. In the light of the apparent tractability of all the subsystem requirements for the Grand Tour Mission, it is strongly recommended that conceptual spacecraft designs be developed and that the complete feasibility of the mission be verified.

REFERENCES

Barone, L., Guidance and Control Division, Jet Propulsion Laboratory, conversation related to Mariner Mars '69 optical tracker experiment and extensions thereof.

Cameron, A. G. W., "The Formation of the Sun and Planets," Icarus, Vol. I, pp. 13-69, 1962.

Cook, A. F. and Franklin, F. A., "Rediscussion of Maxwell's Adams Prize Essay on the Stability of Saturn's Rings," The Astronomical Journal, March 1964, p 173.

Flandro, G., "Fast Reconnaissance Missions to the Outer Solar System Utilizing Energy Derived from the Gravitational Field of Jupiter," Astronautica Acta, Vol. 12, No. 4, 1966.

Franklin, F. A., and Cook, A. F., "Optical Properties of Saturn's Rings. II," The Astronomical Journal, November 1965.

Friedlander, A. L., "Planet-Approach Orbit Determination from Earth-Based Radio Doppler Tracking - PARODE Computer Program," IITRI Technical Memo GC-150, March 1967.

Gates, C. R., and Gordon, H. J., "Planetary Approach Guidance," JPL Technical Report No. 32-631, June 1964.

General Dynamics (Fort Worth Div.) "A Study of Jupiter Flyby Missions," FZM-4625, May 1966.

Goddard Space Flight Center, Series of reports on "Galactic Jupiter Probe," Mission Analysis Office, GSFC, 1967.

Gordon, M. A. and Warwick, J. W., "High Time Resolution Studies of Jupiter's Radio Bursts," Astronomical Journal, Vol. 148, pp. 511-533, 1967.

Hide, R., "On the Circulation of the Atmosphere of Jupiter and Saturn," Planetary and Space Science, Vol. 14, pp 669-675, 1966.

JPL Series, Space Programs Summary, Vol. III, "The Deep Space Network".

Michaux, C. M. (editor), "Handbook of the Physical Properties of the Planet Jupiter," NASA SP-3031, Washington, D.C., 1967.

REFERENCES (Continued)

Minovitch, M. A., "The Determination and Characteristics of Ballistic Interplanetary Trajectories Under the Influence of Multiple Planetary Attractions, JPL TR No. 32-468, October 31, 1963.

Niehoff, J. C., "An Analysis of Gravity Assisted Trajectories in the Ecliptic Plane," ASC/IITRI Report No. T-12, 1965.

Niehoff, J. C., "A Survey of Multiple Missions Using Gravity Assisted Trajectories," ASC/IITRI Report No. M-12, 1966.

Opik, E. J., "Jupiter: Chemical Composition, Structure and Origin of a Giant Planet," Icarus, Vol. I, pp. 200-257, 1962.

Silver, Brent W., "Grand Tours of the Jovian Planets," paper presented at AIAA Guidance, Control and Flight Dynamics Conference, Huntsville, Ala., Aug. 14-16, 1967.

Space Science Board, Directions for the Future, Washington, D.C., 1966.

Strack, W. C. and Huff, V. N., "The N-BODY Code," NASA TN D-1730, November 1963.

Sturms, F. M., Jr., "Statistical Analysis of Three Midcourse Corrections of an Earth-Venus-Mercury Trajectory," JPL Space Programs Summary No. 37-37, Vol. IV, Feb. 1966.

Sturms, F. M., Jr., "Trajectory Analysis of an Earth-Venus-Mercury Mission in 1973," JPL Technical Report No. 32-1062, Jan. 1967.

TRW Systems, "Advanced Planetary Probe," 4547-6007-R0000, July 1966.

APPENDIX A

TARGETING OF INTEGRATED TRAJECTORIES FOR THE MULTIPLE OUTER PLANET MISSION STUDY USING THE N-BODY CODE

APPENDIX A

TARGETING OF INTEGRATED TRAJECTORIES FOR THE MULTIPLE OUTER PLANET MISSION STUDY USING THE N-BODY CODE

The purpose of this appendix is to expand upon the description of the n-body targeting analysis presented in the text of the report and to present some of the results of the n-body targeting program.

The n-body targeting code is used to generate integrated trajectories between Earth and a specified target planet. For the multiple outer planet mission study the target planet was Neptune with the trajectory passing close to Jupiter, Saturn and Uranus. An integrated trajectory serves two purposes, 1) to generate sensitivity matrices for the guidance analysis and 2) to check the accuracy of conic approximations to the trajectory.

Targeting is basically the solution of a two point boundary value problem, where desired final conditions and approximate initial conditions are obtained from the computer program SPARC which provides conic interplanetary and planetary flyby trajectories. The program used for the numerical integration of the equations of motion was the Lewis Research Center's N-Body code, modified to do both the targeting and the guidance analysis.

The following preliminary material will be presented before the actual method of targeting is discussed:

1. The coordinate systems used at Earth and at the other planets.
2. The targeting variables used at Earth and at the other planets.
3. The constraints placed upon the targeting variables.

At Earth the reference plane and axis are the mean equator and equinox of date. The center of the coordinate system is at the Earth's center.

At the other planets, the RST coordinate system is used. In this system, the center of the system is at the center of the planet in question. Unit vectors R, S, T, are defined as follows: The vector S is a vector parallel to the incoming hyperbolic velocity vector. T is a vector normal to S and parallel to the ecliptic plane. Its direction is determined such that the third vector R ($R = S \times T$) in the right-handed system points in the direction of the south pole of the ecliptic. The R-T plane is called the target plane.

In order to perform the integration, a starting time and initial values for the variables x, y, z, $\dot{x}$, $\dot{y}$, and $\dot{z}$ are needed. At Earth these quantities are computed from the magnitude (VHL) and the direction (Φ-declination, Θ-right ascension) of the outgoing hyperbolic excess velocity vector under the following constraints:

1. The day of launch is taken as the launch date of the SPARC conic approximation to the trajectory.
2. The declination of the launch site is constant at 28.3106°, the declination of Cape Kennedy.
3. The launch azimuth, Σ_L, satisfies the following conditions:
   a. $\Sigma_L = 90°$ when $\Phi \leq 28.3106°$
   b. $\Sigma_L - 90° = \text{minimum}$ when $\Phi > 28.3106°$
4. Injection is at perigee at an altitude of 100 nautical miles.
5. The parking time, in a circular parking orbit, is the minimum allowable time greater than 2 minutes.

The variables VHL, Φ and Θ are the variables used for targeting at Earth.

At all other planets, the quantities x, y, z, $\dot{x}$, $\dot{y}$, $\dot{z}$ and time are computed at the target plane from:

VHP - magnitude of the incoming hyperbolic excess velocity

Φ - declination of the incoming asymptote of the ırrival hyperbola

Θ - right ascension of the incoming asymptote of the arrival hyperbola

B·T - the component of B along the T-axis where B is the hyperbolic miss parameter, i.e., the vector in the target plane from the center of the planet to the incoming asymptote of the arrival hyperbola.

B·R - the component of B along the R-axis

t - the time at which the spacecraft pierces the target plane.

The three variables used for targeting at all planets except Earth are B·T, B·R, and t.

The basic procedure in the targeting of any one leg of the trajectory is the determination of the sensitivity of the target variables at any planet to changes in the target variables at the preceeding planet. This is accomplished by computing a matrix of approximate partial derivatives of each of the 3 target variables at the target planet with respect to each of the 3 target variables at the departure planet. The method used to obtain the matrix is that of finite-difference. With the inverse of this matrix it is possible to predict corrections to the values of the target variables at the departure planet which will cancel (or decrease) the error in the values of the target variables at the arrival planet.

It was not known initially how great these sensitivities would be, and hence over how many legs it would be possible to target a trajectory. It turned out that the sensitivities were so great that it was possible to target only one leg at a time. For example, in general to come within 100 km of the aiming point in B·T, B·R in the target plane, it was necessary to make changes in the departure conditions which were in the tenths, hundreths or even thousandths of a kilometer. However, in most cases, it was only necessary to compute one sensitivity matrix to target one leg and it was never necessary to compute more than two matrices. Even though the actual integration is performed in double precision, the targeting subroutines were written in single precision. Because of this, in trying to target two legs at a time, after the first few corrections, the changes in the departure conditions became so small that they could not be handled by the eight place accuracy of single precision arithmetic. For this reason it was not possible to target more than one leg at a time.

In targeting one leg at a time, targeting was started on the Uranus-Neptune leg. An aiming point was selected at Neptune, and the trajectory was integrated from Uranus to to Neptune starting with the SPARC arrival conditions at Uranus as initial conditions. The error in the arrival conditions at Neptune was noted and a sensitivity matrix computed by integrating the Uranus-Neptune leg of the trajectory three more times. Then using the inverse of the sensitivity matrix to predict corrections to the initial conditions, the initial conditions were corrected on successive integrations of the trajectory until convergence was obtained at Neptune. The arrival conditions at Neptune for the converged trajectory were called the n-body converged conditions. The Uranus departure conditions for the converged trajectory became the aiming point at Uranus for the integration of the Saturn-Uranus leg. These departure conditions were called the 'aiming point from n-body convergence.' Targeting was continued in this manner on successive legs until convergence was obtained on the final (Earth-Jupiter) leg. At that time the entire trajectory was considered to be converged.

Because targeting was done using only the three variables, B·T, B·R, and time, there was not complete agreement between the values of VHP, Φ, and Θ for the converged trajectory and the values of VHP, Φ, and Θ at the aiming point. See the last two columns of Tables 1 through 4 for the discrepancies in these values.

Tables 1 through 4 give the convergence histories of the four trajectories studied. On each of these tables are given 1) the values from SPARC of all the pertinent parameters

Table 1

CONVERGENCE HISTORY OF 1977 E TRAJECTORY

Planet	Parameter	SPARC Conditions[1]	Aiming Point from N-Body Convergence[2]	N-Body Converged Conditions
NEPTUNE	B·T (KM)	8.88×10^4	———	8.8725776×10^4
	B·R (KM)	0.0	———	-2.1122848×10^1
	TIME	2447746.85759735	———	2447746.869920335
	E.P.[3]			0.1018
URANUS	B·T (KM)	1.581993×10^5	1.5896784×10^5	1.5891677×10^5
	B·R (KM)	4.09231×10^4	4.1320698×10^4	4.1369825×10^4
	VHP (KPS)	14.7435	14.7435	14.721352
	Ø (DEG)	-1.5304	-1.5304	-1.5395862
	Θ (DEG)	271.1280	271.1280	271.143578
	TIME	2446455.72521209	2446456.33905181	2446456.338873088
	E.P.			0.0712
SATURN	B·T (KM)	3.572481×10^5	3.5841535×10^5	3.5873812×10^5
	B·R (KM)	-1.7228×10^4	-1.7359508×10^4	-1.7746249×10^4
	VHP (KPS)	10.6937	10.6937	10.669641
	Ø (DEG)	2.7472	2.7472	2.7797137
	Θ (DEG)	195.3260	195.3260	195.4885
	TIME	2444842.59416961	2444846.6852323	2444846.684265613
	E.P.			0.5057
JUPITER	B·T (KM)	1.9246066×10^6	1.9387916×10^6	1.9385371×10^6
	B·R (KM)	1.510661×10^5	1.5292970×10^5	1.5287049×10^5
	VHP (KPS)	7.8118	7.[illegible]1180	7.2031271
	Ø (DEG)	-3.0377	-3.0377	-3.6468103
	Θ (DEG)	94.3800	94.379999	92.817464
	TIME	2444070.0	2444090.496979	2444090.496978998
	E.P.			0.35348753
EARTH	VHL (KPS)	9.5426	9.4[illegible]77468	———
	Ø (DEG)	30.5118	32.061232	———
	Θ (DEG)	64.6384	63.501112	———
	TIME	2443388.0	2443388.039231494	———

1. Starting conditions for first n-body convergence run on any leg.
2. Departure conditions corresponding to converged n-body run on any leg.
3. $E.P. = [\,(\text{error in B·T (KM)})^2 + (\text{error in B·R (KM)})^2/1000 + \text{error in time (days)}/.5]$

Table 2

CONVERGENCE HISTORY OF 1977 I TRAJECTORY

Planet	Parameter	SPARC Conditions[1]	Aiming Point from N Body Convergence[2]	N-Body Converged Conditions
NEPTUNE	B·T (KM)	8.88×10^4	————	8.8728759×10^4
	B·R (KM)	0.0	————	4.6033367×10^1
	TIME	2446702.24283599	————	2446702.252454042
	E.P.[3]			0.86743
URANUS	B·T (KM)	5.54577×10^4	5.568189×10^4	5.5598592×10^4
	B·R (KM)	8.9765×10^3	9.0353971×10^3	9.0210702×10^3
	VHP (KPS)	21.2169	21.2169	21.201689
	Ø (DEG)	-1.1496	-1.1496	-1.1556599
	θ (DEG)	266.1723	266.1723	266.703849
	TIME	2445717.68746185	2445717.93804669	2445717.94891575
	E.P.			0.63469172
SATURN	B·T (KM)	1.464489×10^5	1.4674225×10^5	1.4681419×10^5
	B·R (KM)	-5.8615×10^3	-5.8921234×10^3	-5.9170313×10^3
	VHP (KPS)	16.6908	16.6908	16.693921
	Ø (DEG)	2.3789	2.3789	2.3890921
	θ (DEG)	192.0425	192.0425	192.1512
	TIME	2444477.21163177	2444478.9283927	2444478.950747013
	E.P.			0.80600794
JUPITER	B·T (KM)	7.537491×10^5	7.5512495×10^5	7.5519466×10^5
	B·R (KM)	4.74979×10^4	4.7697880×10^4	4.7649485×10^4
	VHP (KPS)	12.1601	12.1601	11.683219
	Ø (DEG)	-1.2147	-1.2147	-1.2812889
	θ (DEG)	99.1286	99.1286	98.958305
	TIME	2443902.0	2443910.3168511	2443910.350936017
	E.P.	2443902.0	2443910.3168511	0.91673776
EARTH	VHL (KPS)	10.6865	10.534982	————
	Ø (DEG)	25.5477	25.614623	————
	θ (DEG)	70.4962	69.296594	————
	TIME	2443391.0	2443391.037413678	————

1. Starting conditions for first n-body convergence run on any leg.
2. Departure conditions corresponding to converged n-body run on any leg.
3. E.P. = [(error in B·T (KM))^2 + (error in B·R (KM))^2/100 + error in time (days)/.5]

Table 3

CONVERGENCE HISTORY OF 1978 E TRAJECTORY

Planet	Parameter	SPARC Conditions[1]	Aiming Point from N-Body Convergence[2]	N-Body Converged Conditions
NEPTUNE	B·T (KM)	8.88×10^4	————	8.8787349×10^4
	B·R (KM)	0.0	————	-.53713876
	TIME	2447795.03485107	————	2447795.046940632
	E.P.[3]	.		.03684153
URANUS	B·T (KM)	1.624708×10^5	$1.6[illegible]99 \times 10^5$	1.6354962×10^5
	B·R (KM)	4.6898×10^4	4.7365698×10^4	4.7173301×10^4
	VHP (KPS)	15.0754	15.075400	15.052522
	Ø (DEG)	-1.6495	-1.6495	-1.6585941
	θ (DEG)	272.3912	272.3912	272.392575
	TIME	2446535.58604431	2446536.28276522	2446536.299654782
	E P.			0.37185594
SATURN	B·T (KM)	3.277183×10^5	3.2866481×10^5	3.2933279×10^5
	B·R (KM)	-1.54493×10^4	-1.5571016×10^4	-1.5028893×10^4
	VHP (KPS)	11.0191	11.0191	10.976001
	Ø (DEG)	3.4277	3.4277	3.4624565
	θ (DEG)	193.0302	193.0302	193.14326
	TIME	2445014.45593261	2445018.1242855	2445018.126545787
	E.P.			0.86480821
JUPITER	B·T (KM)	2.5733328×10^6	2.576358×10^6	2.5767222×10^6
	B·R (KM)	3.072777×10^5	3.0856215×10^5	3.0800495×10^5
	VHP (KPS)	10.4459	10.4459	9.99934091
	Ø (DEG)	-1.0682	-1.0682	-1.1806979
	θ (DEG)	131.3308	131.3308	130.92092
	TIME	2444370.0	2444379.1380357	2444379.181606578
	E.P.			
EARTH	VHL (KPS)	10.1703	10.051029	————
	Ø (DEG)	31.4611	31.803824	————
	θ (DEG)	102.5632	101.07521	————
	TIME	2443788.0	2443788.045681285	————

1. Starting conditions for first n-body convergence run on any leg.
2. Departure conditions corresponding to converged n-body run on any leg.
3. E.P. = [(error in B·T (KM))^2 + (error in B·R (KM))^2/100 + error in time (days)/.5]

Table 4

CONVERGENCE HISTORY OF 1978 I TRAJECTORY

Planet	Parameter	SPARC Conditions[1]	Aiming Point from N-Body Convergence[2]	N-Body Converged Conditions
NEPTUNE	B·T (KM)	88,800.0	———	88,813.824
	B·R (KM)	0.0	———	7.2100276
	TIME	2446869.64882278	———	2446869.658390037
	E.P.[3]			.17504714
URANUS	B·T (KM)	62,403.537	62.399.409	62,381.158
	B·R (KM)	12,092.542	12,078.476	12,066.347
	VHP (KPS)	21,2430	21.2430	21.225333
	Ø (DEG)	-1.3550	-1.3550	-1.3611881
	θ (DEG)	268.8005	268.8005	268.821909
	TIME	2445902.36242700	2445902.30991744	2445902.30990082
	E.P.			.21916501
SATURN	B·T (KM)	149,578.26	149,880.85	149,842.04
	B·R (KM)	-6,561.51	-6,598.2403	-6,560.6399
	VHP (KPS)	16.6754	16.6754	16.661244
	Ø (DEG)	3.1370	3.1370	3.1495592
	θ (DEG)	193.7356	193.7356	193.80042
	TIME	2444729.30791854	2444730.7871652	2444730.80984527
	E.P.			.58567327
JUPITER	B·T (KM)	1,212,719.8	1,213,580.0	1,213,546.3
	B·R (KM)	112,404.55	112,727.92	112,732.28
	VHP (KPS)	14.2022	14.2022	13.860628
	Ø (DEG)	-.3391	-.3391	-.35889586
	θ (DEG)	132.5223	132.52230	132.45347
	TIME	2444265.50000000	2444270.2575305	2444270.29616476
	E P.			
EARTH	VHL (KPS)	11.237559	11.243561	———
	Ø (DEG)	28.186442	28.155887	———
	θ (DEG)	108.03907	107.30312	———
	TIME	2443790.50000000	2443790.991008502	———

1. Starting conditions for first n-body convergence run on any leg.
2. Departure conditions corresponding to converged n-body run on any leg.
3. E.P. = [(error in B·T (KM))^2 + (error in B·R (KM))^2/100 + error in time (days)/.5]

at all the planets and 2) the initial (aiming point from n-body convergence) and final (n-body converged conditions) conditions from each leg of the converged n-body trajectories. On any one leg there is good agreement between the conic and integrated trajectories with the exception of the time of flight.

Table 5 gives the complete convergence history of the Jupiter-Saturn leg of the trajectory for the 1977 exterior ring passage. The initial and final conditions, as well as the corrections to the initial conditions, are given for each successive integration of the trajectory. In this case only one sensitivity matrix was used to obtain convergence. Also, for most of the other legs, fewer corrections were needed to obtain convergence.

Tables 6 and 7 give the sensitivity matrices generated during convergence for all legs of the trajectories corresponding to the 1977 exterior ring passage, and the 1977 interior ring passage. A comparison of the sensitivity matrices in Tables 6 and 7 shows that the sensitivities are greater for the interior ring passage (Table 7) than the exterior ring passage (Table 6). For the trajectory corresponding to the 1977 interior ring passage it was necessary to generate two sensitivity matrices for the Earth-Jupiter and Jupiter-Saturn legs in order to obtain convergence. The sensitivity matrices were retained upon convergence for the midcourse guidance analysis.

Table 5

CONVERGENCE HISTORY OF JUPITER-SATURN LEG FOR 1977 E TRAJECTORY

	Parameter	SPARC Initial Conditions	First Run	Corrections	Second Run	Corrections	Third Run	Corrections
JUPITER	B·T (KM)	1,924,606.6	1,924,606.6	16,497.6	1,941,104.2	-2886.6	1,938,217.6	777.6
	B·R (KM)	151,066.10	151,066.10	1226.26	152,292.36	648.63	152,940.98	-22.72
	VHP (KPS)	7.8118	7.8118		7.8118		7.8118	
	Ø (DEG)	-3.0377	-3.0377		-3.0377		-3.0377	
	Θ (DEG)	94.3799	94.3799		94.3799		94.3799	
	TIME	2444070. 00000000	2444070. 00000000	21.561264	2444091. 561264	-1.2584095	2444090. 302854	.29456893
		N-Body Aiming Point						
SATURN	B·T (KM)	358,415.35	4,998,310.8		496,732.79		291,326.92	
	B·R (KM)	-17,359.508	-173,760.34		216.031.72		-39,355.652	
	VHP (KPS)	10.6937	10.822137		10.661842		10.671063	
	Ø (DEG)	2.7472	2.7430736		2.7654006		2.7808117	
	Θ (DEG)	195.3260	195.04878		194.48274		195.49266	
	TIME	2444846. 61852323	2444826. 85295868		2444847. 77484107		2444846. 435048818	
	BIMISS (KM) 1)		4,642,530.6		271,299.06		70,602.32	
	ETIME (Days) 2)		19.832273		-1.0896087		.250183	
	E.P. 3)		4682.1951		273.47827		71.102682	

1) BIMISS = $(\text{error in B·T (KM)})^2 + \text{error in B·R (KM)})^2$
2) ETIME = error in time of arrival
3) E P. = $[\,(\text{error in B·T (KM)})^2 + (\text{error in B·R (KM)})^2/1000 + \text{error in time (days)}/.5]$

Table 5 (Cont.)

CONVERGENCE HISTORY OF JUPITER-SATURN LEG FOR 1977 E TRAJECTORY

Parameter	Fourth Run	Corrections	Fifth Run	Corrections	Sixth Run
B·T (KM)	1,938,995.2	-187.4	1,938,807.8	-16.1	1,938,791.6
B·R (KM)	152,918.26	20.5	152,938.74	- 9.03	152,929.7
VHP (KPS)	7.8118		7.8118		7.8118
Ø (DEG)	-3.0377		-3.0377		-3.0377
θ (DEG)	94.3799		94.3799		94.3799
TIME	597423	-.0808015	2444090. 5116621	-.01964204	2444090. 496979
	N-Body Aiming Point				
B·T (KM)	369,447.43		355,063.52		358,738.12
B·R (KM)	-79,728.391		-19,304.993		-17,746.25
VHP (KPS)	10.668896		10.669496		10.669641
Ø (DEG)	2.7792466		2.7798719		2.7797137
θ (DEG)	195.48814		195.48886		195.4885
TIME	2444846. 7549548		2444846. 70319819		2444846. 68426561
BIMISS (KM)	14,485.038		3875.5		503.739
ETIME (Days)	-.069722		-.017965		-.0009667
E.P.	14.624483		3.911453		.50567

Table 6

SENSITIVITY MATRICES
1977 E TRAJECTORY

		$B \cdot T_F$*	$B \cdot R_F$	$Time_F$
EARTH-JUPITER	VHL	1.4524449×10^{10}	$-1.7320846 \times 10^{10}$	-257.02057
	Φ	-1.3078390×10^{9}	-8.0286081×10^{8}	6.8216719
	Θ	-4.6717345×10^{9}	5.7470956×10^{8}	6.3153312
		$B \cdot T_F$	$B \cdot R_F$	$Time_F$
JUPITER-SATURN	$B \cdot T_I$*	241.85600	16.936000	$-.38146972 \times 10^{-7}$
	$B \cdot R_I$	77.952000	-266.15400	$-.76293944 \times 10^{-8}$
	$Time_I$	-404685180	9432296.0	.94943237
		$B \cdot T_F$	$B \cdot R_F$	$Time_F$
SATURN-URANUS	$B \cdot T_I$	3963.5840	-435.8500	$-.85449219 \times 10^{-6}$
	$B \cdot R_I$	-736.0000	-3854.8930	$.10681152 \times 10^{-6}$
	$Time_I$	-85910912	-167873.00	.66708374
		$B \cdot T_F$	$B \cdot R_F$	$Time_F$
URANUS NEPTUNE	$B \cdot T_I$	2814.7200	1540.5820	$.76293944 \times 10^{-7}$
	$B \cdot R_I$	1629.7280	-2798.2185	$.30517578 \times 10^{-7}$
	$Time_I$	-916262.40	1309212.0	.91964722

*The subscripts F and I refer to the target variables at the arrival (final) and departure (initial) planets respectively.

Table 7

SENSITIVITY MATRICES
1977 I TRAJECTORY

		$B \cdot T_F$	$B \cdot R_F$	$Time_F$
EARTH- JUPITER MATRIX #1	VHL Φ Θ	$.39089154 \times 10^{11}$ $-.11769157 \times 10^{10}$ $-.61185418 \times 10^{10}$	$-.44512973 \times 10^{10}$ $-.21622508 \times 10^{10}$ $.41952192 \times 10^{9}$	-101.97067 1.5725325 4.1982886
		$B \cdot T_F$	$B \cdot R_F$	$Time_F$
EARTH- JUPITER MATRIX #2	VHL Φ Θ	$.39388928 \times 10^{11}$ $-.12265990 \times 10^{10}$ $-.59155179 \times 10^{10}$	$-.49738721 \times 10^{10}$ $-.20714486 \times 10^{10}$ $.4283892 \times 10^{9}$	-98.93036 1.1833571 2.1417473
		$B \cdot T_F$	$B \cdot R_F$	$Time_F$
JUPITER- SATURN	$B \cdot T_I$ $B \cdot R_I$ $Time_I$	834.91199 113.28000 $-.20933776 \times 10^{9}$	77.974000 -745.13599 $.17943218 \times 10^{8}$	$-.38146972 \times 10^{-7}$ $-.22888184 \times 10^{-7}$ .74314630
		$B \cdot T_F$	$B \cdot R_F$	$Time_F$
SATURN- URANUS MATRIX #1	$B \cdot T_I$ $B \cdot R_I$ $Time_I$	12732.416 -676.16000 $.99752256 \times 10^{8}$	-1328.3794 -11670.457 $.13437109 \times 10^{8}$	$-.19531250 \times 10^{-5}$ $-.12207031 \times 10^{-6}$ .70349120

Table 7 (Cont.)

SENSITIVITY MATRICES
1977 I TRAJECTORY

SATURN-URANUS MATRIX #2	$B \cdot T_I$	12400.823	-1009.7776	$.97961425 \times 10^{-5}$
	$B \cdot R_I$	-1027.5015	-11470.189	$.10467529 \times 10^{-4}$
	$Time_I$	$.97545045 \times 10^{8}$	$-.13392877 \times 10^{8}$	.73211670
URANUS-NEPTUNE	$B \cdot T_I$	13253.760	4330.6870	$.53405762 \times 10^{-7}$
	$B \cdot R_I$	10267.904	-12880.946	$-.44403076 \times 10^{-5}$
	$Time_I$	$-.35868352 \times 10^{8}$	$.59646740 \times 10^{7}$	.90330505